

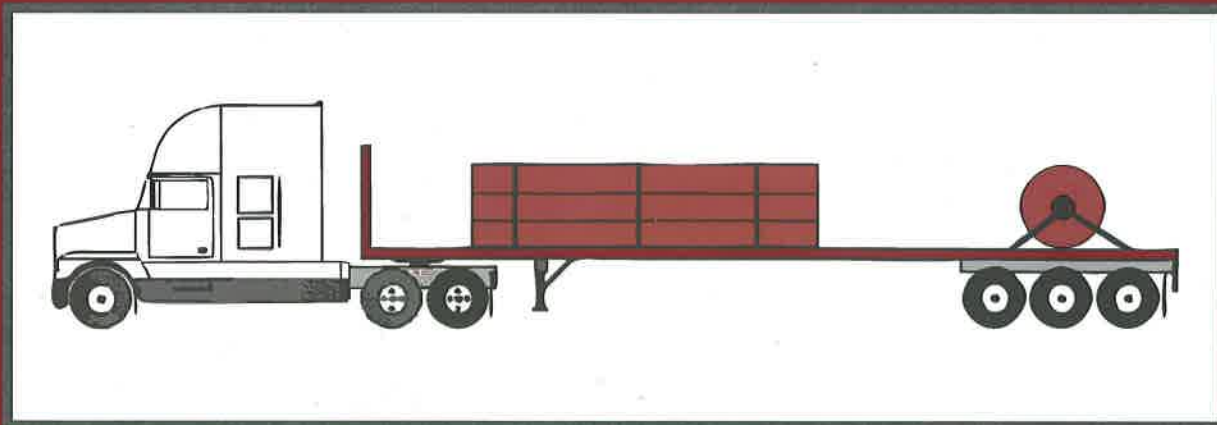
---

# CCMTA Load Security Research Project

---

Report # 2

## EXPERIMENTAL EVALUATION OF FRICTION COEFFICIENTS OF TYPICAL LOADS AND TRAILER DECKS UNDER VERTICAL VIBRATION



**CCMTA • CCATM**

CANADIAN COUNCIL OF MOTOR TRANSPORT ADMINISTRATORS  
CONSEIL CANADIEN DES ADMINISTRATEURS EN TRANSPORT MOTORISÉ

---

# *CCMTA Load Security Research Project*

---

Report # 2

## **EXPERIMENTAL EVALUATION OF FRICTION COEFFICIENTS OF TYPICAL LOADS AND TRAILER DECKS UNDER VERTICAL VIBRATION**

*Prepared for*

Canadian Council of Motor Transport Administrators  
Load Security Research Management Committee

*By*

S. Rakheja, P. Sauvé and D. Juras  
CONCAVE Research Centre  
Concordia University  
1455 de Maisonneuve Blvd. West  
Montreal, Quebec H3G 1M8

April 1997

## Disclaimer

This report is one of a series commissioned by the sponsors of the *CCMTA Load Security Research Project*. Readers are cautioned on the use of the data and the conclusions drawn from this particular aspect of the research program as this report is only one of a series related to this multi-faceted issue. The report and the results are not intended to be used in any way as a basis for establishing civil liability.

The material presented in this text was carefully researched and presented. However, no warranty expressed or implied is made on the accuracy of the contents or their extraction from reference to publications; nor shall the fact of distribution constitute responsibility by CCMTA or any of the sponsors, researchers or contributors for omissions, errors or possible misrepresentation that may result from use or interpretation of the material contained herein.

©1997 Canadian Council of Motor Transport Administrators/  
Conseil canadien des administrateurs en transport motorisé

ISBN 0-921795-30-0

Canadian Council of Motor Transport Administrators  
2323 St. Laurent Blvd.  
Ottawa, Ontario  
K1G 4J8

Telephone: (613) 736-1003  
Fax: (613) 736-1395

E-mail: [ccmta-secretariat@ccmta.ca](mailto:ccmta-secretariat@ccmta.ca)  
Internet Web site: [www.ccmta.ca](http://www.ccmta.ca)

## **North American Cargo Securement Standard**

CCMTA is serving to coordinate the development of a revised North American Cargo Securement Standard. To this end the research results in this report are being reviewed and discussed by interested stakeholders throughout North America.

**Those readers interested in participating in the development of the North American Cargo Securement Standard through 1997 are invited to visit the project Web site at [www.ab.org/ccmta/ccmta.html](http://www.ab.org/ccmta/ccmta.html) to secure additional project information.**



# TABLE OF CONTENTS

	<i>Page</i>
SUMMARY	
ACKNOWLEDGMENTS	
1. INTRODUCTION	1
2. OBJECTIVES OF THE STUDY	4
3. TEST PROGRAM AND METHODOLOGY	5
3.1 Test Apparatus	5
3.2 Signal Generation and Data Capture	10
3.2.1 Validation of the Laboratory Synthesis of Trailer Vibration	12
3.3 Test Matrix	19
3.4 Test Procedures	23
4. DATA ANALYSIS AND DISCUSSION OF RESULTS	25
4.1 Friction Forces in the Vibration Free Environment	25
4.1.1 Discussion of Results (Static)	33
4.2 Friction Forces Under Sinusoidal Vibrations	39
4.2.1 Discussion of Results (Sinusoidal Vibrations)	45
4.2.1.1 Coarse Hardwood Deck	46
4.2.1.2 Y-Groove Aluminum Deck	56
4.2.1.3 Smooth Hardwood Deck	64
4.2.1.4 X-Groove Aluminum Deck	86
4.3 Friction Coefficients Under Random Vibrations	103
4.3.1 Discussion of Results (Random Vibration)	105
4.3.1.1 Coarse Hardwood Deck	105
4.3.1.2 Smooth Hardwood Deck	116

## TABLE OF CONTENTS (Continued)

	<i>Page</i>
4.3.1.3 Y-Groove Aluminum Deck	121
4.3.1.4 X-Groove Aluminum Deck	125
5. CONCLUSIONS	130
6. REFERENCES	132

APPENDIX - Statistical Analysis

# EXPERIMENTAL EVALUATION OF FRICTION COEFFICIENTS OF TYPICAL LOADS AND TRAILER DECKS UNDER VERTICAL VIBRATION

## SUMMARY

Friction coefficients of selected deck and skid materials are measured under static, and deterministic and field measured random vibration environments. From the analysis of the measured data, it is apparent that the friction coefficients are strongly dependent upon the properties of the mating surfaces, normal load, magnitude and frequency of vibration, and flexibility of the deck and skid materials. A comparison of the published data, and between the measured and reported data reveals considerable discrepancies due to lack of standardized test procedures and reporting guidelines. The measurement of breakaway friction, specifically, necessitates high sampling rate. The breakaway friction is strongly dependent upon the degree of contact or adhesion between the mating surfaces, and thus cannot be relied upon in formulating the load security guidelines.

The sliding friction coefficients further depend upon the normal load in a significant manner. A general pattern, however, can not be established due to varying flexibility of the different mating surfaces. A guideline based upon mean values alone thus may lead to considerable concerns. The trailer vertical vibration further influences the magnitude of friction forces between the mating surfaces significantly. The vertical vibration may lead to either higher or lower instantaneous friction forces, depending upon the direction of vertical acceleration. Sinusoidal vertical vibration result in extreme high and low values of friction coefficients during a vibration cycle. The analysis of the measured data showed that lowest values of friction coefficients can be as low as 20% of the static value under 0.5g vertical acceleration. Since the extreme low values occur during a short portion of the vibration cycle, consideration of these low values will perhaps lead to highly conservative guidelines.



The measurements performed under field measured random vibration are therefore analyzed to determine the amplitude distribution of the coefficients of friction. The amplitude distribution can provide significant knowledge leading to friction coefficients and their corresponding frequency of occurrence. The frequent occurrence of lower values of friction coefficients in conjunction with braking and directional maneuvers can lead to significant load shift, when the loads are not adequately secured. The analysis of the results showed that friction coefficients, in most cases, fall below 75% of the mean or static value for durations as high as 25% of the total test duration.

## ACKNOWLEDGEMENTS

The work described in the present report is part of the Load Security Research Project of the Canadian Council of Motor Transport Administrators (CCMTA). The CCMTA Load Security Research Management Committee is chaired by Mr. M. Schmidt of the U.S. Federal Highway Administration (Albany, New York). The project was funded jointly by the following agencies:

- Allegheny Industrial Associates;
- Alberta Transportation and Utilities;
- American Trucking Associations;
- British Columbia Ministry of Transportation and Highways;
- Canadian Trucking Research Institute;
- Commercial Vehicle Safety Alliance (CVSA);
- Forest Engineering Research Institute of Canada;
- Manitoba Highways and Transportation;
- Ministère des Transports du Québec;
- New Brunswick Ministry of Transportation;
- Newfoundland Ministry of Transportation and Public Works;
- New York State Department of Transportation;
- Nova Scotia Ministry of Transportation;
- Ontario Ministry of Transportation;
- Prince Edward Island Department of Transportation;
- Saskatchewan Government Insurance;
- Saskatchewan Highways and Transportation;
- Société de l'Assurance Automobile du Québec;
- Transport Canada, Road and Motor Vehicle Safety Directorate;
- Transport Canada, Transportation Development Centre; and
- United States Department of Transportation, Federal Highway Administration.

The experimental work was conducted through technical consultations with the *Strategic Transportation Research Branch* of the *Ontario Ministry of Transportation* (MTO). Different decking and skidder materials, and accessories were provided by the MTO.

The authors acknowledge the support provided by the *Forestry Engineering Research Institute of Canada* (FERIC), Eastern division, in creating the opportunities to characterize the vertical vibration spectra of their logging trailer. The experimental work was further assisted by Mr. Dale Rathwell and Mr. Ajai Singh at CONCAVE Research Centre.

# 1. INTRODUCTION

The freight transportation industry has been employing different types of load securement mechanisms to minimize the occurrences of load spills. The dynamic forces and moments developed during various directional maneuvers can lead to movement of certain types of cargo relative to the trailer bed. The dynamic relative movements of such cargo and thus the load shift may impose amplified forces and moments leading to reduce handling and control limits of vehicle and potential load spill situations. The friction forces arising within the cargo layers and between the cargo and the trailer bed, are known to offer definite resistance to the dynamic forces and moments induced by the directional maneuvers [1]. While the significant role of these friction forces related to the load security has been recognized, there exists a lack of reliable database on the friction forces between typical loads and trailer decks, specifically under dynamic vehicular environment [2, 3].

Although friction coefficients of different sliding surfaces in a static environment have been extensively reported in the published literature, considerable variations can be observed among the values reported by different authors [4, 5, 6]. Such variations can be attributed to lack of standardized test methods and highly nonlinear dependency of the localized rubbing friction on various material and environment factors. The friction forces, primarily arising from physicomechanical and chemical properties of the sliding surfaces and subsurface layers of solids, are known to be strongly influenced by: (i) the surface conditions and roughness; (ii) type of material; (iii) thermal properties of materials; (iv) humidity and temperature; (v) normal load on the sliding surfaces; and (vi) the molecular structure and plastic deformations of the surface layers. The properties of surface layers experience significant changes during friction, when an intensive deformation of the surface layers takes place. The friction

then tends to generate higher temperatures, which further accelerates the physical and chemical processes of the interactions between the surfaces and the surrounding environment [4]. The magnitude of variations among the reported values of friction coefficients in a static environment suggests that there exists a need for development of standardized measurement procedures and further measurements for different mating surfaces.

The friction forces are further influenced by the vibration environment encountered in freight vehicles. The inertia forces developed by the load vibration influence the magnitude of dynamic friction forces within the load layers, and between the load and the trailer bed surfaces. The influence of vertical vibration on the friction force can be demonstrated through a simple example of a solid sliding on a rigid surface, shown in Figure 1.1. When a solid of mass  $m$  is subject to a periodic vertical acceleration  $a(t)$ , the normal force  $N$  is related to the acceleration in the following manner:

$$N = m (g - A \sin \omega t) \quad (1.1)$$

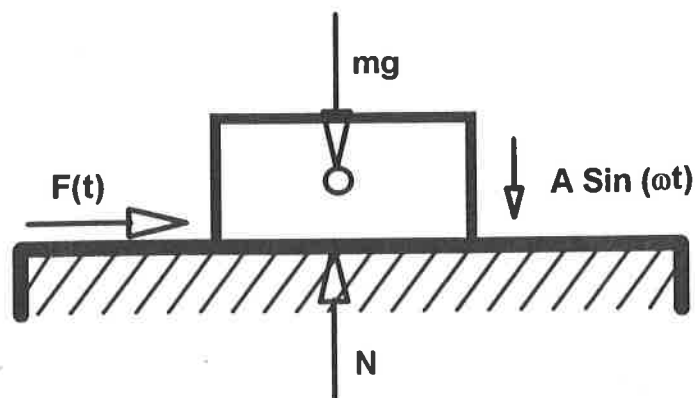


Figure 1.1: Friction force developed between sliding surfaces subject to vertical vibration.

where  $g$  is the acceleration due to gravity,  $A$  is the magnitude of vertical acceleration, and  $\omega$  is the frequency of vibration. The instantaneous friction force, assuming ideal friction, can then be expressed as:

$$F(t) = \mu m (g - A \sin \omega t) \quad (1.2)$$

where  $\mu$  is the coefficient of friction and  $F(t)$  is the instantaneous friction force. From equation (1.2), it is apparent that the instantaneous friction force is different from the friction force measured in the absence of vibration ( $F_0 = \mu mg$ ), and is dependent upon the magnitude and direction of the vertical vibration. The vehicular vibration imposing downward acceleration on the load can lead to significantly lower instantaneous friction forces, which may influence the effectiveness of the load securement in an adverse manner. While the friction coefficients between different surfaces have been reported extensively for vibration free environment, the influence of vertical vibration on the friction coefficients has not been reported, with the exception of studies on tire-road friction and friction drives [4,8,9].

## 2. OBJECTIVES OF THE STUDY

In view of the lack of knowledge, and upon recognition of the significance of vehicle vibration in relation to the load securement [3], this study was undertaken to characterize the friction forces under vertical vibration. The overall objective of this study was formulated to contribute to the *CCMTA Load Security Program* through experimental characterization of friction properties of selected loads and deck surfaces under vertical vibration.

The specific objectives of the study included the following:

- a. Characterize the breakaway and sliding friction coefficients between selected loads and deck surfaces in a vibration free environment.
- b. Characterize the breakaway and sliding friction coefficients between selected loads and deck surfaces under sinusoidal vertical vibration, as a function of
  - Magnitude of vibration;
  - Frequency of vibration
  - Normal load; and
  - Properties of the interface.
- c. Correlate the friction coefficients measured under sinusoidal vibration with those measured in a static environment.
- d. Measure the vibration response of a typical trailer and synthesize the trailer vibration in the laboratory.
- e. Characterize the breakaway and sliding friction coefficients between selected loads and deck surfaces under field measured trailer vibration synthesized in the laboratory.

### 3. TEST PROGRAM AND METHODOLOGY

#### 3.1 TEST APPARATUS

A test fixture, comprising a deck structure and a horizontal hydraulic actuator, was designed, as shown in Figure 3.1, to perform the experimental study. A deck support structure, comprising three load bearing I-beams and three cross-members, was fabricated, as shown in Figure 3.2. The selected deck material was installed on the 1.83m x 1.32m frame structure. The different skid materials were attached to a steel sled, provided by MTO, which was placed on the flat deck surface. The skid materials representing steel pads and machine feet were directly attached to the sled, while the materials such as rubber, paper and plastic were attached to the smooth bottom surface of the sled. Different vertical loads were realized through either one or two concrete blocks (0.61 X 1.22 X 0.53 m) placed on the sled, as illustrated in Figure 3.3. The study of concrete skid surface was performed by placing the concrete block directly on the deck surface.

A hydraulic actuator with load capacity of approximately 45kN and displacement of 0.3m was mounted horizontally on the frame to generate the necessary pull force. A 50 kN compression-tension force transducer, mounted to the actuator piston rod, was coupled to the sled as shown in the pictorial view in Figure 3.4. The frame structure with the hydraulic actuator was installed on two electro-hydraulic vibration exciters, each with stall force capacity of 53kN. The frame structure was installed using linear rails on one of the actuator and cylindrical bushings on the second actuator, in order to minimize the side loads. The installation further provided the capability to generate rotational vibration, which was outside the scope of this study. Figure 3.5 illustrates the frame mounting comprising linear rails. A position sensor was installed within the horizontal actuator to achieve the motion of the loaded sled in the displacement



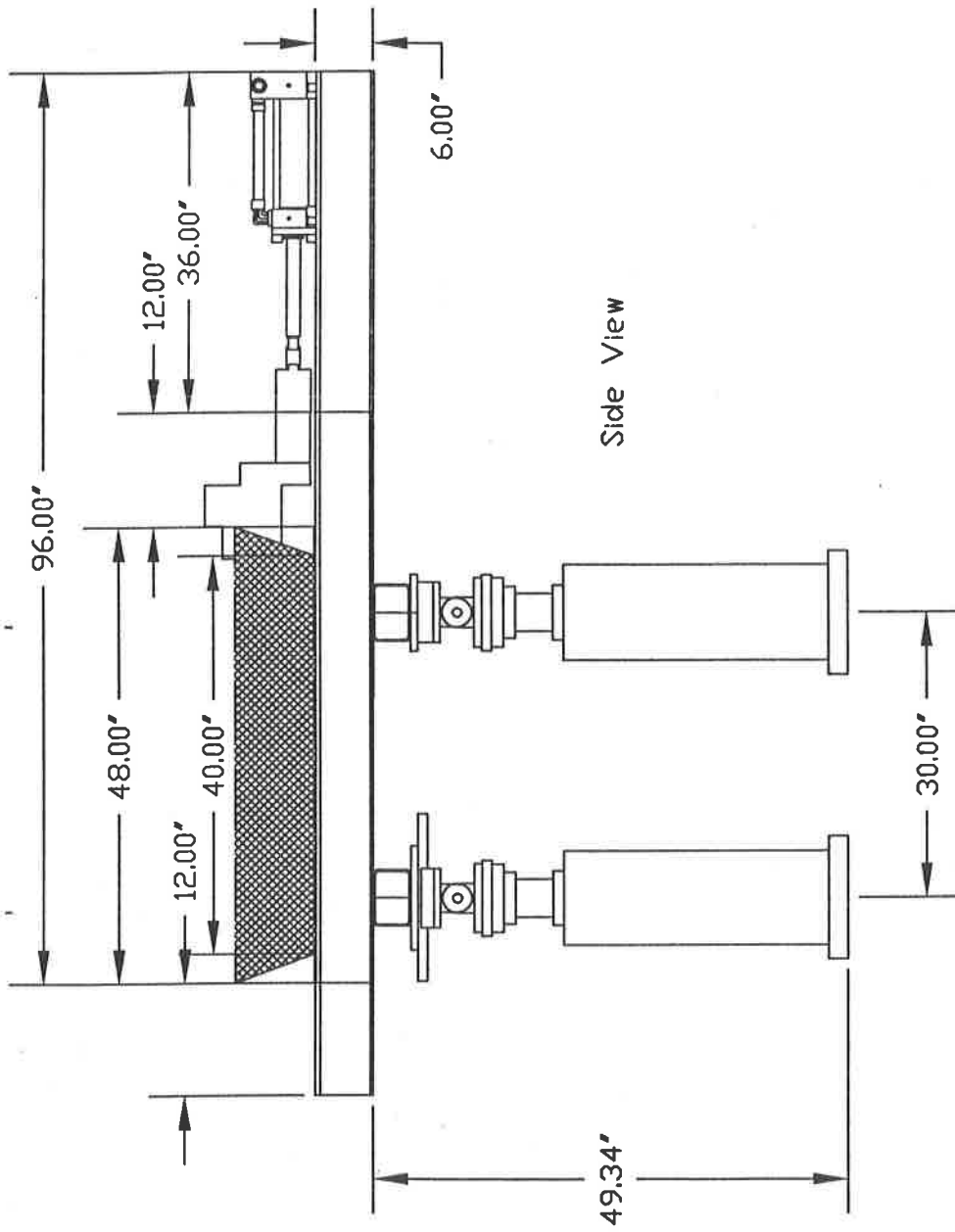
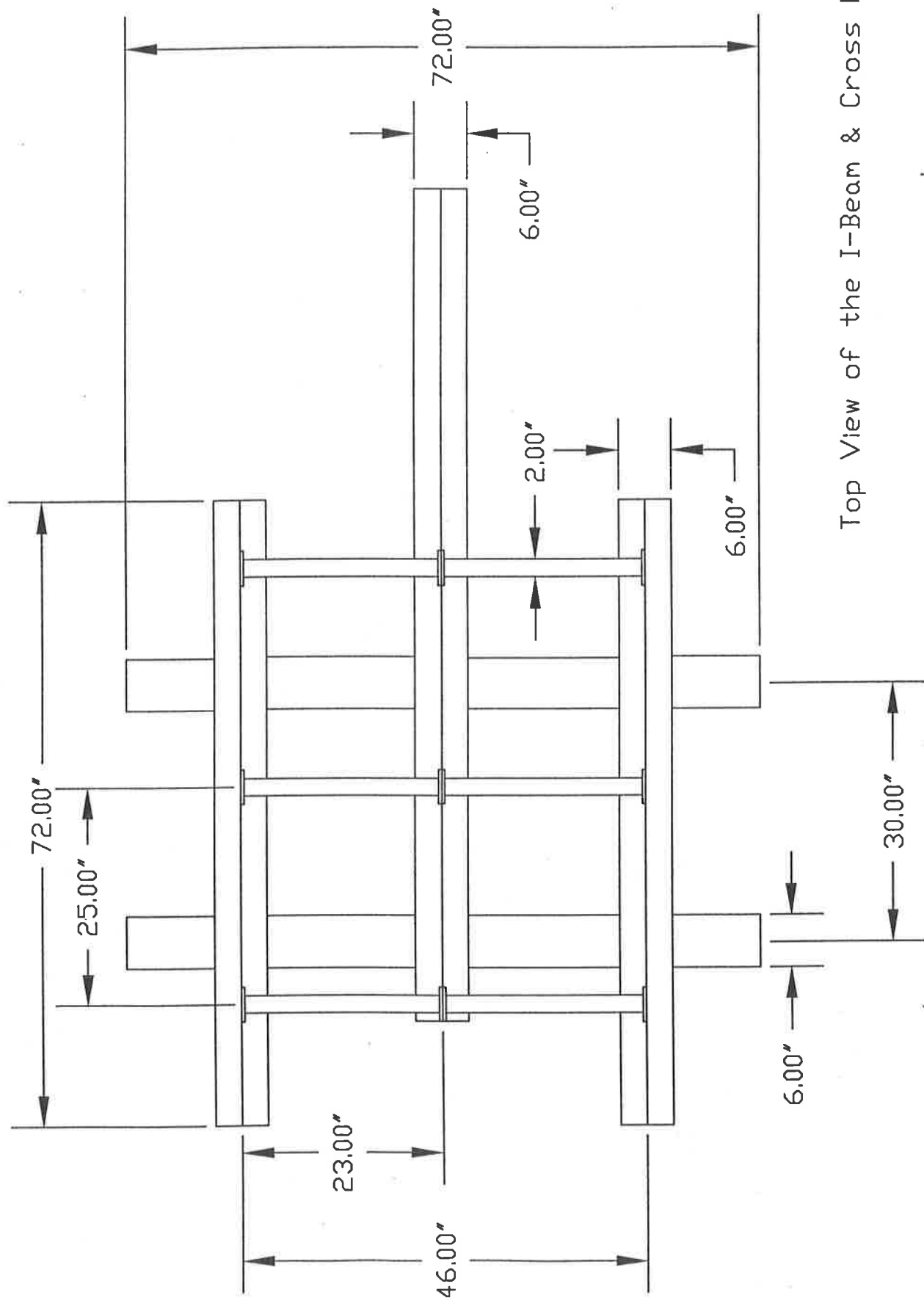


Figure 3.1: The test fixture.



Top View of the I-Beam & Cross Members

Figure 3.2 : Design of the frame structure

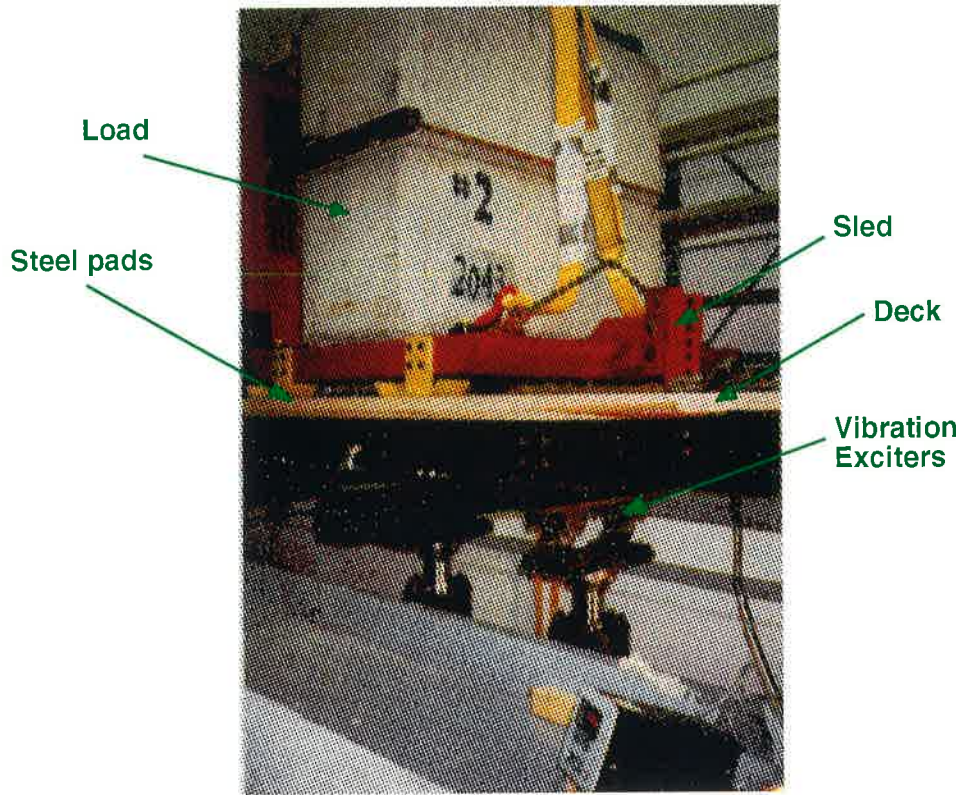


Figure 3.3: A pictorial view of the test apparatus indicating the placement of vertical load on the sled.

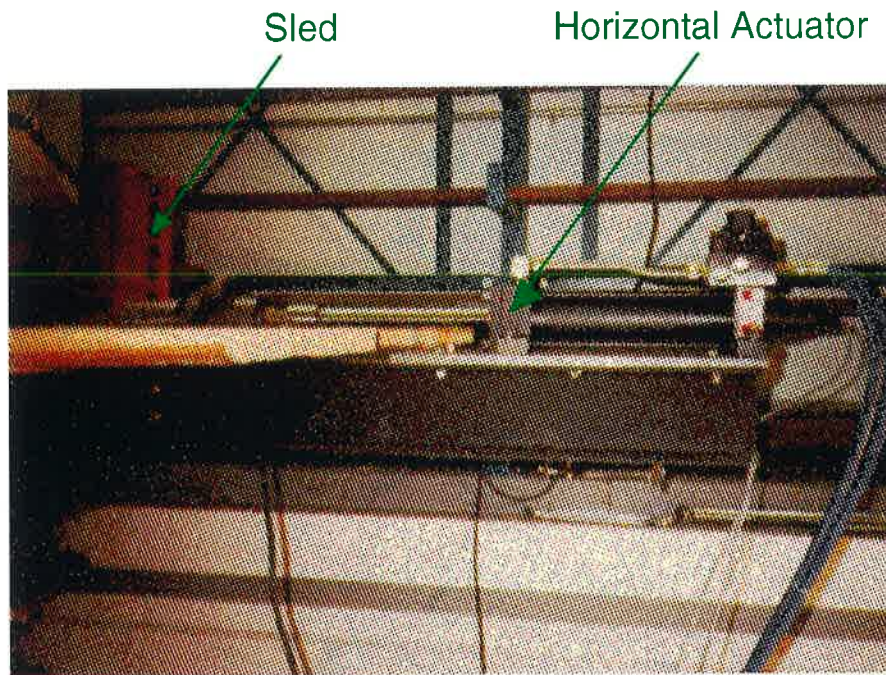


Figure 3.4: A pictorial view of the hydraulic actuator and the coupling.

feedback control mode. A B&K accelerometer was installed on the frame structure to monitor and control the acceleration input to the deck surface.

### **3.2 SIGNAL GENERATION AND DATA CAPTURE**

In view of the large number of repetitive tests required for the study, a signal generation and data capture software was developed in order to automate the test by linking the various computers and data acquisition hardware. Figures 3.6 and 3.7 illustrate the schematics of the signal generation and data capture hardware used for sinusoidal and random vibration tests, respectively. The sinusoidal vibration signals were generated using a multi-channel *Wavetek* signal generator coupled to the servo controller and the vibration exciters. The software generated the position signal for the horizontal pulling actuator at a rate of 2.54 cm/s (1.0 in/s) through the output board of the personal computer *PC2*. The software was developed to generate the position command signal to create a series of 5 pulls (5 cm or 2.0 in each), where each pull occurred over a duration of 2s. The command signal also allowed a rest period of 2s between the successive pulls. The command signal was filtered through a low pass filter with cut-off frequency of 2 Hz and trigger signals were embedded to synchronize the motion of all the horizontal and vertical exciters. The *Wavetek* signal generator was triggered through an IEEE bus, and the ramp displacement of the horizontal actuator and the EGAA data acquisition were triggered, when the vertical actuator displacement reached the peak value.

A multi-channel data acquisition board and associated software (*PC3*) were configured to record the vertical acceleration, friction force, horizontal actuator displacement, and the displacements of the two vertical vibration exciters. The experiments in a vibration free environment were also performed using this setup, while the position gains for the vertical exciters were suppressed.

End View

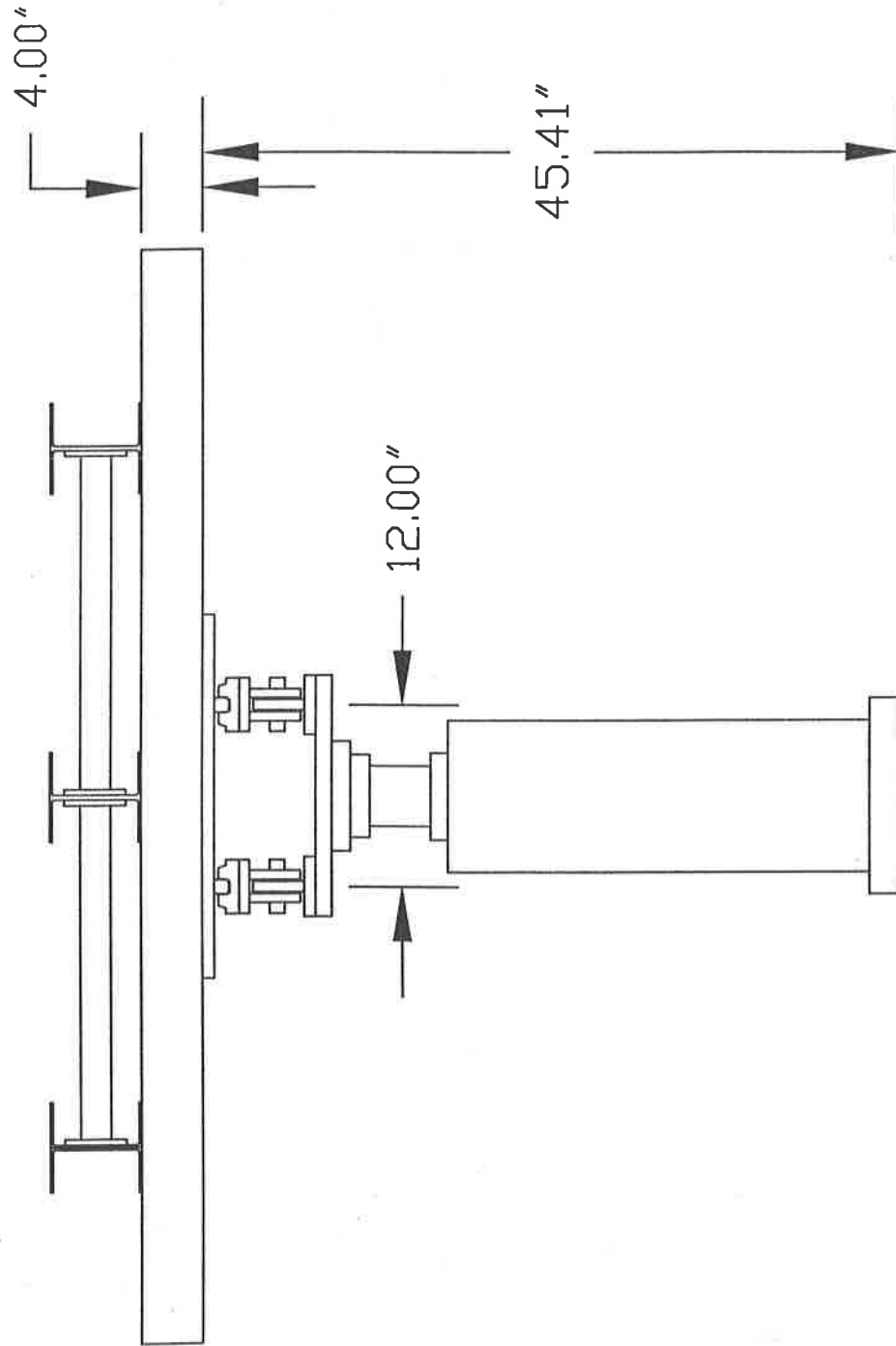


Figure 3.5: Schematic design of the linear rail mountings between the frame structure and the electro-hydraulic exciter.

The tests under field measured random vibration were performed using the setup described in Figure 3.7. The vertical vibration response characteristics of a modern trailer were measured, while operating on asphalt and gravel roads. The measurements were performed in collaboration with Eastern Division of the *Forestry Engineering Research Institute of Canada* (FERIC). The measured data was analyzed and corresponding drive files were generated in the *Dadisp* software. The personal computer (*PC1*) was configured to generate the drive file signals using D/A output board and *Visual Designer* software. A trigger signal, similar to the one described for sinusoidal vibration, was embedded in the drive file to synchronize the EGAA data acquisition and the motions of all the actuators. The measured data were recorded at a sampling rate of 1000 samples/s in order to capture the breakaway friction force. The measured acceleration and friction force signals were also analyzed using the two-channel *B&K Signal Analyzer*, and the measured signals were recorded in terms of power spectral density (PSD). In case of random vibration tests, the horizontal actuator drive software was modified to generate the ramp displacement over the entire stroke instead of the 5 ramps used in the sinusoidal vibration tests. This allowed the measurement of friction force under representative vibration excitations of longer duration. Each test, however, was repeated three times in order to examine the repeatability of measurements.

### **3.2.1 Validation of the Laboratory Synthesis of Trailer Vibration**

The field measured random vibration response of the trailer bed was analyzed and processed in order to generate the corresponding drive files. The drive files developed for both asphalt and gravel roads, were validated by comparing the measured response of the vibration exciters in the laboratory with the field measured data. Figure 3.8 illustrates the systematic procedures employed for synthesis and

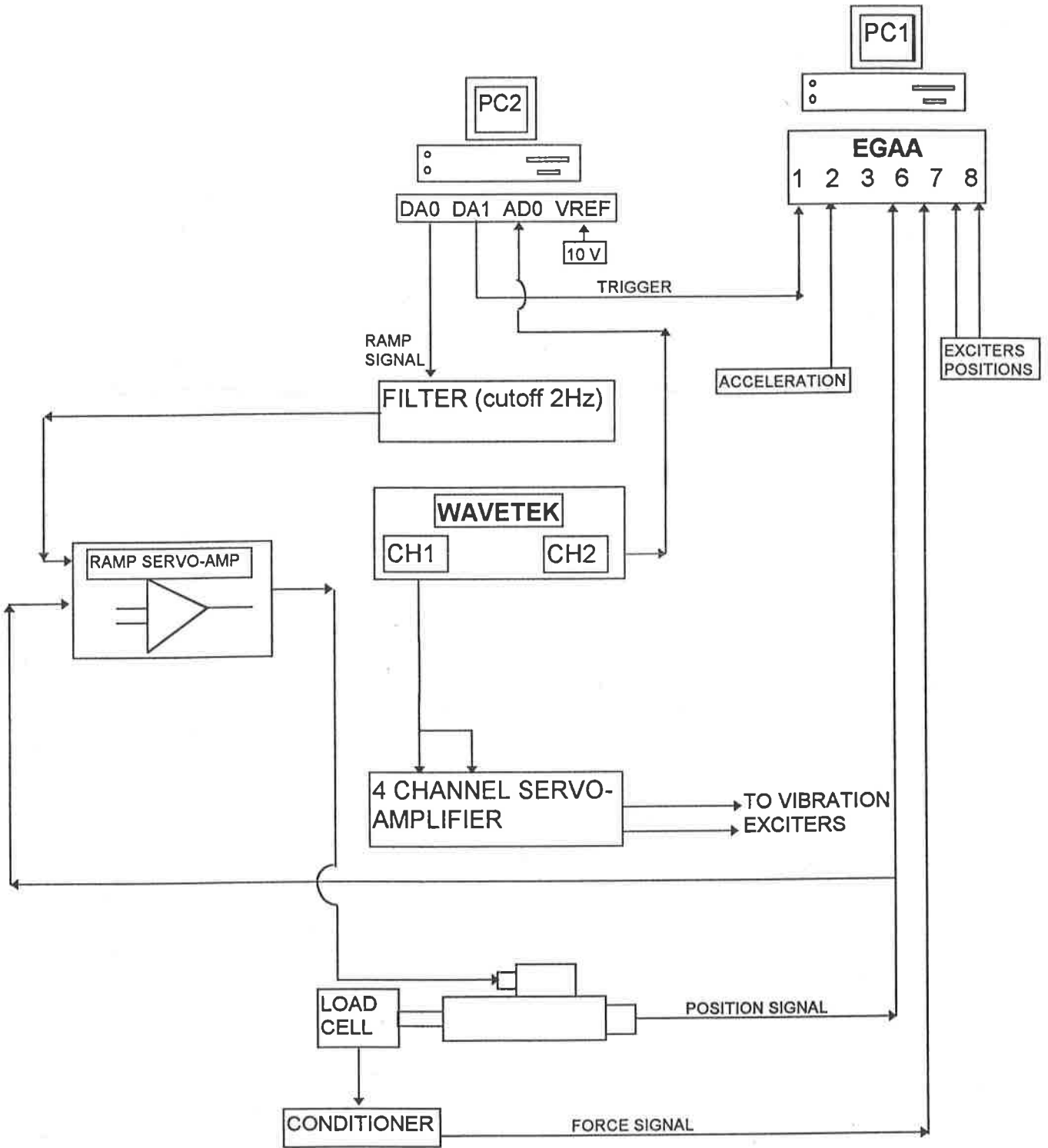


Figure 3.6 : Schematic of the signal generation and data capture systems (sinusoidal excitations).



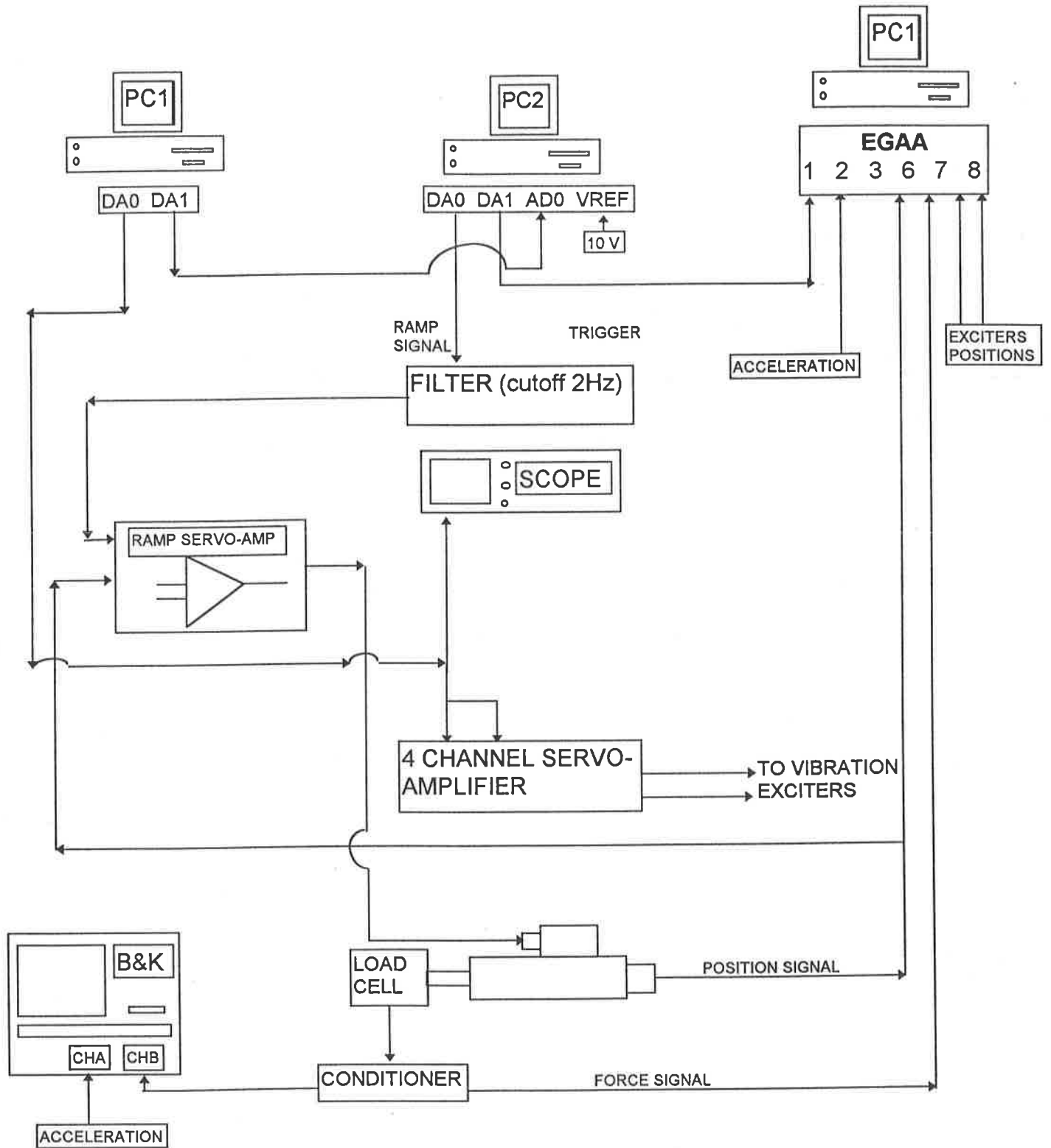


Figure 3.7 : Schematic of the signal generation and data capture systems (random excitations).

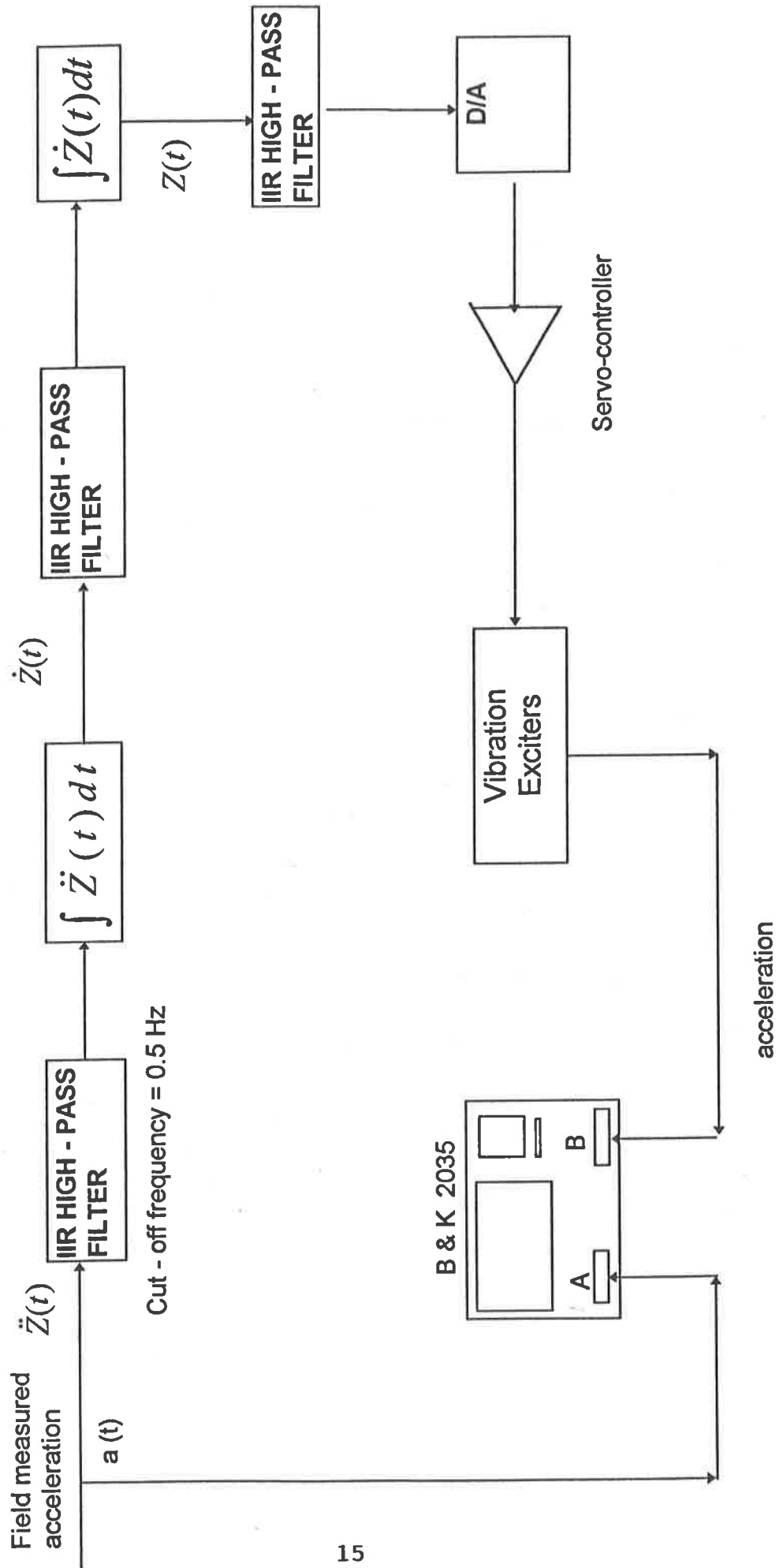


Fig. 3.8 Signal processing employed for synthesis of field measured acceleration data

validation of the field measured random vibration data. The field measured acceleration data was initially filtered using a high-pass (HP) filter with cut-off frequency of 0.5 Hz in order to eliminate the dc components. The filtered signal is integrated twice in order to derive the corresponding displacement signal. An A/D conversion is then performed to generate the drive file, which is interfaced with the servo controller using the *Visual Designer* output board. The resulting acceleration response of the trailer bed is then measured and analyzed using the *B&K Signal Analyzer*.

The power spectral density (PSD) of the synthesized acceleration response of the trailer bed is compared with that of the field measured acceleration response, while driving on asphalt and gravel roads, as shown in Figures 3.9 and 3.10, respectively. The results clearly show a good correlation between the synthesized and the field measured data in the entire frequency range, except in the 0 - 0.5 Hz frequency band. The PSD of laboratory synthesized acceleration in this low frequency range is considerably lower due to the high-pass filter used in the study. The levels of vibration in this frequency band, however, are significantly low, as shown in the Figures. The results clearly show predominant vibration in the vicinity 1.5 Hz, which is attributed to the resonant frequency of the sprung mass of the trailer supported on air suspension. The results further reveal high vibration near 3 Hz, most likely attributed to the pitching mode of the trailer, and relatively low level vibration in the 12 - 16 Hz frequency range attributed to wheel-hop motions. The results also show that the asphalt and gravel roads exhibit very similar trailer response in both the magnitude and frequency components of vibration. The asphalt road used in the study was considered to be quite rough, while the gravel road was levelled prior to the measurements. The measurements performed on the two roads thus resulted in similar spectra, with the exception of slightly higher vertical acceleration encountered on the gravel road in the vicinity of trailer pitch and wheel-hop frequencies.

# PSD of Synthesized vs Measured Highway Profile

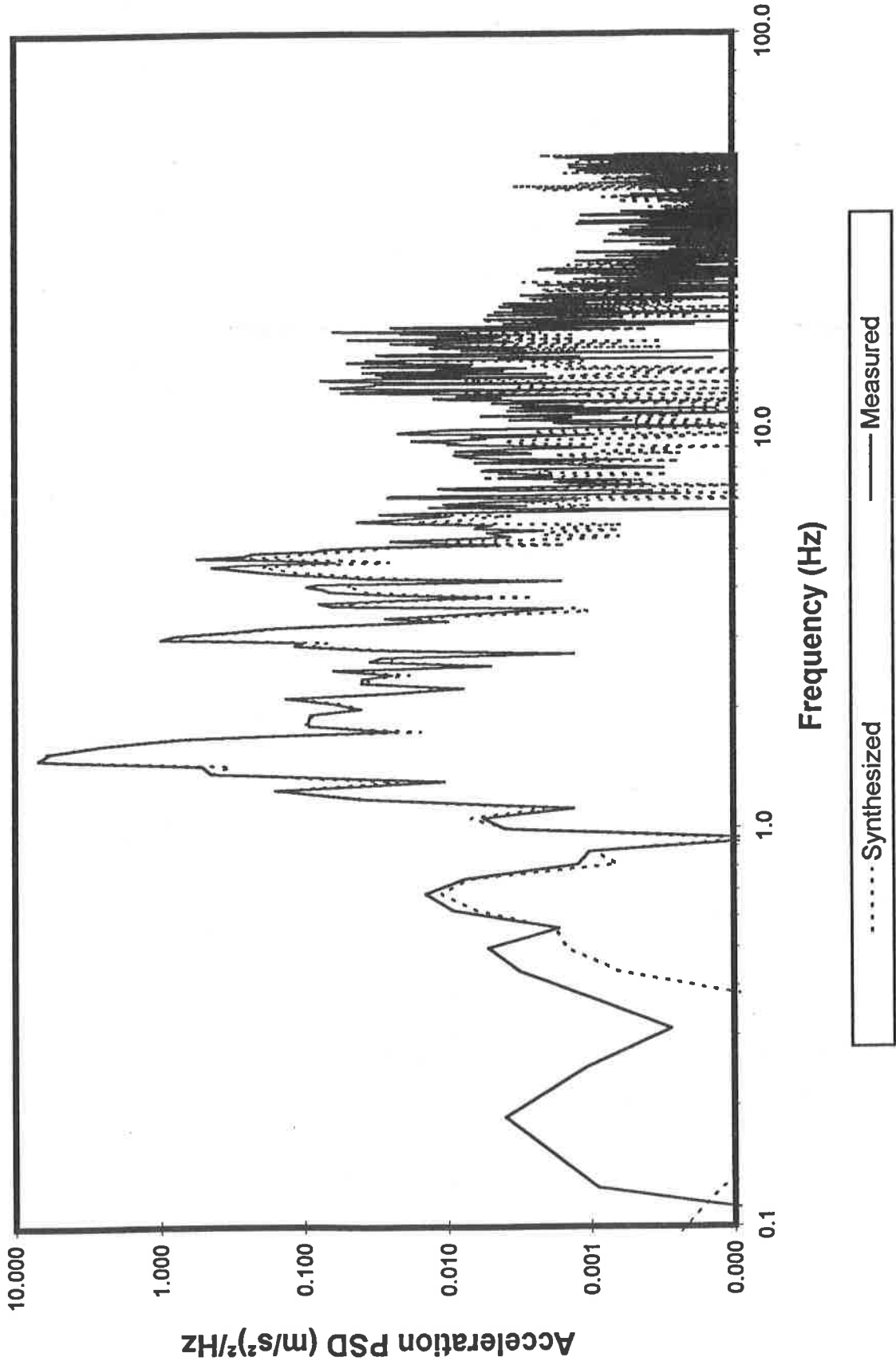


Figure 3.9: Comparison of PSD of acceleration measured in the laboratory with that of the field measured acceleration (Asphalt Road).

# PSD of Synthesized vs Measured Gravel road profile

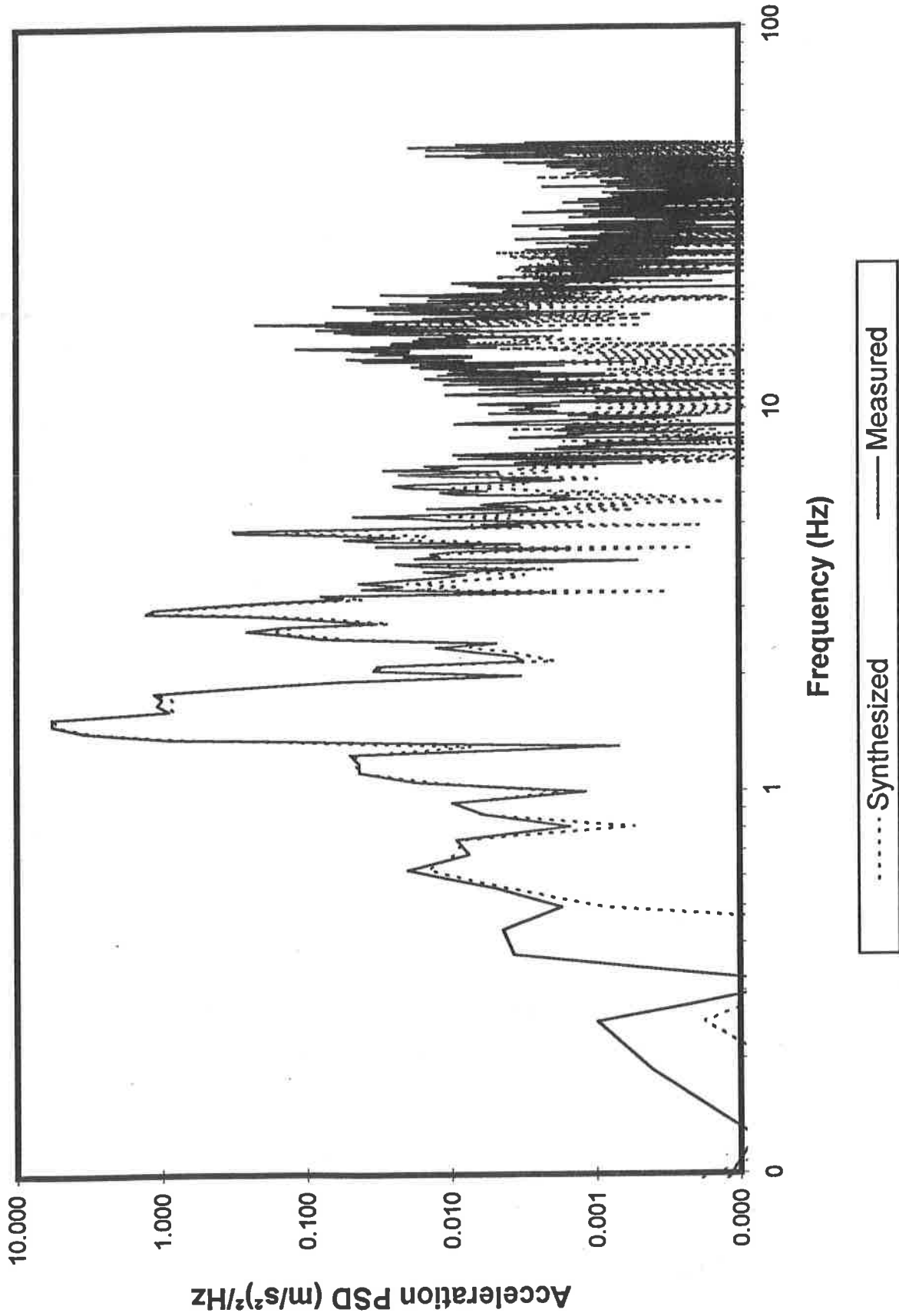


Figure 3.10: Comparison of PSD of acceleration measured in the laboratory with that of the field measured acceleration (Gravel Road).

### 3.3 TEST MATRIX

The study was performed to characterize the friction coefficients between different skid and deck materials. A total of four deck and nine skid materials were identified for the study in consultation with MTO, as outlined in Table 3.1. The tests were conducted under different vertical loads, referred to as low (L), medium (M) and high (H), which are summarized in Table 3.2. The low vertical load corresponds to the sled and skid material, while the medium and high loads are realized by adding one and two concrete blocks, respectively, to the sled. The experiments involving rubber and paper, however, could not be performed under high load due to frequent failure of the skid surface during the test. All the tests were performed with clean and dry surfaces only. The friction forces between each deck and skid material were evaluated under static as well as vertical vibrations. Although the study of friction forces under representative vehicular vibration are considered to be most relevant to the load security program, a study under deterministic vibration is vital to gain an understanding of the important trends. Two types of vertical vibrations were selected for the study: (i) sinusoidal; (ii) field measured random vibration. The tests under sinusoidal vibration were performed with different magnitudes and frequencies of vibration. Three different acceleration levels were selected as: 0.1g, 0.25g and 0.5g peak. The experiments under higher levels of vibration (0.75g and 1.0g) could not be performed due to separation of the skid and deck materials under these levels. While different discrete frequencies in the 1 - 12 Hz range (1, 1.5, 2, 4, 8, 10 and 12 Hz) were selected, the experiments under low level acceleration and higher frequencies were not performed due to extremely small vertical motion. Furthermore, the tests under high level acceleration (0.5g) at low frequencies (1.0 and 1.5 Hz) were not performed due to separation of loads caused by high magnitudes of vertical displacements. The selected frequency range represents the predominant frequency components of heavy vehicle

Table 3.1: Test Matrix

Deck Material	Skid Material	Sinusoidal Vertical Vibration											Field Measured Vehicular Vibration		Vertical Load							
		Magnitude (g)	Frequencies (Hz)											Asphalt Road	Gravel Road	L	M	H				
			1	1.5	2	4	8	10	12													
Aluminum Grooves (X-axis)	Plastic skid	0.1	X	X	X	X																
		0.25	X	X	X	X	X								X					X	X	X
		0.5		X	X	X	X	X														
	Concrete	0.1	X	X	X	X																
		0.25	X	X	X	X	X								X						X	X
		0.5		X	X	X	X	X														
	Steel Pads	0.1	X	X	X	X																
		0.25	X	X	X	X	X								X						X	X
		0.5		X	X	X	X	X														
Aluminum Grooves (Y-axis)	Plastic skid	0.1	X	X	X	X																
		0.25	X	X	X	X	X								X					X	X	
		0.5		X	X	X	X	X														
	Concrete	0.1	X	X	X	X																
		0.25	X	X	X	X	X								X						X	X
		0.5		X	X	X	X	X														
	Steel Pads	0.1	X	X	X	X																
		0.25	X	X	X	X	X								X						X	X
		0.5		X	X	X	X	X														
Coarse Hardwood	Machine Fe	0.1	X	X	X	X																
		0.25	X	X	X	X	X								X					X	X	
		0.5		X	X	X	X	X														
	Concrete	0.1	X	X	X	X																
		0.25	X	X	X	X	X								X						X	X
		0.5		X	X	X	X	X														
	Spruce	0.1	X	X	X	X																
		0.25	X	X	X	X	X								X						X	X
		0.5		X	X	X	X	X														
Steel Pads	0.1	X	X	X	X																	
	0.25	X	X	X	X	X								X						X	X	
	0.5		X	X	X	X	X															

Deck Material	Skid Material	Sinusoidal Vertical Vibration											Field Measured Vehicular Vibration		Vertical Load																		
		Magnitude (g)	Frequencies (Hz)											Asphalt Road	Gravel Road	Load																	
			1	1.5	2	4	8	10	12	L	M	H																					
Smooth Hardwood	Paper	0.1	X	X	X	X																											
		0.25	X	X	X	X	X	X						X															X	X			
		0.5		X	X	X	X	X	X					X																			
	Rubber	0.1	X	X	X	X	X																										
		0.25	X	X	X	X	X	X						X																X	X		
		0.5		X	X	X	X	X	X					X																			
	Plastic Skid	0.1	X	X	X	X	X																										
		0.25	X	X	X	X	X	X						X																X	X	X	
		0.5		X	X	X	X	X	X					X																			
	Smooth Steel	0.1	X	X	X	X	X																										
		0.25	X	X	X	X	X	X						X																X	X	X	X
		0.5		X	X	X	X	X	X					X																X	X	X	X



**TABLE 3.2: VERTICAL LOADS EMPLOYED IN DIFFERENT TESTS.**

Skid Material	Vertical Load (kN)		
	L	M	H
Plastic	1.989	11.164	20.054
Steel Pads	1.933	11.108	19.997
Concrete		8.889	18.011
Machine Feet	1.844	11.019	19.908
Spruce	1.938	11.014	20.003
Kraft Paper	1.874	11.029	
Rubber	1.951	11.126	20.015
Smooth Steel	1.775	10.950	19.838

vertical vibration associated with the deflection modes of the sprung (suspension frequency: 1.5 - 2.5 Hz) and unsprung masses (wheel hop: 9 - 15 Hz), and fundamental flexural modes of the trailer (6 - 8 Hz). The amplitudes of sinusoidal vibration are also considered to represent the range of vibration encountered while operating on smooth and rough roads.

### **3.4 TEST PROCEDURES**

The experiments were performed using the following procedures:

- i)* For each test series, install the deck material on the frame structure mounted on the two electro-hydraulic vibration exciters.
- ii)* Install the base and the skid material on the sled and place the sled on the deck. In case of concrete skid material, the concrete block was placed directly on the deck. The smooth steel skid surface was realized by placing the sled directly on the deck. The sled or the concrete block was then coupled with the horizontal actuator comprising a 22 kN load cell.
- iii)* Place either one or two concrete blocks on the sled to represent the selected load condition.
- iv)* Install an accelerometer on the frame and connect the accelerometer and load cell signals to appropriate signal conditioners.
- v)* Connect the conditioned signals from the load cell, accelerometer, horizontal actuator displacement sensor, and vertical exciters LVDT's to the data acquisition system.
- vi)* Install a potentiometer in conjunction with the horizontal actuator displacement sensor to adjust the actuator position.
- vii)* Extend the horizontal actuator to the extreme position through the command signal generated by the software and adjust the potentiometer to release the residual load on the coupling.
- viii)* Generate the ramp displacement command signal to realize five pulls of the load, and acquire the force, displacement and acceleration data.

- ix)* Activate the *Wavetek* waveform generator and the associated software to perform tests under sinusoidal vertical vibration. Select the excitation frequency and connect the trigger signals to the *Wavetek*. Select the servo-controller gain to achieve desired acceleration of the base frame, and extend the horizontal actuator, as described in (vii).
- x)* Run the software to generate vertical vibration and the command signal to conduct five consecutive pulls in a synchronized manner and record the measured data.
- xi)* Repeat steps (ix) and (x) to perform measurements under vertical vibration of different magnitudes and frequencies.
- xii)* Disconnect the *Wavetek* and connect the random signal from *PC1* to the servo controller. Run the *Visual Designer* file and set the servo gain to the preset values for either gravel or asphalt roads. Perform the tests as described in steps (ix) and (x). It should be noted that under random vibrations the ramp displacement signal was configured to yield a 0.30m pull.
- xiii)* Repeat each test under random vibration three times.

## **4. DATA ANALYSIS AND DISCUSSION OF RESULTS**

The friction forces between the selected skid and deck materials were measured under both static (in the absence of vertical vibration) and vertical vibration environment. Each test under static and sinusoidal vibration conditions was performed five times using the automated ramp signal. The first pull allowed the alignment of the sled, and synchronization between the vertical vibration and horizontal actuator displacement. Since each subsequent pull was synchronized with the vertical displacement, the last pull in the series was performed only for the remainder of either the command signal to the actuator stroke. The data acquired during the first and last pulls were therefore rejected during the analyses. The analyses performed with the measured data acquired under static and dynamic environment are described in the following sections.

### **4.1 FRICTION FORCES IN THE VIBRATION FREE ENVIRONMENT**

The measurements were initially performed in a vibration free environment in order to establish the breakaway and sliding friction coefficients between the selected skid and deck materials. These measurements provided the essential data to study the influence of vertical vibration on the coefficients of friction. Figures 4.1 to 4.3 illustrate the time histories of friction forces and the horizontal displacement measured with some of the selected skid and deck materials. It should be noted that these figures illustrate the plot of the directly measured data. All the figures clearly illustrate high degree of repeatability, specifically for the pulls #2, 3 and 4. The results show that the sharp breakaway friction force can be adequately captured using the selected sampling rate of 1000 samples/s. The measurements also reveal considerable residual load on the coupling between the sled and the horizontal actuator, between the successive pulls, which is attributed to relatively tight coupling. The matching holes on the sled

Deck: Smooth Hardwood

Normal Load: 1873 N

Skid: Kraft Paper

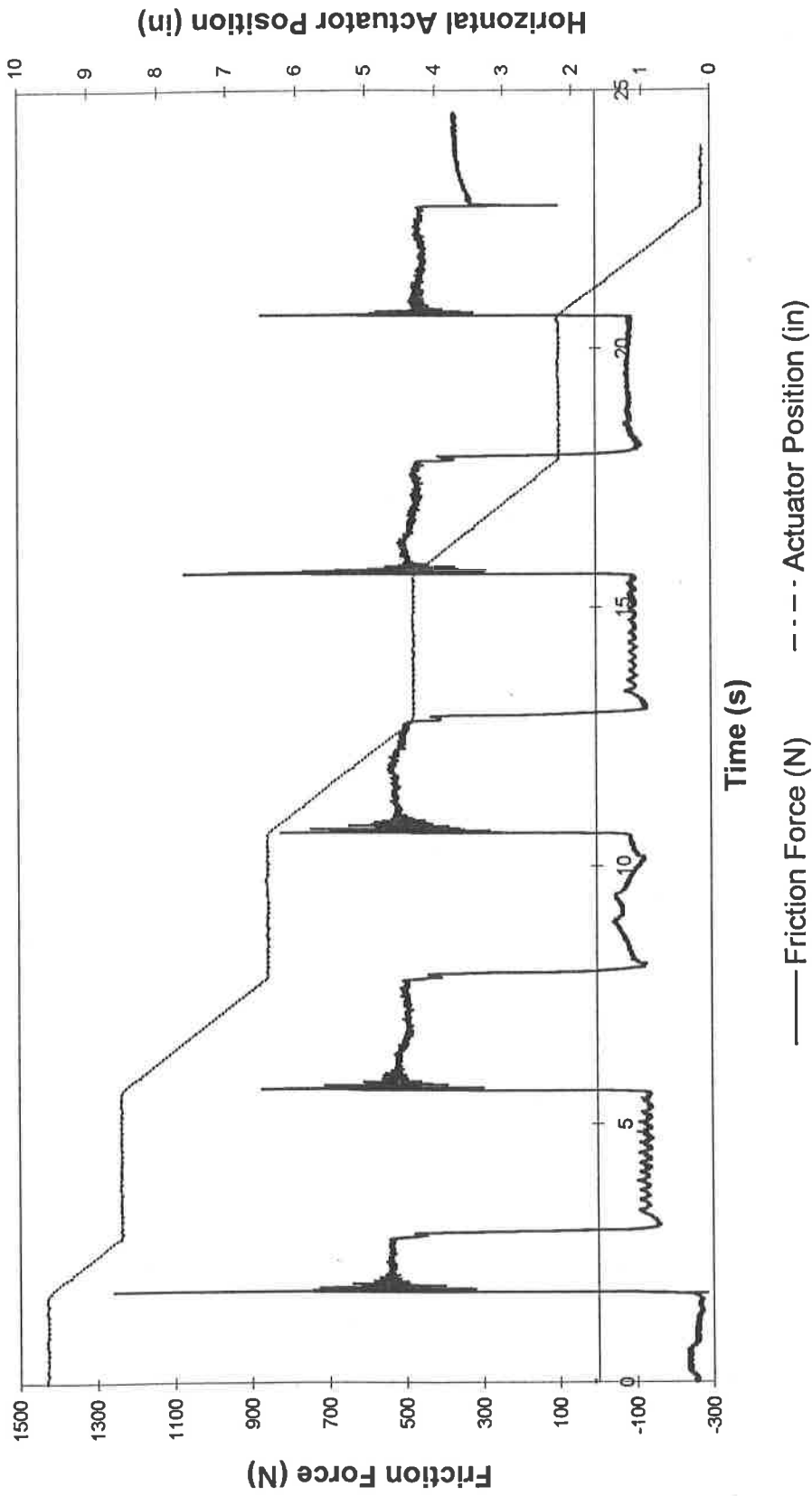


Figure 4.1: Time history of the friction force and load displacement under static condition

Deck: Smooth Hardwood      Normal Load: 11164 N      Skid: Kraft Paper

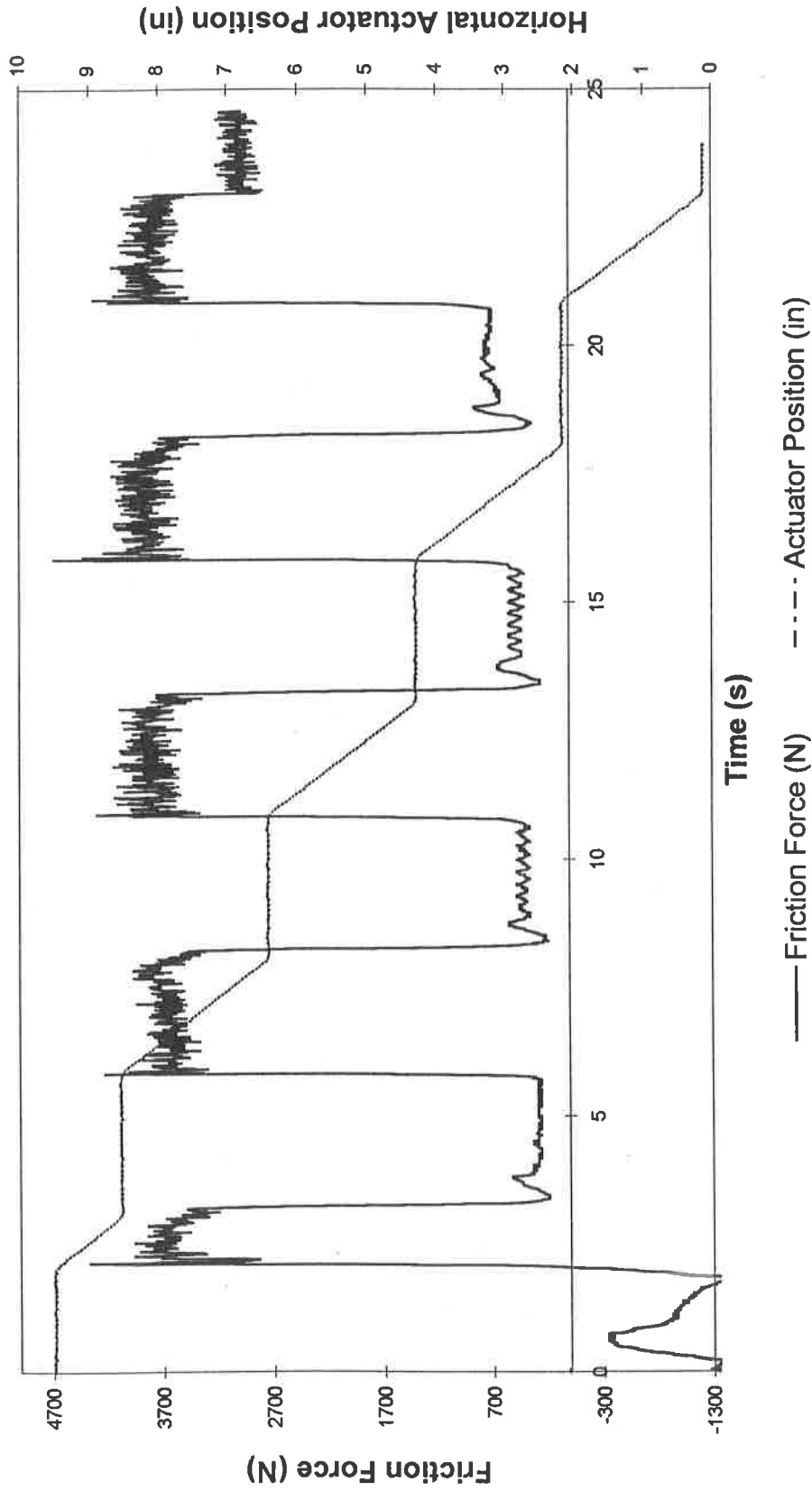


Figure 4.2: Time history of the friction force and load displacement under static condition

Deck: X-Groove Aluminum

Normal Load: 18011 N

Skid: Concrete

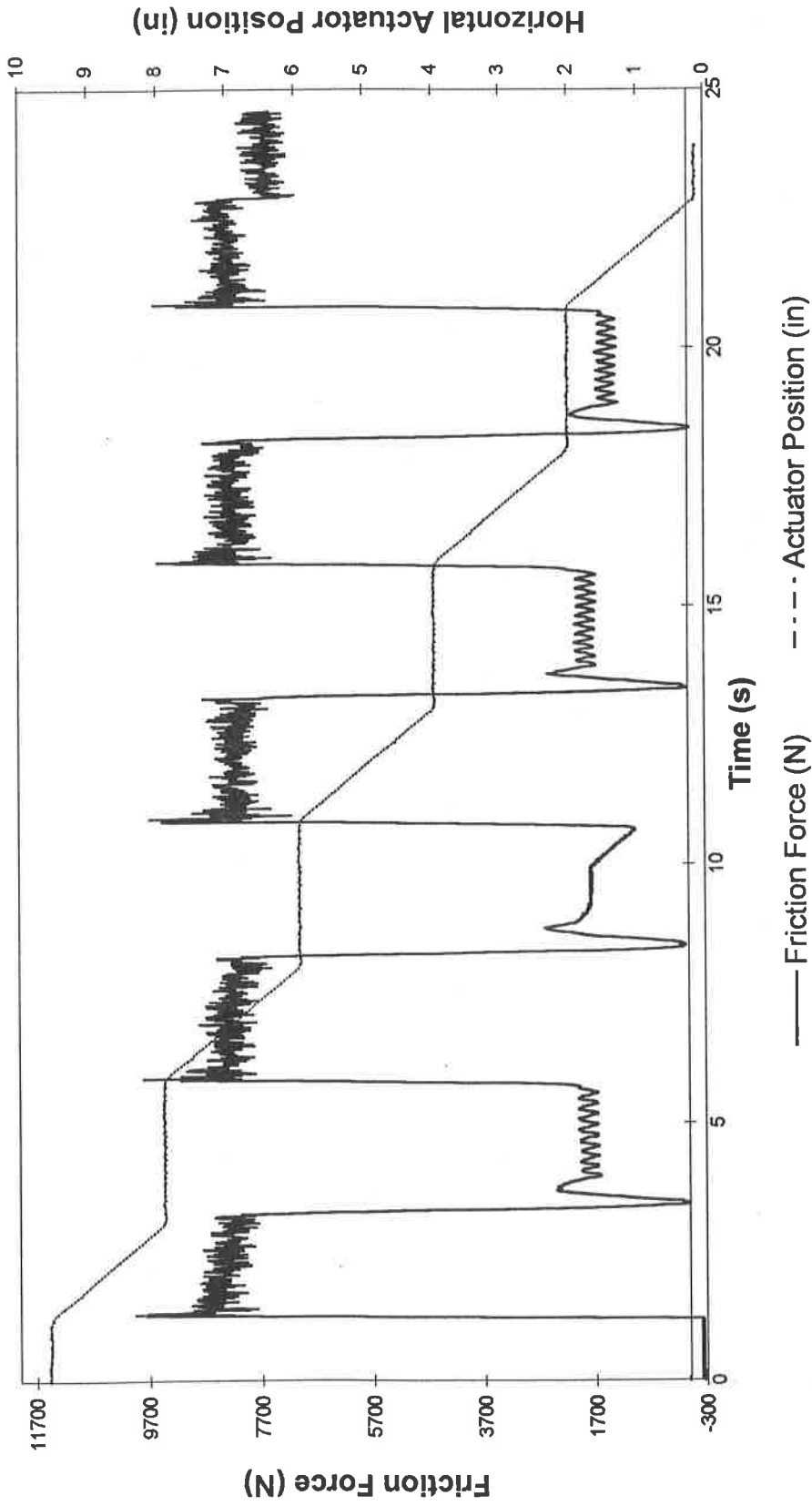


Figure 4.3: Time history of the friction force and load displacement under static condition

provided by the MTO were thus relaxed for tests performed with Y-groove aluminum, coarse hardwood and smooth hardwood decks. The force signals, however, did not approach their initial values during all the tests, which is most likely attributed to the lock-up, inertia of the moving sled and the inability of the coupling to release the load completely. The measurements also reveal low frequency oscillations in the force signal acquired between the successive pulls, when horizontal actuator is stationary. These oscillations are most likely attributed to the inertia forces developed due to braking of the sled and stick-slip motion.

The data acquired during the pulls #2, 3 and 4 were adjusted to account for the residual forces. The breakaway friction forces measured during the pulls were extracted. The measured data revealed oscillations in the sliding friction force, which are most likely attributed to micro variations in the surfaces, transients following the breakaway, and signal noise. An averaging was therefore performed on the sliding friction force data to derive the mean sliding friction force corresponding to each trial (pull). The breakaway and average sliding friction forces derived corresponding to each trial are normalized with respect to the vertical load to determine the breakaway and sliding friction coefficients,  $\mu_o$  and  $\mu_s$ , respectively. Table 4.1 summarizes the values of  $\mu_o$  and  $\mu_s$  derived from each trial as a function of the normal load, together with their mean values. The data derived during each test are thoroughly examined for repeatability. While a majority of the measurements revealed high degree of repeatability, only six measurements (indicated by an asterisk in Table 4.1) revealed inconsistent measurements of the breakaway friction during either one or two pulls. The mean values of friction coefficients, derived upon excluding the values considered inconsistent, are also summarized in Table 4.1.



**TABLE 4.1: SUMMARY OF BREAKAWAY AND SLIDING FRICTION COEFFICIENTS MEASURED DURING DIFFERENT TRIALS.**

Deck Material	Skid Material	Normal Load (kN)	Friction Coefficient							
			Breakaway ( $\mu_0$ )				Sliding ( $\mu_s$ )			
			Trial # 2	Trial # 3	Trial # 4	Mean	Trial # 2	Trial # 3	Trial # 4	Mean
Aluminum X-Grooves	Plastic	1.989	0.314*	0.360	0.366	0.363	0.250	0.251	0.258	0.255
		11.164	0.272	0.275	0.272	0.273	0.232	0.234	0.236	0.234
		20.054	0.313	0.309	0.308	0.310	0.270	0.267	0.269	0.269
Aluminum Y-Grooves	Steel Pads	1.933	0.385	0.385	0.338	0.370	0.272	0.276	0.272	0.274
		11.108	0.362	0.373	0.380	0.372	0.313	0.323	0.345	0.327
		19.997	0.481*	0.422	0.388	0.405	0.369	0.361	0.356	0.362
Aluminum Y-Grooves	Concrete	8.889	0.400	0.413	0.392	0.402	0.343	0.330	0.327	0.333
		18.011	0.561	0.560	0.573	0.565	0.473	0.469	0.473	0.472
		1.989	0.357	0.352	0.328	0.346	0.216	0.207	0.207	0.210
Aluminum Y-Grooves	Steel Pads	11.164	0.240	0.235	0.229	0.235	0.222	0.210	0.197	0.210
		20.054	0.218	0.219	0.213	0.217	0.186	0.183	0.172	0.180
		1.933	0.654	0.668	0.635	0.652	0.475	0.470	0.465	0.470
Aluminum Y-Grooves	Steel Pads	11.108	0.412*	0.434	0.408*	0.434	0.412	0.380	0.408	0.400
		19.997	0.502	0.437*	0.454*	0.502	0.467	0.437	0.454	0.452

**TABLE 4.1: SUMMARY OF BREAKAWAY AND SLIDING FRICTION COEFFICIENTS MEASURED DURING DIFFERENT TRAILS. (Continued)**

Deck Material	Skid Material	Normal Load (kN)	Friction Coefficient							
			Breakaway ( $\mu_0$ )				Sliding ( $\mu_s$ )			
			Trial # 2	Trial # 3	Trial # 4	Mean	Trial # 2	Trial # 3	Trial # 4	Mean
Aluminum Y-Grooves	Concrete	8.889	0.422	0.427	0.384	0.411	0.349	0.322	0.330	0.333
		18.011	0.506	0.501	0.486	0.498	0.440	0.449	0.437	0.442
Coarse Hardwood	Machine Feet	1.844	0.805	0.806	0.811	0.807	0.582	0.589	0.547	0.573
		11.019	0.588	0.610	0.573	0.591	0.493	0.508	0.510	0.503
	Concrete	19.908	0.669	0.666	0.661	0.665	0.596	0.593	0.585	0.591
		8.889	0.664	0.670	0.640	0.658	0.516	0.524	0.521	0.520
	Spruce	18.011	0.681	0.697	0.705	0.694	0.558	0.578	0.557	0.564
		1.938	0.704	0.622	0.642	0.656	0.458	0.465	0.459	0.461
	Steel Pads	11.014	0.603	0.586	0.584	0.591	0.486	0.484	0.486	0.485
		20.003	0.623	0.594	0.596	0.604	0.525	0.510	0.504	0.513
	Steel Pads	1.933	0.586	0.548	0.574	0.569	0.512	0.496	0.463	0.490
		11.108	0.588	0.570	0.570	0.576	0.527	0.516	0.512	0.518
		19.997	0.601	0.569	0.559	0.576	0.532	0.508	0.514	0.518

**TABLE 4.1: SUMMARY OF BREAKAWAY AND SLIDING FRICTION COEFFICIENTS MEASURED DURING DIFFERENT TRAILS. (Continued)**

Deck Material	Skid Material	Normal Load (kN)	Friction Coefficient							
			Breakaway ( $\mu_0$ )				Sliding ( $\mu_s$ )			
			Trial # 2	Trial # 3	Trial # 4	Mean	Trial # 2	Trial # 3	Trial # 4	Mean
Smooth Hardwood	Paper	1.874	0.720	0.743	0.699	0.721	0.400	0.410	0.385	0.398
		11.029	0.463	0.467	0.469	0.466	0.368	0.381	0.388	0.379
	Rubber	1.951	0.706	0.716	0.701	0.708	0.665	0.674	0.671	0.670
		11.126	0.658*	0.757	0.770	0.764	0.658	0.690	0.699	0.682
		20.015	0.645	0.717	0.712	0.681	0.618	0.636	0.631	0.627
			0.616	0.606	0.656	0.626	0.419*	0.463	0.463	0.463
	Smooth Steel	10.950	0.528*	0.561	0.572	0.567	0.439*	0.487	0.471	0.479
		19.838	0.482	0.509	0.518	0.503	0.430*	0.466	0.460	0.463
	Plastic	1.989	0.222	0.224	0.228	0.225	0.152	0.148	0.151	0.150
		11.164	0.174	0.165	0.172	0.170	0.137	0.133	0.135	0.135
		20.054	0.182	0.176	0.177	0.178	0.144	0.144	0.139	0.142

#### 4.1.1 Discussion of Results (Static)

The results of the static measurements, summarized in Table 4.1, clearly illustrate considerable influence of vertical load on the friction coefficient. Although the friction coefficients reported in majority of the published literature do not emphasize on the influence of normal load [5, 6], the role of normal load on the frictional properties (in a static environment) has been thoroughly described by Kragelskii and Mikhin [4], and Damian and Pascu [8]. It is speculated that the friction coefficients reported in the literature represent the mean values, which may be considered valid within certain range of variations in the normal load. Such a practice of reported the friction coefficients, however, can lead to considerable errors. A comparison of the mean and mean of mean values revealed that errors in static breakaway and sliding friction coefficients approach as high as 27% and 21%, respectively, when the influence of variations in the load is neglected.

The variations in friction coefficients with changes in the normal load are strongly dependent upon the relative flexibility of the skid and deck materials. The relative flexibility of the mating surfaces affects the areas of contact and density of distribution of the individual contact areas, which depend upon many factors, such as roughness of the contacting surfaces and their mechanical properties, surface waviness, intensity of normal load, elastic or elastoplastic deformations of the asperities leading to localized flat zones, and interpenetration of the surfaces. Non-uniform flattening of asperities and interpenetration of the surfaces have been reported for interfaces comprising hard and soft surfaces [4, 8]. A general pattern of dependency on the normal load, however, can not be established for different materials. In light of the significant variations in the coefficients of friction with the normal load and surface

properties, the measured data is examined for each skid material to establish the pattern.

Apart from the significant influence of normal load, the friction coefficients are strongly influenced by many other factors discussed in section 1. The reliability of the measured data is therefore examined by comparing the measured values with the mean values reported by MTO for the selected materials [7]. While the measured friction coefficients for some materials were comparable, significant differences were observed in other cases, specifically in the breakaway coefficients. The differences and similarities between the measurements are discussed below for each skid material.

**CONCRETE:** The relatively high stiffness of concrete can yield considerable localized deformation of the deck surface. The magnitude of normal load thus affects the coefficient of friction in a significant manner, as evident in Table 4.2. The breakaway and sliding friction coefficients between concrete, and X- grooved aluminum deck increase by 41%, when normal load is increased from 8.889 kN to 18.011 kN. The corresponding increases between concrete and Y-grooved aluminum deck are 21% and 33%, respectively. The variations in friction coefficients for the coarse hardwood deck surface, however, are relatively small, 5.5% and 8.5% in  $\mu_o$  and  $\mu_s$ , respectively. The flattening of local asperities within the aluminum surface yields considerable variations in the friction forces. The molecular structure of the coarse hardwood permits flattening of wider areas even under smaller loads and thus leads to only lower variations in  $\mu_o$  and  $\mu_s$ . The results further show similar values of  $\mu_o$  and  $\mu_s$  for both directions (X- and Y-) of the grooved aluminum floor. A comparison with the values reported by MTO [7] revealed significant differences, which are discussed below:

- The mean values of coefficients of friction measured between concrete and coarse hardwood ( $\mu_o=.676$ ,  $\mu_s=0.542$ ) are considerably higher than those

reported by MTO ( $\mu_o=0.46$ ,  $\mu_s=0.40$ ). These differences are primarily attributed to three factors:

- (i) The experimental data capture by MTO was performed at a rate of 200 samples/s, while a sampling rate of 1000 samples/s was used in this study. The lower values of  $\mu_o$  reported by MTO are most likely attributed to the lower sampling rate.
  - (ii) The coarse hardwood used in this study was extremely rough, which was used in conjunction with only four skid materials. The MTO tests utilized the coarse hardwood for significantly large number of surface conditions and skid materials. Repetitive tests performed by MTO perhaps resulted in smoothening of the surface conditions.
  - (iii) The experiments in this study were performed in the laboratory with controlled environment, while the MTO tests were performed in a relatively large garage. The differences in the humidity and temperature conditions may have also contributed to variations in the results.
- The mean values of friction coefficients measured between concrete and X-groove aluminum ( $\mu_o=.483$ ,  $\mu_s=0.403$ ) are slightly higher than those measured with Y-groove aluminum deck ( $\mu_o=.455$ ,  $\mu_s=.388$ ). The values reported by MTO for the X-groove aluminum ( $\mu_o=0.59$ ,  $\mu_s=0.55$ ) are considerably larger than those reported for the Y-groove aluminum deck ( $\mu_o=0.34$ ,  $\mu_s=0.33$ ). The results reported by MTO further exhibit only small differences between the sliding and breakaway coefficients. While the differences in the  $\mu_o$  values can be attributed to the different sampling rates used in two studies, the sliding friction coefficients reported for Y-groove aluminium in the two studies are quite similar. The considerable variation in  $\mu_s$  values for the X-groove aluminum deck may be attributed to different test conditions such as temperature, humidity and concrete surface.

**Table 4.2: Influence of normal load on the friction coefficients between concrete and different deck materials.**

Deck Material	Aluminum X-Grooves	Aluminum Y-Grooves	Hardwood Coarse	Aluminum X-Grooves	Aluminum Y-Grooves	Hardwood Coarse
Load (kN)	Breakaway Friction Coefficient			Sliding Friction Coefficient		
8.889	0.402	0.411	0.658	0.333	0.333	0.520
18.011	0.565	0.498	0.694	0.472	0.442	0.564
MEAN	0.483	0.455	0.676	0.403	0.388	0.542

**PLASTIC:** Table 4.3 summarizes the mean values of friction coefficients measured between the plastic skid and different deck materials. The friction coefficients measured with the aluminum deck clearly reveal the significant influence of vertical load, which is attributed to the relative flexibility of the plastic skid and the aluminum floor. The high values of  $\mu_o$  and  $\mu_s$  measured with X-groove aluminum are most likely due to penetration of aluminum deck into the plastic skid. The friction coefficients tend to decrease when the load is increased from L to M. A further increase in the normal load yields increase in the coefficients measured with X-groove aluminum, which may be attributed to increased interpenetration. The influence of normal load on the friction coefficients measured between the smooth hardwood and plastic skid, however, is considerable small due to more uniform contact.

A comparison with the values reported by MTO [7] reveals very good correlation for the hardwood deck surface. The coefficients associated with aluminum deck surface, however, differ. While the large difference in the  $\mu_o$  values are most likely attributed to the sampling rate, the differences in the sliding values are relatively small.

**Table 4.3: Influence of normal load on the friction coefficients between plastic skid and different deck materials.**

Deck Material	Aluminum X-Grooves	Aluminum Y-Grooves	Hardwood Smooth	Aluminum X-Grooves	Aluminum Y-Grooves	Hardwood Smooth
Load (kN)	Breakaway Friction Coefficient			Sliding Friction Coefficient		
1.989	0.363	0.346	0.225	0.255	0.210	0.150
11.164	0.273	0.235	0.170	0.234	0.210	0.135
20.054	0.310	0.217	0.178	0.269	0.180	0.142
MEAN	0.315	0.266	0.191	0.253	0.200	0.142

**STEEL PADS:** The mean values of friction coefficients and the significance of normal load are summarized in Table 4.4 It can be seen that the influence of normal load on the sliding friction between steel pads and the coarse hardwood is relatively

insignificant, as observed earlier for the plastic and smooth hardwood interface. The sliding friction coefficients between the steel pads and the grooved aluminum deck, however, are affected by the normal load, although the influence is not as pronounced. This variation can be attributed to varying localized deformation of the deck encountered in the vicinity of the steel pads under varying loads. Errors as high as 15% are obtained when the influence of normal load is neglected in the case of grooved aluminum deck. The friction coefficients obtained with coarse hardwood ( $\mu_o=.574$ ,  $\mu_s=.509$ ) were observed to be considerably higher when compared to those reported by MTO ( $\mu_o=0.26$ ,  $\mu_s=0.193$ ). These differences are most likely attributed to the factors discussed earlier.

**Table 4.4 Influence of normal load on the friction coefficients between steel pads and different deck materials.**

Deck Material	Aluminum X-Grooves	Aluminum Y-Grooves	Hardwood Coarse	Aluminum X-Grooves	Aluminum Y-Grooves	Hardwood Coarse
Load (kN)	Breakaway Friction Coefficient			Sliding Friction Coefficient		
1.933	0.370	0.652	0.569	0.274	0.470	0.490
11.108	0.372	0.434	0.576	0.327	0.400	0.518
29.997	0.405	0.502	0.576	0.362	0.452	0.518
MEAN	0.382	0.529	0.574	0.321	0.441	0.509

**MACHINE FEET:** The friction measurements were performed with only coarse hardwood deck surface, which revealed considerable variations in the coefficient of friction with the normal load. During experiments, under light loads, the machine feet revealed poor leveling of the surfaces of different feet, which resulted in considerable stick-slip behaviour and thus considerably high friction, as shown in Table 4.1. The addition of load, however, resulted in improved levelling of the machine feet, and relatively less significance of the normal load. The consideration of mean values of



friction coefficients ( $\mu_o=0.687$ ,  $\mu_s=0.556$ ), derived upon rejecting the values obtained for light load and neglecting the variations in the normal loads, yields only 17% and 6% errors, respectively in  $\mu_o$  and  $\mu_s$ .

**SPRUCE**: The friction measurements were performed with only coarse hardwood deck surface, which revealed relatively less significance of the normal load, as shown in Table 4.1. The mean values, obtained upon neglecting the influence of normal load, reveal maximum errors below 4% and 5%, respectively, in  $\mu_o$  and  $\mu_s$ . The measured values are observed to be considerably larger than those reported in [7], due to the factors described earlier.

**PAPER**: The measured friction between paper and smooth hardwood surface revealed most distinct breakaway friction forces. While the breakaway friction force was observed to be strongly dependent upon the normal load, the influence of normal load on the sliding friction coefficients was relatively insignificant, as illustrated in Table 4.1. The sliding friction coefficient can thus be adequately represented by its mean value ( $\mu_s=0.388$ ), while the breakaway friction tends to decrease considerably with increase in the load.

**RUBBER**: The breakaway and sliding friction forces measured between rubber and smooth hardwood revealed insignificant influence of variations in the normal load. The variations in the normal load considered in this study resulted in peak variations in the breakaway and sliding friction coefficients well below 6% and 5%, respectively. The measured values also correlated very well with those reported by MTO [7].

**SMOOTH STEEL**: The breakaway friction coefficients measured between smooth steel and smooth hardwood tend to decrease with increase in the normal load, as illustrated in Table 4.1. The breakaway friction coefficient with light load is considerably high

most likely due to poor levelling of the deck and thus the poor contact between the mating surfaces. The sliding friction coefficients, however, do not vary significantly with variations in the normal load. Upon neglecting the measurements indicated by an asteriks in Table 4.1, the mean values of breakaway and sliding friction coefficients are obtained as:  $\mu_o=0.569$  and  $\mu_s=0.468$ . The consideration of these mean values can yield respective errors of 12% and 2% with variations in the load considered in this study. A comparison with the values reported by MTO [7] revealed good correlation of the breakaway and sliding friction coefficients.

From the above discussions, it is apparent that the friction coefficients are strongly influenced by many factors. The differences between the reported values necessitate the development of standardized test and reporting guidelines. The role of normal load and flexibility of the skid materials merit further considerations in formulating the load security guidelines. While the normal load factor can be conveniently eliminated when hardwood deck structures are used, the variations in normal load form an important consideration with deck structures likely to experience local deformation of asperities. In the latter case, it is perhaps more appropriate to consider the lowest values of friction measured in the weight range of interest. Furthermore, the breakaway friction is strongly dependent upon the contact area and levelling of the mating surfaces. Since the levelling of the skid cannot be ensured in the realistic freight transportation environment, the load security guidelines should be based upon the sliding friction coefficients only.

#### **4.2 FRICTION FORCES UNDER SINUSOIDAL VERTICAL VIBRATION**

The friction forces between the selected skid and deck materials were measured under sinusoidal vibration of varying magnitudes at different discrete frequencies, as

illustrated in Table 3.1. The measured friction forces and acceleration signals were analyzed to derive the following:

- The maximum, minimum and mean values of friction forces between the selected materials as a function of magnitude and frequency of vertical vibration.
- The influence of magnitude of vibration on the maximum and minimum friction force.
- The influence of frequency of vibration on the maximum and minimum friction force.

Figures 4.4 to 4.7 present the measured friction forces and vertical acceleration excitation for selected surfaces. The measurements reveal considerable oscillations in the friction force, which are mostly attributed to stick-slip phenomenon occurring during each cycle of vibration. The friction forces in most cases were observed to be in-phase with the vertical acceleration of the deck frame. The peak force occurs when the acceleration approaches its peak value, while the friction force approaches its lowest value corresponding to minimum instantaneous acceleration. The measurements involving flexible skid materials, however, resulted in phase difference between the friction force and the deck material, which is attributed to the dynamics associated with the flexible skid material. The occurrence of stick-slip also resulted in the phase difference between the force and acceleration. While the breakaway friction forces were observed to be quite apparent in some of the measurements, other measurements did not reveal distinct breakaway. Most experiments, however, revealed breakaway corresponding to lowest instantaneous vertical acceleration, as shown in Figure 4.4. The measurements performed with the same surfaces, however, did not reveal distinct breakaway friction, as shown in Figure 4.5 during every cycle, due to low level vertical acceleration. The measurements performed under high frequency vibration revealed highly inconsistent breakaway friction. The measured data presented in Figures 4.4 to

Deck: Smooth Hardwood      Normal Load: 1989 N      Skid: Plastic Skid

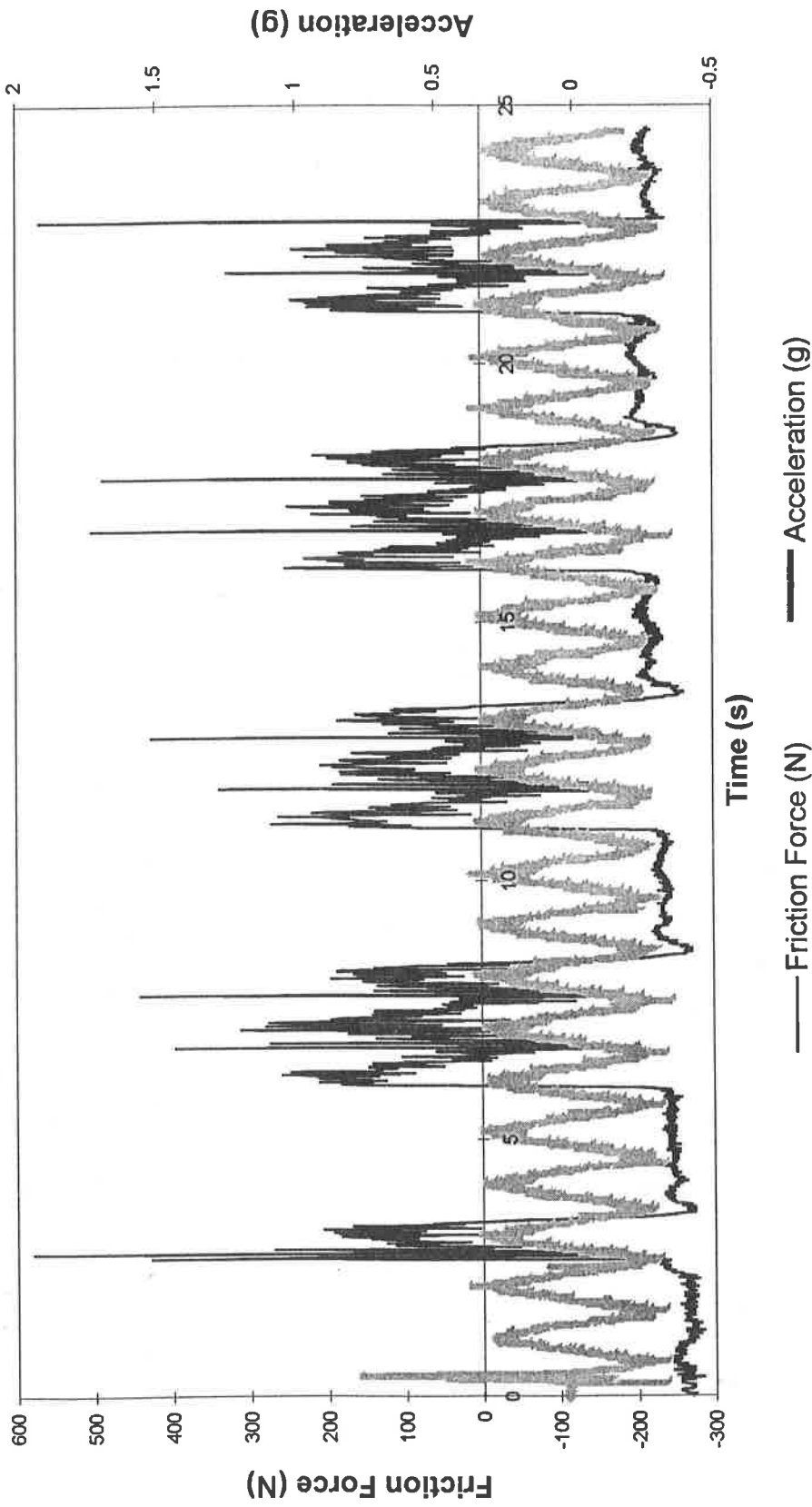


**Figure 4.4: Time history of vertical acceleration and measured friction force  
(Frequency: 1.0 Hz ; Acceleration: 0.25g peak)**

Deck: Smooth Hardwood      Normal Load: 1989 N      Skid: Plastic Skid

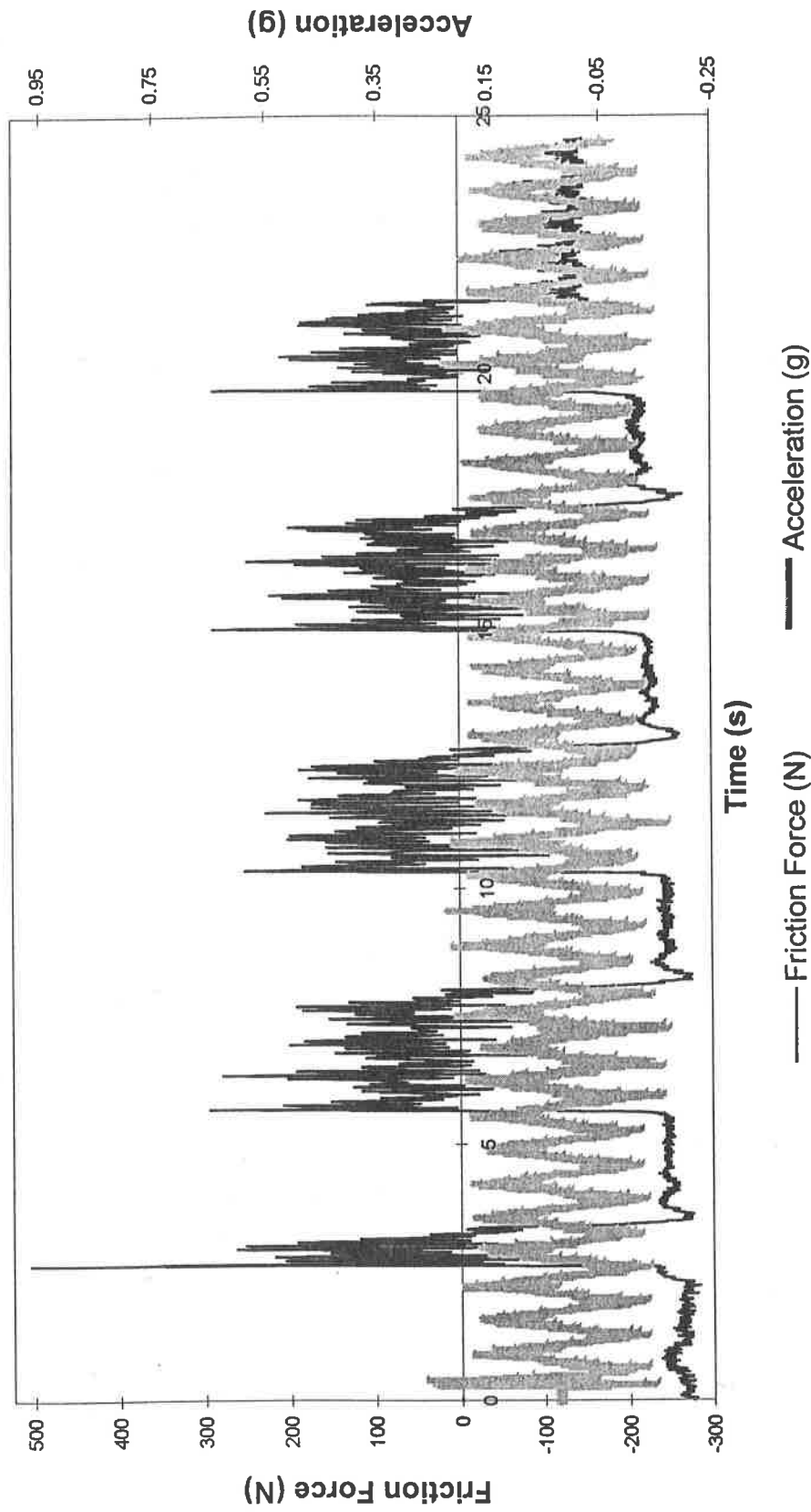


Figure 4.5: Time history of vertical acceleration and measured friction force  
(Frequency: 1.5 Hz ; Acceleration: 0.1g peak)

Deck: Coarse Hardwood      Normal Load: 20003 N      Skid: Spruce Board

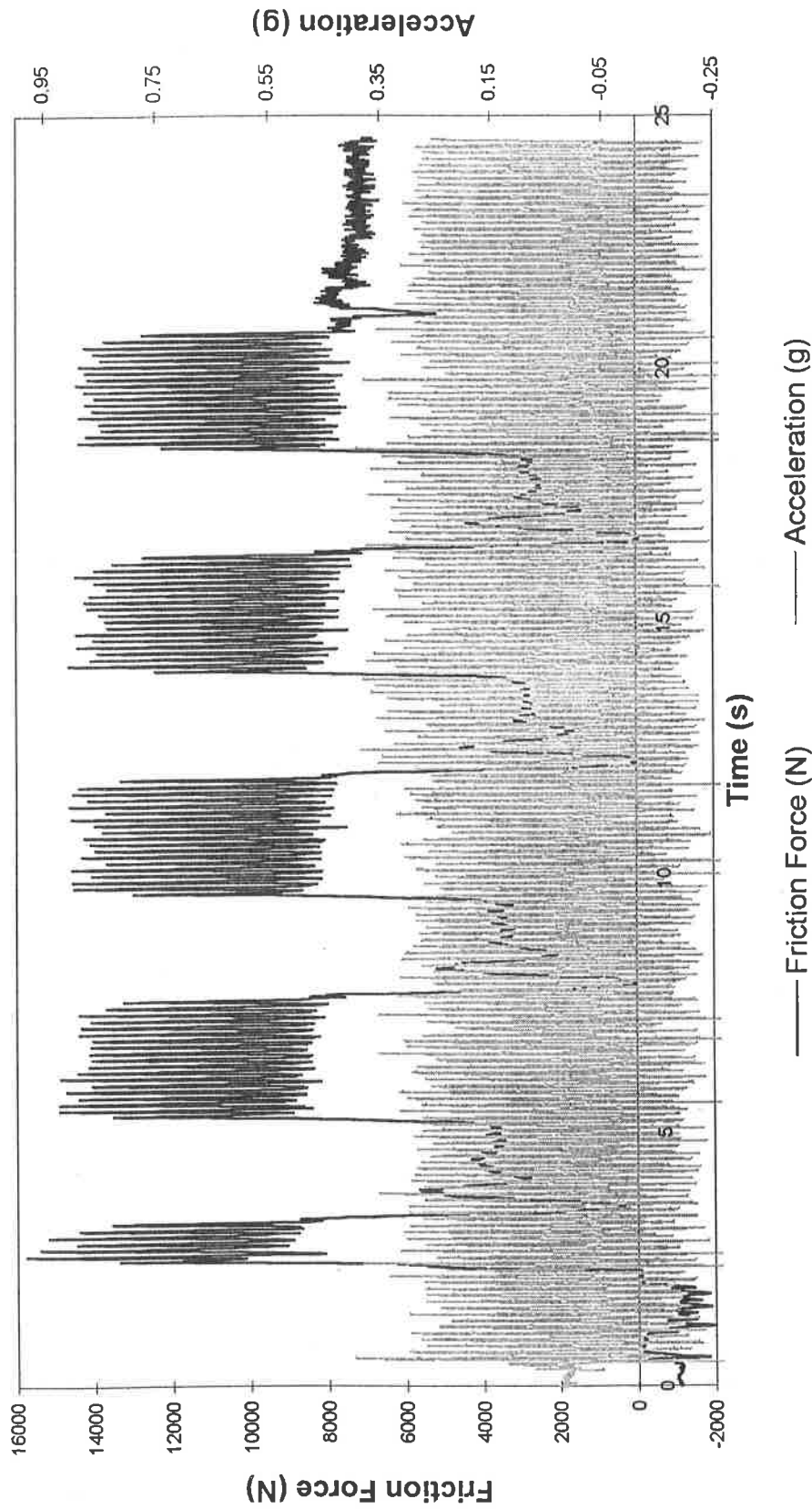
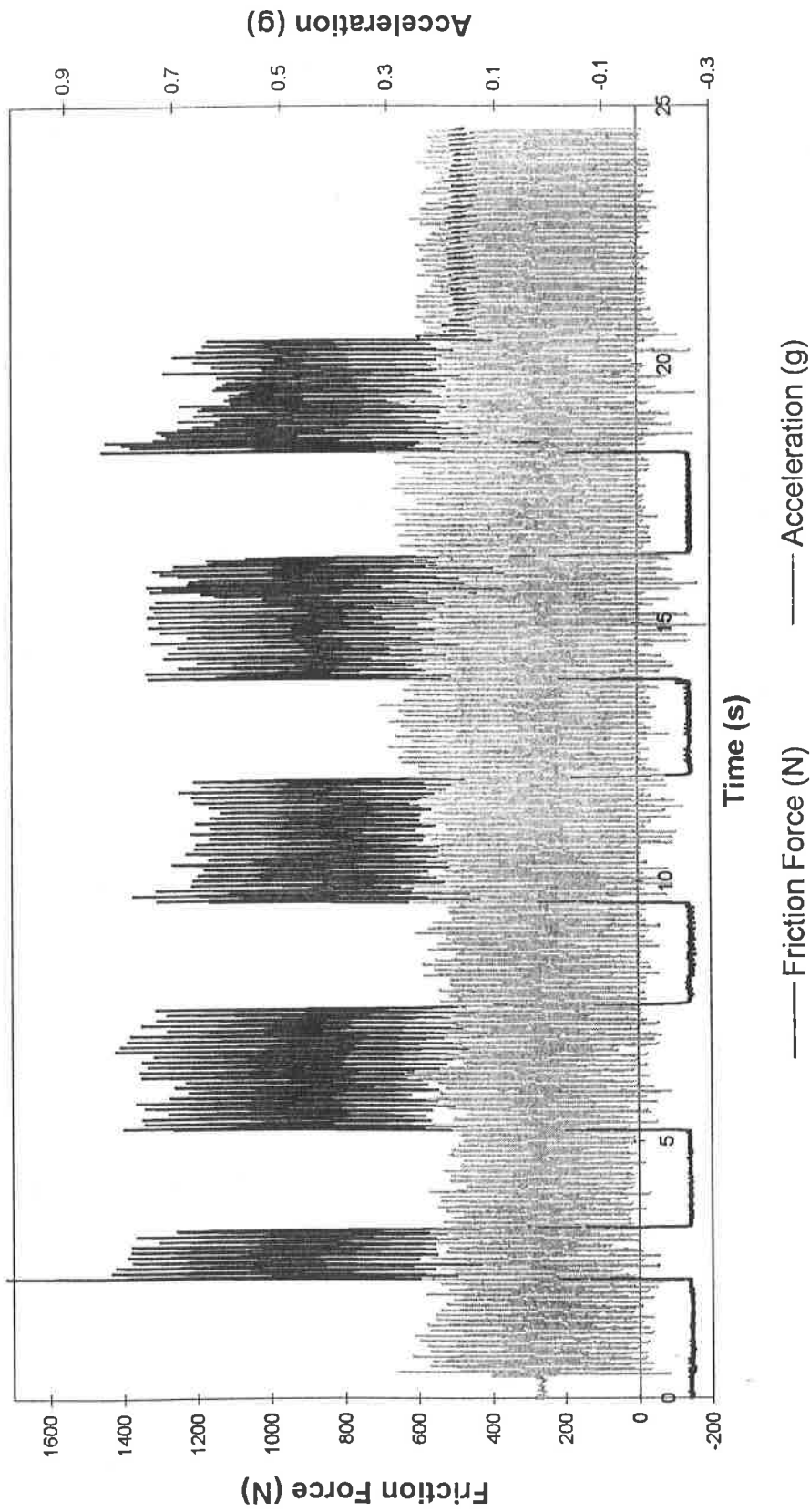


Figure 4.6: Time history of vertical acceleration and measured friction force  
(Frequency: 8.0 Hz ; Acceleration: 0.25g peak)

Deck: Coarse Hardwood

Normal Load: 1938 N

Skid: Spruce Board



**Figure 4.7: Time history of vertical acceleration and measured friction force  
(Frequency: 10.0 Hz ; Acceleration: 0.25g peak)**

4.7, however, reveal repeatability and trends, when oscillatory sliding friction alone is considered. In view of the inconsistent patterns in breakaway friction, no attempts are made to identify the breakaway friction forces. Furthermore, in the context of load security under vertical vibration, it is most appropriate to formulate the guidelines based upon sliding friction alone. The breakaway friction forces under vertical vibration, apart from the factors discussed under static conditions, are strongly dependent upon the frequency of vibration, dynamics of the mating surfaces, degree of contact or adhesion, and magnitude of vibration. Furthermore, the magnitude of friction force is related to not only the vibration excitation but also the vibration response of the skid and the load. Although the measurement of vibration response of the skid was beyond the scope of this study, amplified vibration of the load were observed at certain excitation frequencies.

The friction force and acceleration signals acquired under vertical vibration at different discrete frequencies were filtered to eliminate the high frequency components arising from the coupled dynamics of the sled and the deck, and the frequent stick-slip motion. The filtered data was then analyzed to determine the mean, maximum and minimum values of sliding friction coefficients ( $\mu_v = F/mg$ ), as a function of the mating surfaces, magnitude of vertical vibration and frequency of vibration.

#### **4.2.1 Discussion of Results (Sinusoidal Vibration)**

The sliding friction forces measured between different skid and deck materials are presented in terms of mean, maximum and minimum coefficients of friction ( $\mu_v$ ). The measurements obtained from three different trials (pull # 2, 3 and 4) are averaged and presented as a function of the magnitude and frequency of vibration. The results, presented in Figures 4.8 to 4.58, illustrate the coefficients of friction measured under vertical sinusoidal vibration for different mating surfaces. Although the measurements



were performed under excitations up to 12 Hz, for acceleration levels of 0.25 g and 0.5 g, the results are presented only in the 0-10 Hz range due to only insignificant variations in  $\mu_v$  at higher frequencies. For low level vertical acceleration (0.1g), the tests were performed only up to 4Hz due to extremely low displacement at higher frequencies. The results are discussed below for each deck surface.

#### 4.2.1.1 COARSE HARDWOOD DECK

Figures 4.8 to 4.10 illustrate the mean, maximum and minimum values of coefficient of friction measured between spruce and coarse hardwood deck. The results clearly illustrate the symmetry between the maximum and minimum values of  $\mu_v$ , irrespective of the magnitude and frequency of excitation, and the variations in the load. The mean values of coefficient of friction is observed to be quite close to the coefficient of friction measured under static conditions, irrespective of the excitation frequency and magnitude. The maximum and minimum values of  $\mu_v$ , however, are strongly dependent upon the magnitude of acceleration and the normal load. The results, presented in Figures 4.8 to 4.10, exhibit considerable variations in the friction coefficients under vertical vibration. The maximum and minimum values of  $\mu_v$  tend to differ considerably from the respective  $\mu_s$  values. While the maximum and minimum values tend to be considerable higher and lower, respectively, with the excitation frequency in the low frequency range, the values remain relatively constant at frequencies above 4 Hz. While the application of vertical vibration yields oscillatory friction forces of magnitudes, which may be either higher or lower than those measured under static conditions, the lowest values of  $\mu_v$  need to be emphasized in the context of load security. The minimum values of  $\mu_v$  measured under light load and 0.1g acceleration are observed to be 9% lower than  $\mu_s$  (measured under static conditions). The minimum values of  $\mu_v$  tend to decrease significantly under higher loads, 15% and

Deck: Coarse Hardwood

Load: L

Skid: Spruce Board

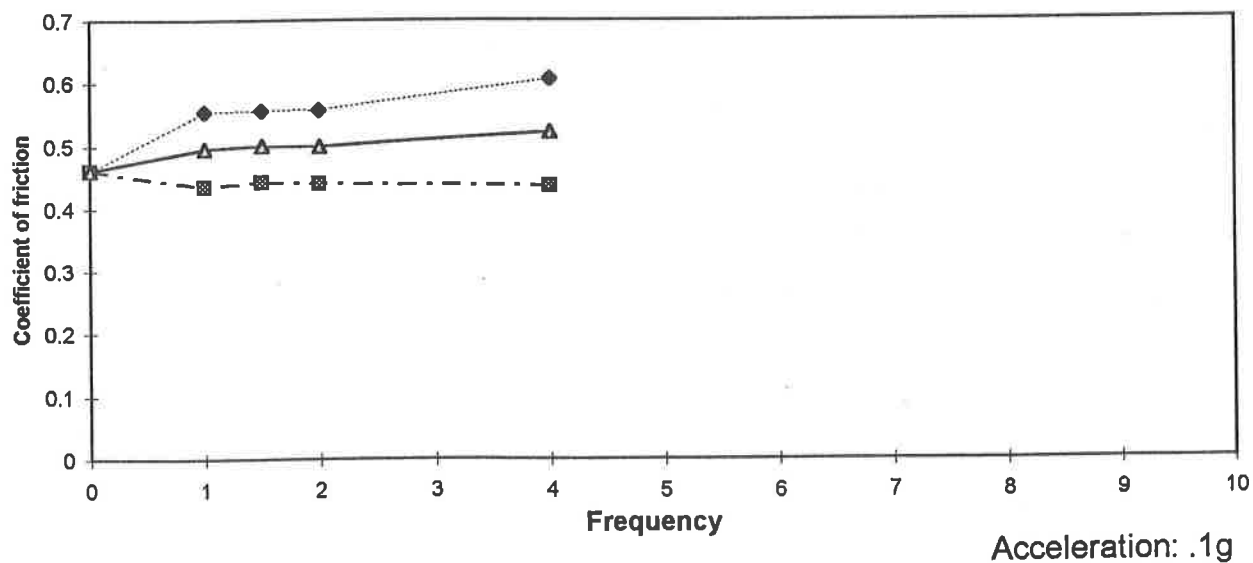
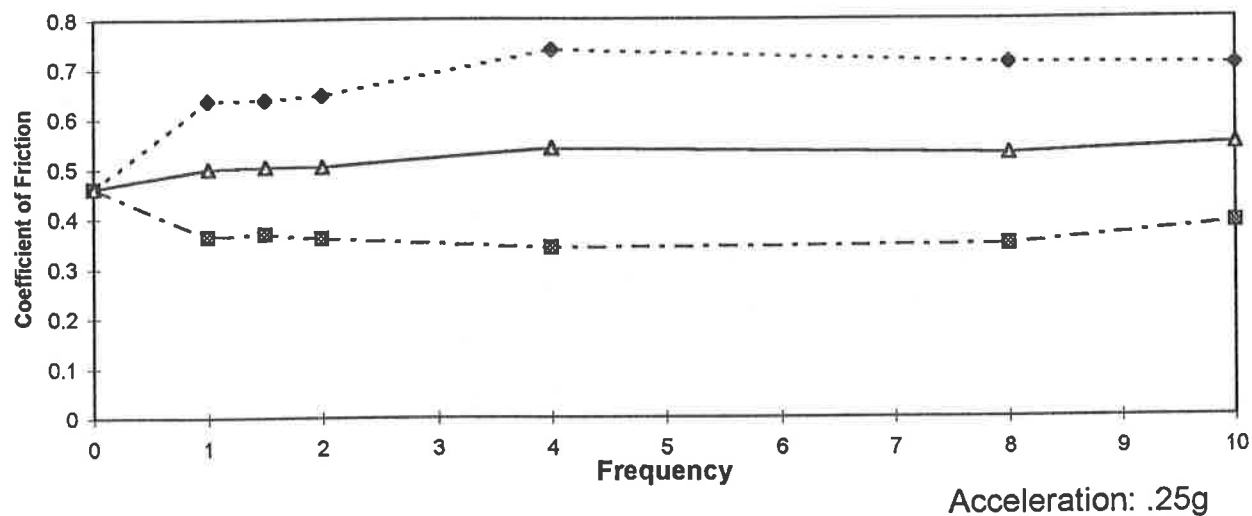
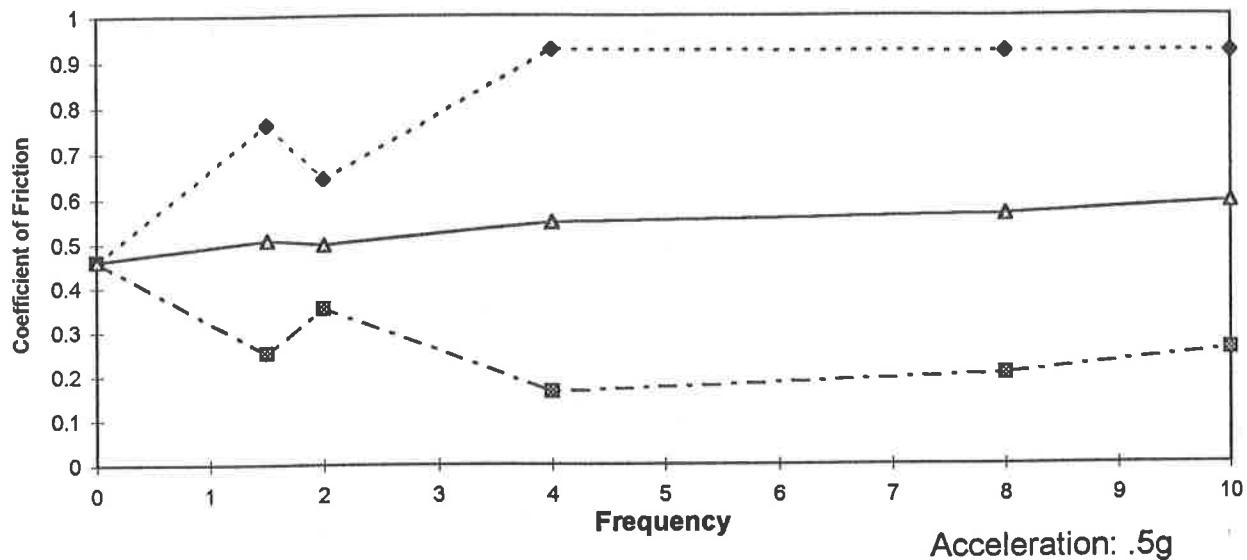


Figure 4.8: Influence of vertical vibration on the coefficient of friction

Deck: Coarse Hardwood      Load: M      Skid: Spruce Board

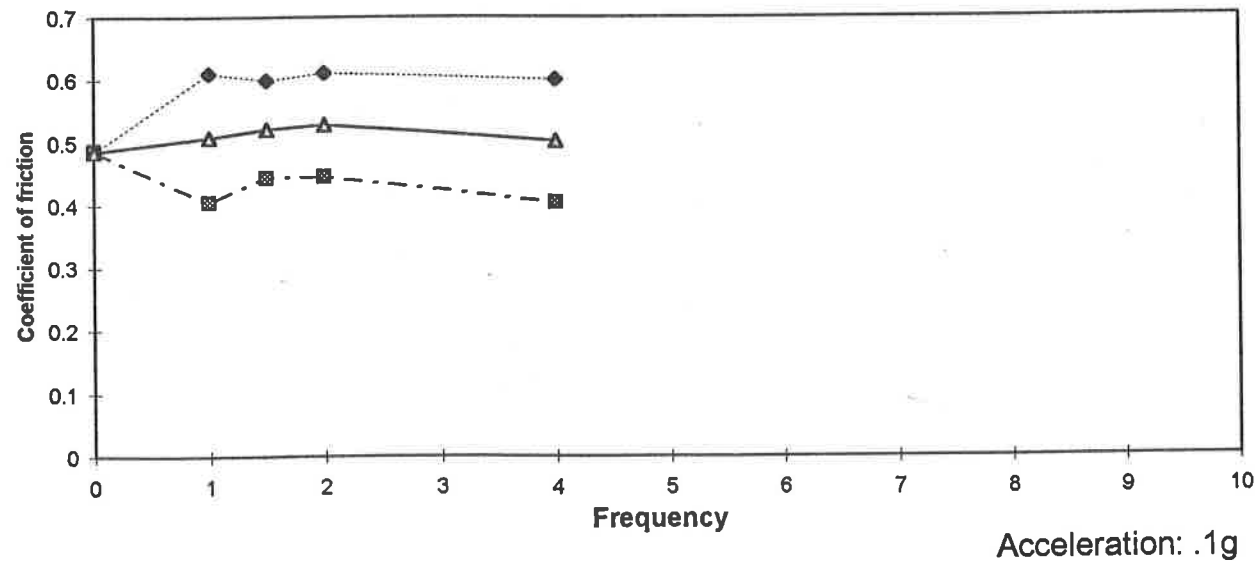
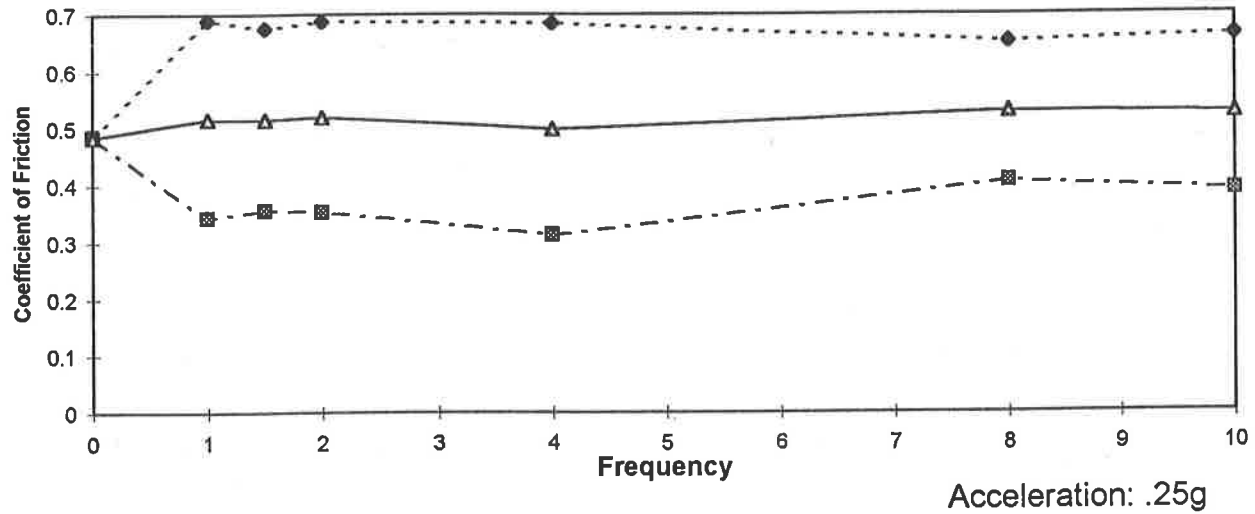
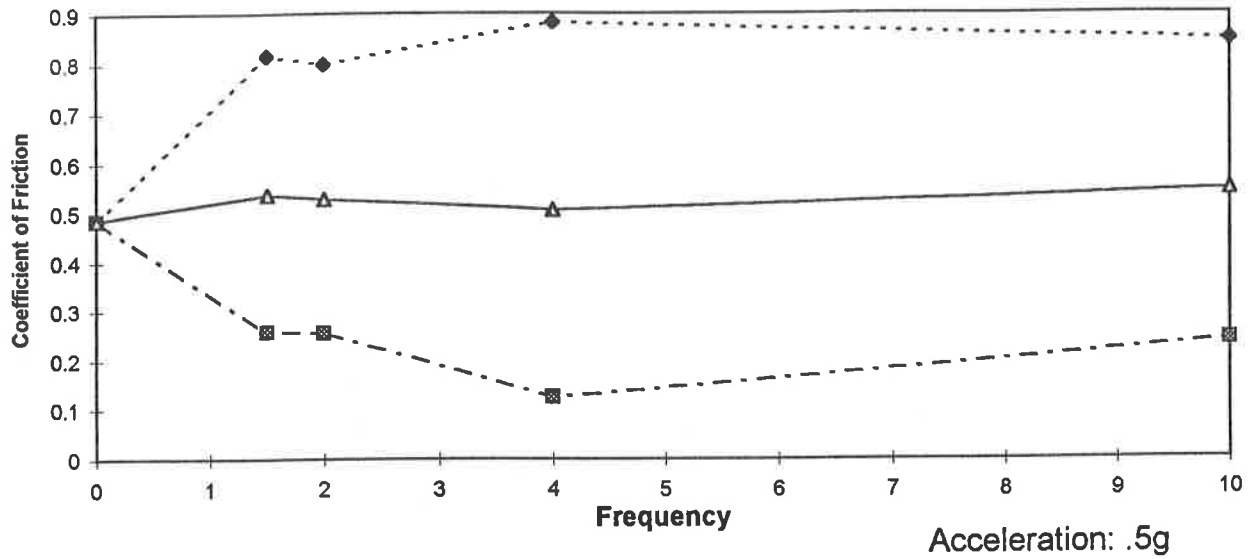


Figure 4.9: Influence of vertical vibration on the coefficient of friction

Deck: Coarse Hardwood

Load: H

Skid: Spruce Board

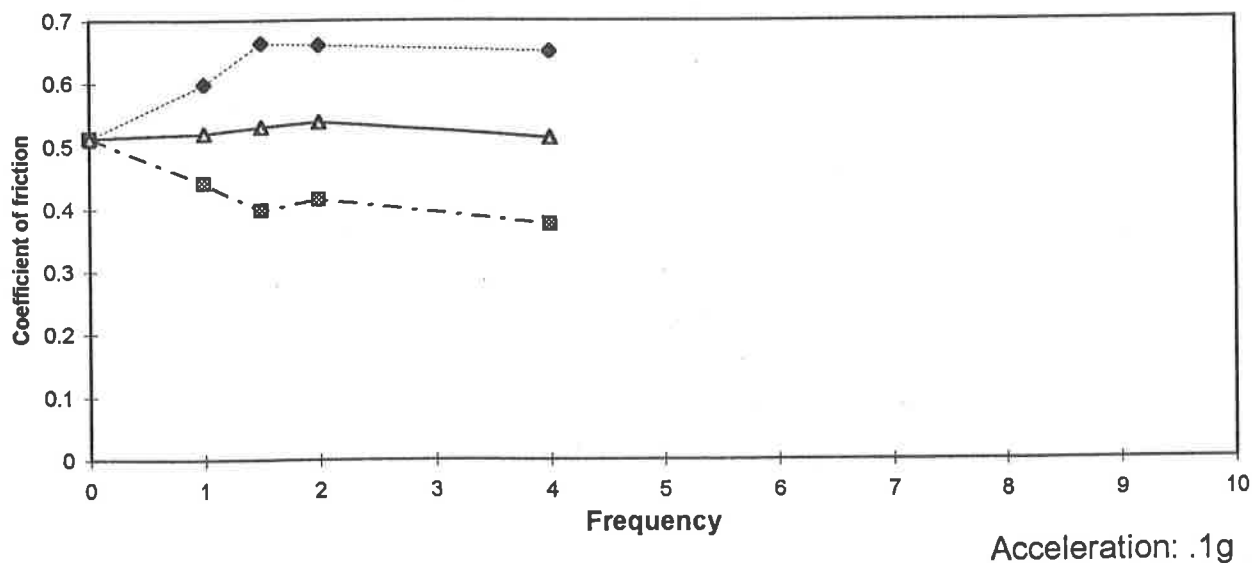
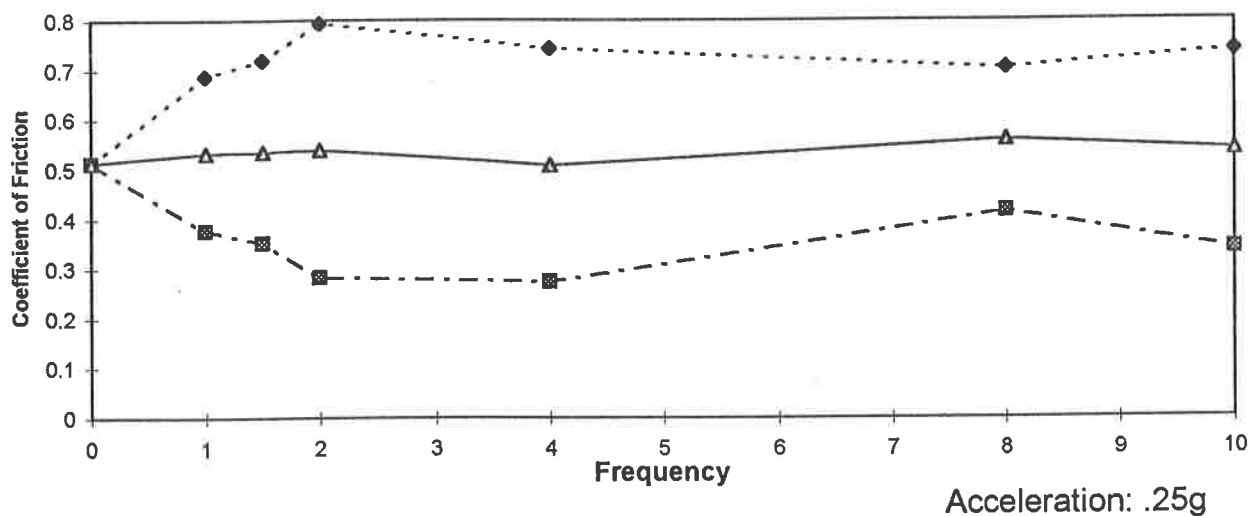
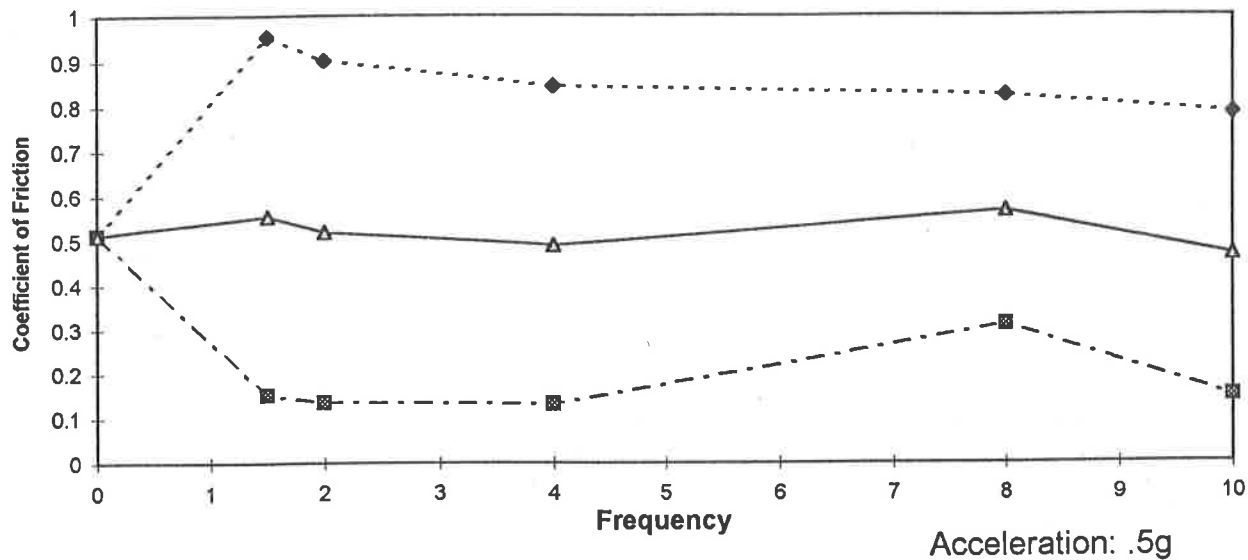


Figure 4.10: Influence of vertical vibration on the coefficient of friction

Deck: Coarse Hardwood

Skid: Spruce Board

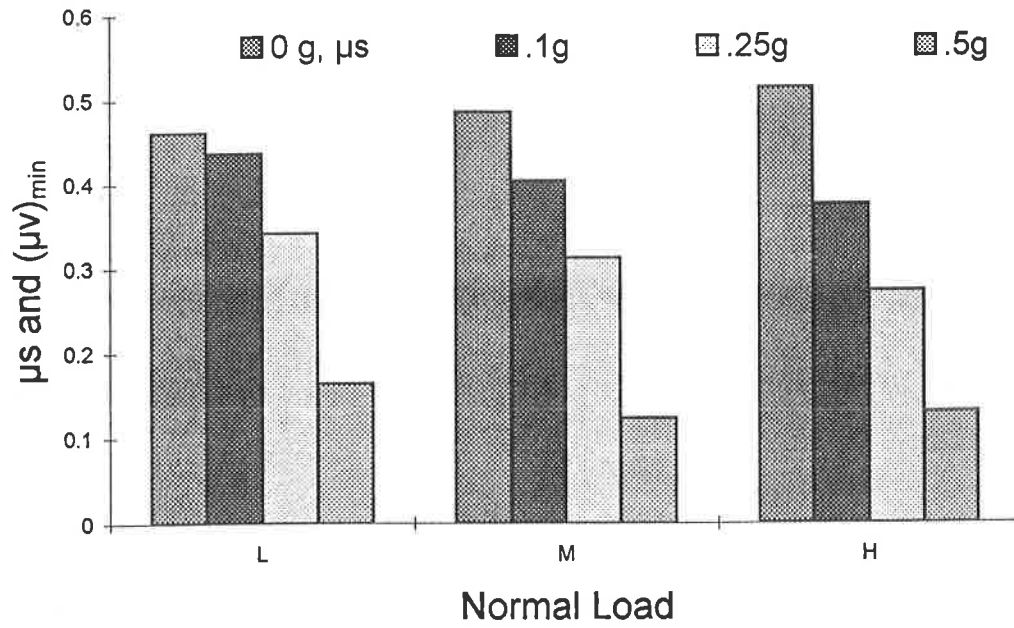


Figure 4.11: Influence of vertical acceleration and normal load on the minimum value of friction coefficient

20%, respectively for medium and high loads. Further reduction in the minimum values with increase in load is attributed to the dynamics associated with increased inertia.

An increase in the magnitude of acceleration of the vertical vibration yields considerable variations between the maximum and minimum values of  $\mu_v$ , as illustrated in the figures. Under low normal load, the minimum value of  $\mu_v$  is almost 60% lower than  $\mu_s$ , when the amplitude of acceleration is increased to 0.5g. The corresponding reduction in the minimum value of  $\mu_v$  under medium and high loads are obtained as 73% and 75%, respectively. Figure 4.11 illustrates the influence of normal load and amplitude of acceleration on the  $\mu_s$  and minimum values of  $\mu_v$ .

Figures 4.12 to 4.14 illustrate the mean, minimum and maximum values of  $\mu_v$  measured between steel pads and coarse hardwood deck, as a function of the normal load, and magnitude and frequency of vertical vibration. Figure 4.15 summarizes the variations in minimum values of  $\mu_v$  as a function of normal load and magnitude of acceleration. The results show trends similar to those described for the spruce skid material. The steel pads with medium and high normal load, however, exhibit peak variation in  $\mu_v$  under vertical excitations near 4 Hz, specifically in the minimum value of  $\mu_v$ . This variation is caused by contact vibration between the mating surfaces, which was observed to be excessive at excitation frequency of 4 Hz. The contact vibrations, mostly occurred when acceleration approached its minimum value or immediately after the vertical displacement approached its maximum value. This effect became more pronounced with increase in the acceleration level, as shown in Figures 4.13 and 4.14. The lowest value of  $\mu_v$  is 21% to 36% lower than the  $\mu_s$  value, depending upon the normal load, under 0.1g vertical acceleration. The minimum values are observed to be 63% to 80% lower, when acceleration level is increased to 0.5g. It should be noted that the mean value of friction coefficient ( $\mu_v$ ) under excitations at certain frequencies

Deck: Coarse Hardwood      Load: L      Skid: Steel Pads

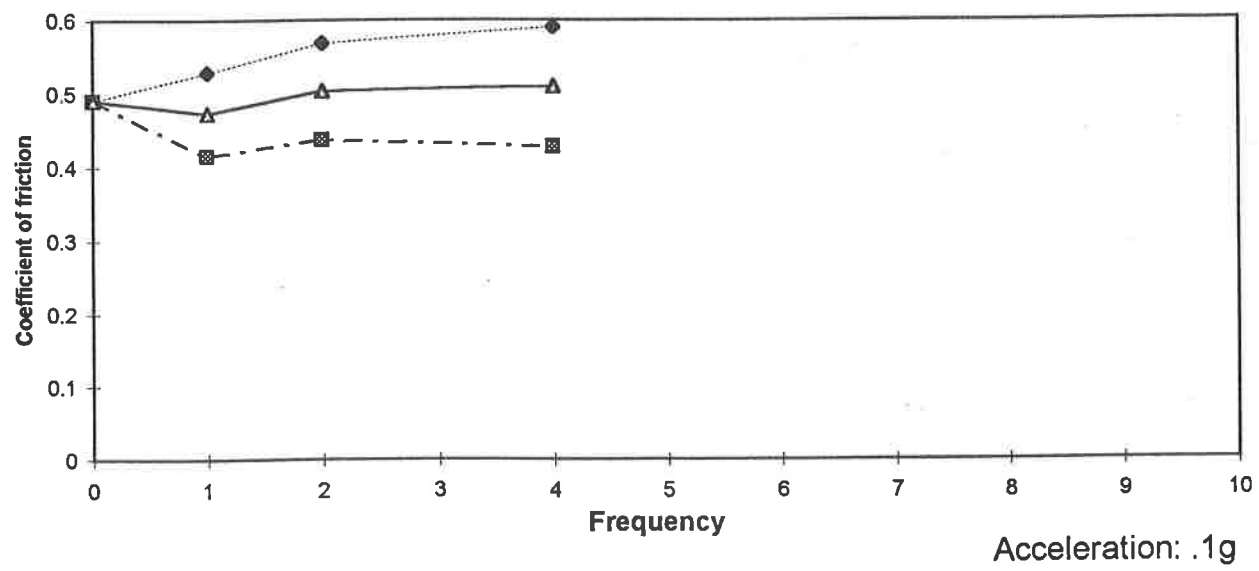
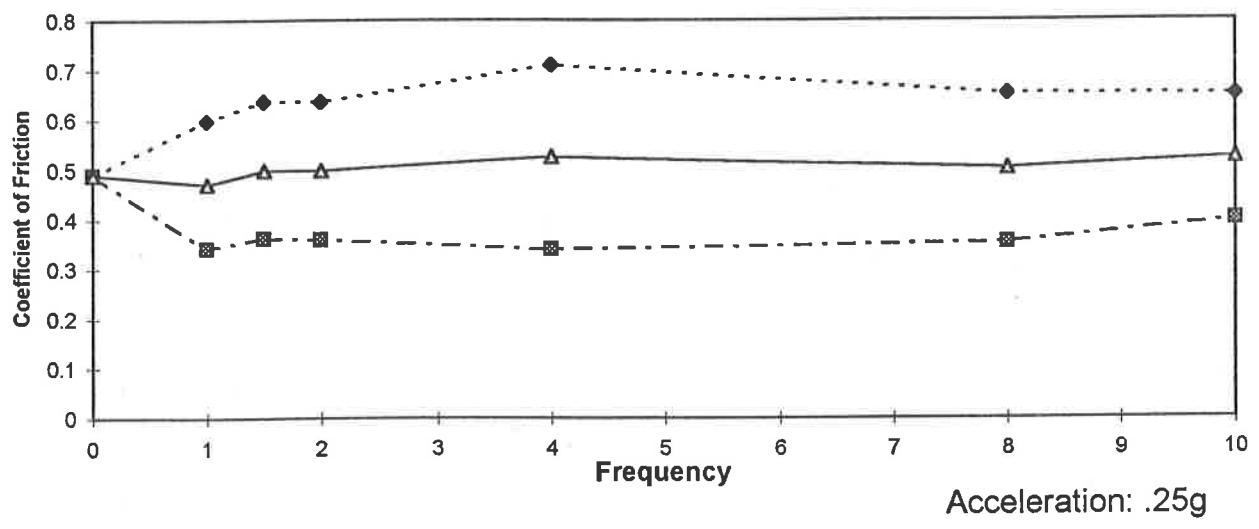
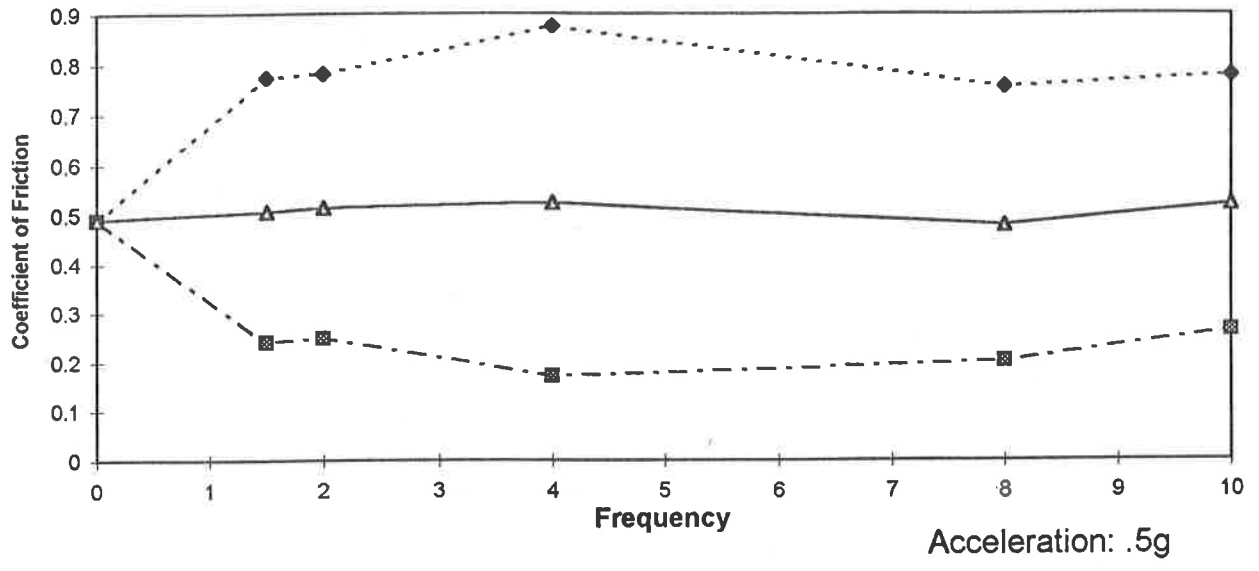


Figure 4.12: Influence of vertical vibration on the coefficient of friction

Deck: Coarse Hardwood

Load: M

Skid: Steel Pads

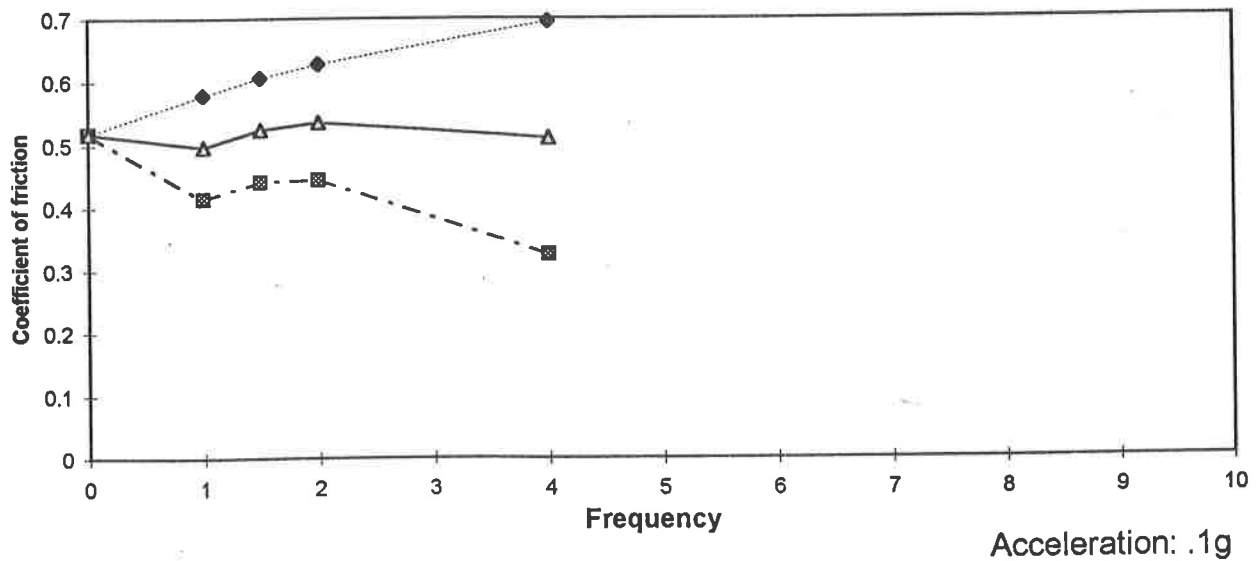
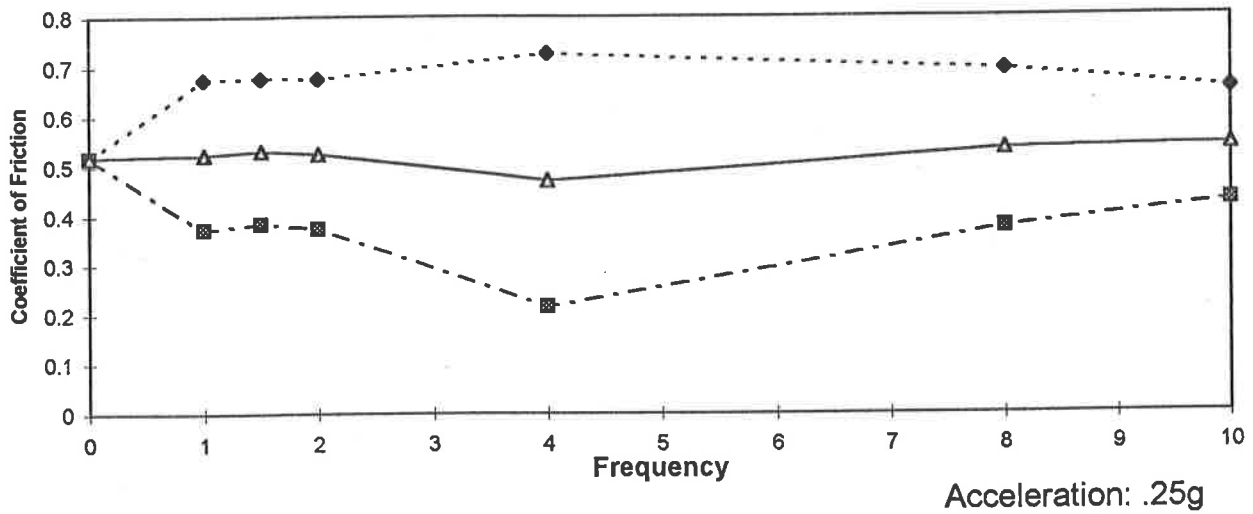
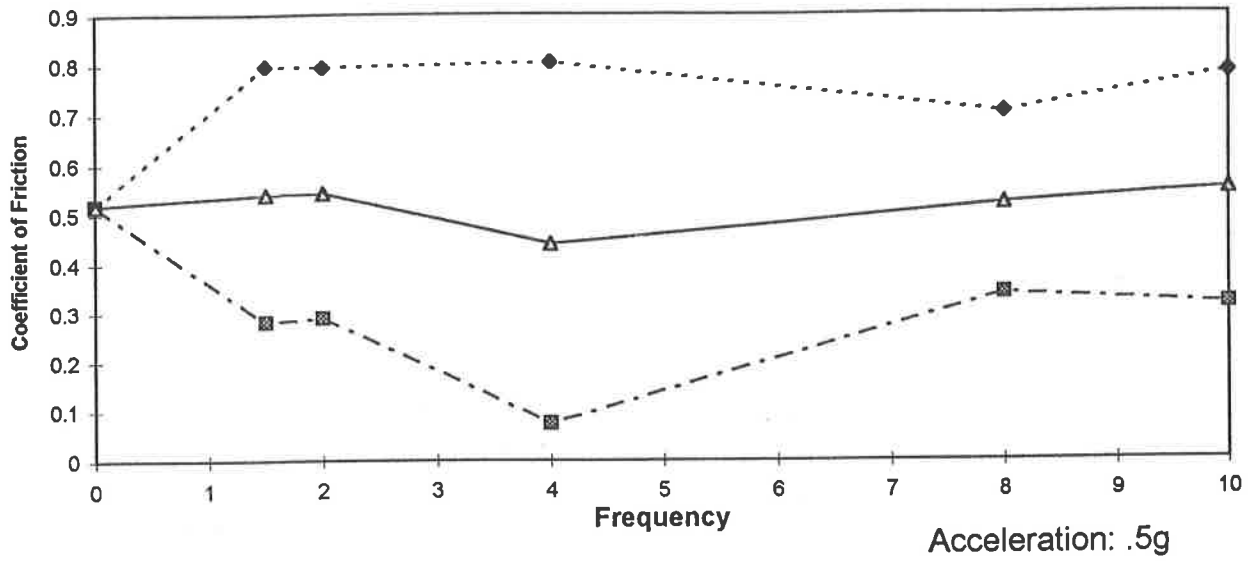


Figure 4.13: Influence of vertical vibration on the coefficient of friction



Deck: Coarse Hardwood

Load: H

Skid: Steel Pads

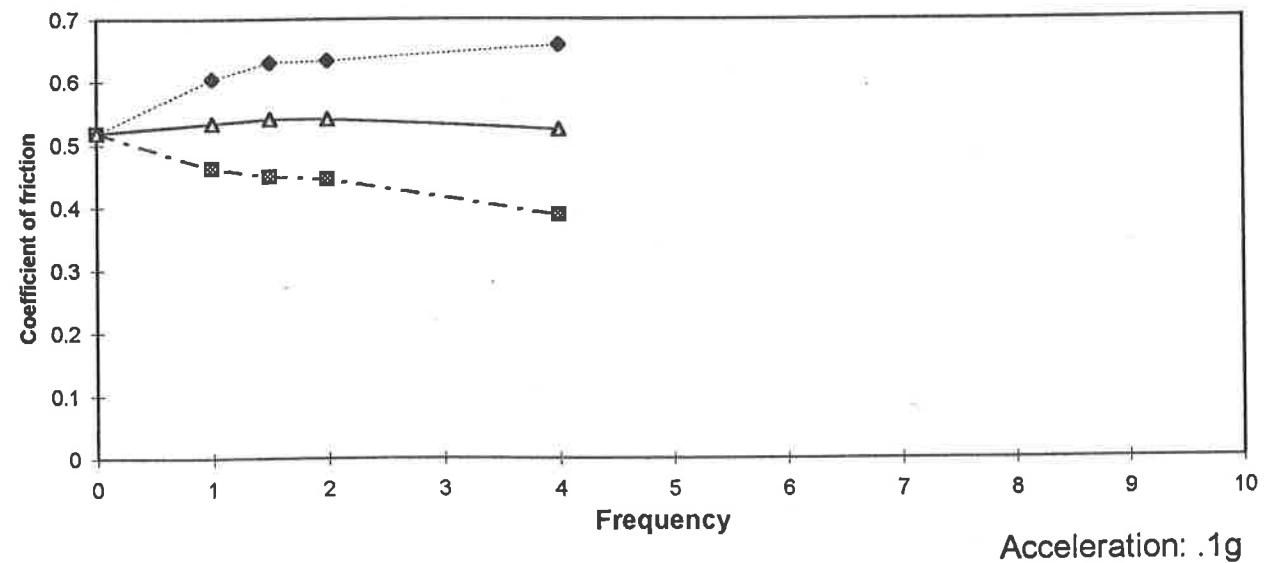
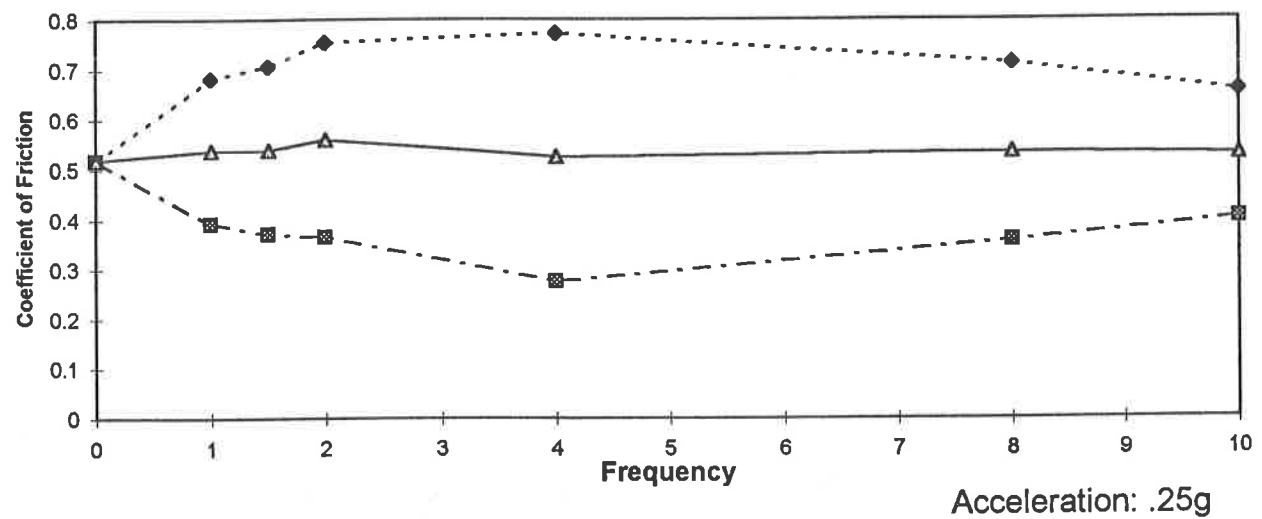
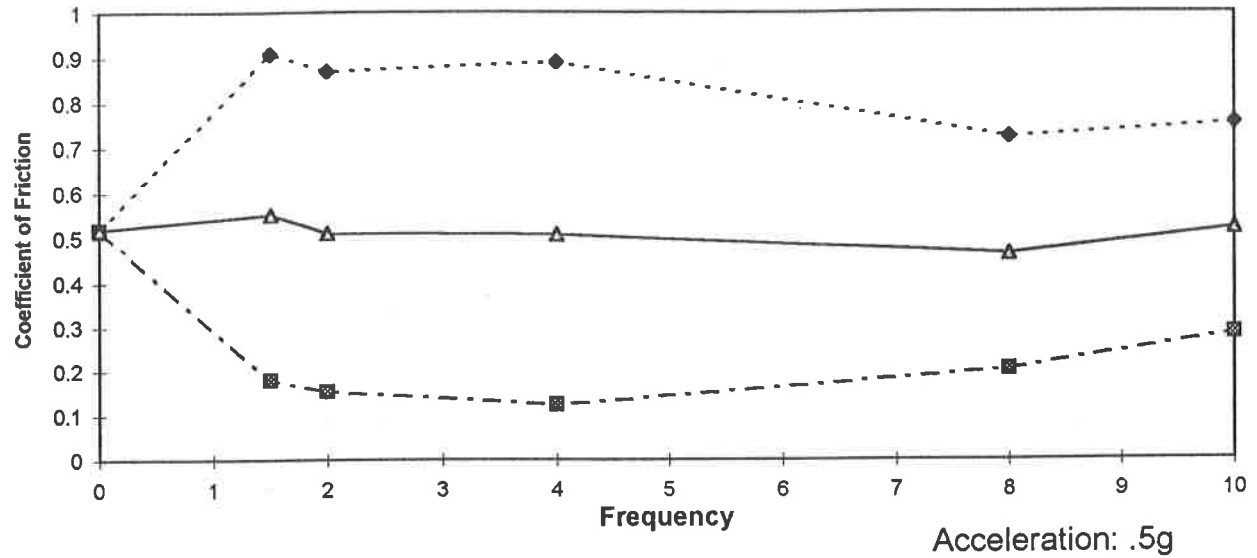


Figure 4.14: Influence of vertical vibration on the coefficient of friction

Deck: Coarse Hardwood

Skid: Steel Pads

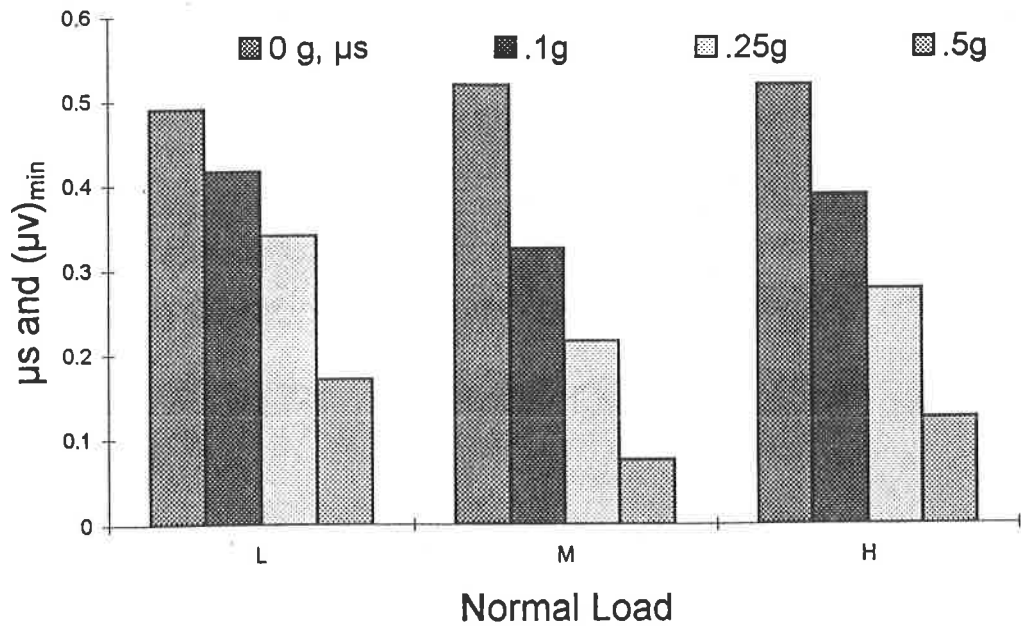


Figure 4.15: Influence of vertical acceleration and normal load on the minimum value of friction coefficient

approaches a value slightly higher than  $\mu_s$ , which is attributed to occurrence of stick-slip motion.

The influence of vertical vibration on the maximum and minimum values of coefficients of friction between the concrete and coarse hardwood is illustrated in Figures 4.16 to 4.18. The results show trends similar to those described above. The results show the existence of minimum values of  $\mu_v$  near 4 Hz, which is most likely caused by the excessive contact vibration at this frequency. The minimum values of  $\mu_v$  are observed to be nearly 16% and 42% lower than the  $\mu_s$  value with medium and high loads subject 0.1g vertical acceleration. The corresponding values of  $\mu_v$  under 0.5g vertical acceleration are nearly 70% lower than the  $\mu_s$  value. The minimum values of  $\mu_v$  decrease considerably with increase in both the vertical load and the magnitude of vertical vibration.

The influence of vertical vibration on the mean, minimum and maximum friction coefficients obtained for machine feet and coarse hardwood deck are presented in Figures 4.19 to 4.21. Figure 4.22 summarizes the influence of normal load and the magnitude of vertical acceleration on the minimum values of  $\mu_v$ . The results clearly illustrate considerable reduction in minimum values of  $\mu_v$  with increase in normal load and level of vibration.

#### 4.2.1.2 Y-GROOVE ALUMINUM DECK

Figures 4.23 to 4.33 present the influence of normal load, and frequency and magnitude of vertical vibration on the mean, maximum and minimum values of  $\mu_v$  measured with concrete, steel pads and plastic skid materials. The results exhibit trends similar to those discussed in section 4.2.1.1. The minimum values of  $\mu_v$  tend to decrease with increase in the vertical load and acceleration magnitude, while the mean

Deck: Coarse Hardwood      Load: M      Skid: Concrete Blocks

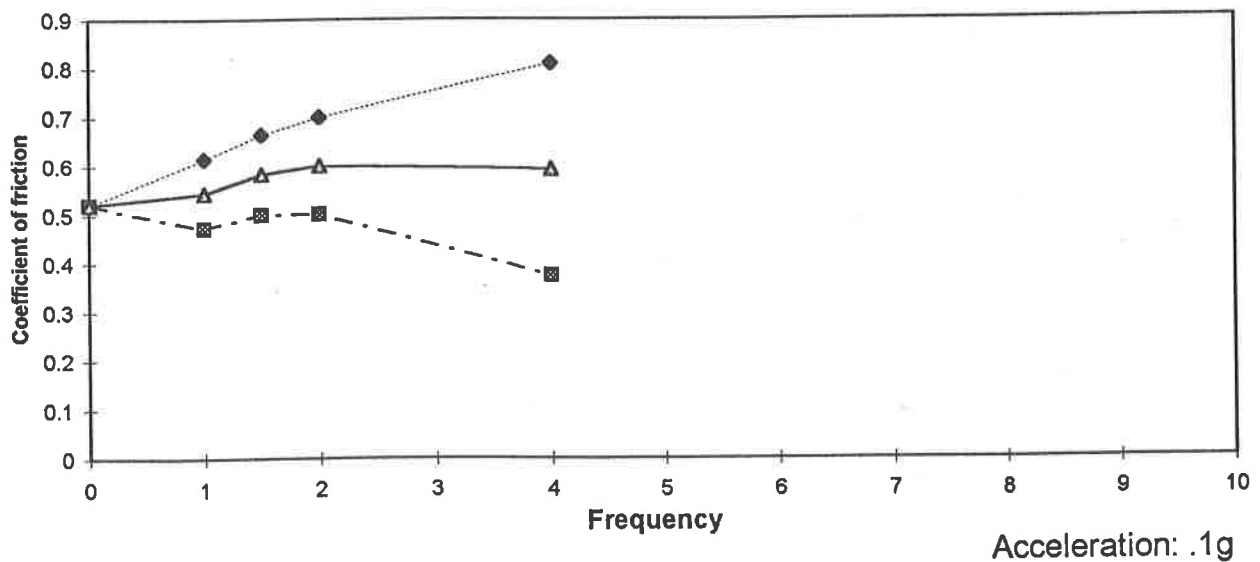
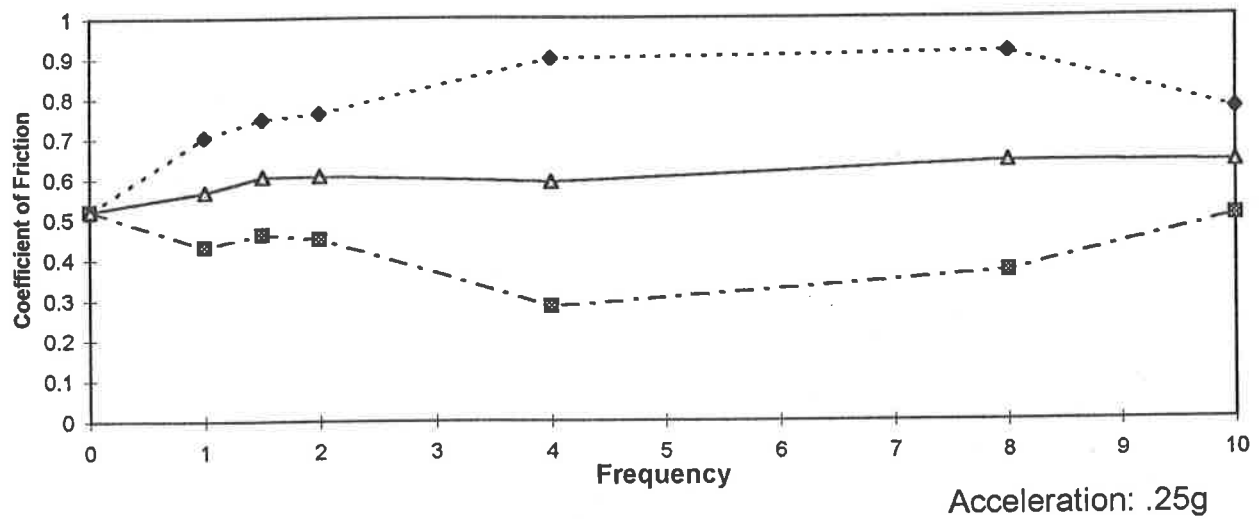
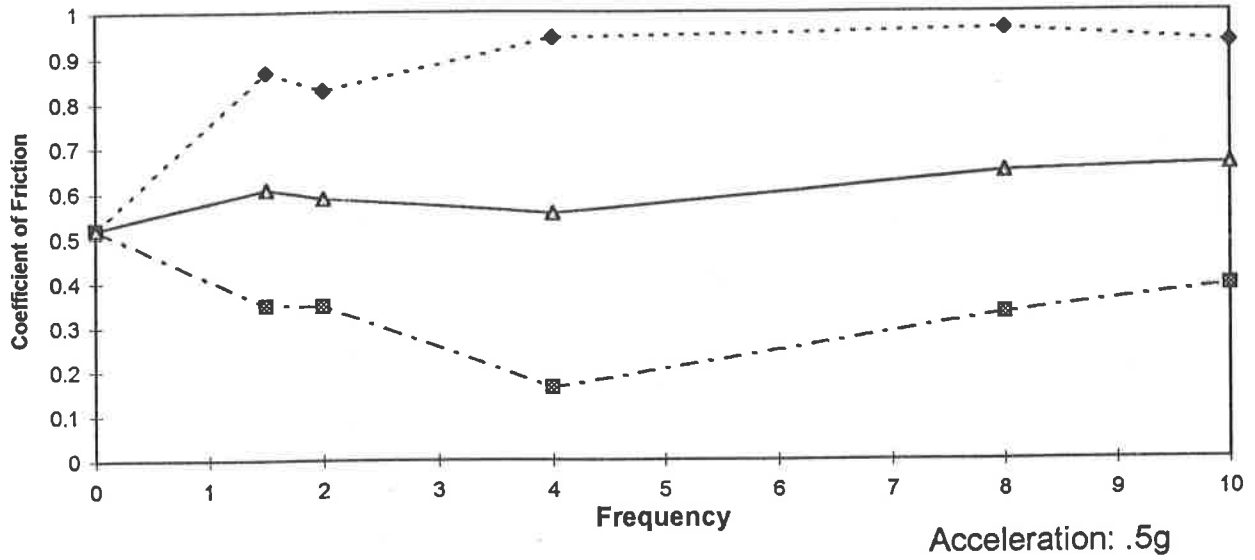


Figure 4.16: Influence of vertical vibration on the coefficient of friction

Deck: Coarse Hardwood      Load: H      Skid: Concrete Blocks

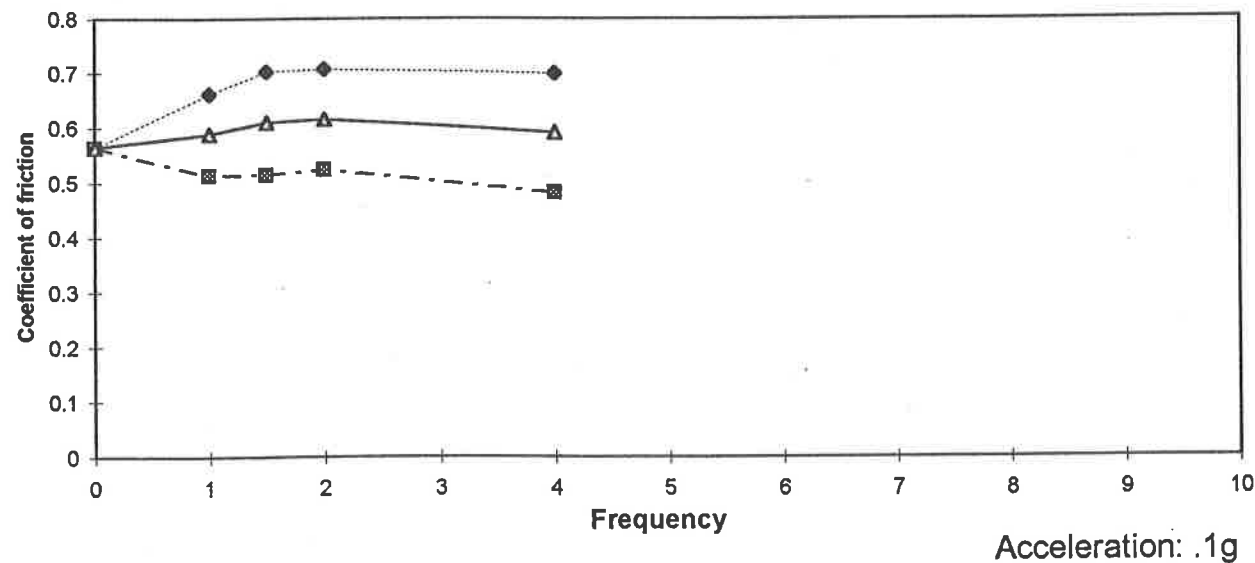
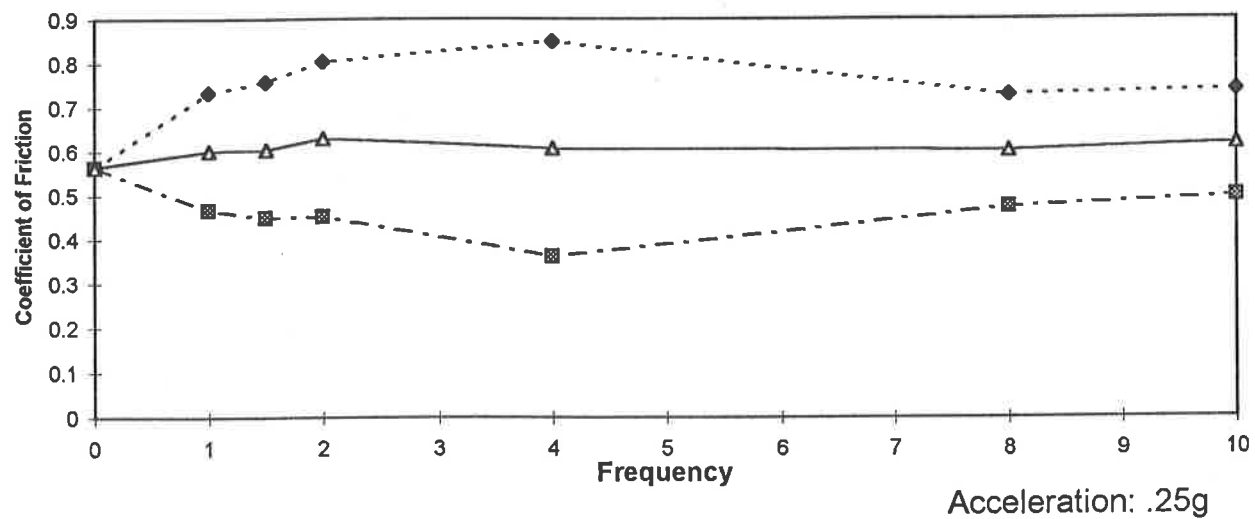
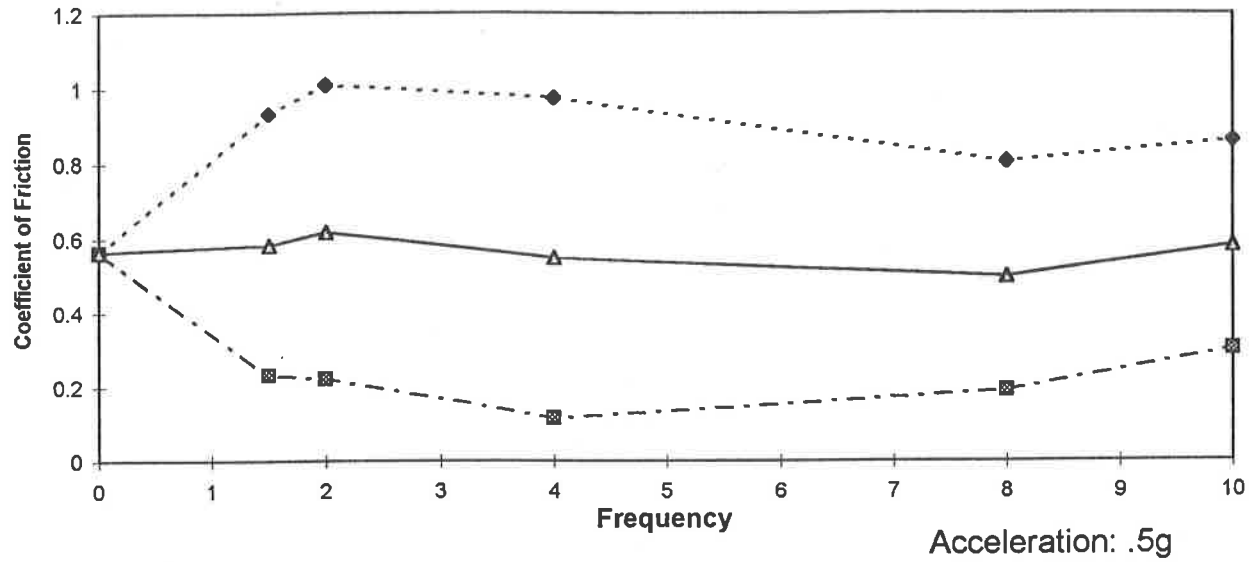


Figure 4.17: Influence of vertical vibration on the coefficient of friction

Deck: Coarse Hardwood

Skid: Concrete Blocks

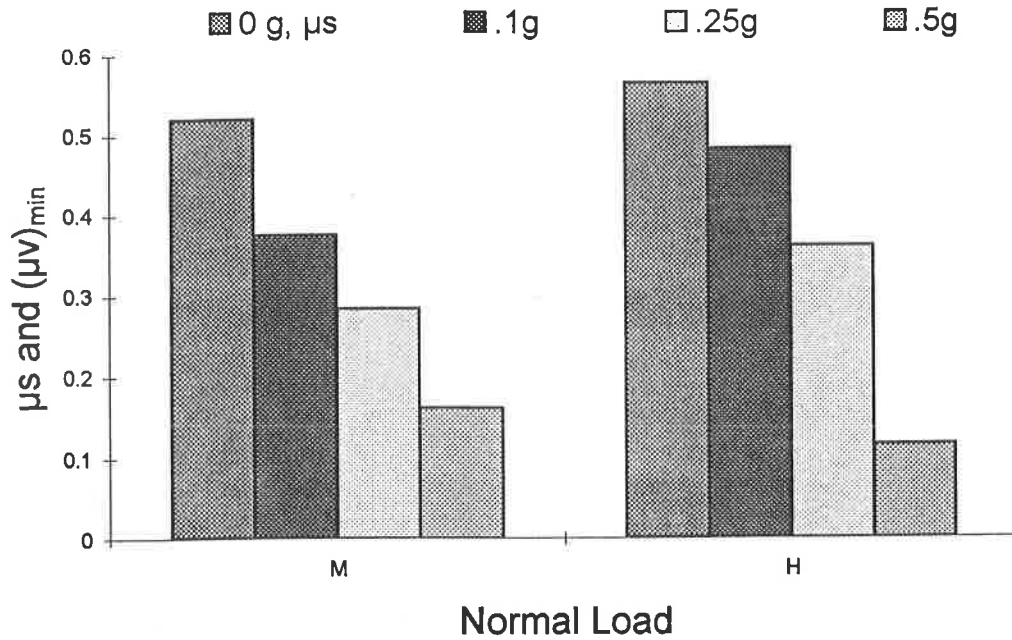


Figure 4.18: Influence of vertical acceleration and normal load on the minimum value of friction coefficient

Deck: Coarse Hardwood

Load: L

Skid: Machine Feet

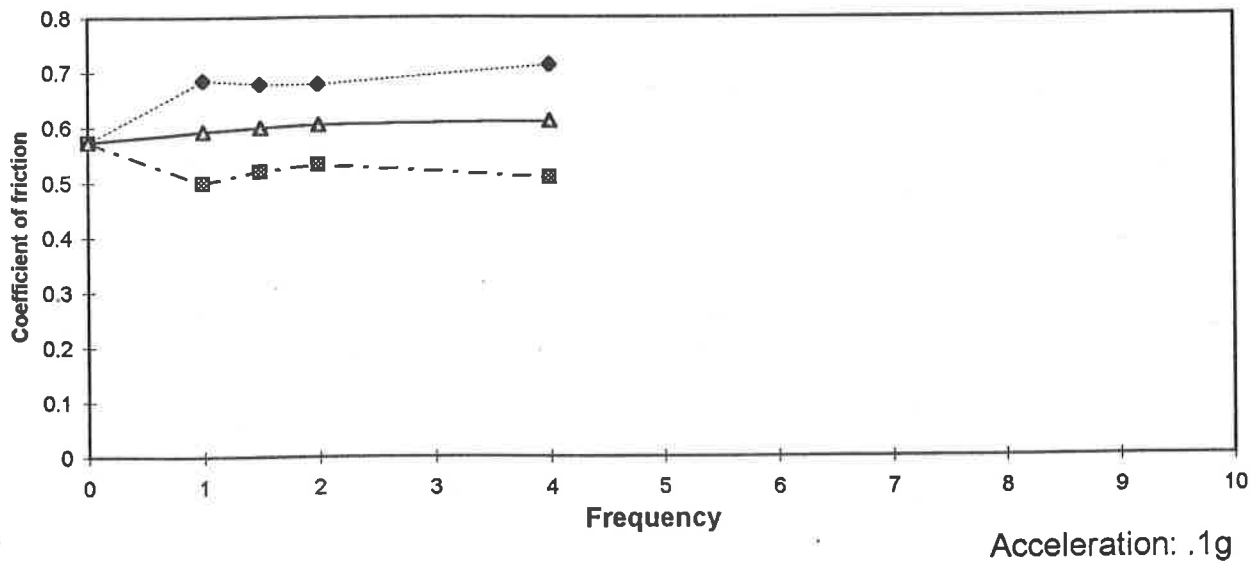
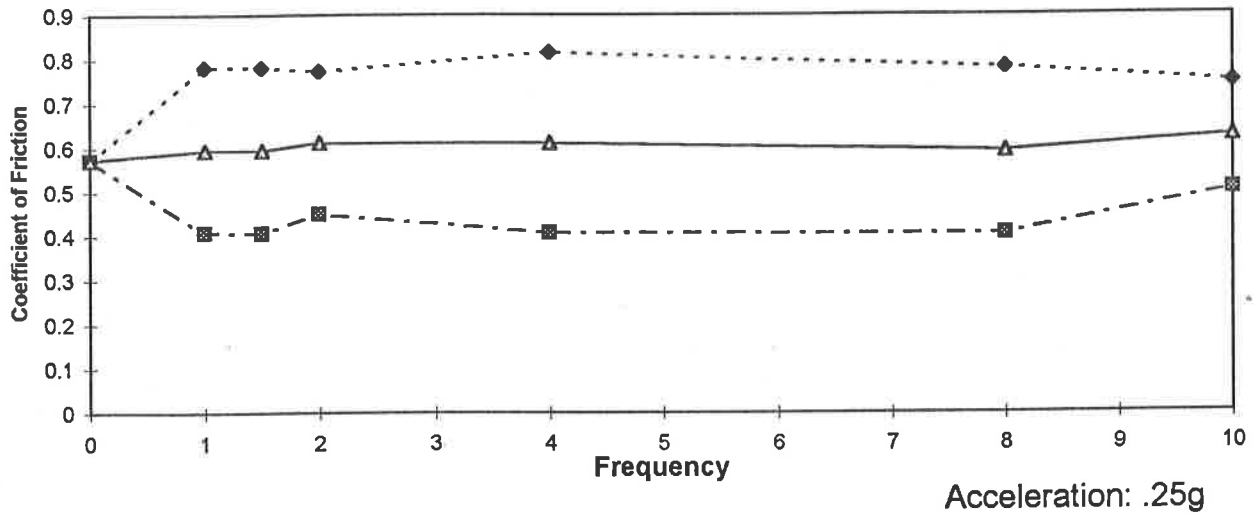
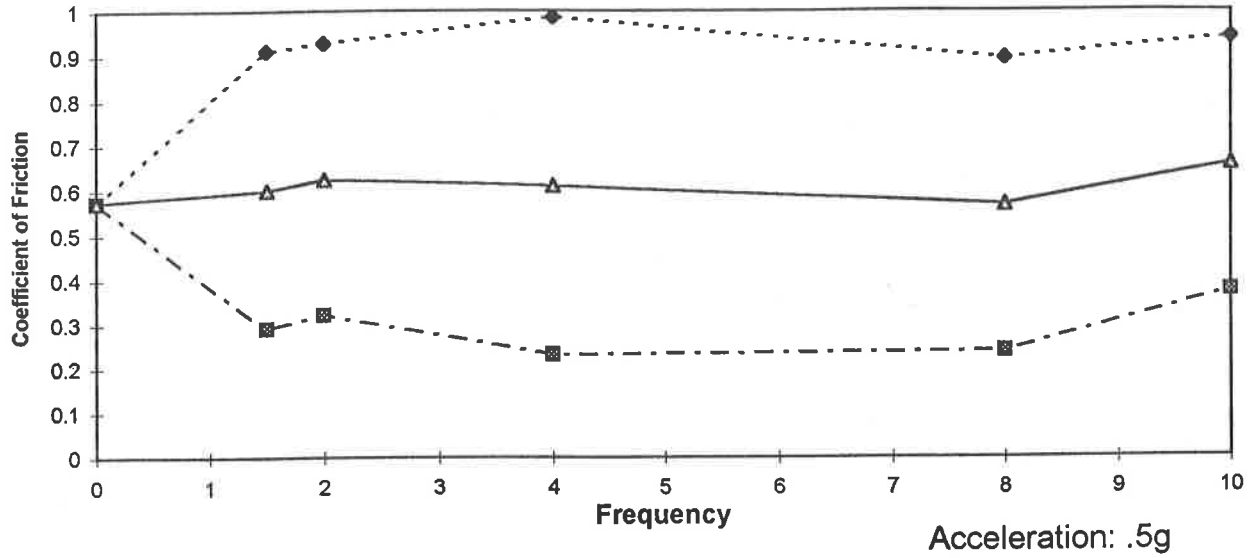


Figure 4.19: Influence of vertical vibration on the coefficient of friction

Deck: Coarse Hardwood      Load: M      Skid: Machine Feet

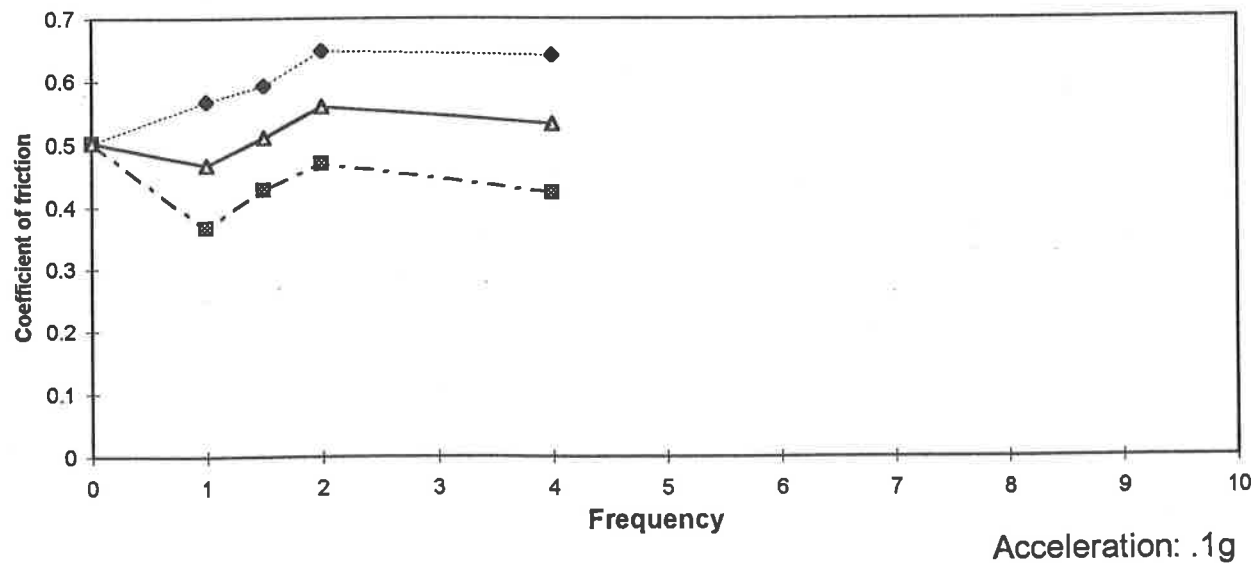
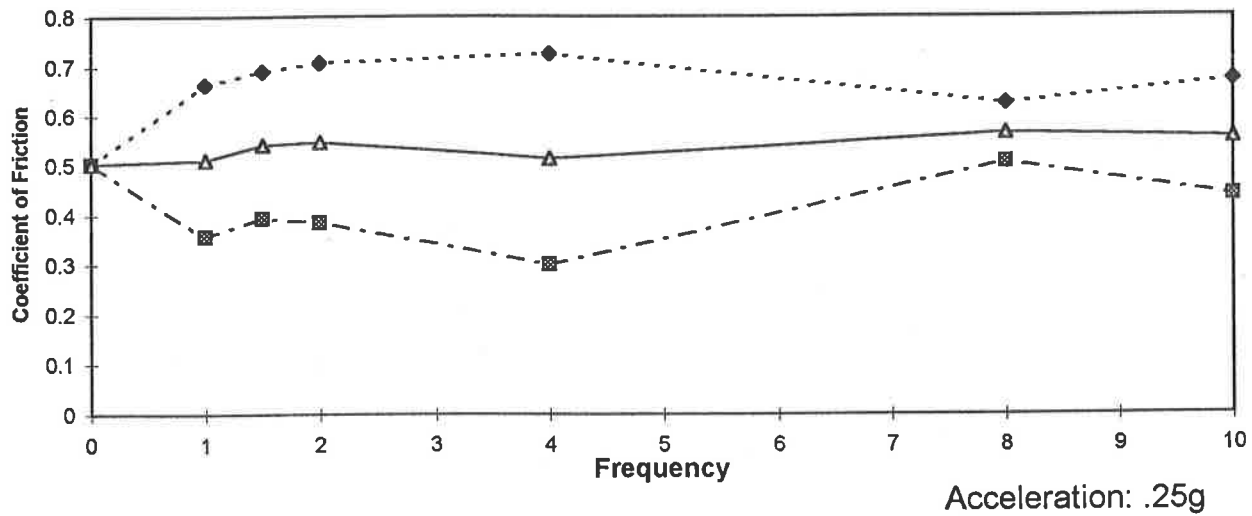
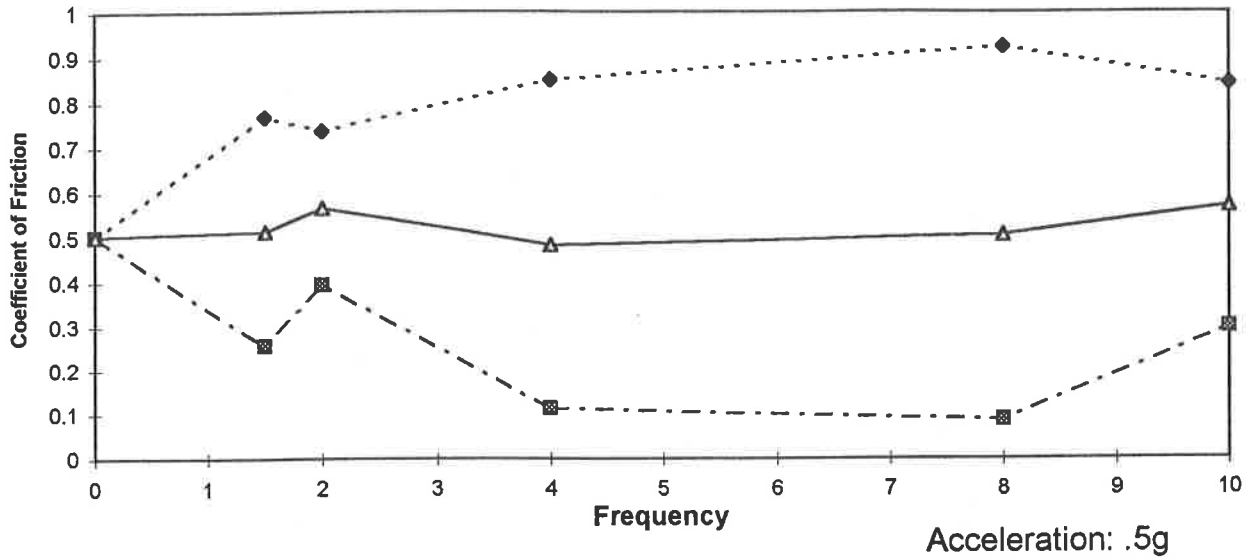


Figure 4.20: Influence of vertical vibration on the coefficient of friction



Deck: Coarse Hardwood

Load: H

Skid: Machine Feet

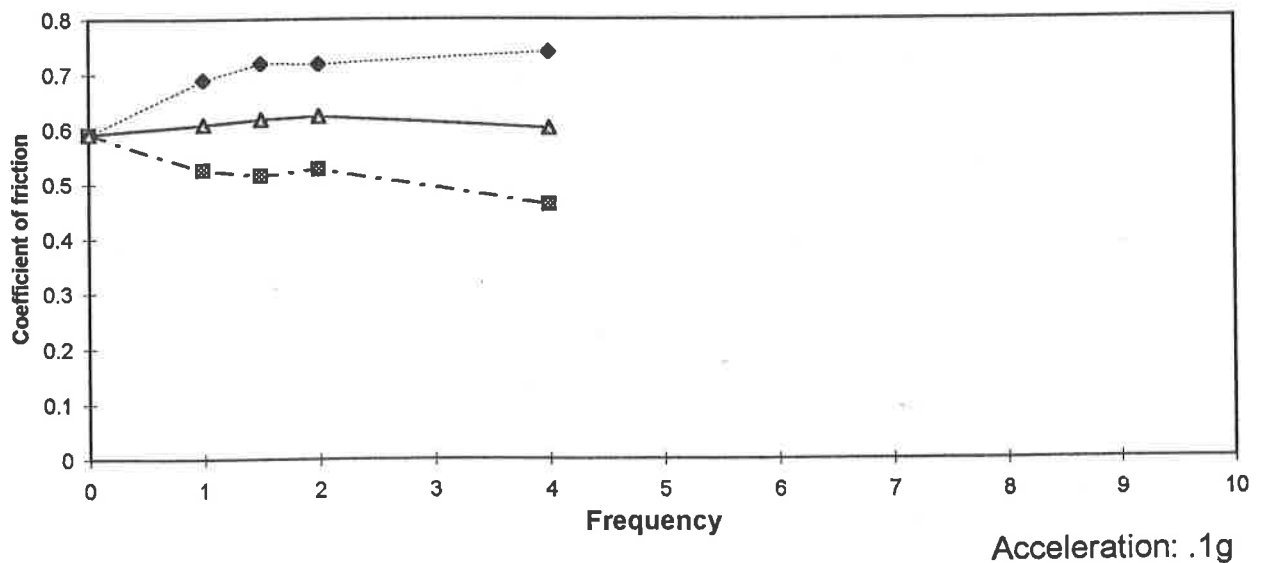
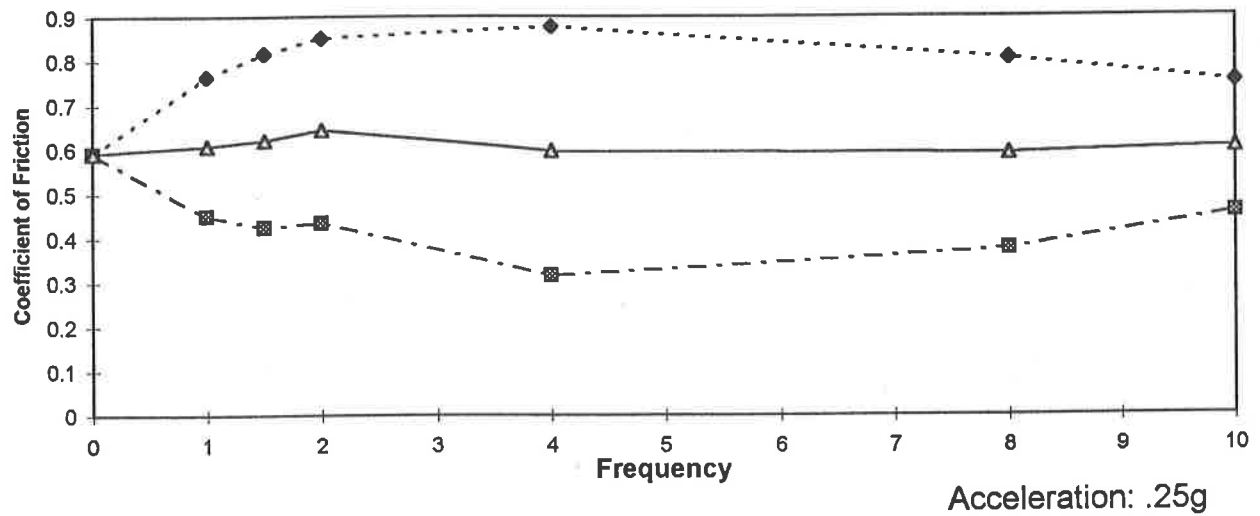
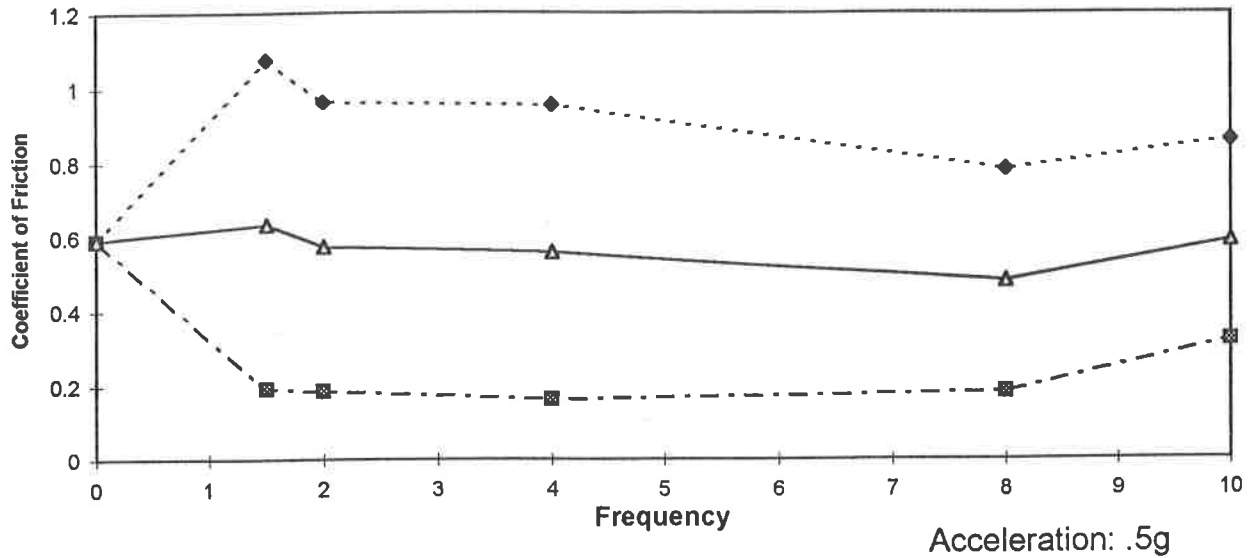


Figure 4.21: Influence of vertical vibration on the coefficient of friction

Deck: Coarse Hardwood

Skid: Machine Feet

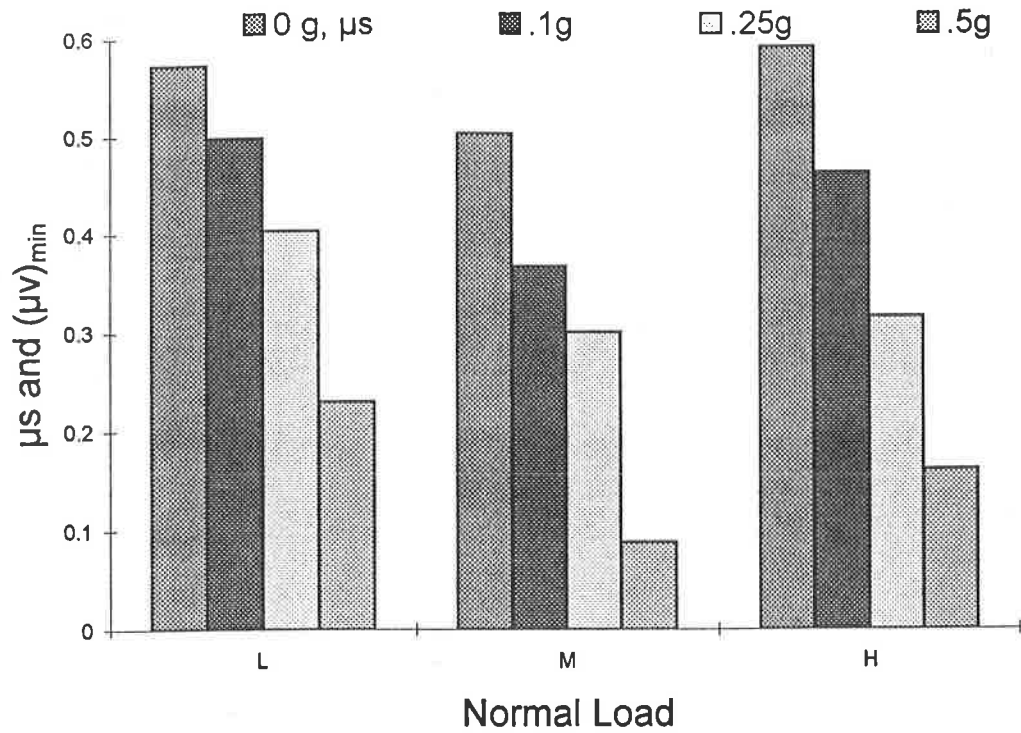


Figure 4.22: Influence of vertical acceleration and normal load on the minimum value of friction coefficient

values remain comparable with the respective  $\mu_s$  values in almost entire frequency range.

The concrete skid material exhibits lowest friction in the 4-8 Hz frequency range, irrespective of the normal load and the magnitude of vertical acceleration, as shown in Figures 4.23 and 4.24. The high vertical load in conjunction with 0.5g peak vertical acceleration yields almost loss of contact between the skid and deck surfaces at frequencies near 4.0 Hz. The steel pads also exhibit low friction values in the 4-8 Hz frequency range (Figures 4.26 to 4.28), while plastic skid exhibits lowest values in the 2-4 Hz frequency range (Figures 4.30 to 4.32).

The plastic skid material with light load reveals lowest friction coefficients of 0.11, 0.07 and 0.03, respectively, under 0.1g, 0.25g and 0.5g vertical acceleration. These values are approximately 47%, 67% and 88% lower than the respective  $\mu_s$  value. The lowest values of friction coefficients further decrease with increase in the vertical load. A loss of contact between the plastic skid and aluminum deck is observed under high normal load and 0.5g vertical acceleration. The steel pads, however, exhibit relatively lower reduction in the minimum values of  $\mu_v$ , ranging from 19% to 61%, under low level acceleration. The steel pads also exhibit near loss of contact under medium load and 0.5g vertical excitations at 8Hz.

#### 4.2.1.3 SMOOTH HARDWOOD DECK

Figures 4.34 and 4.35 illustrate the influence of vertical vibration on the mean, maximum and minimum values of friction coefficients obtained for paper on the smooth hardwood deck. The mean value of  $\mu_v$  tends to increase slightly with increase in the excitation frequency, specifically under low level vibration. This increase in  $\mu_v$  is attributed to frequent stick-slip motion and relatively high breakaway friction between

Deck: Y-Groove Aluminum      Load: M      Skid: Concrete Blocks

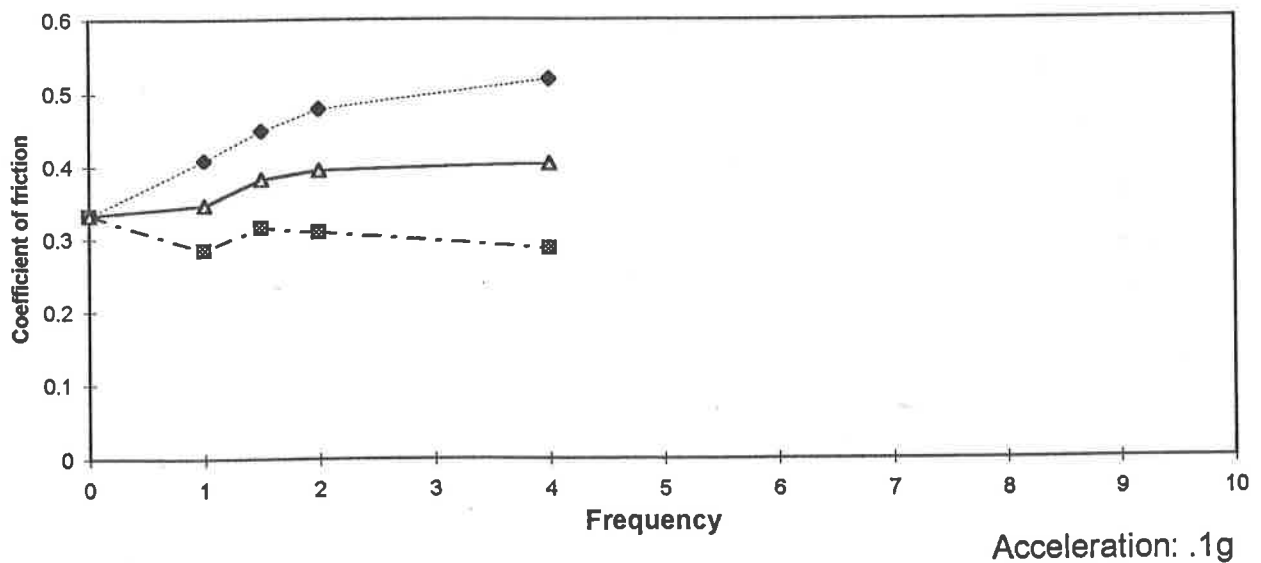
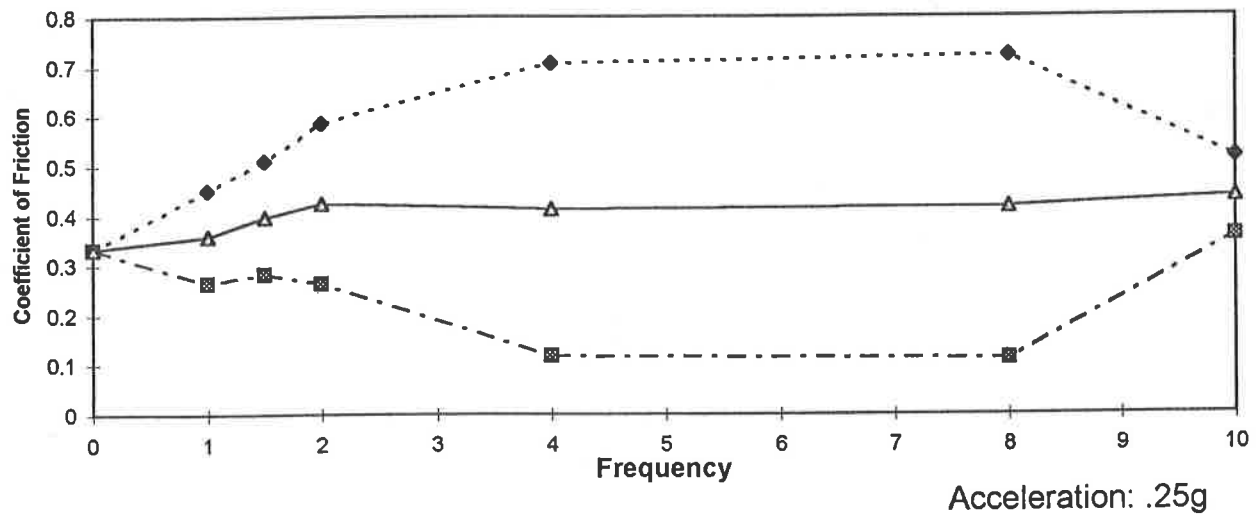
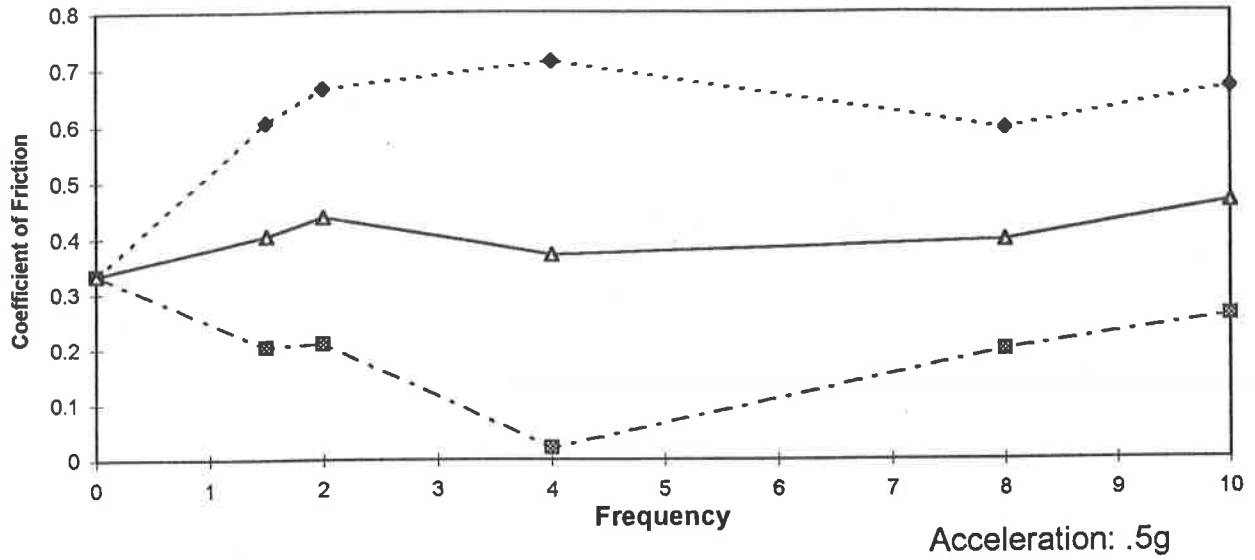


Figure 4.23: Influence of vertical vibration on the coefficient of friction

Deck: Y-Groove Aluminum      Load: H      Skid: Concrete Blocks

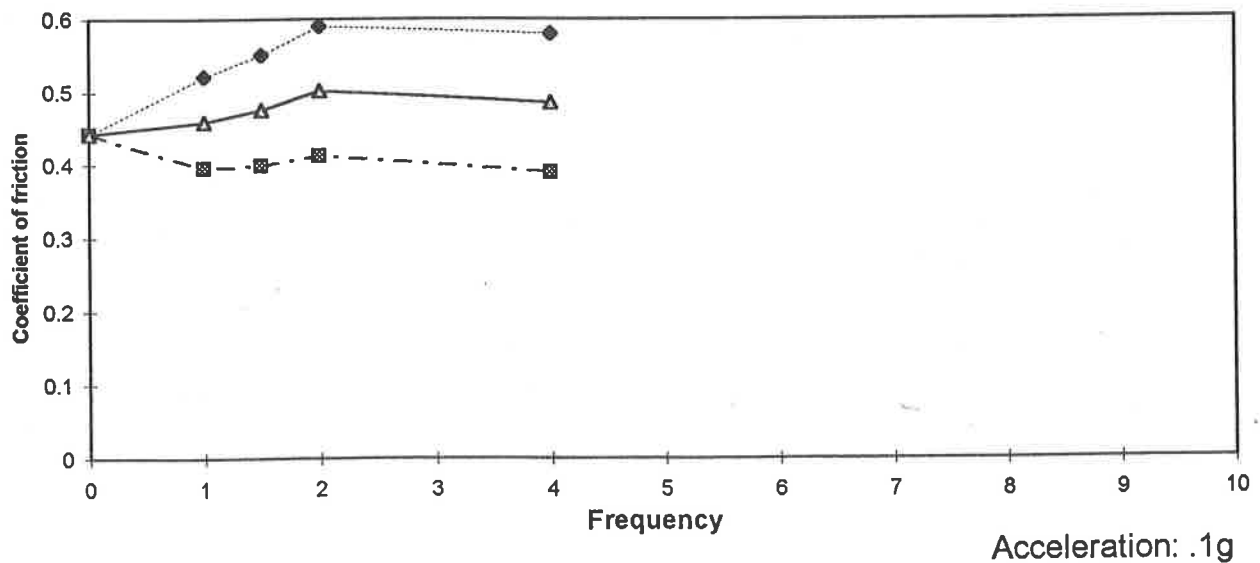
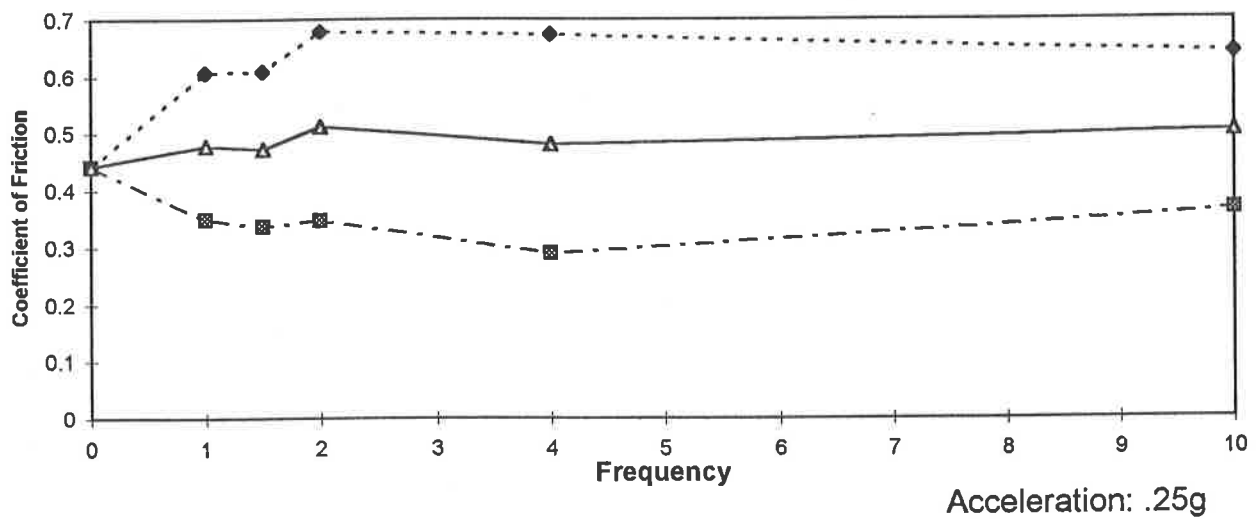
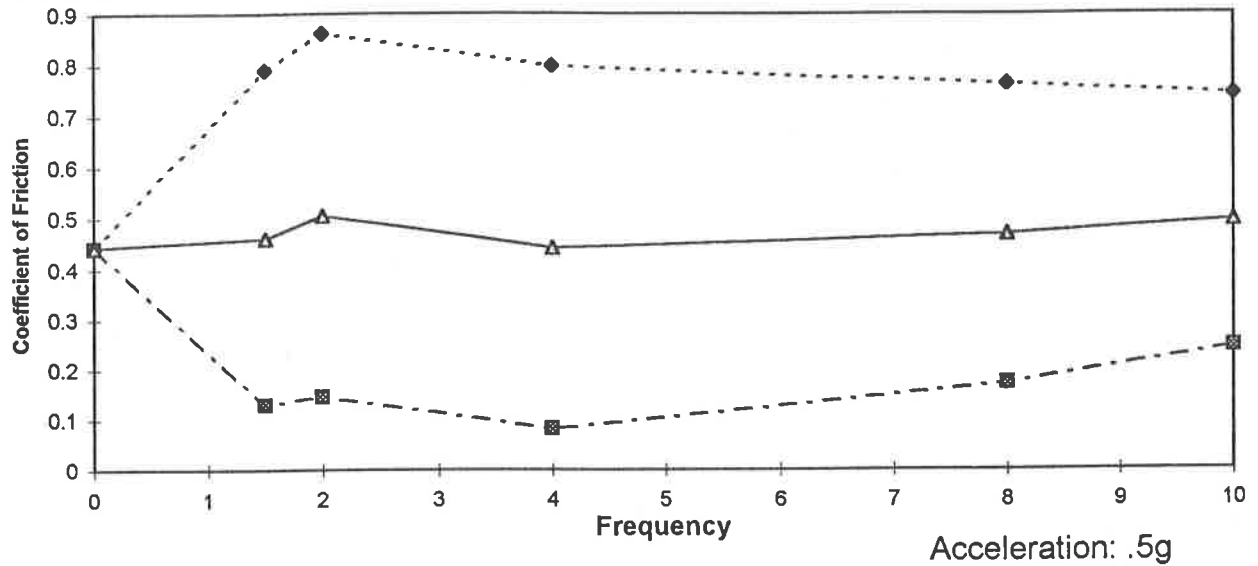


Figure 4.24: Influence of vertical vibration on the coefficient of friction

Deck: Y-Groove Aluminum

Skid: Concrete Blocks

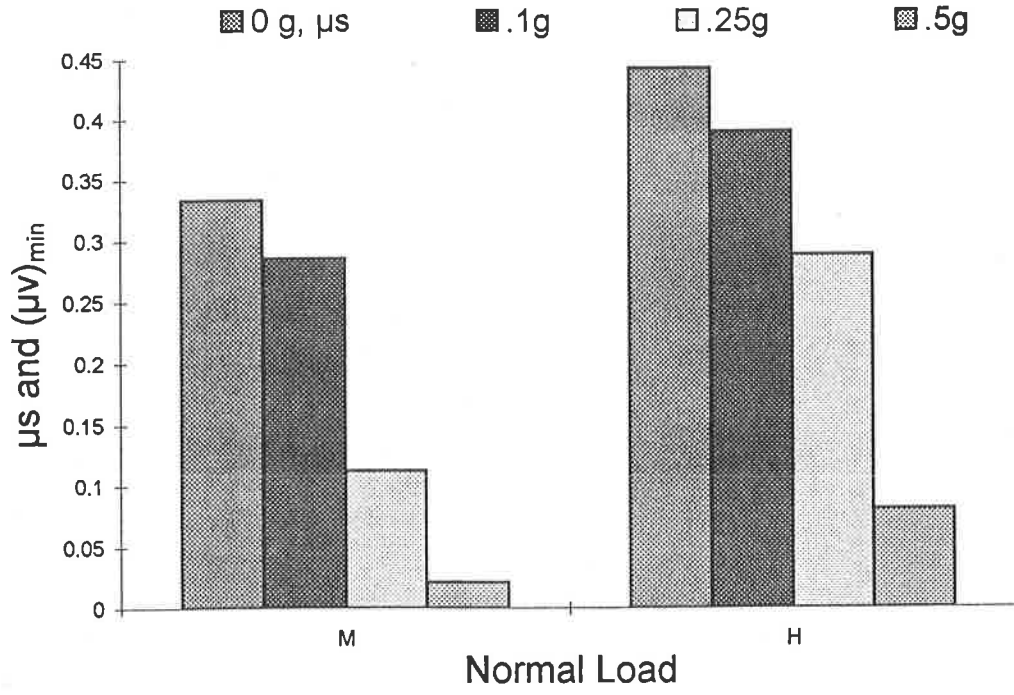


Figure 4.25: Influence of vertical acceleration and normal load on the minimum value of friction coefficient

Deck: Y-Groove Aluminum

Load: L

Skid: Steel Pads

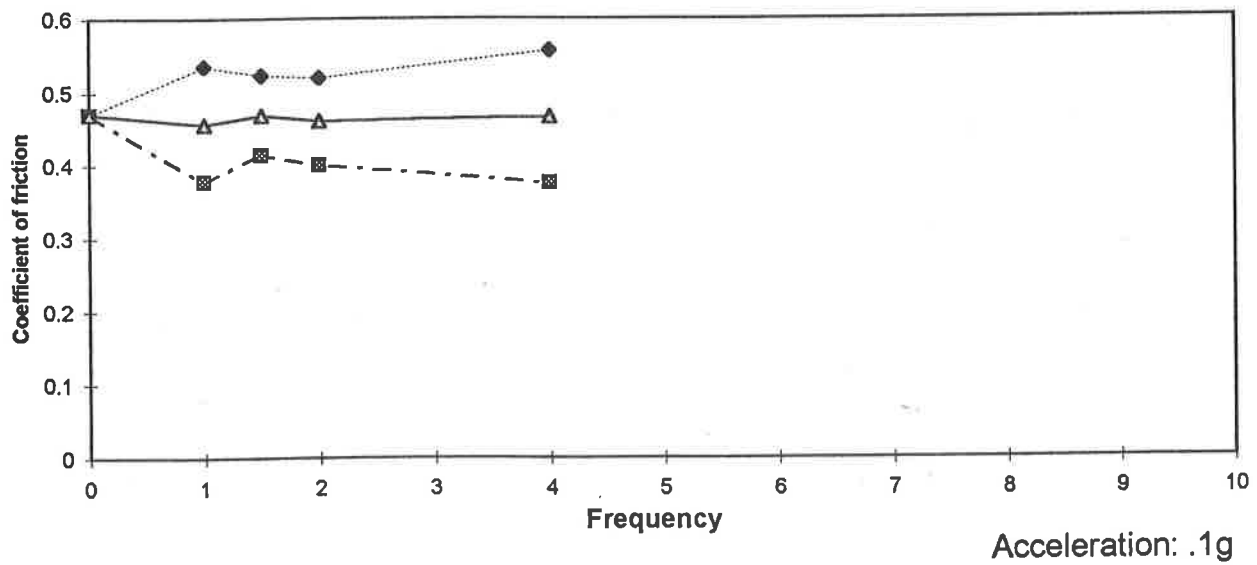
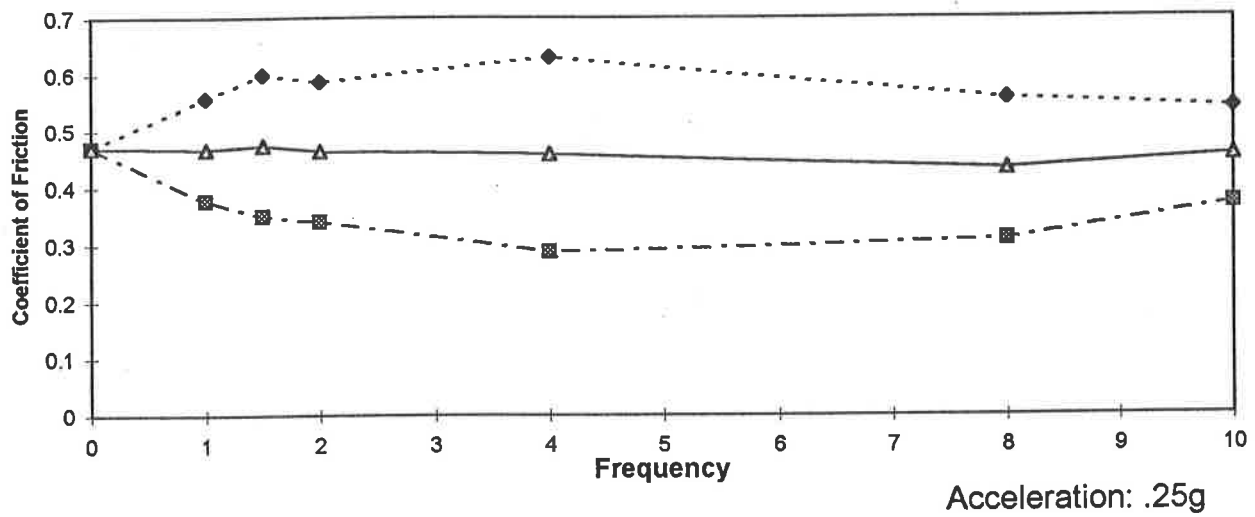
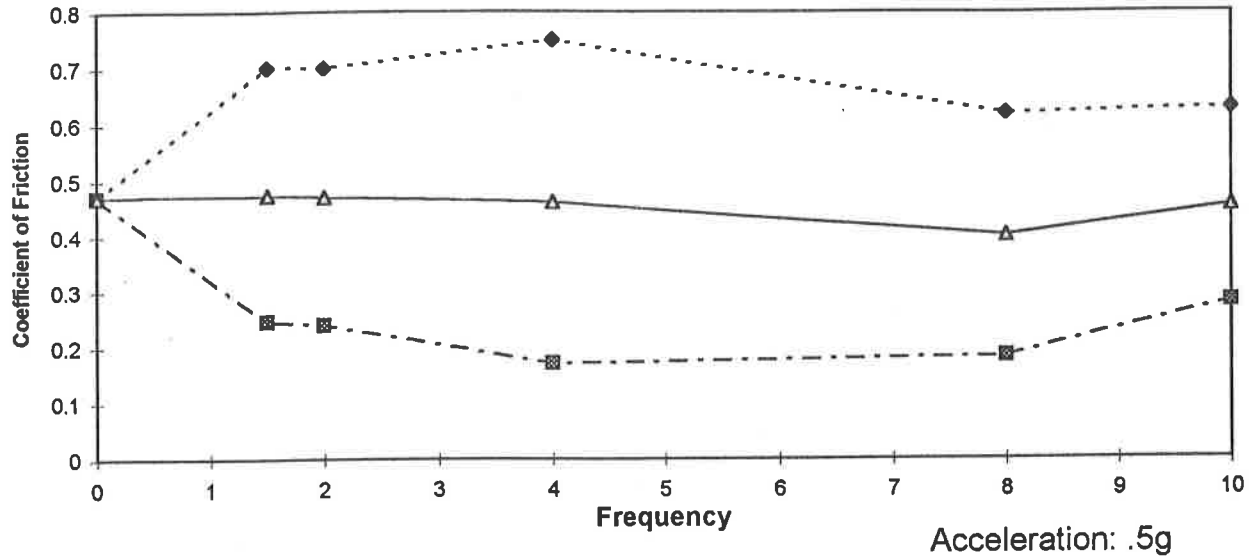


Figure 4.26: Influence of vertical vibration on the coefficient of friction

Deck: Y-Groove Aluminum

Load: M

Skid: Steel Pads

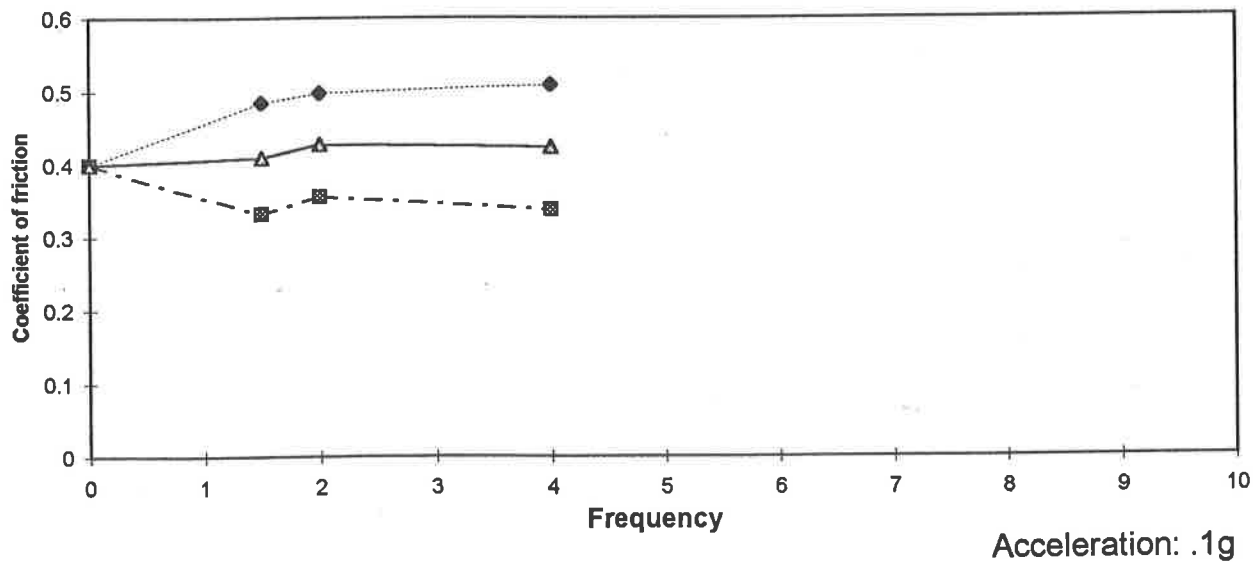
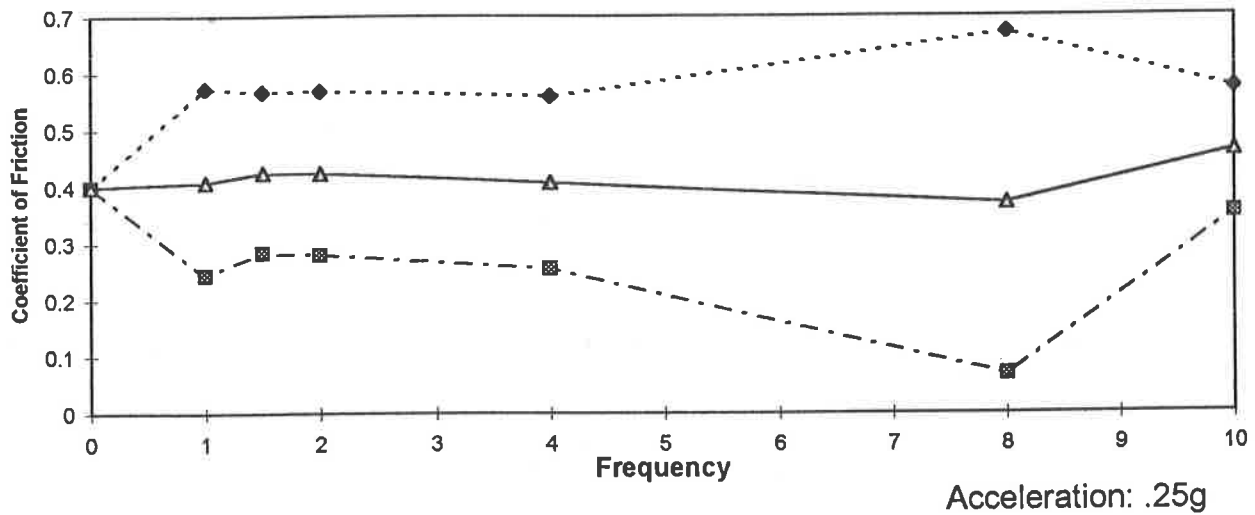
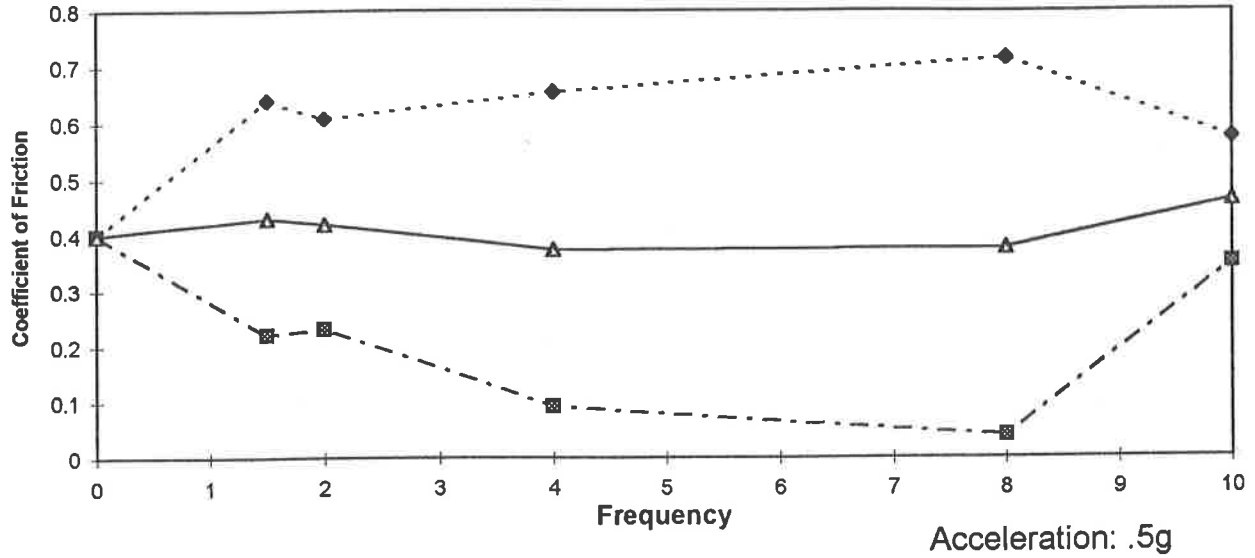


Figure 4.27: Influence of vertical vibration on the coefficient of friction



Deck: Y-Groove Aluminum      Load: H      Skid: Steel Pads

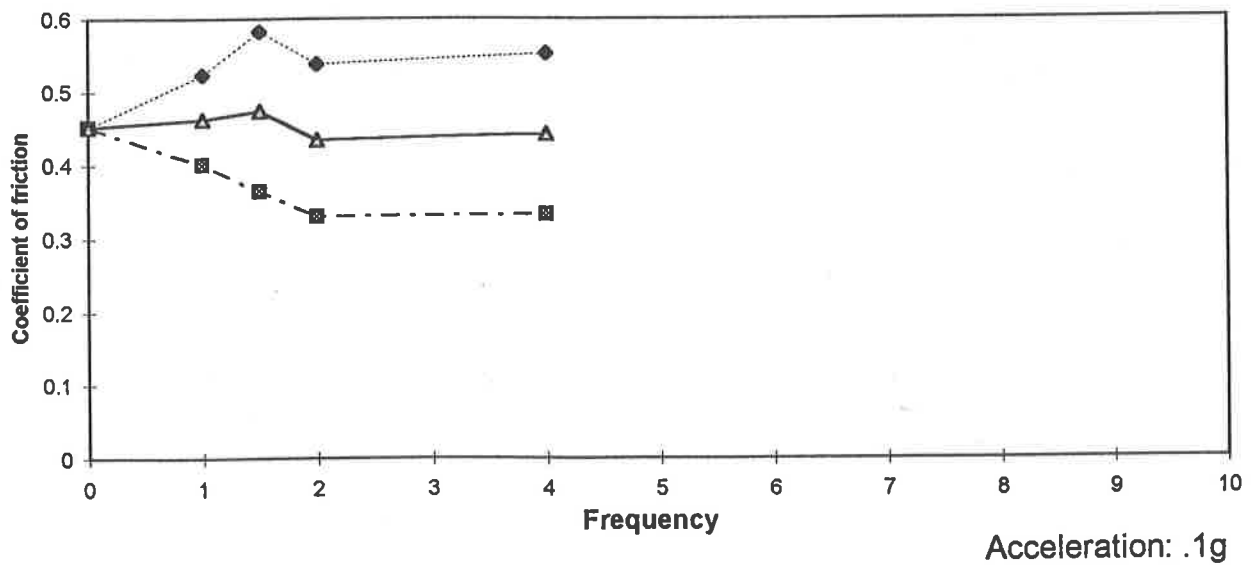
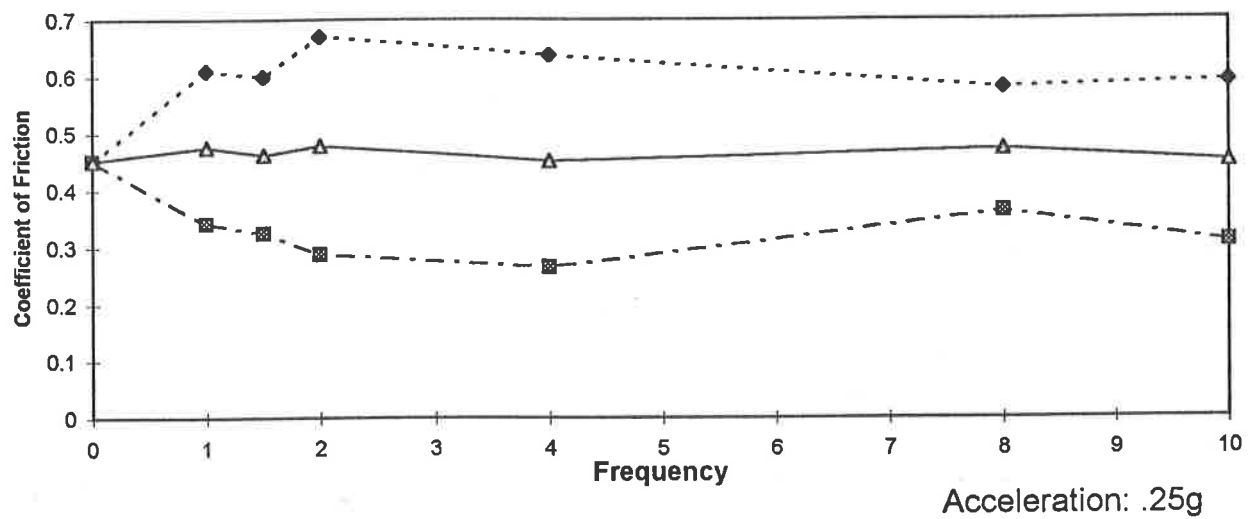
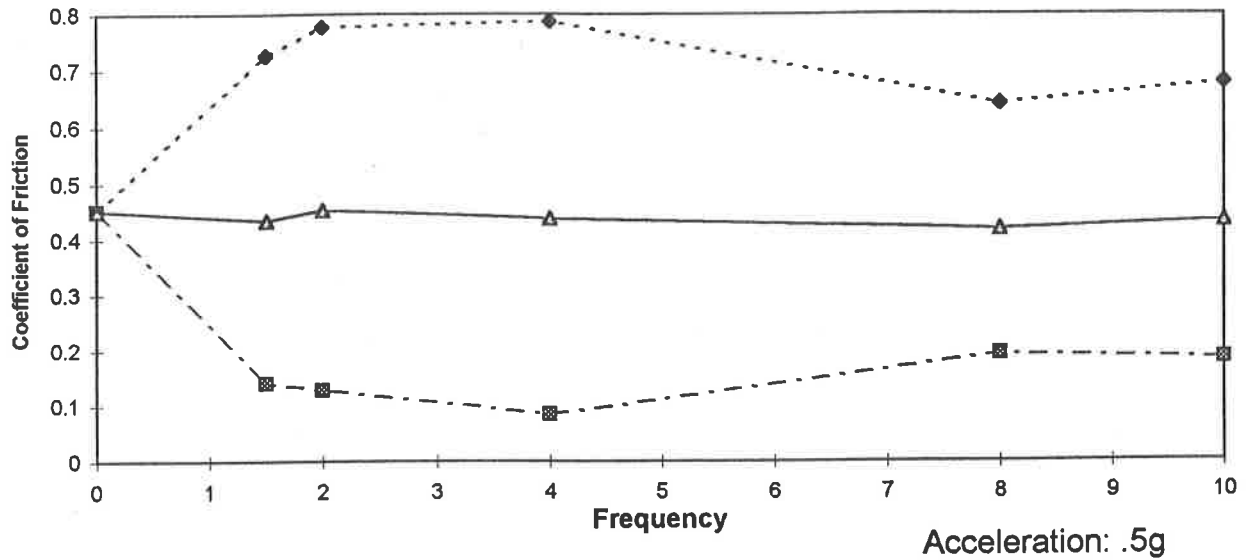


Figure 4.28: Influence of vertical vibration on the coefficient of friction

Deck: Y-Groove Aluminum

Skid: Steel Pads

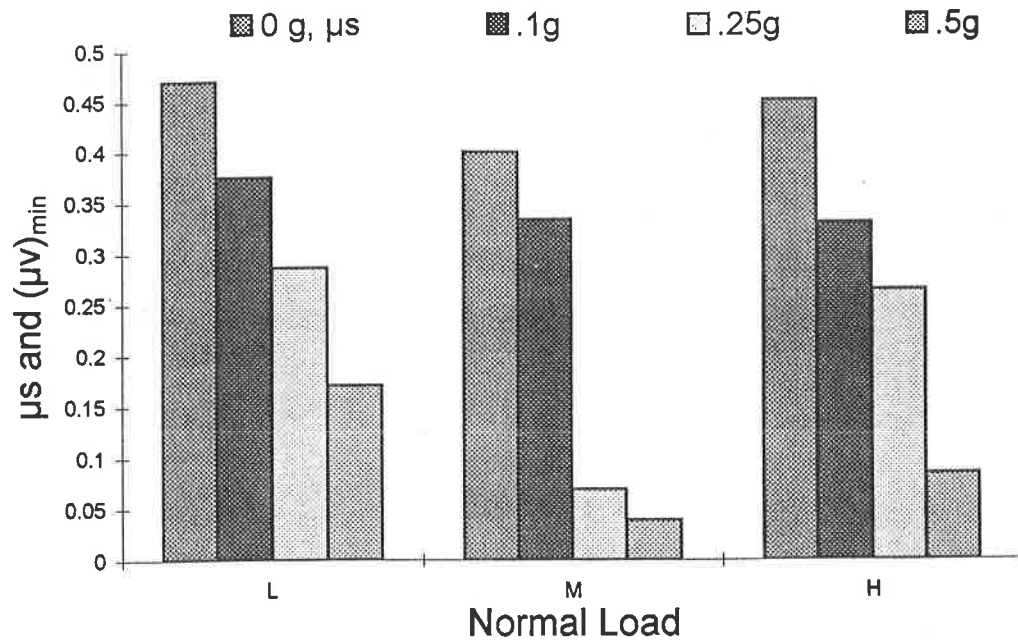


Figure 4.29: Influence of vertical acceleration and normal load on the minimum value of friction coefficient

Deck: Y-Groove Aluminum

Load: L

Skid: Plastic Skid

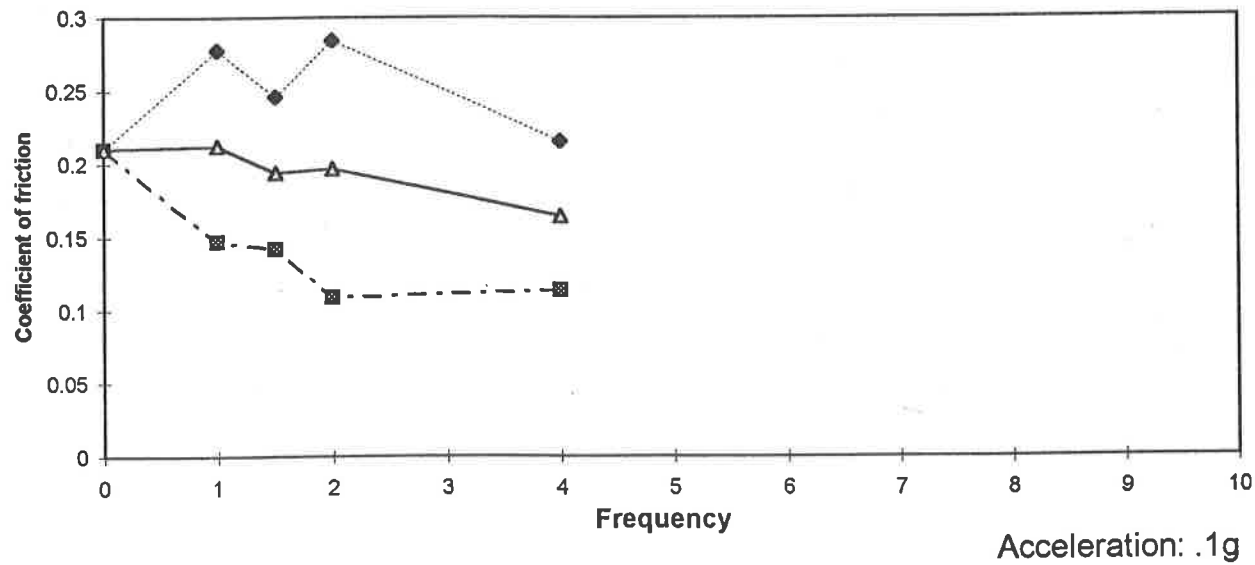
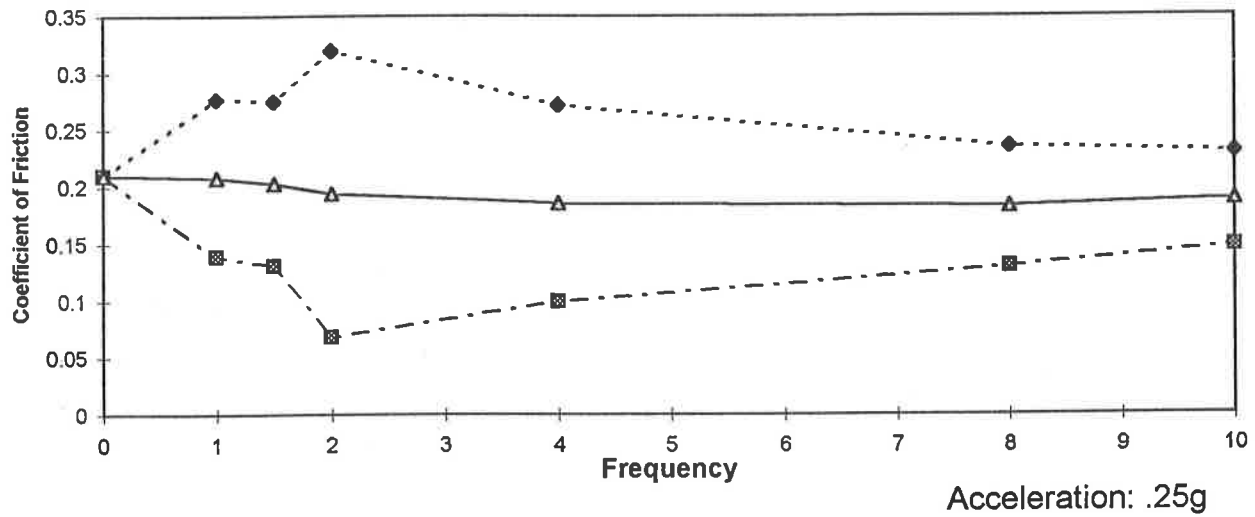
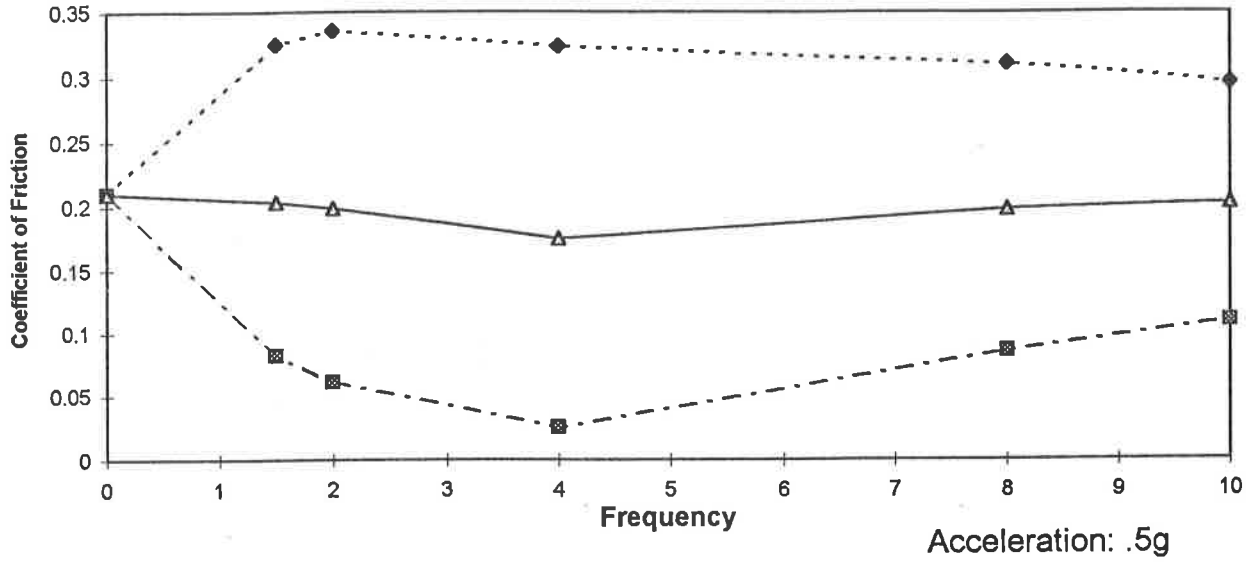


Figure 4.30: Influence of vertical vibration on the coefficient of friction

Deck: Y-Groove Aluminum      Load: M      Skid: Plastic Skid

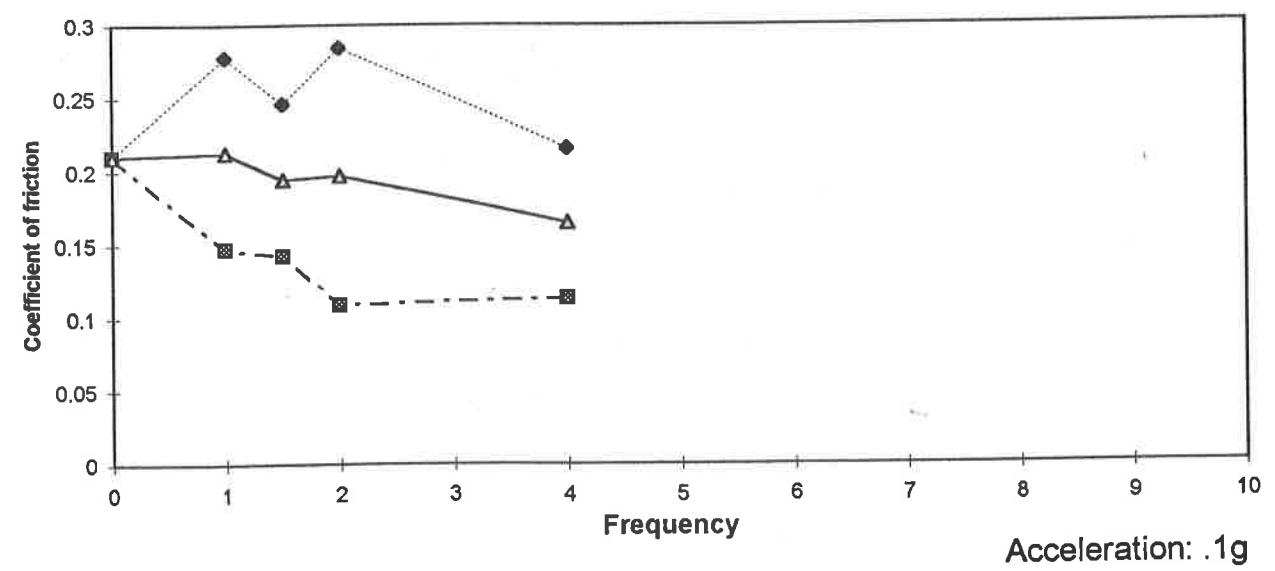
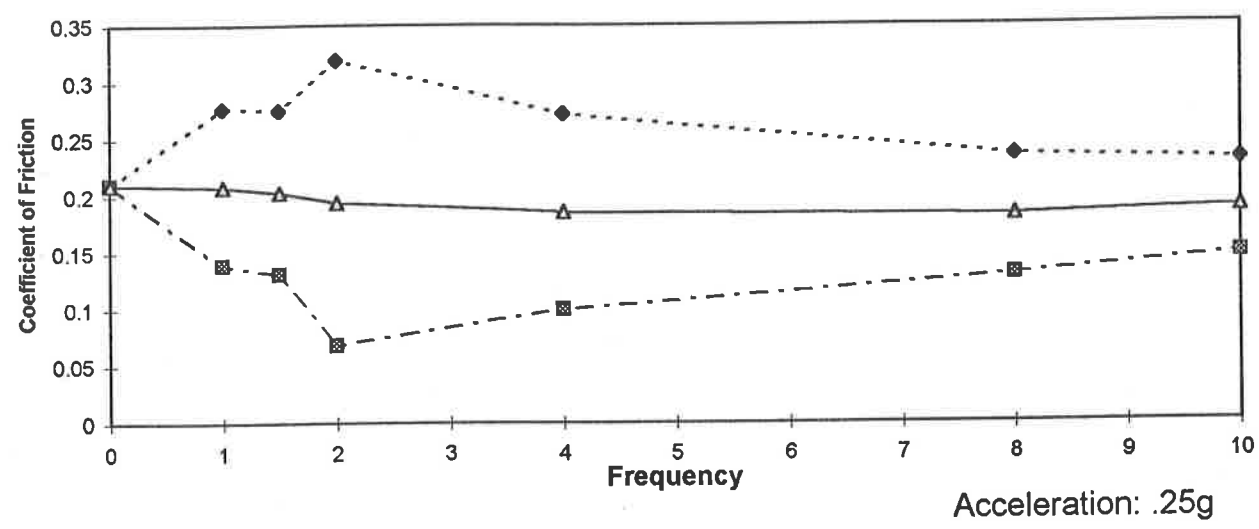
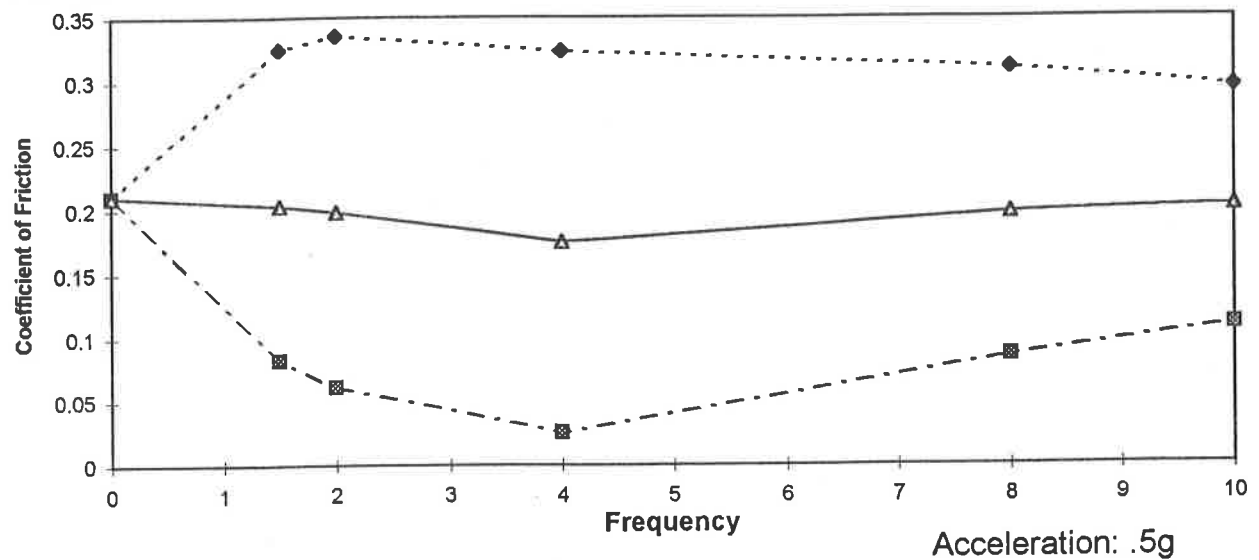


Figure 4.31: Influence of vertical vibration on the coefficient of friction

Deck: Y-Groove Aluminum

Load: H

Skid: Plastic Skid

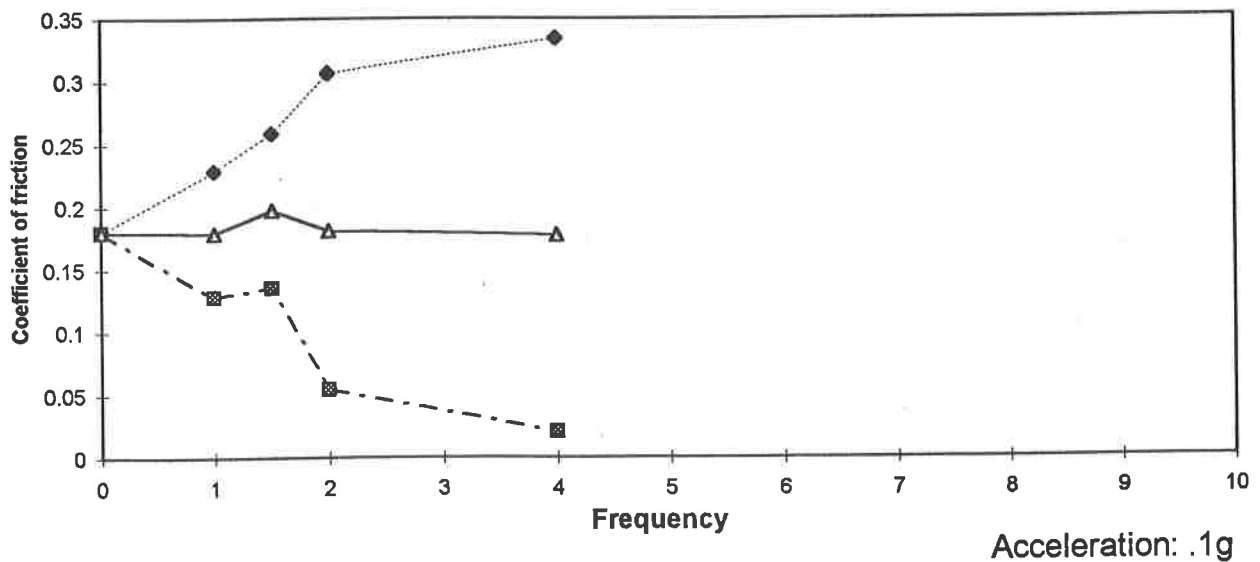
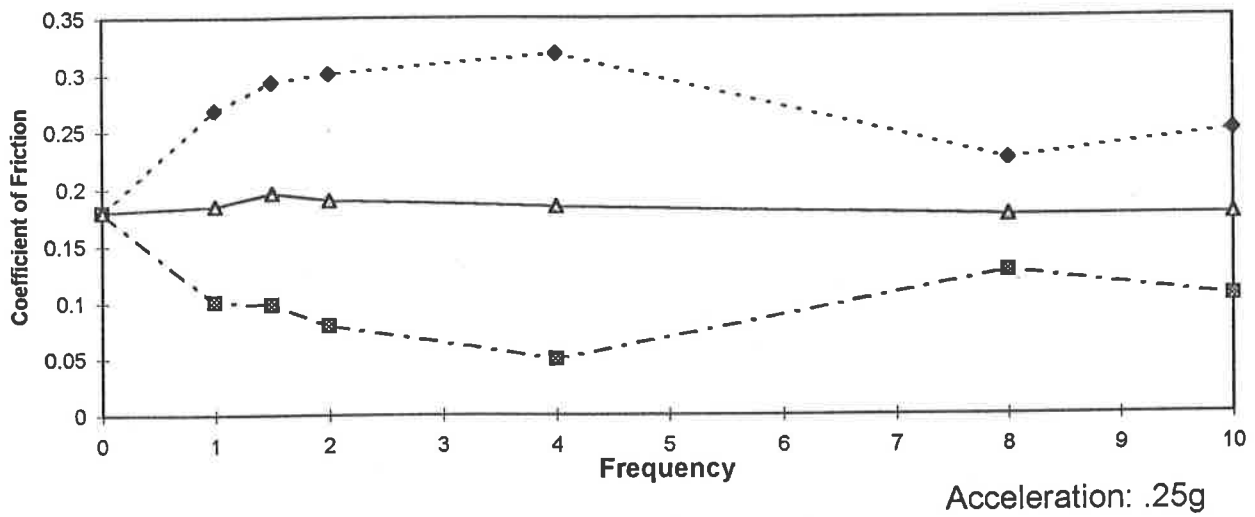
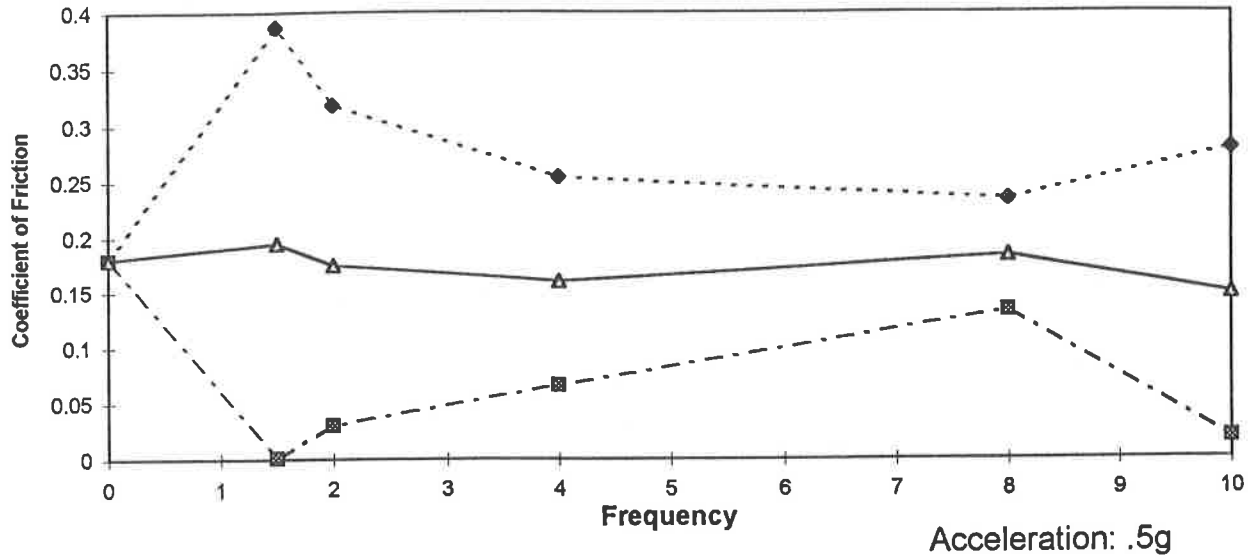


Figure 4.32: Influence of vertical vibration on the coefficient of friction

Deck: Y-Groove Aluminum

Skid: Plastic Skid

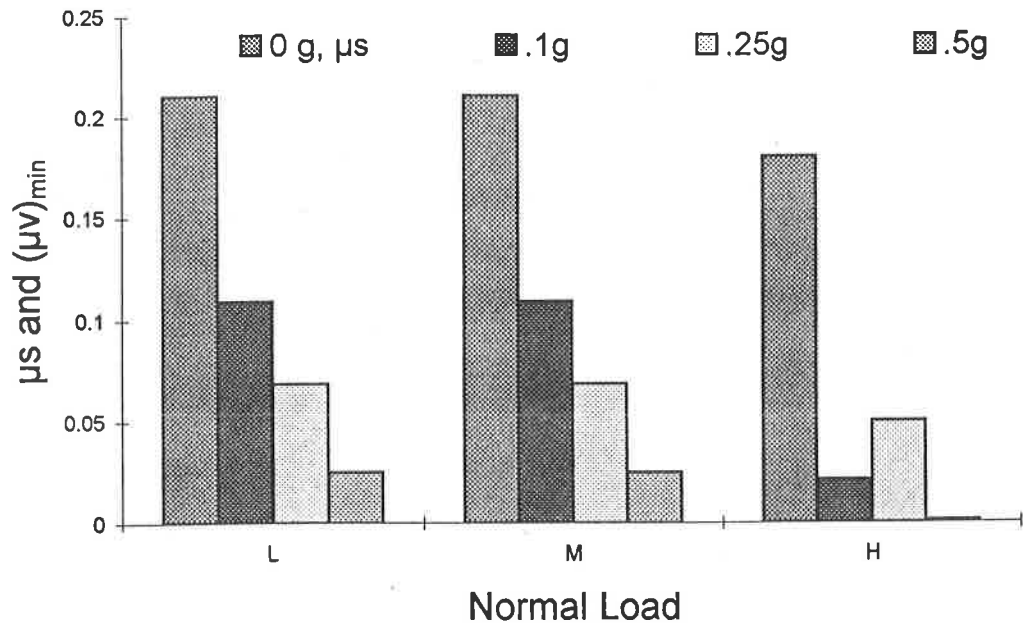


Figure 4.33: Influence of vertical acceleration and normal load on the minimum value of friction coefficient

paper and smooth hardwood. The measurements reveal most significant variation in  $\mu_v$  in the 4-8 Hz frequency range, irrespective of the normal load and the magnitude of vertical acceleration. Under light normal load and 0.1g vertical acceleration, the minimum value of  $\mu_v$  is observed to be only 7.5% lower than the  $\mu_s$  value. The minimum value, however, decreases by nearly 47% when normal load is increased to medium value, and by nearly 87% when magnitude of vertical acceleration is also increased to 0.5g, as shown in Figure 4.36.

The mean, maximum and minimum values of  $\mu_v$  measured between rubber and smooth hardwood also exhibit similar trends, as shown in Figures 4.37 and 4.38. The measurements under medium load, however, reveal most significant decrease in  $\mu_v$  in the 2-4 Hz frequency range. The decrease in minimum value of  $\mu_v$  occurs irrespective of the magnitude of vertical acceleration and is attributed to the flexibility of the rubber mat. The frequency range of significant reduction in  $\mu_v$  may further decrease with higher loads. The selection of a rubber mat thus needs appropriate consideration of the resonant frequency of the loaded rubber mat to ensure that it does not coincide with resonant frequency of the sprung weight, which occurs in the 1.5 to 2.5 Hz depending upon the type of suspension. Figure 4.39 summarizes the minimum values obtained as a function of the normal load and magnitude of vertical acceleration.

The friction coefficients measured between plastic skid and smooth hardwood deck subject to vertical vibration, shown in Figures 4.40 to 4.42, also reveal similar patterns. The minimum values of friction coefficient tend to decrease considerably with increase in normal load and the magnitude of vertical vibration. The most significant decrease in the  $\mu_v$  occurs in the 2-4 Hz frequency range, depending upon the normal load. High normal load yields most significant decrease near 2 Hz, which is most likely attributed to the lower resonant frequency of the loaded plastic skid material. The

Deck: Smooth Hardwood

Load: L

Skid: Kraft Paper

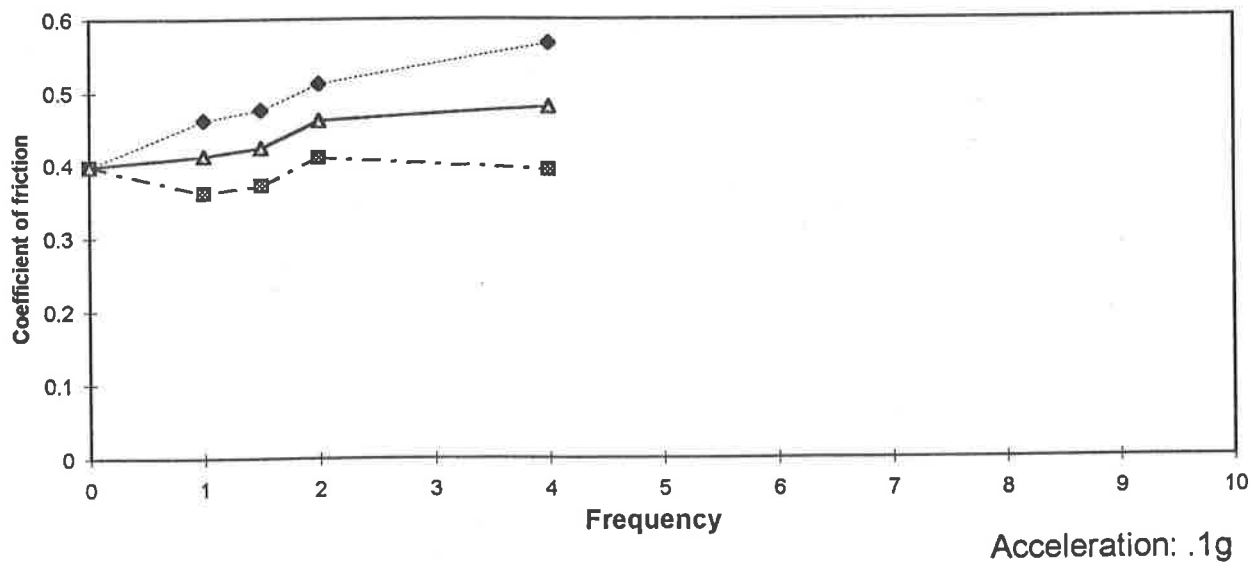
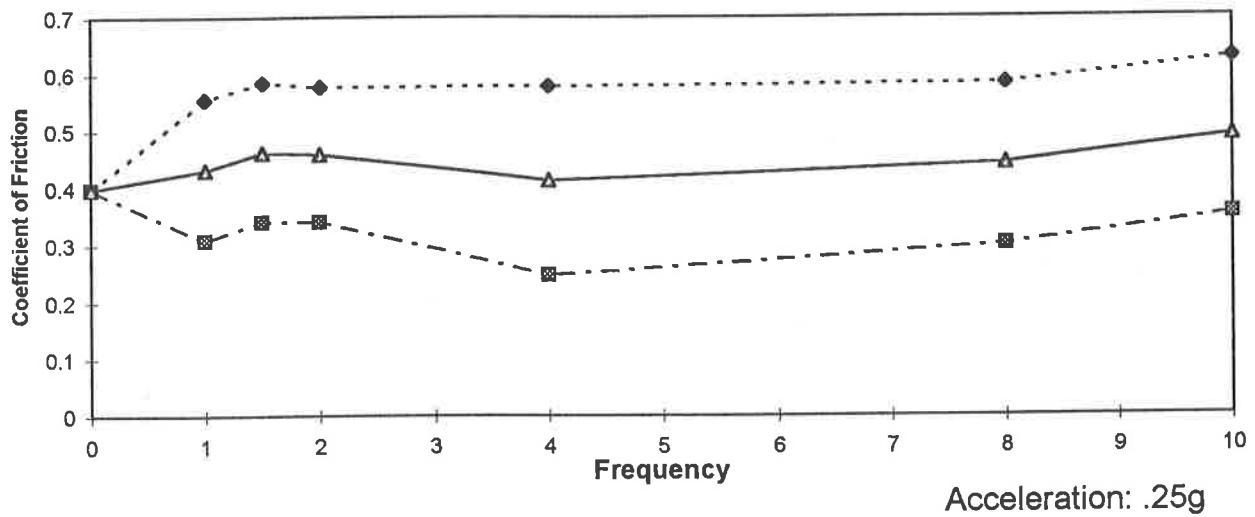
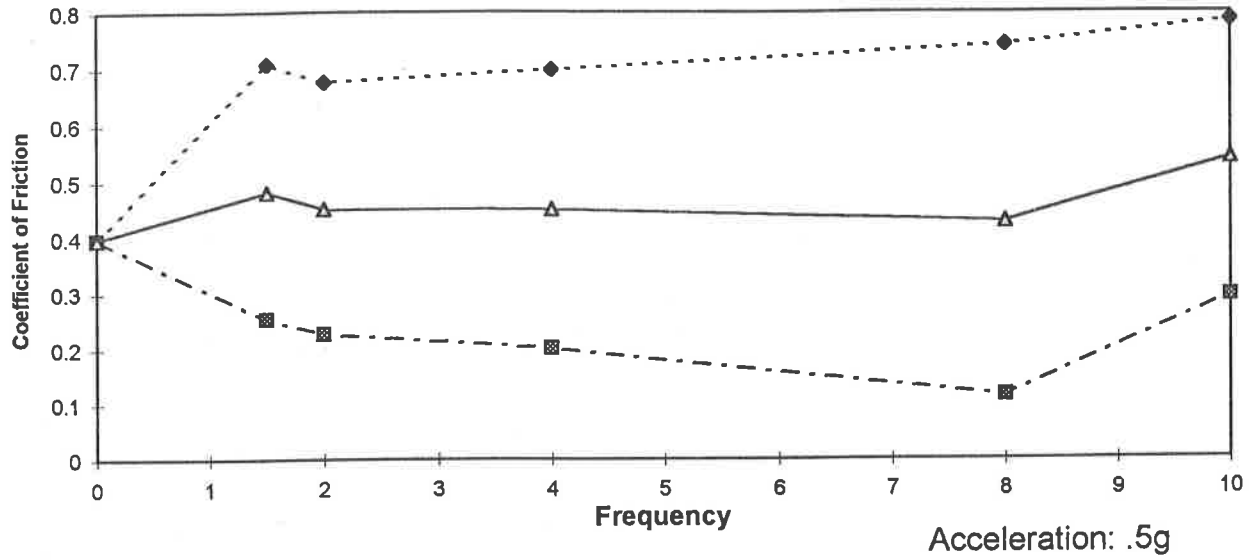


Figure 4.34: Influence of vertical vibration on the coefficient of friction



Deck: Smooth Hardwood      Load: M      Skid: Kraft Paper

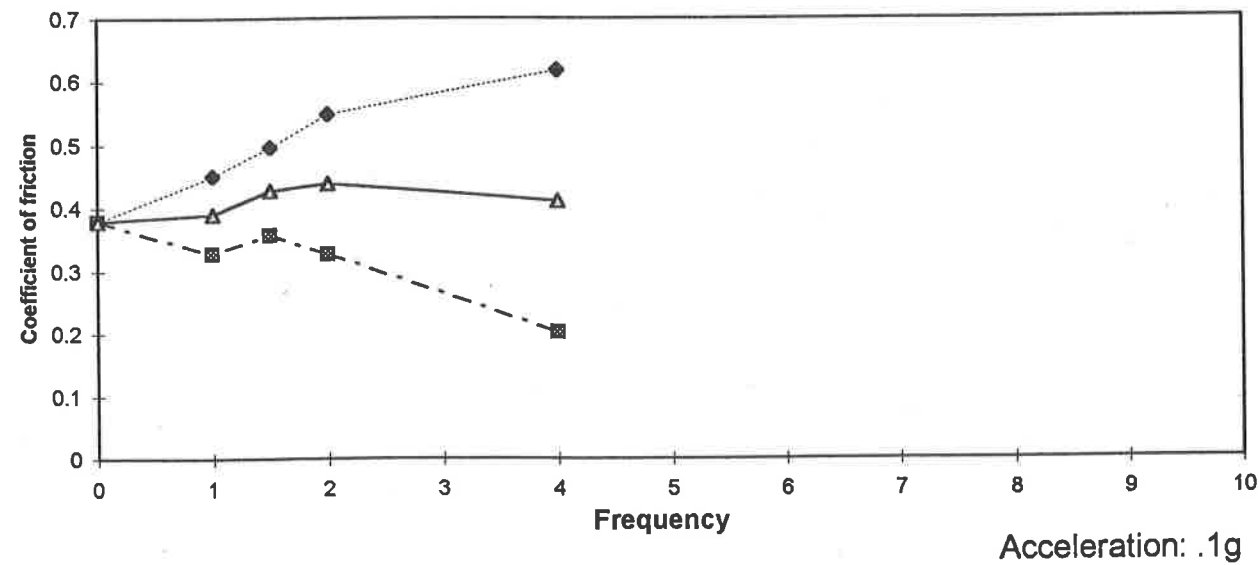
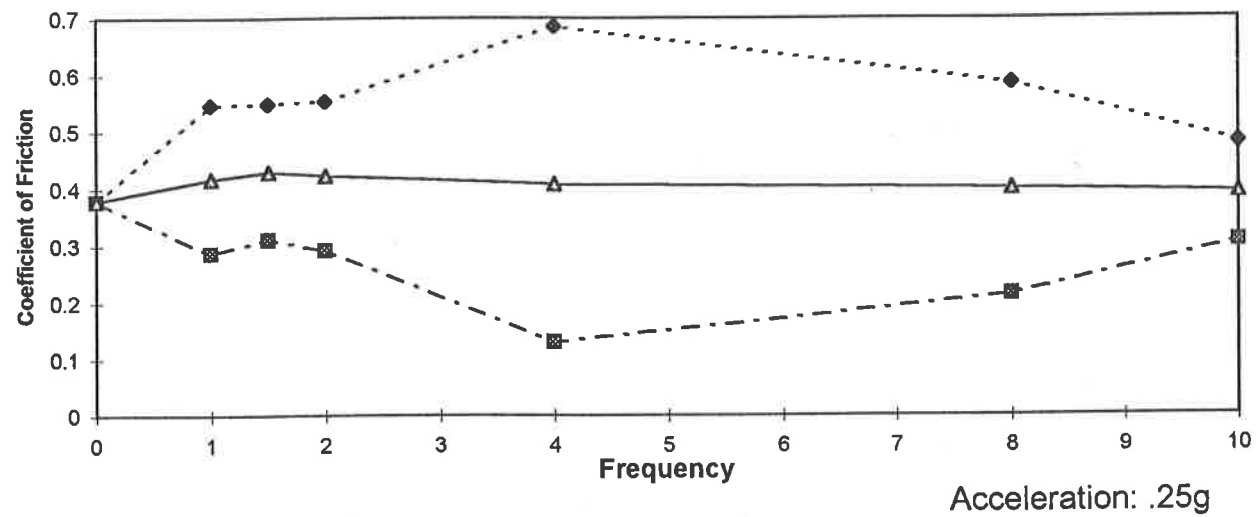
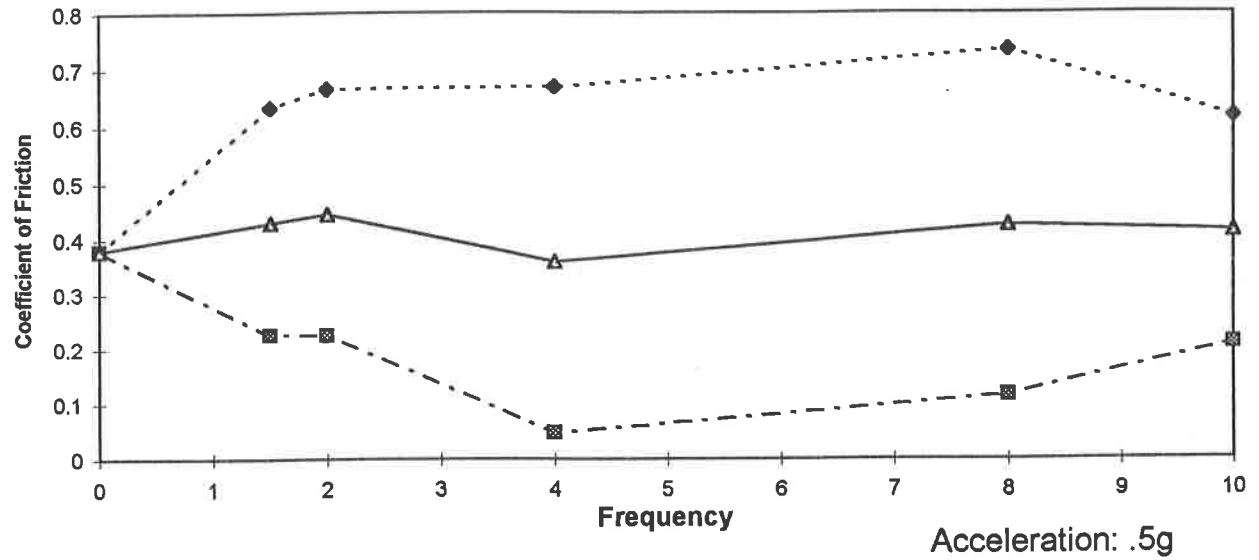


Figure 4.35: Influence of vertical vibration on the coefficient of friction

Deck: Smooth Hardwood

Skid: Kraft Paper

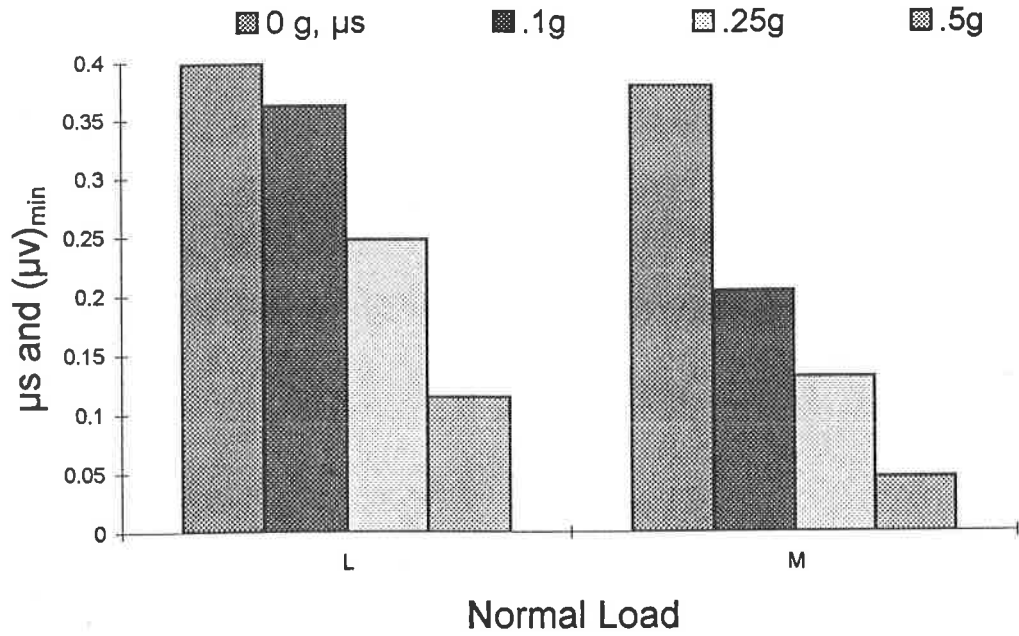


Figure 4.36: Influence of vertical acceleration and normal load on the minimum value of friction coefficient

Deck: Smooth Hardwood      Load: L      Skid: Rubber Mat

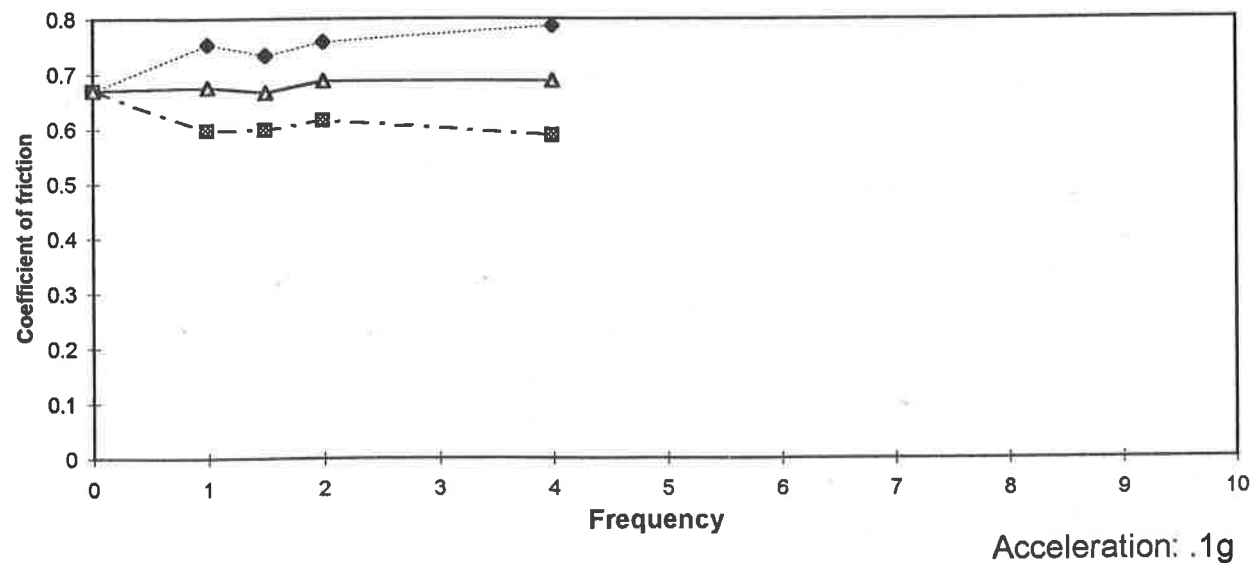
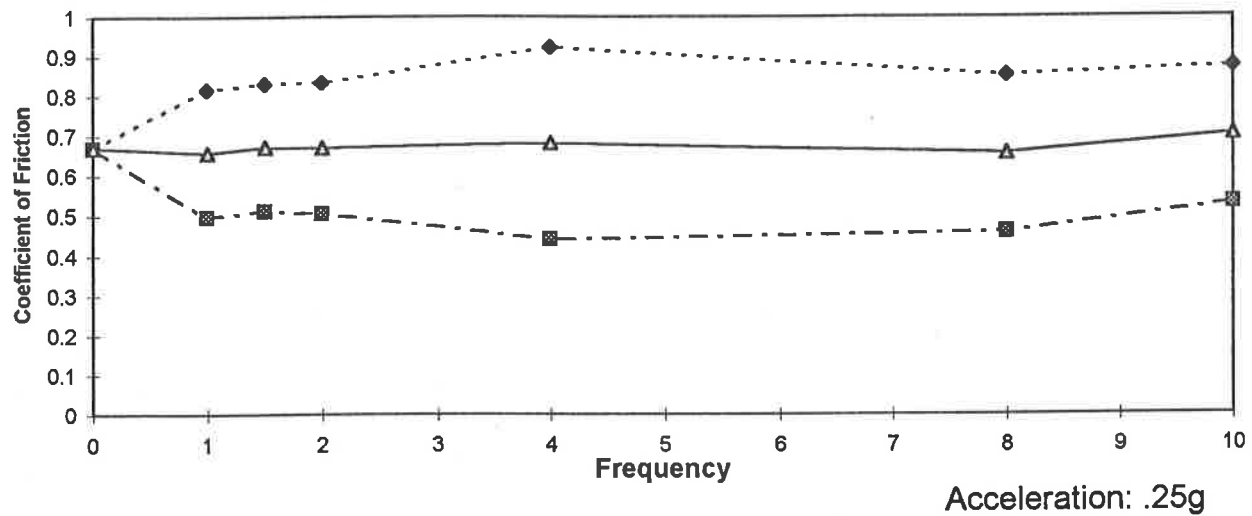
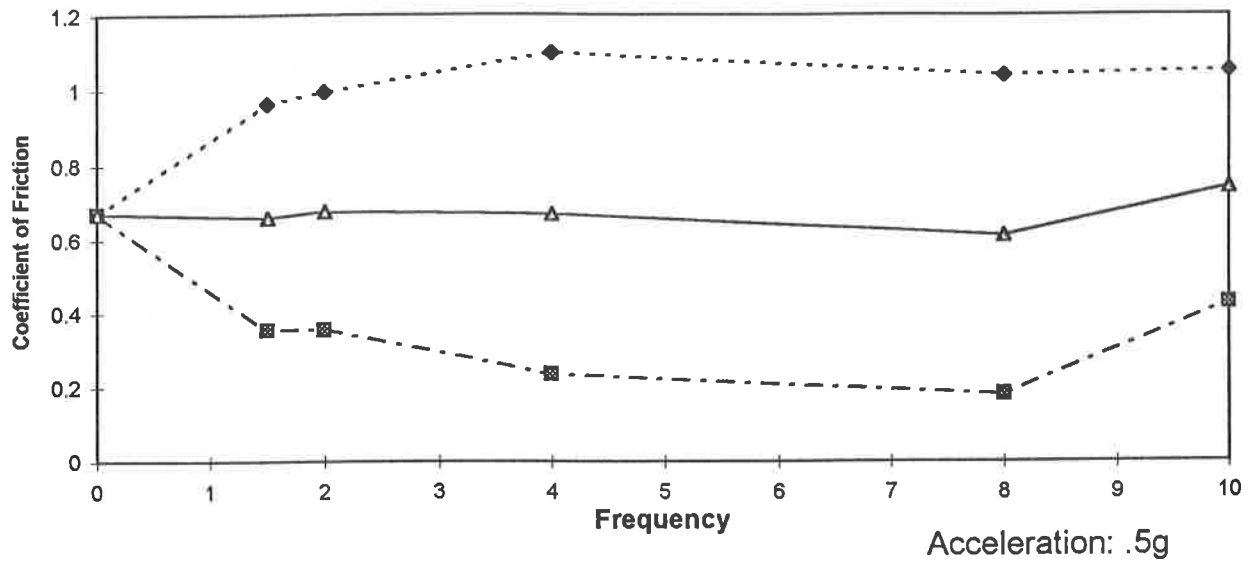


Figure 4.37: Influence of vertical vibration on the coefficient of friction

Deck: Smooth Hardwood

Load: M

Skid: Rubber Mat

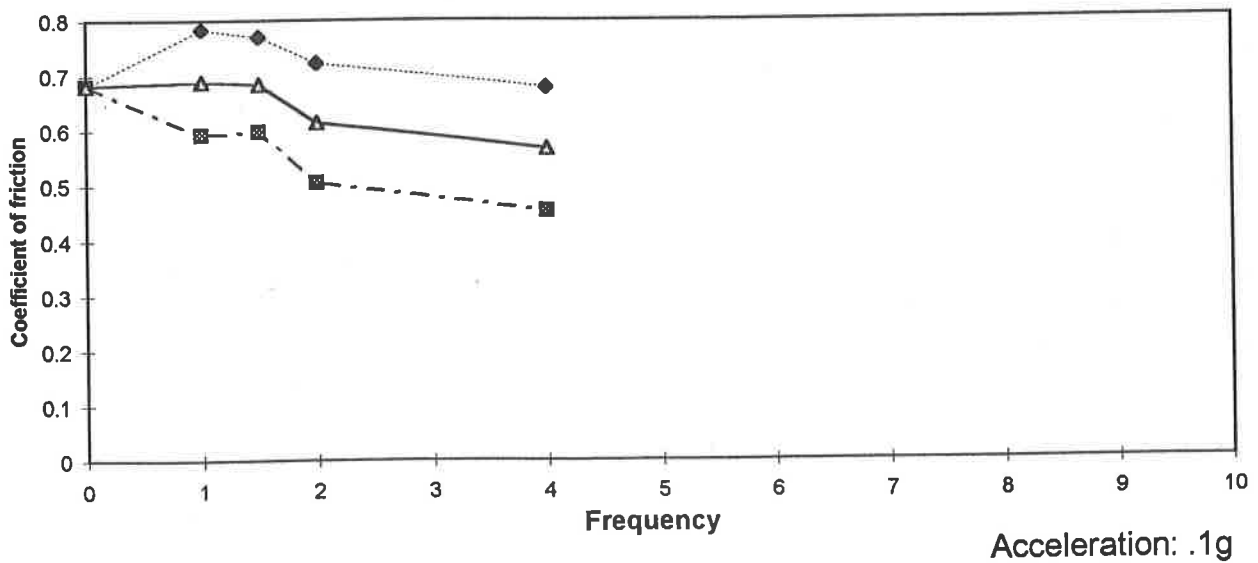
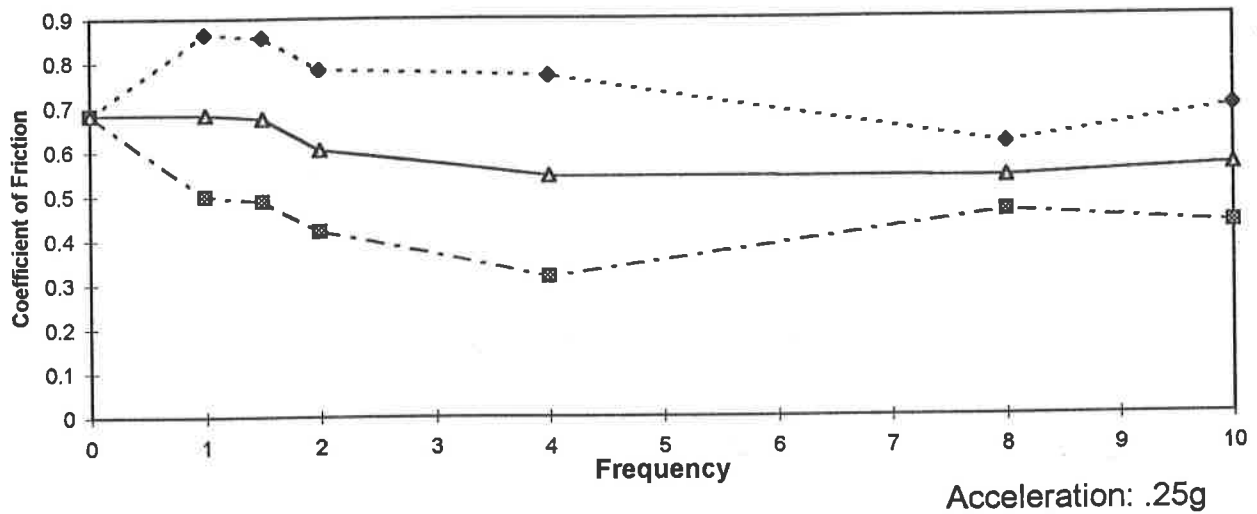
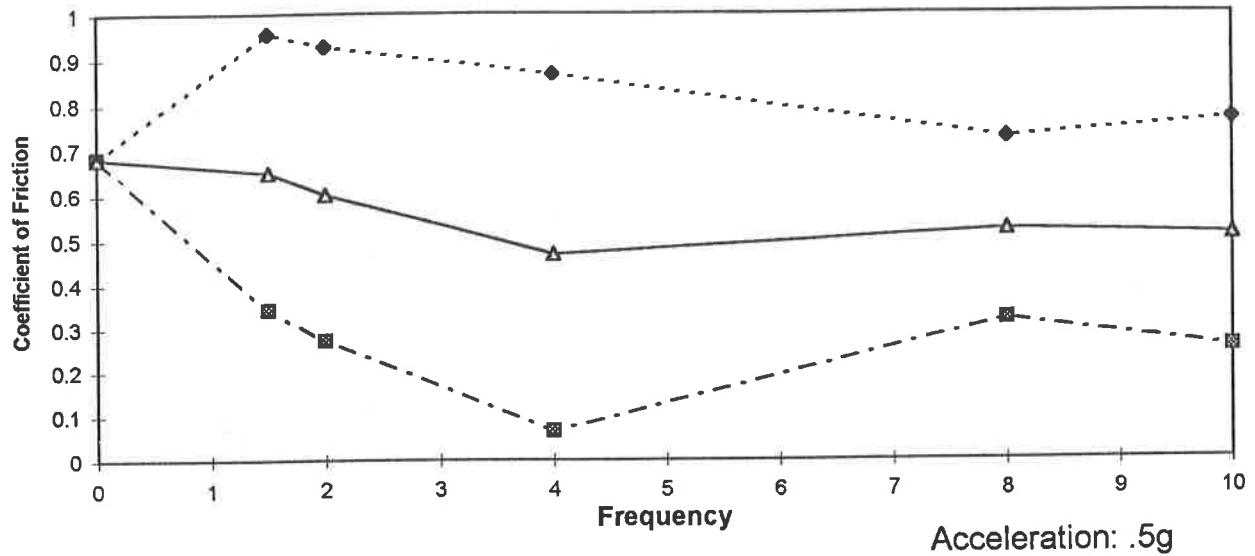


Figure 4.38: Influence of vertical vibration on the coefficient of friction

Deck: Smooth Hardwood

Skid: Rubber Mat

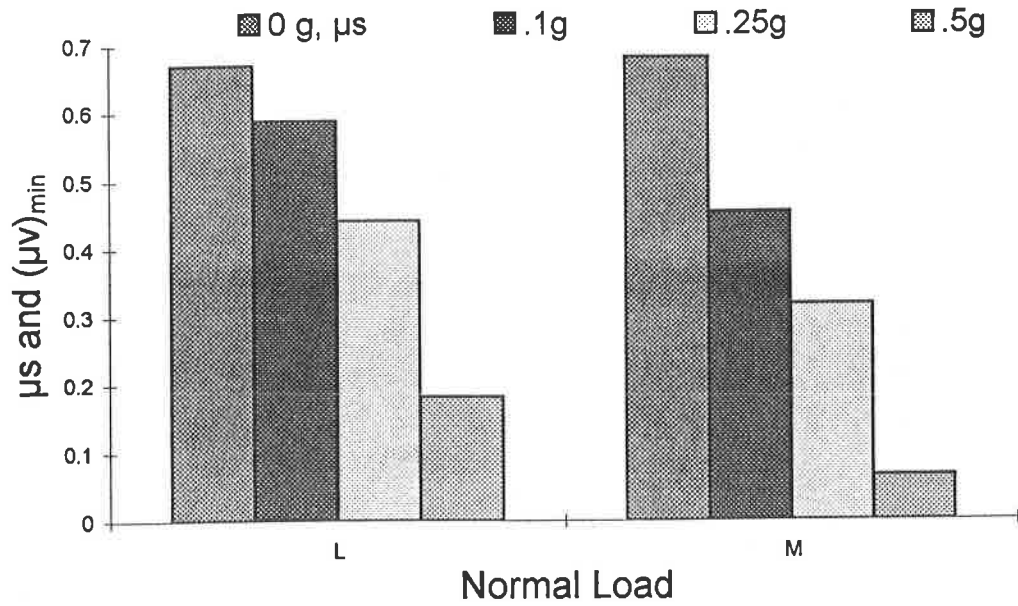


Figure 4.39: Influence of vertical acceleration and normal load on the minimum value of friction coefficient

Deck: Smooth Hardwood

Load: L

Skid: Plastic Skid

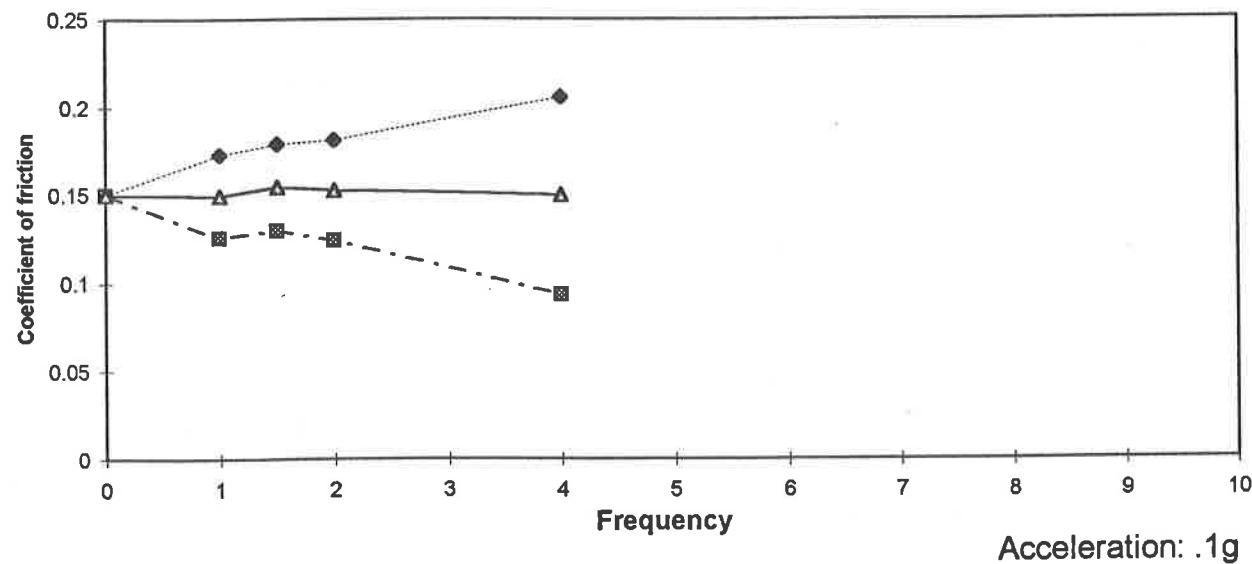
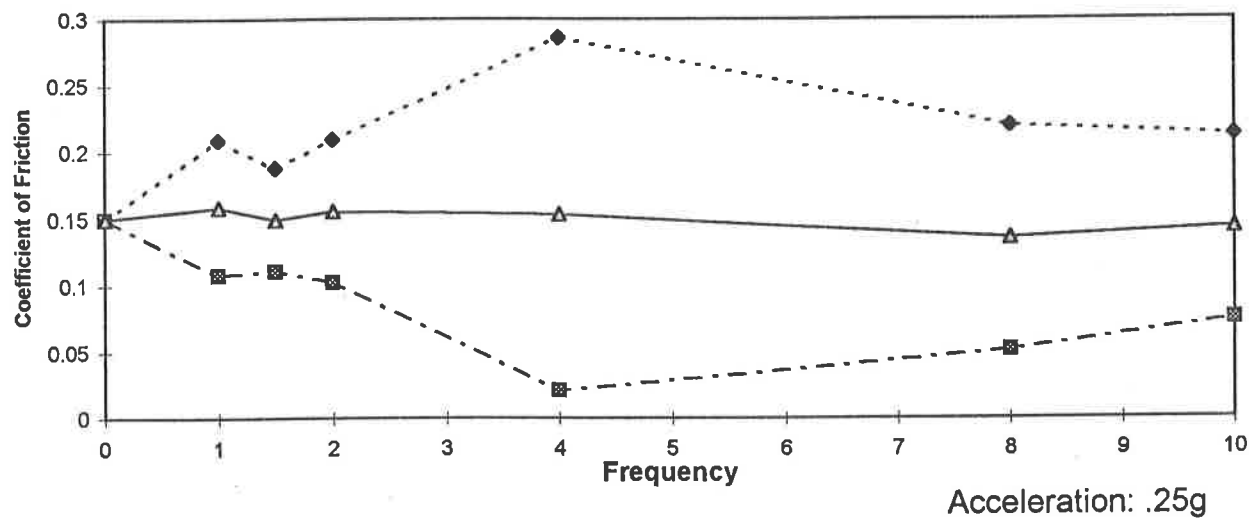
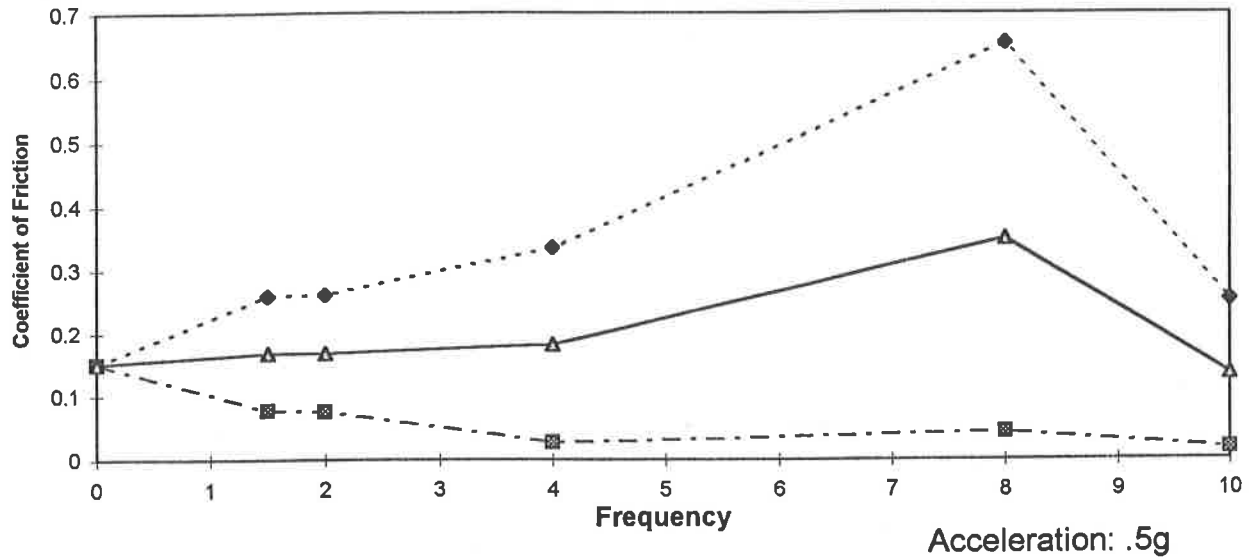


Figure 4.40: Influence of vertical vibration on the coefficient of friction

Deck: Smooth Hardwood      Load: M      Skid: Plastic Skid

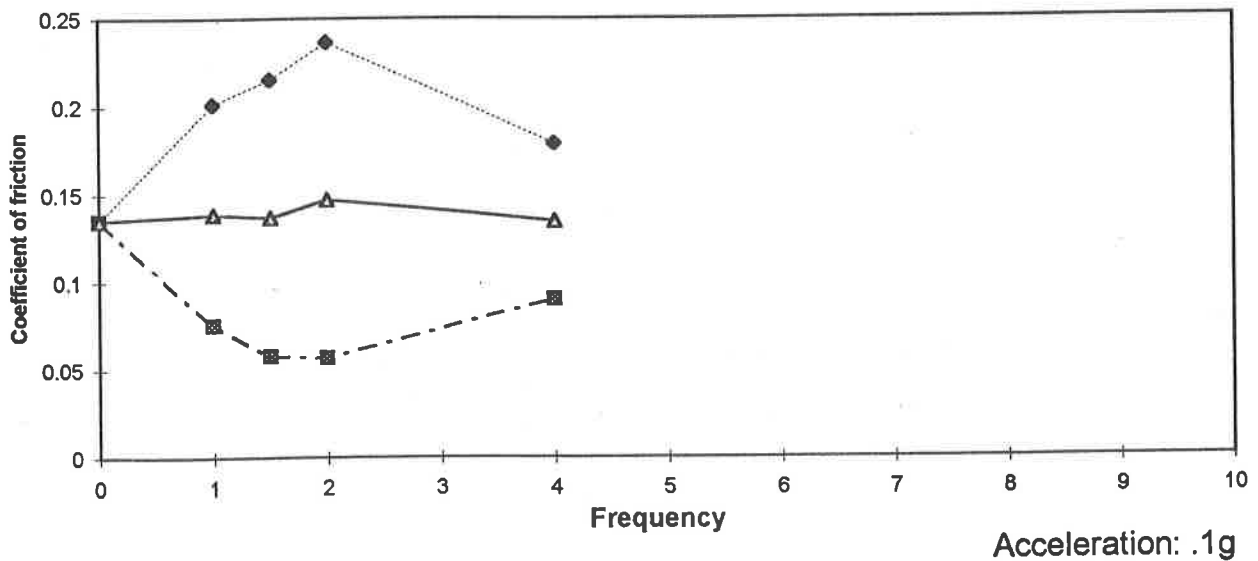
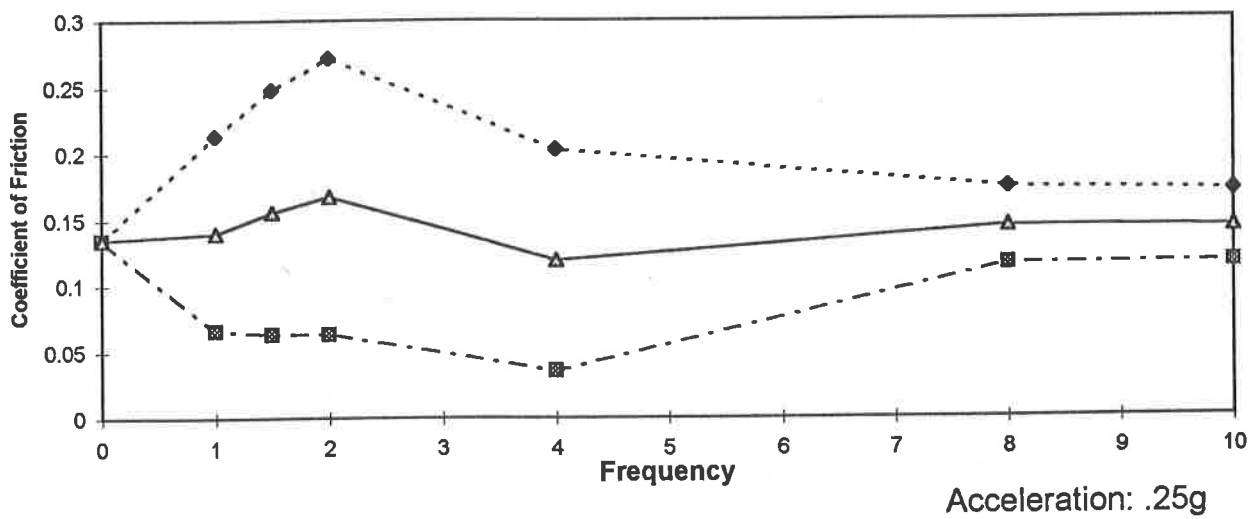
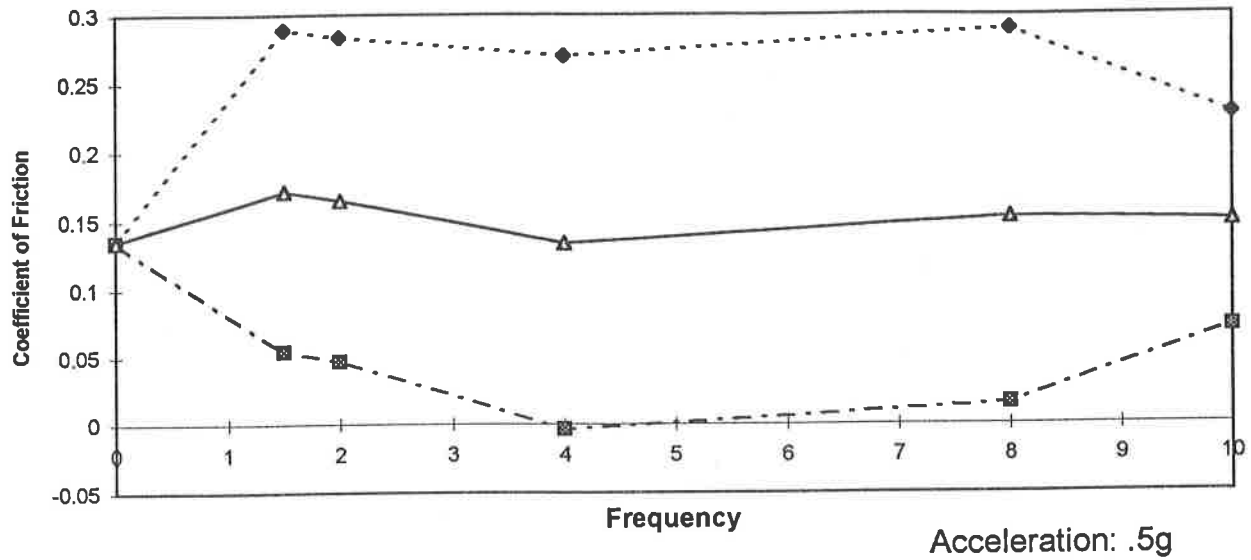


Figure 4.41: Influence of vertical vibration on the coefficient of friction

Deck: Smooth Hardwood

Load: H

Skid: Plastic

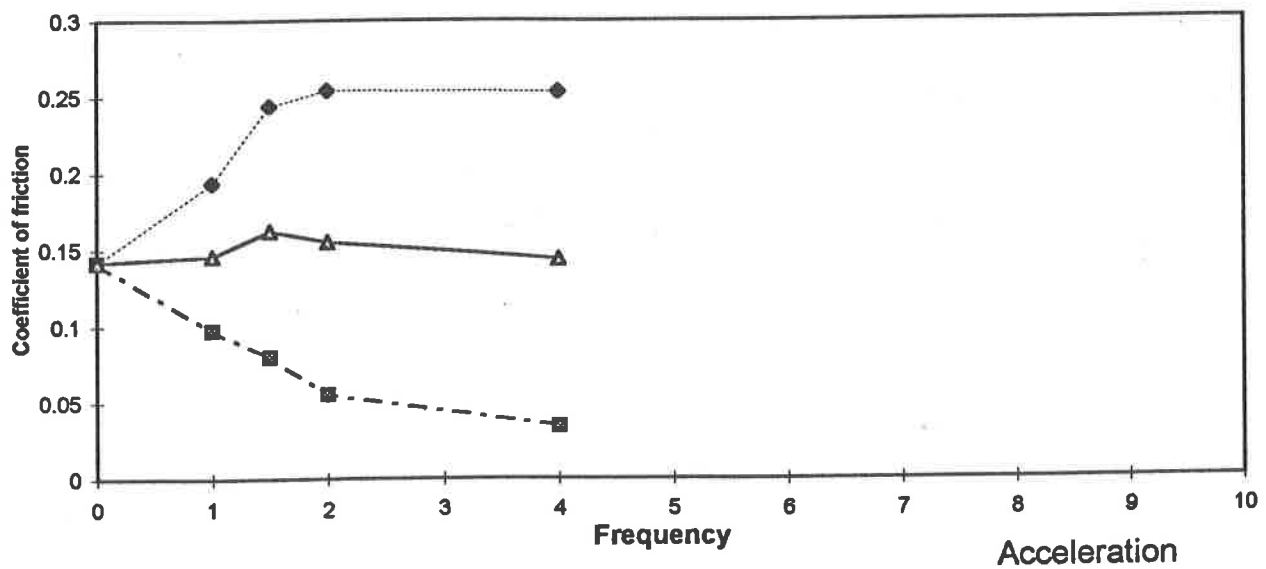
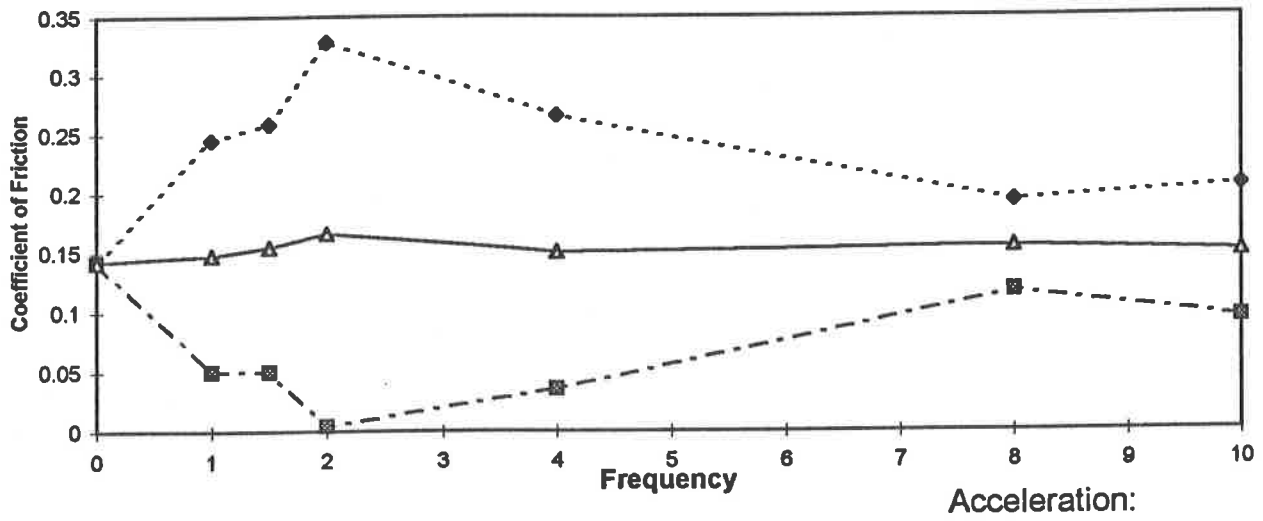
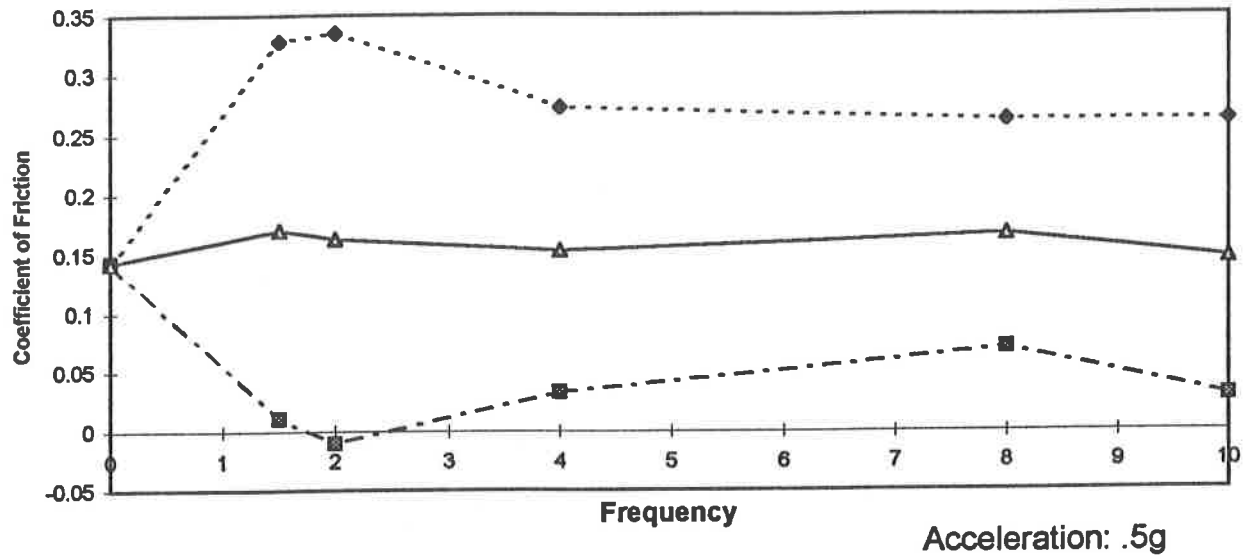


Figure 4.42: Influence of vertical vibration on the coefficient of friction



plastic skid also resulted in loss of contact in the 2-4 Hz frequency range under medium and high normal loads, as shown in Figure 4.43.

The friction coefficients measured between smooth steel and smooth hardwood deck subject to vertical vibration are presented in Figures 4.44 to 4.47. The mean coefficient under medium and high loads and low level acceleration in the 1-2 Hz frequency range is observed to be higher than the corresponding  $\mu_s$  values. The results show similar trends in variations in minimum and mean values of  $\mu_v$  measured under sinusoidal vibration. The minimum values of  $\mu_v$  are observed to be lowest in the 4-10 Hz frequency range, as shown in the figures, irrespective of the normal load. Figure 4.47 summarizes the influence of normal load and magnitude of vertical acceleration on the minimum values of  $\mu_v$ .

#### 4.2.1.4 X-GROOVE ALUMINUM DECK

The measurements performed with different skid materials and X-groove aluminum deck also revealed similar trends in the mean, maximum and minimum values of coefficients of friction. Each combination revealed significantly lower values of minimum friction coefficients under vibration, while the mean values were observed to be comparable with those measured under static conditions. The minimum values of friction coefficients decreased considerably with increase in both the normal load and the magnitude of acceleration.

The mean, maximum, and minimum values of friction coefficients obtained for steel pads, concrete and plastic skid materials are presented in Figures 4.48-4.50, 4.52-4.53 and 4.55-4.57, respectively. Figures 4.51, 4.54 and 4.58 summarize the influence of normal load and the magnitude of vertical acceleration on the minimum

Deck: Smooth Hardwood

Skid: Plastic Skid

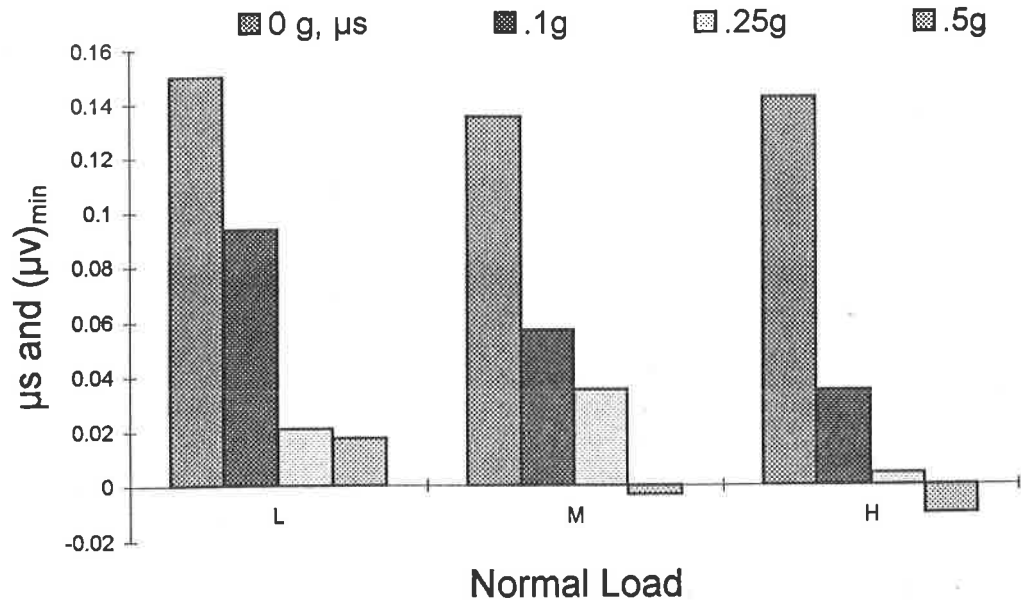


Figure 4.43: Influence of vertical acceleration and normal load on the minimum value of friction coefficient

Deck: Smooth Hardwood

Load: L

Skid: Smooth Steel

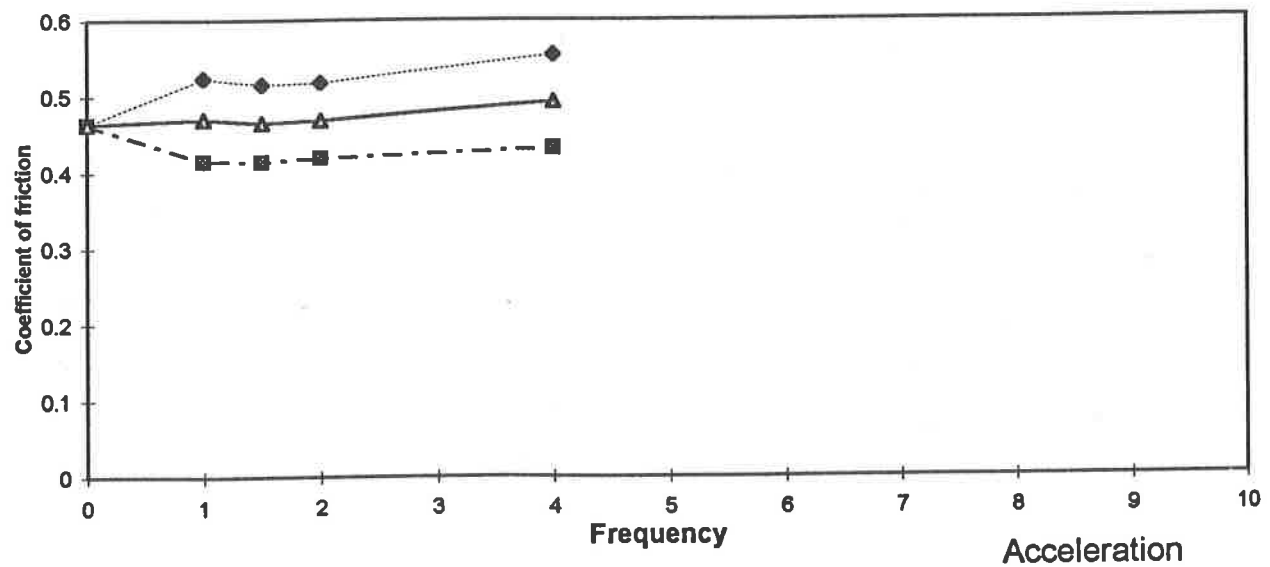
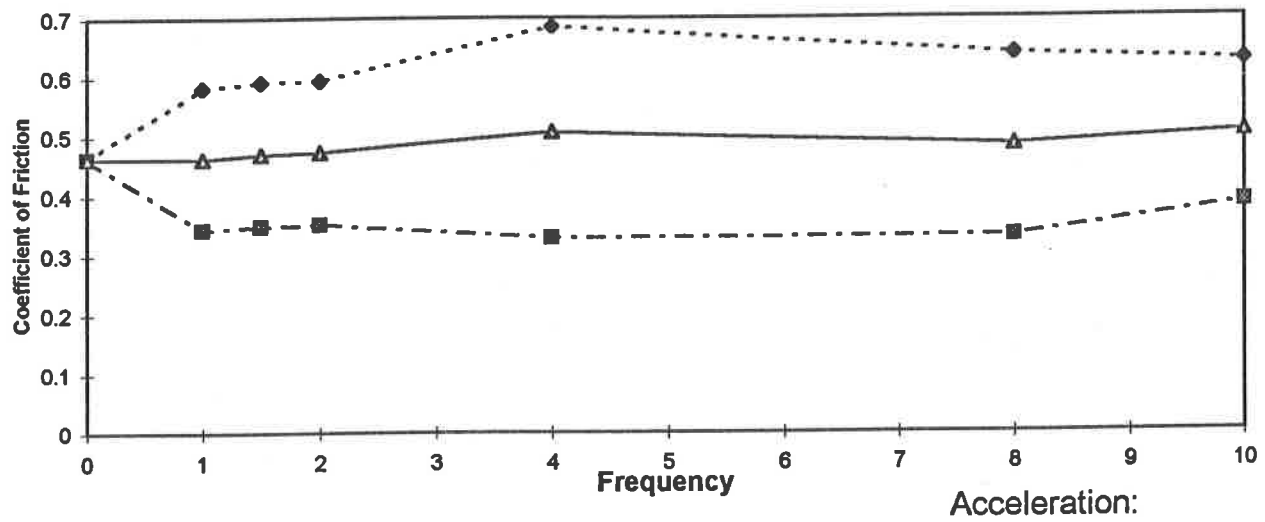
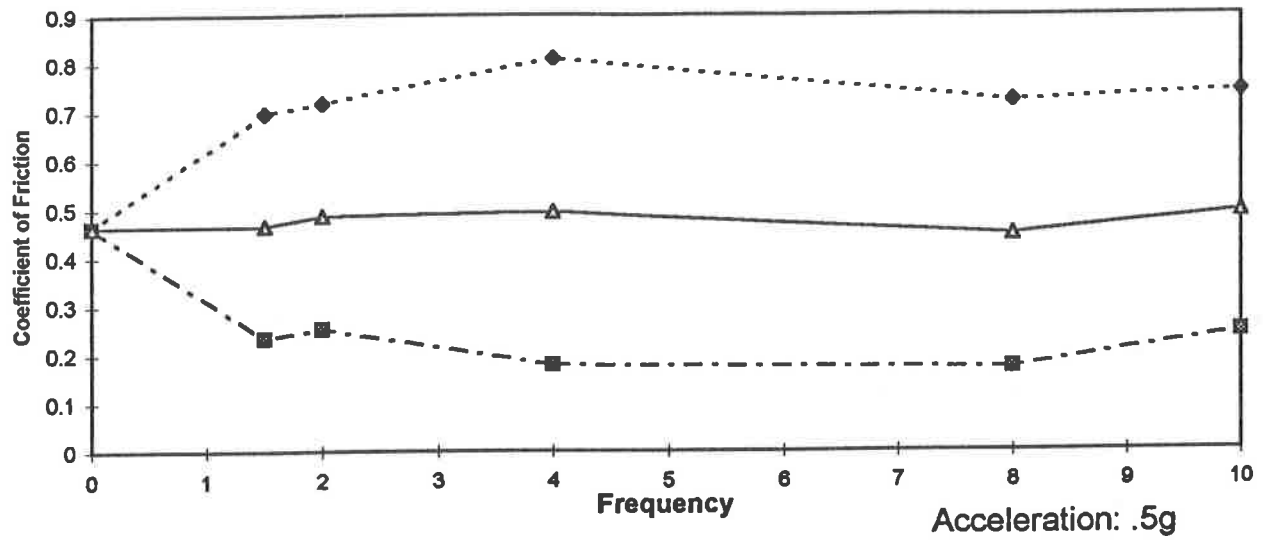


Figure 4.44: Influence of vertical vibration on the coefficient of friction

Deck: Smooth Hardwood      Load: M      Skid: Smooth Steel

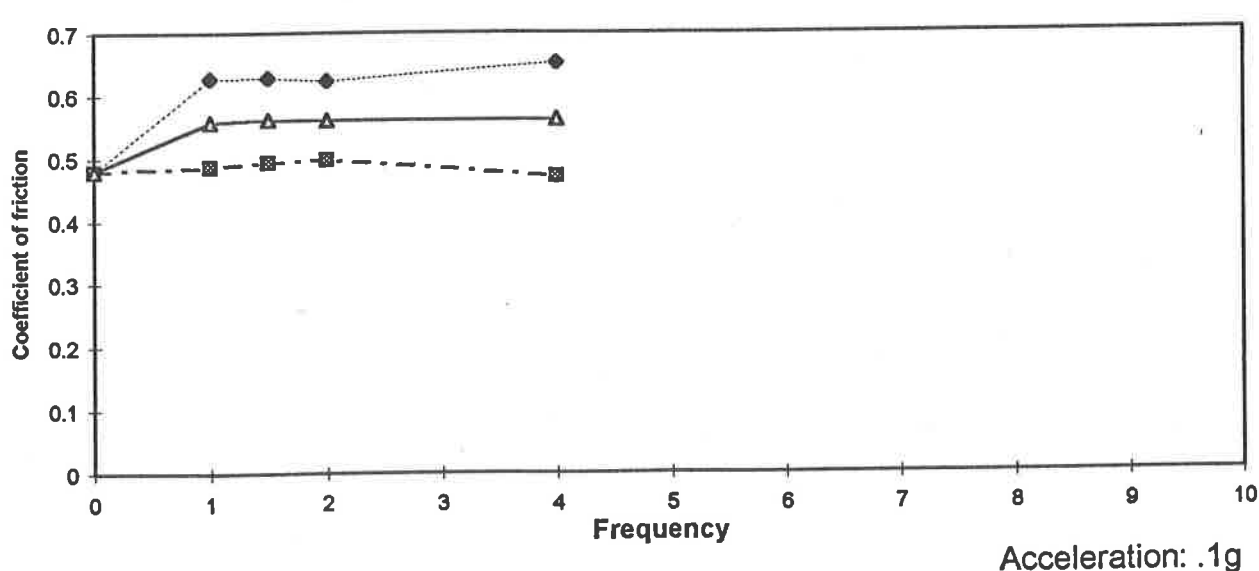
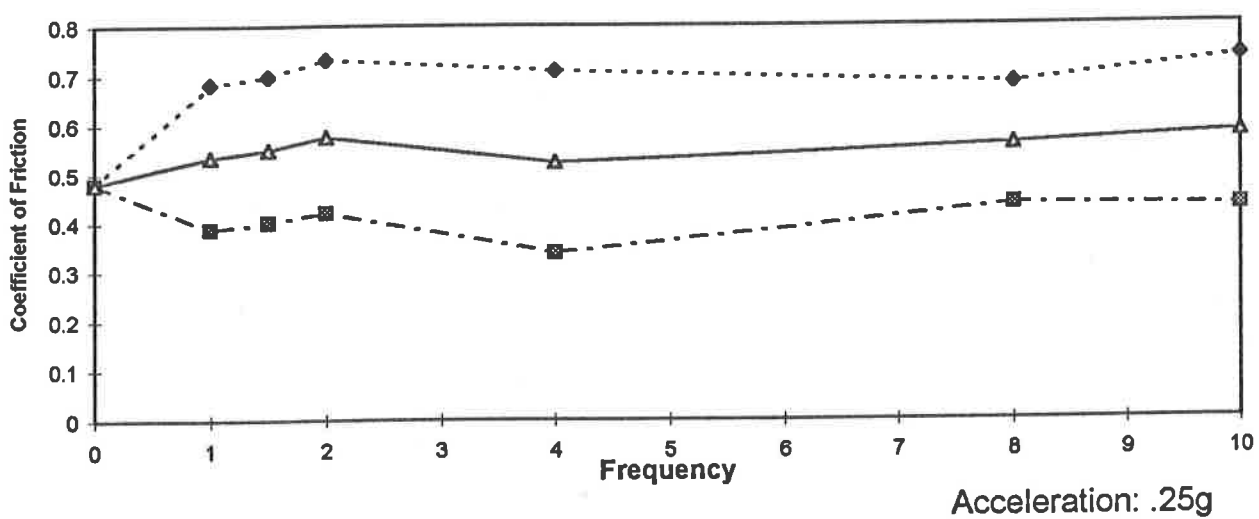
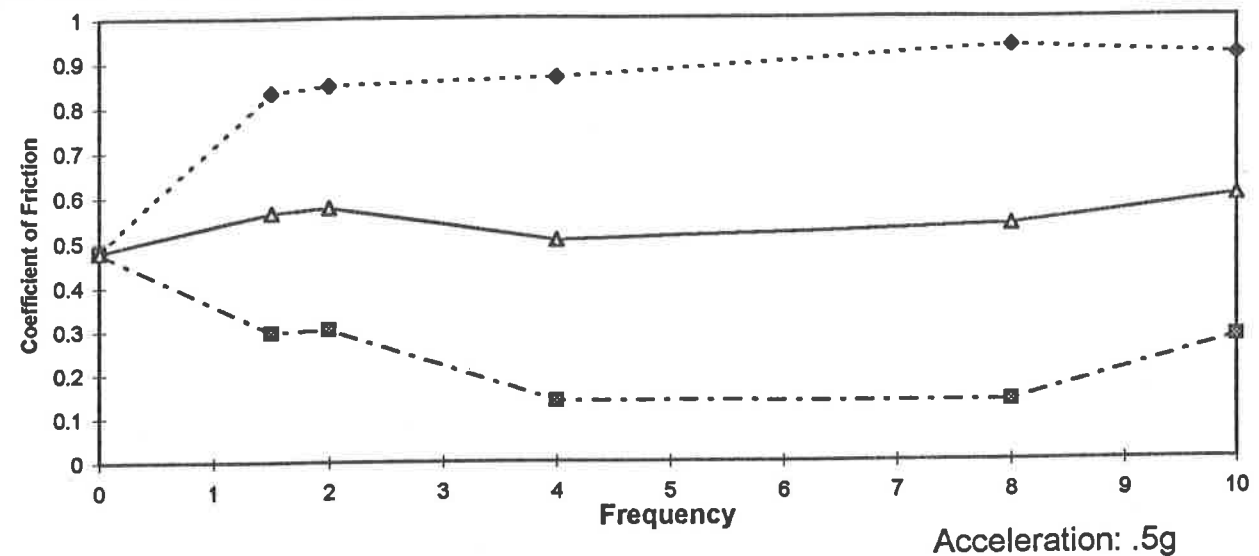


Figure 4.45: Influence of vertical vibration on the coefficient of friction

Deck: Smooth Hardwood

Load: H

Skid: Smooth Steel

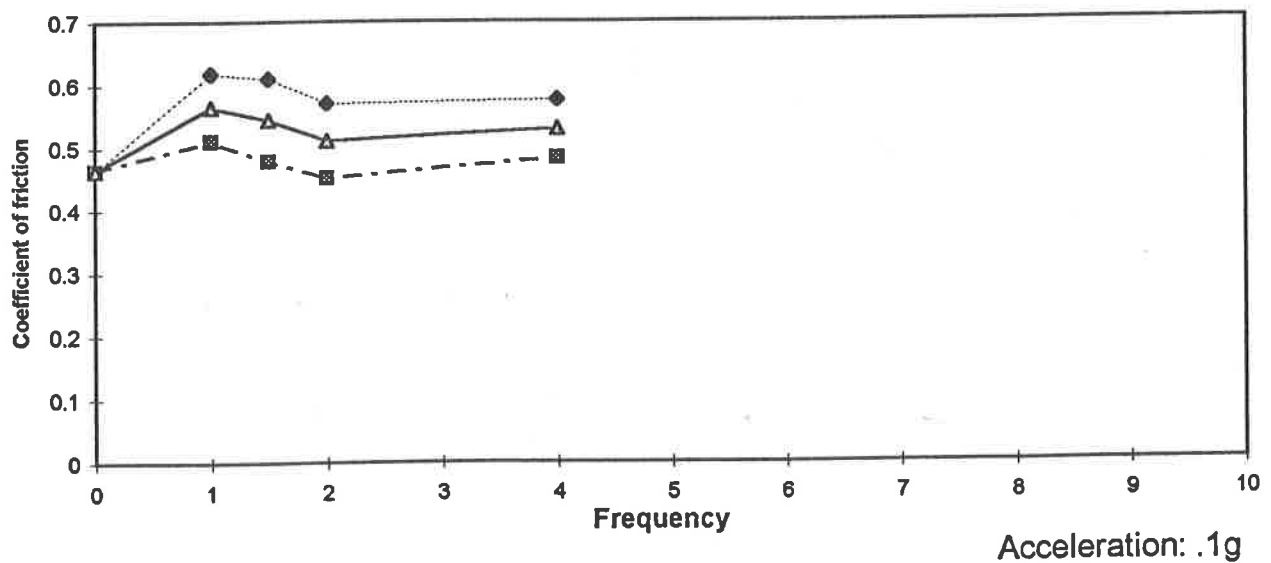
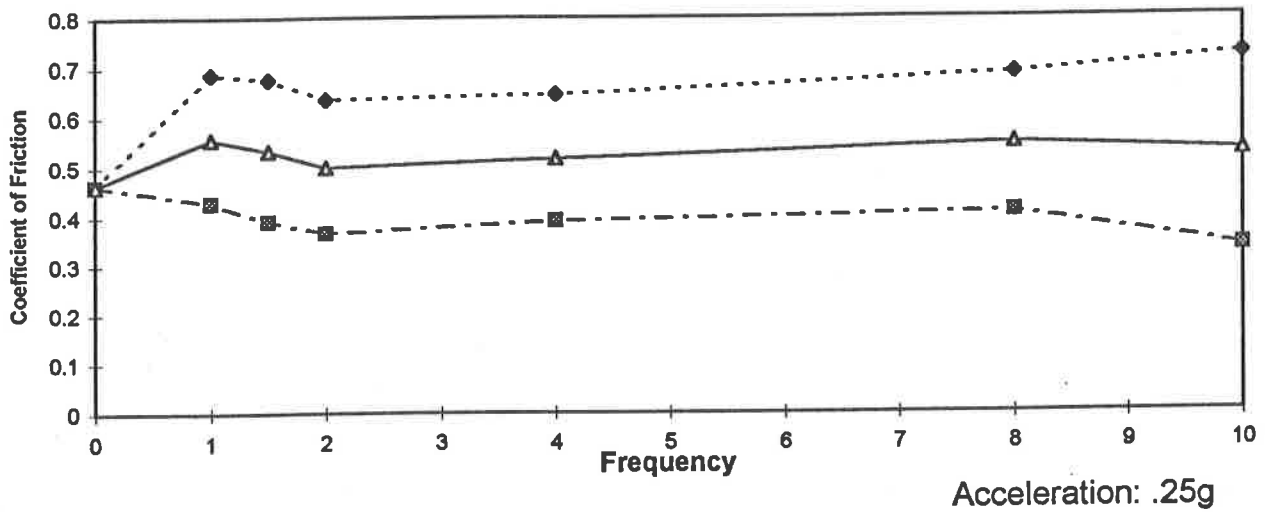
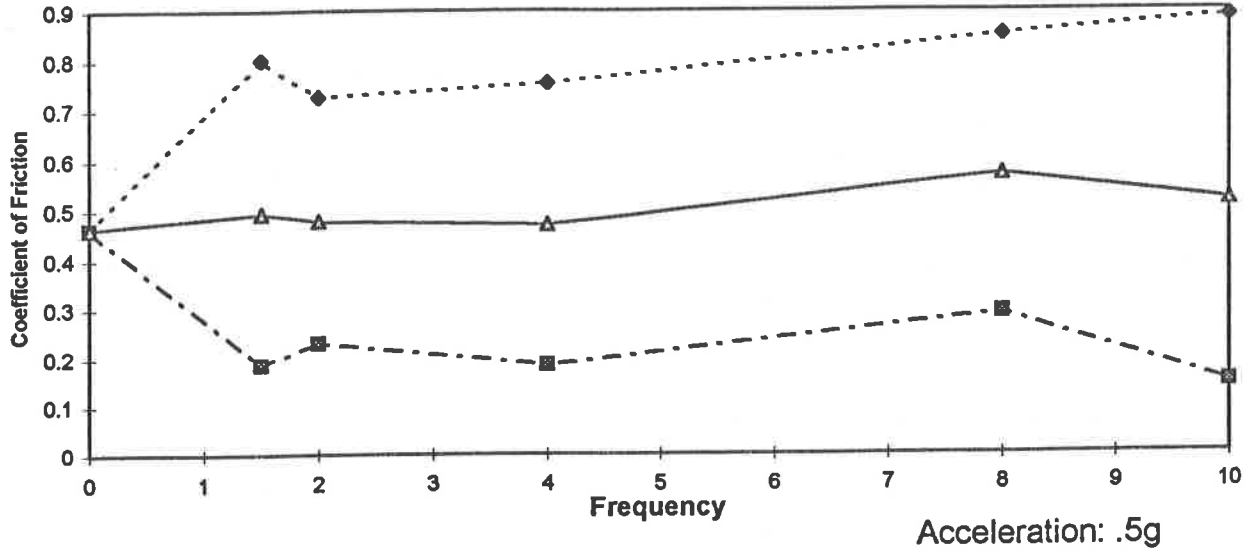


Figure 4.46: Influence of vertical vibration on the coefficient of friction

Deck: Smooth Hardwood

Skid: Smooth Steel

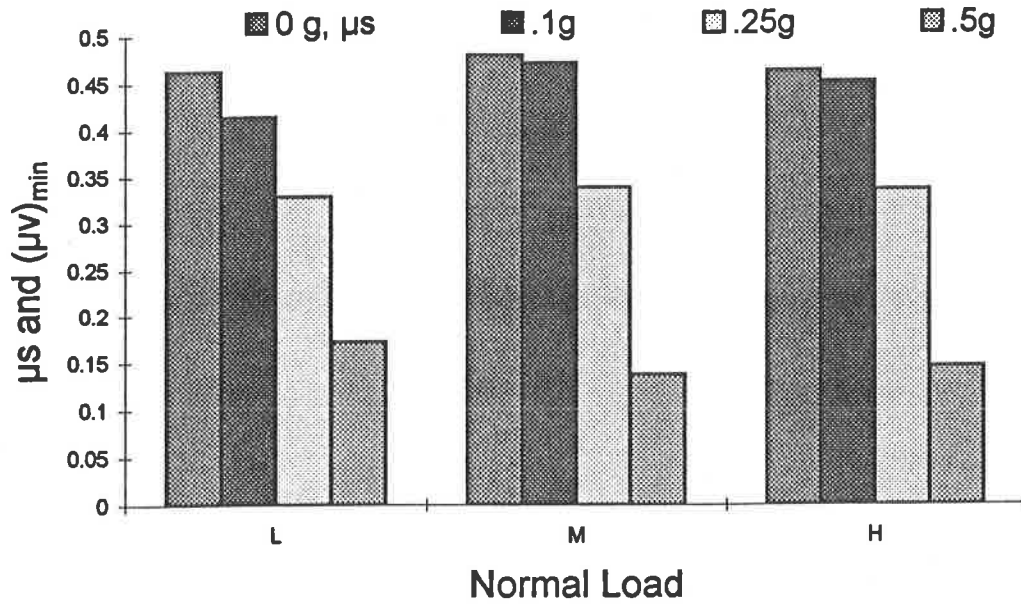


Figure 4.47: Influence of vertical acceleration and normal load on the minimum value of friction coefficient

Deck: X-Groove Aluminum

Load: L

Skid: Steel Pads

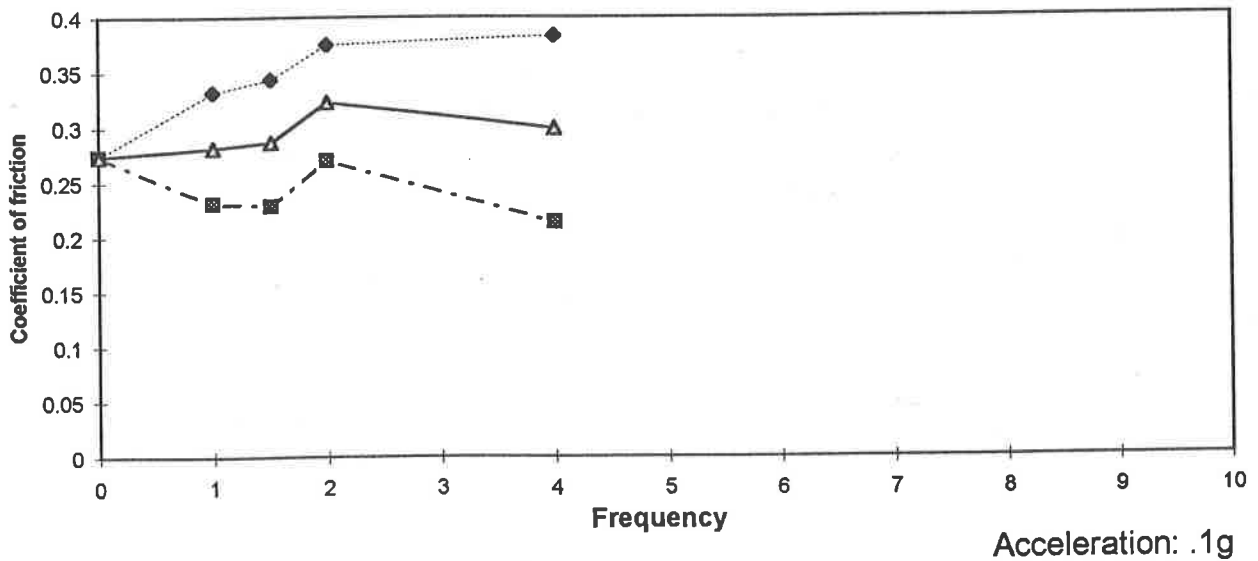
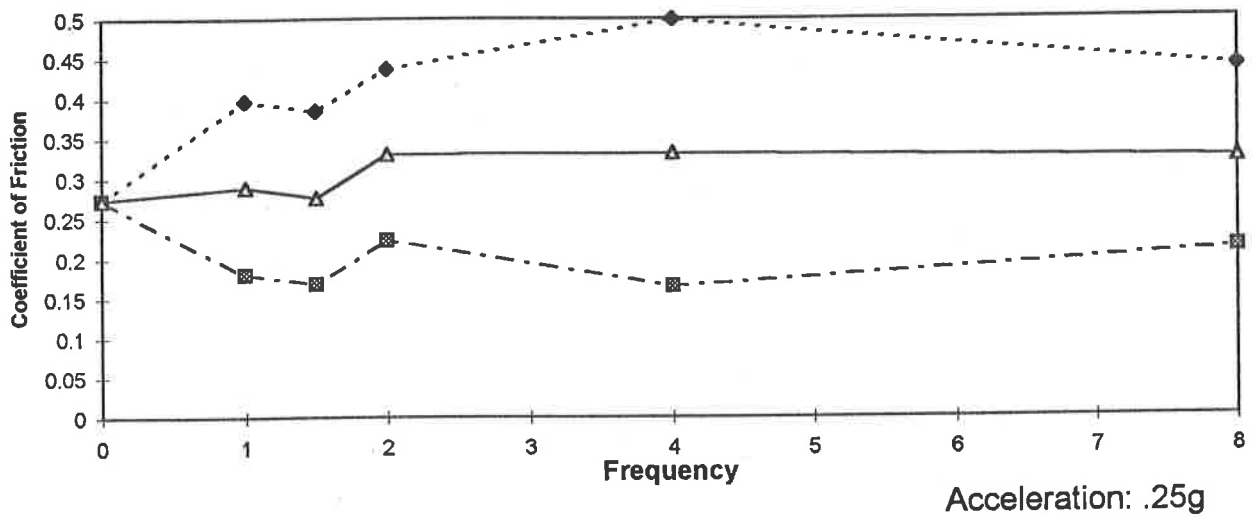
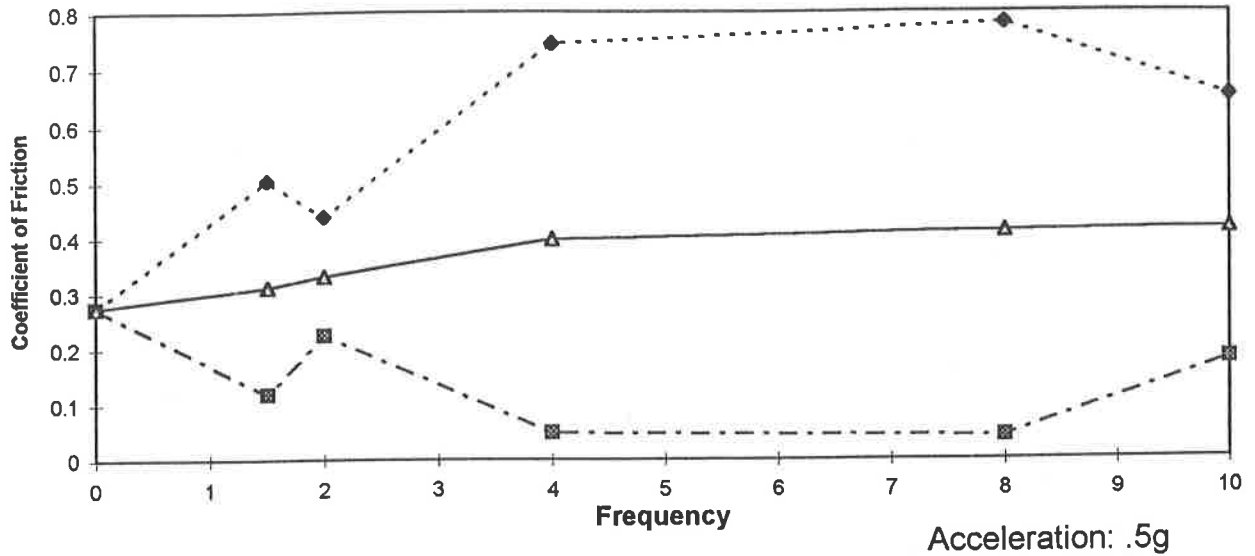


Figure 4.48: Influence of vertical vibration on the coefficient of friction

Deck: X-Groove Aluminum

Load: M

Skid: Steel Pads

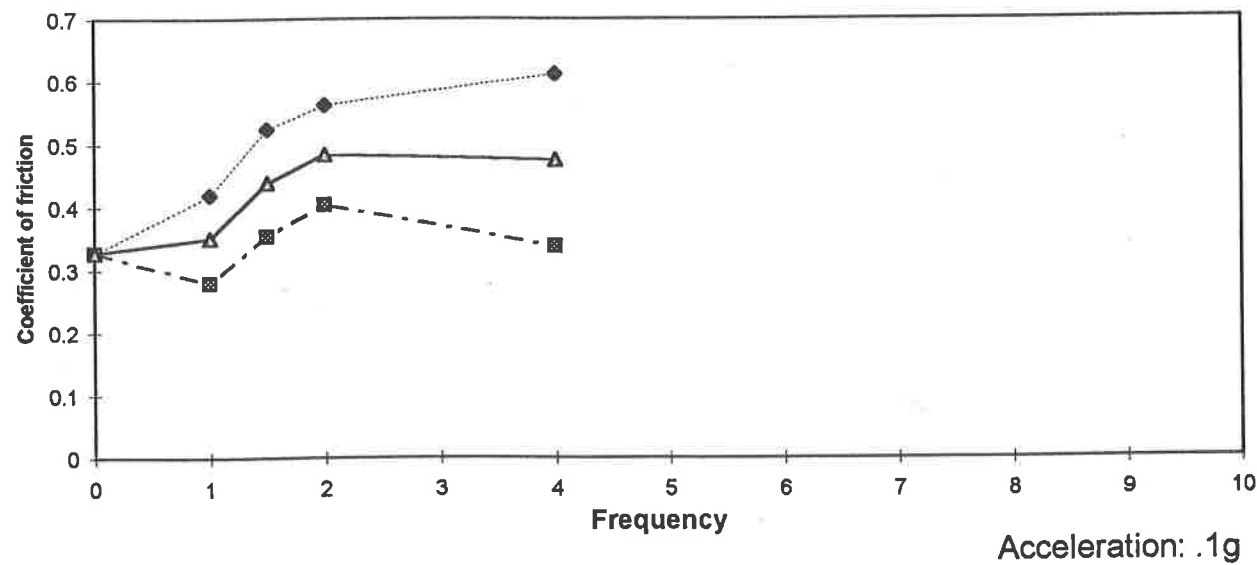
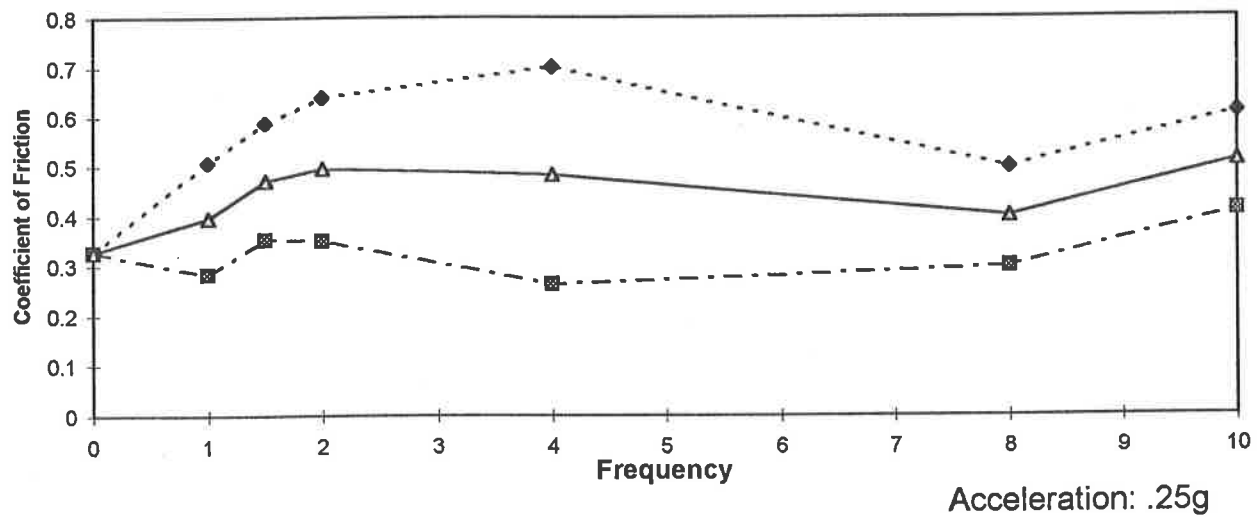
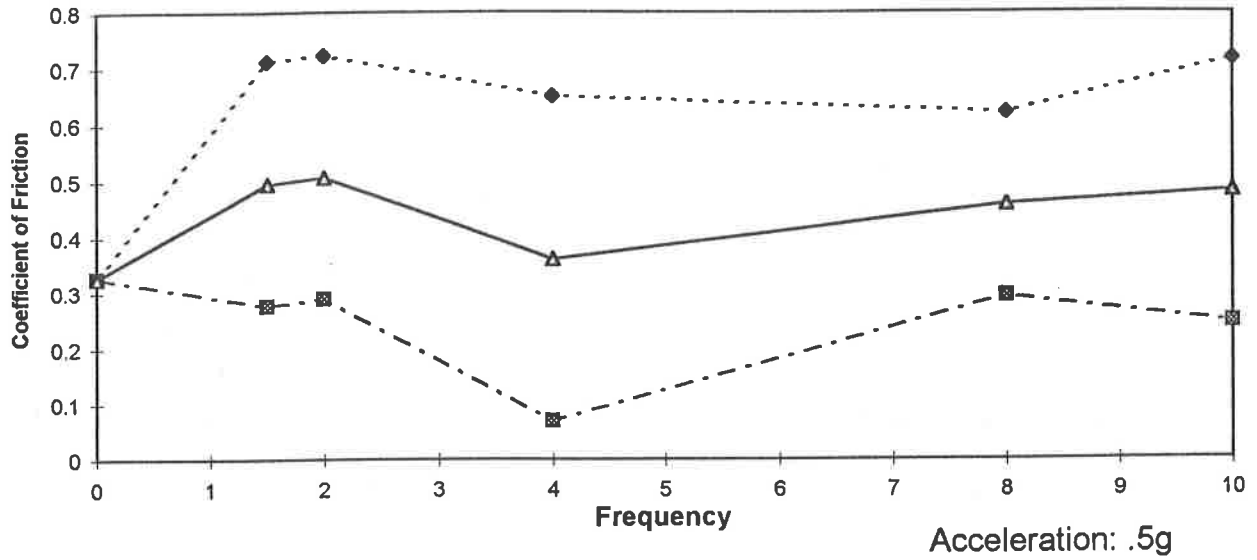


Figure 4.49: Influence of vertical vibration on the coefficient of friction



Deck: X-Groove Aluminum

Load: H

Skid: Steel Pads

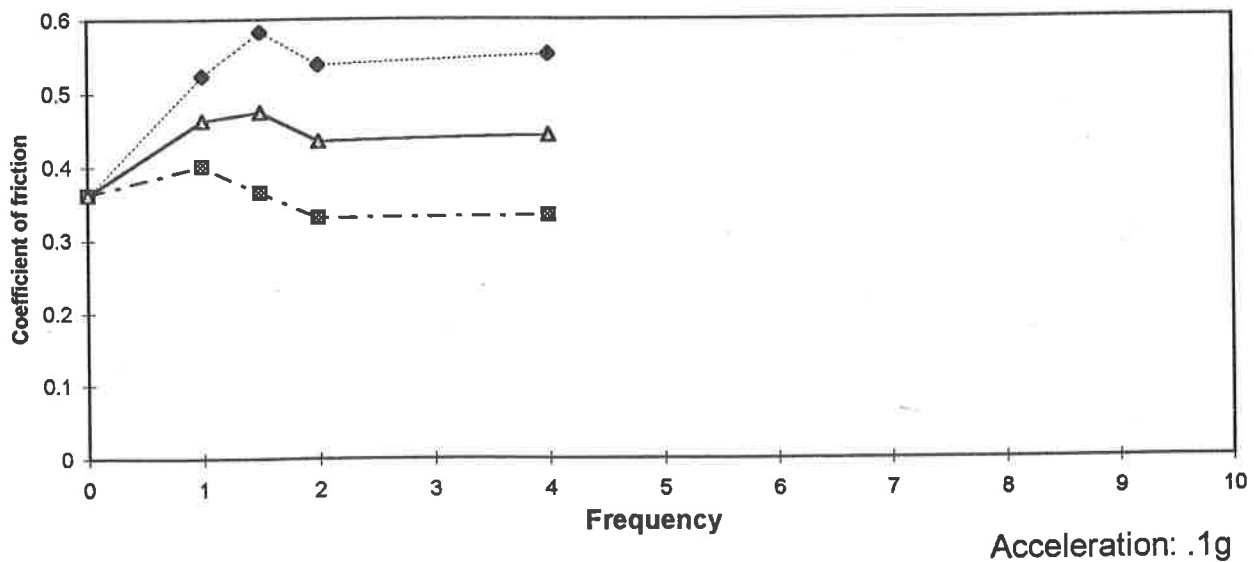
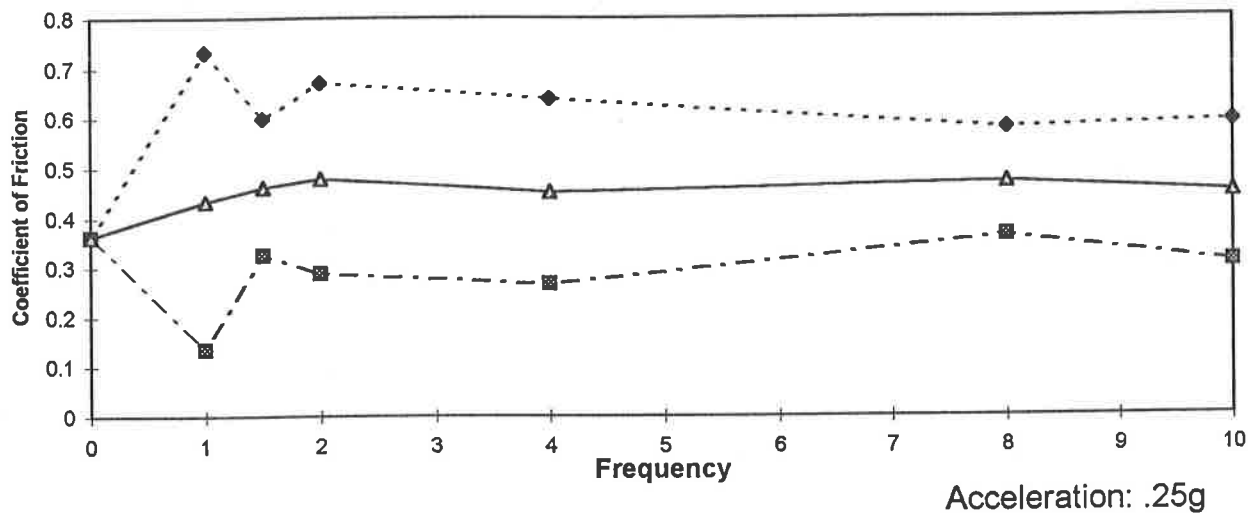
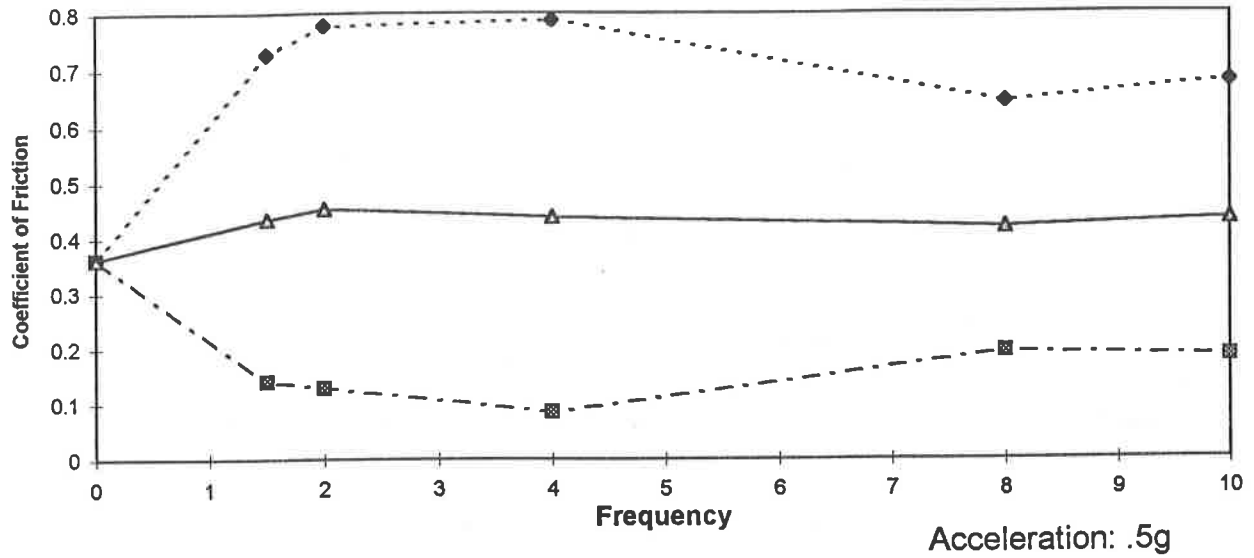


Figure 4.50: Influence of vertical vibration on the coefficient of friction

Deck: X-Groove Aluminum

Skid: Steel Pads

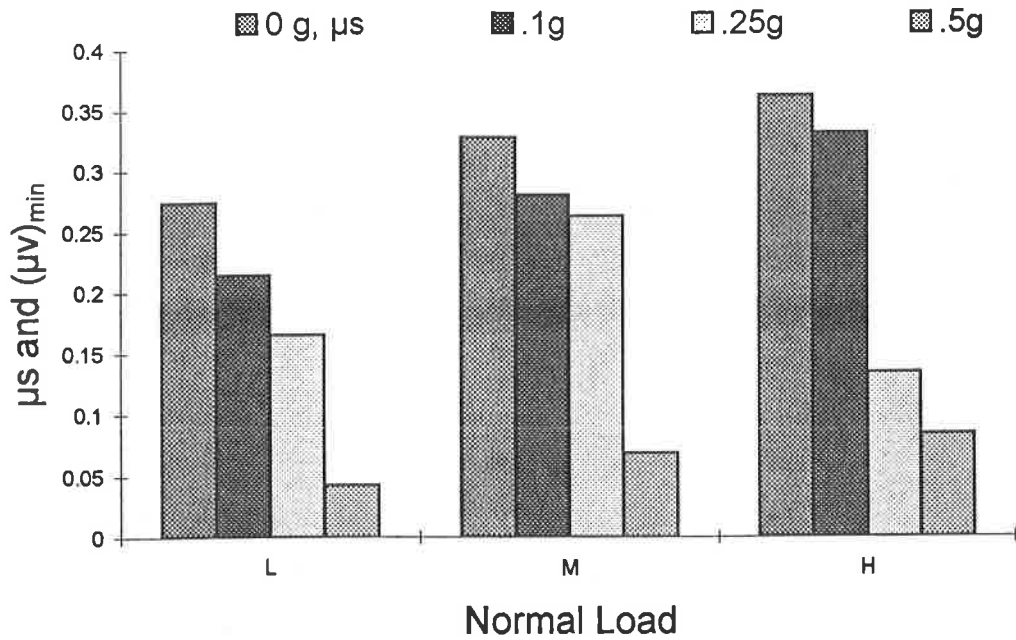


Figure 4.51: Influence of vertical acceleration and normal load on the minimum value of friction coefficient

Deck: X-Groove Aluminum      Load: M      Skid: Concrete Blocks

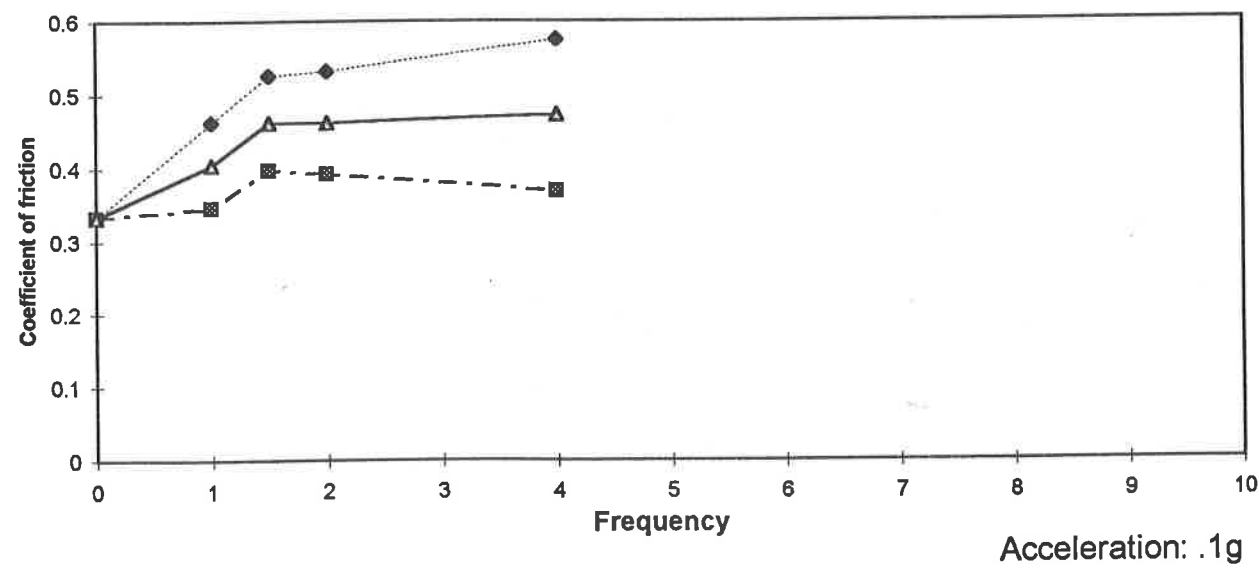
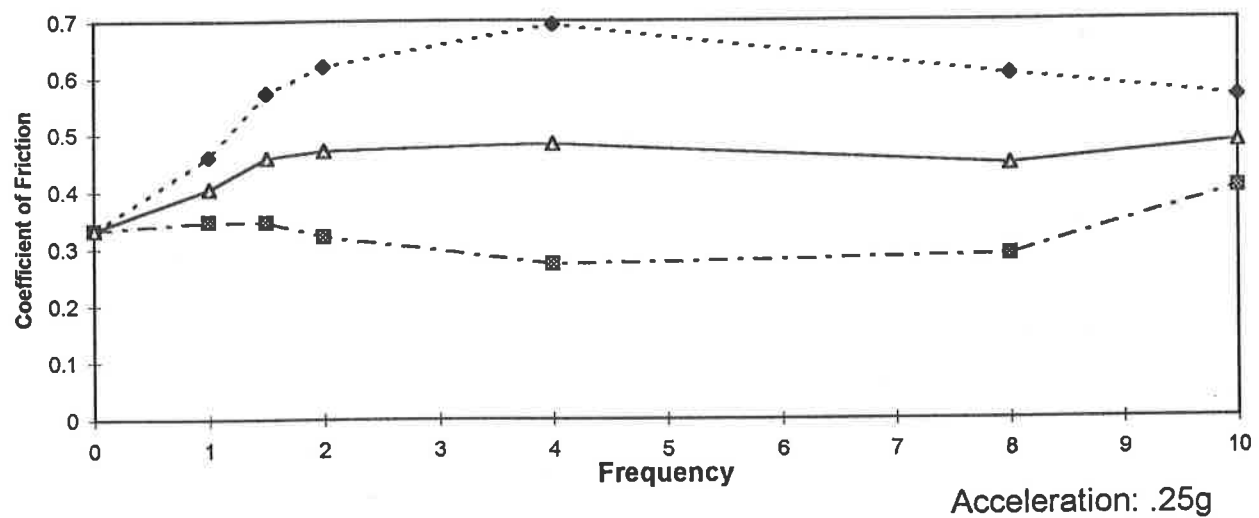
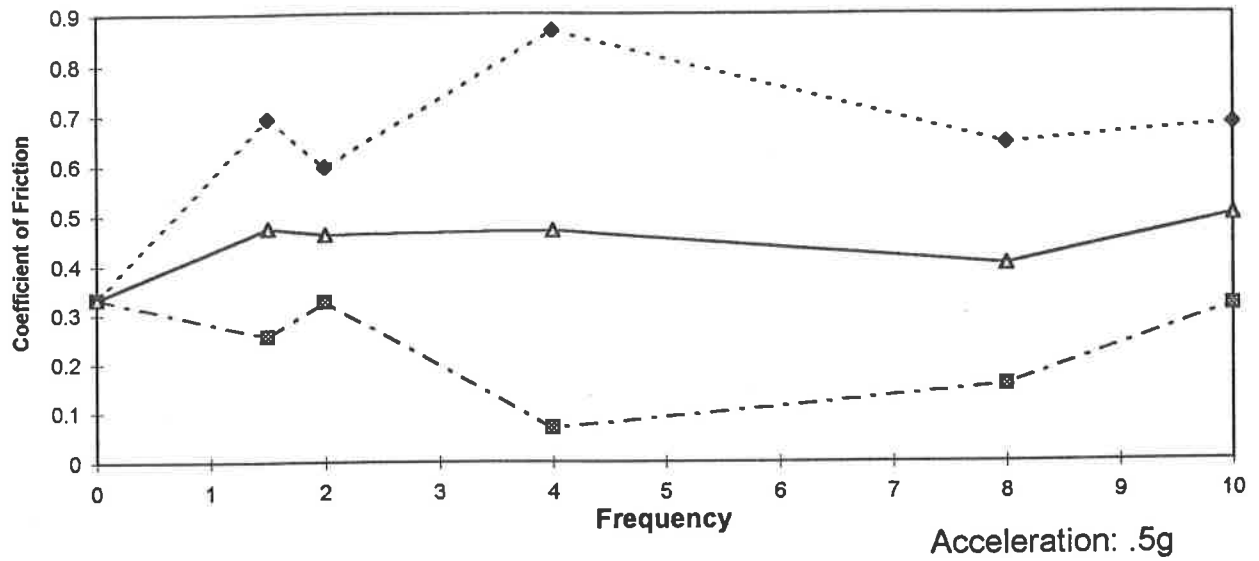


Figure 4.52: Influence of vertical vibration on the coefficient of friction

Deck: X-Groove Aluminum      Load: H      Skid: Concrete Blocks

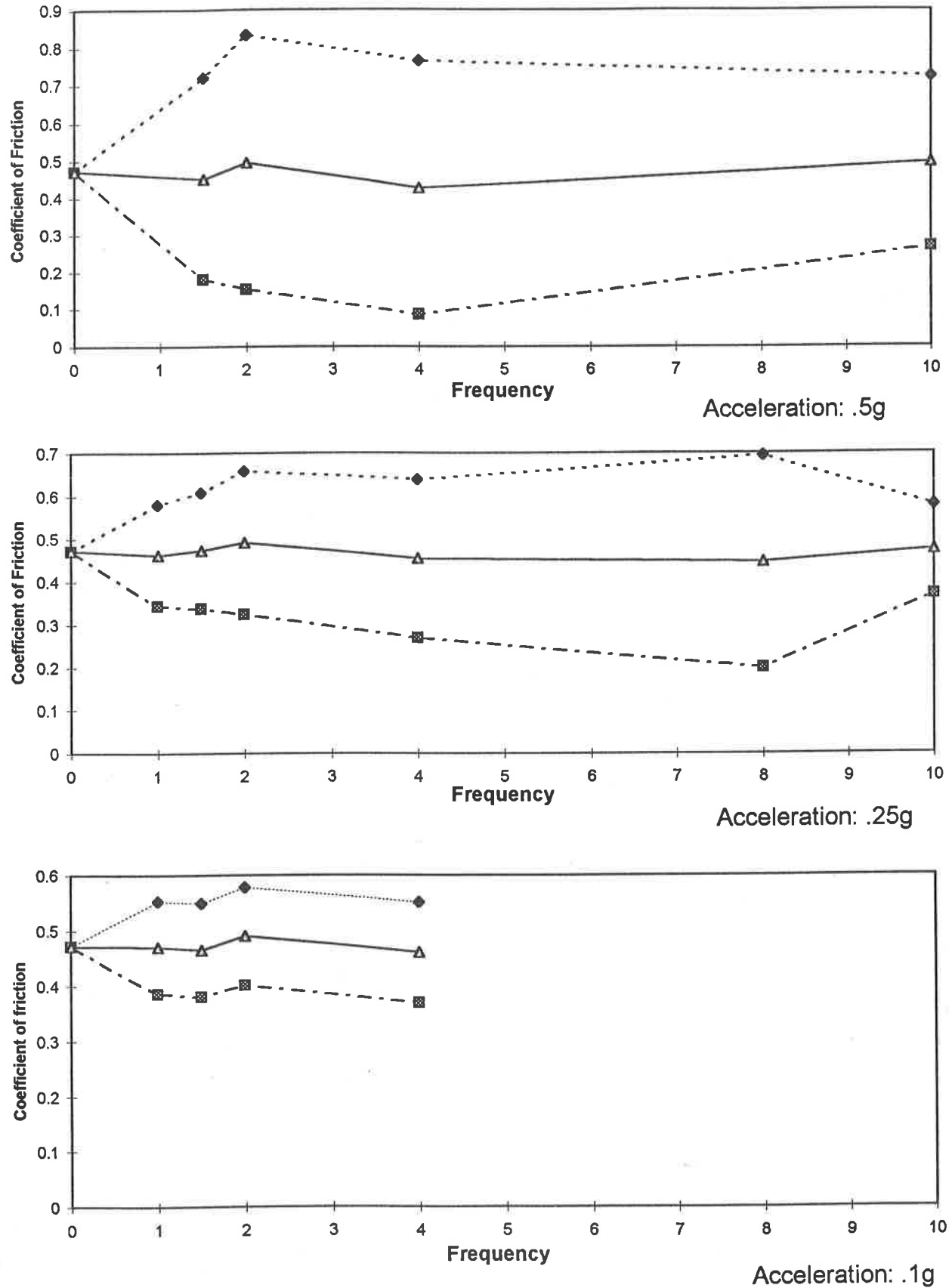


Figure 4.53: Influence of vertical vibration on the coefficient of friction

Deck: X-Groove Aluminum

Skid: Concrete Blocks

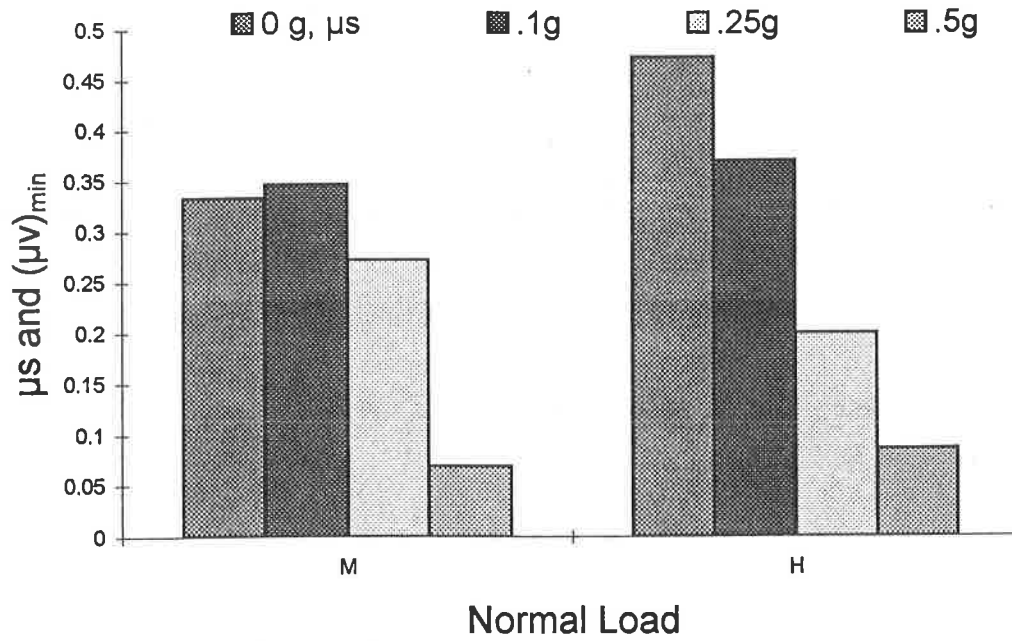


Figure 4.54: Influence of vertical acceleration and normal load on the minimum value of friction coefficient

Deck: X-Groove Aluminum

Load: L

Skid: Plastic Skid

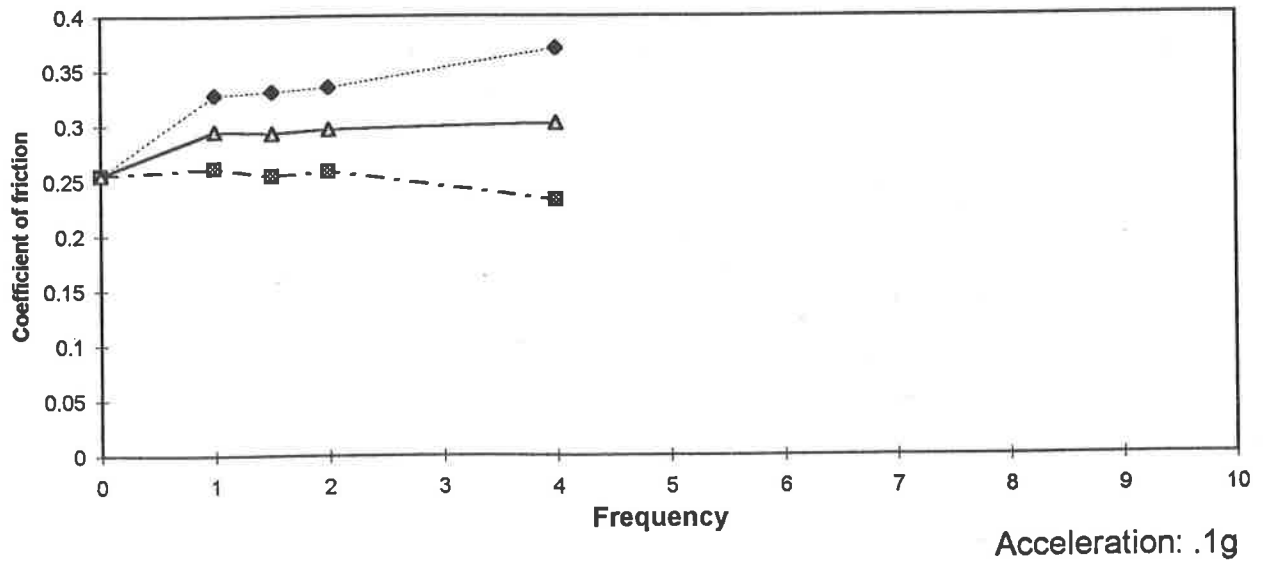
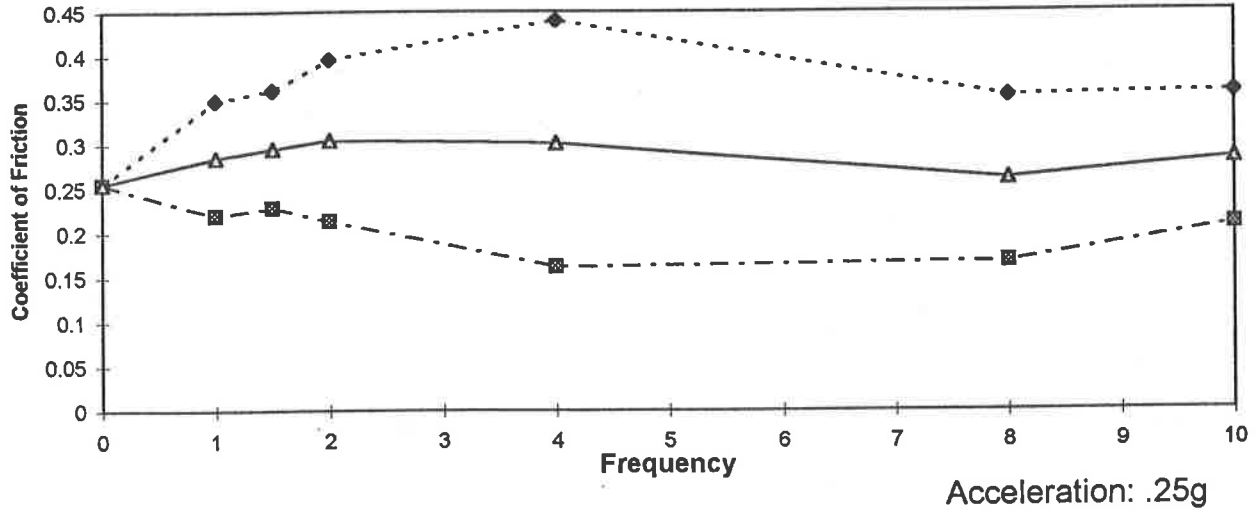
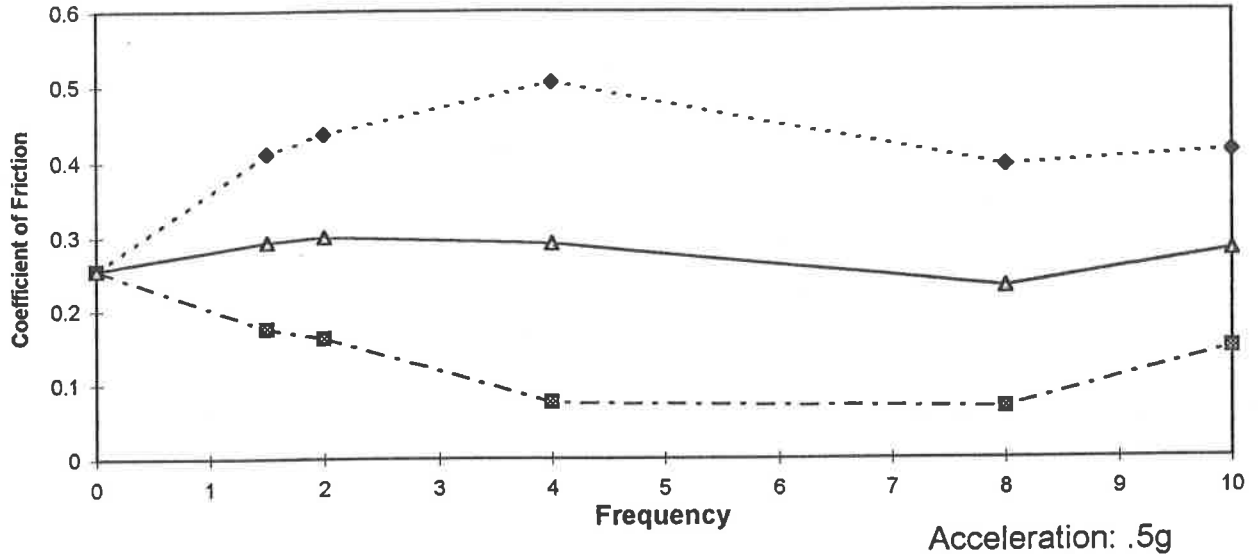


Figure 4.55: Influence of vertical vibration on the coefficient of friction

Deck: X-Groove Aluminum

Load: M

Skid: Plastic Skid

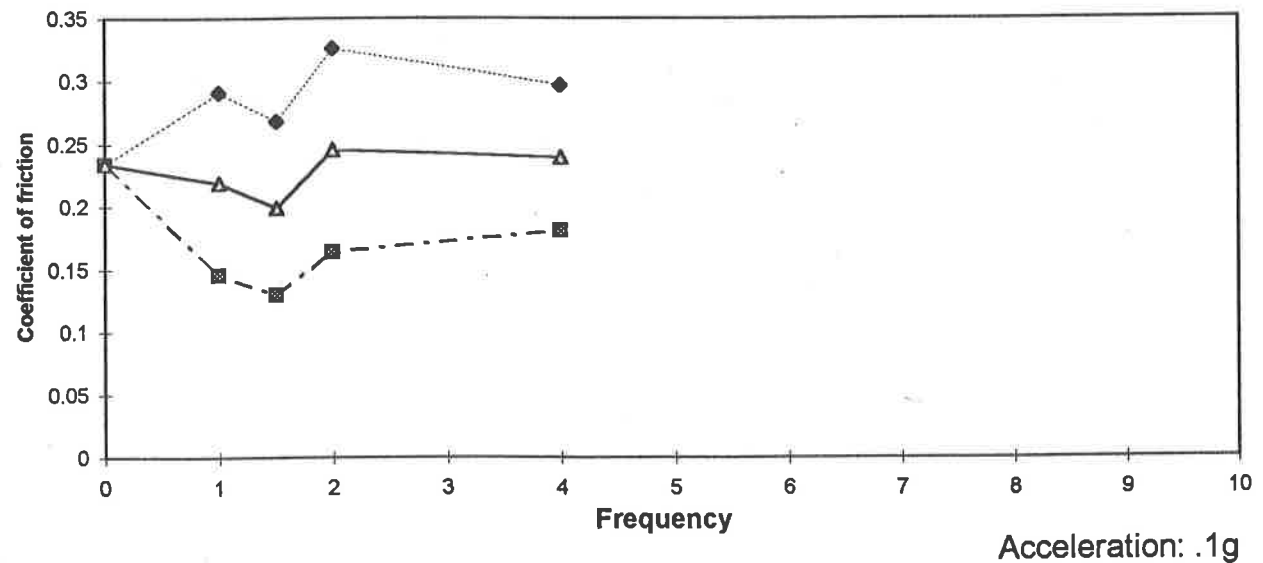
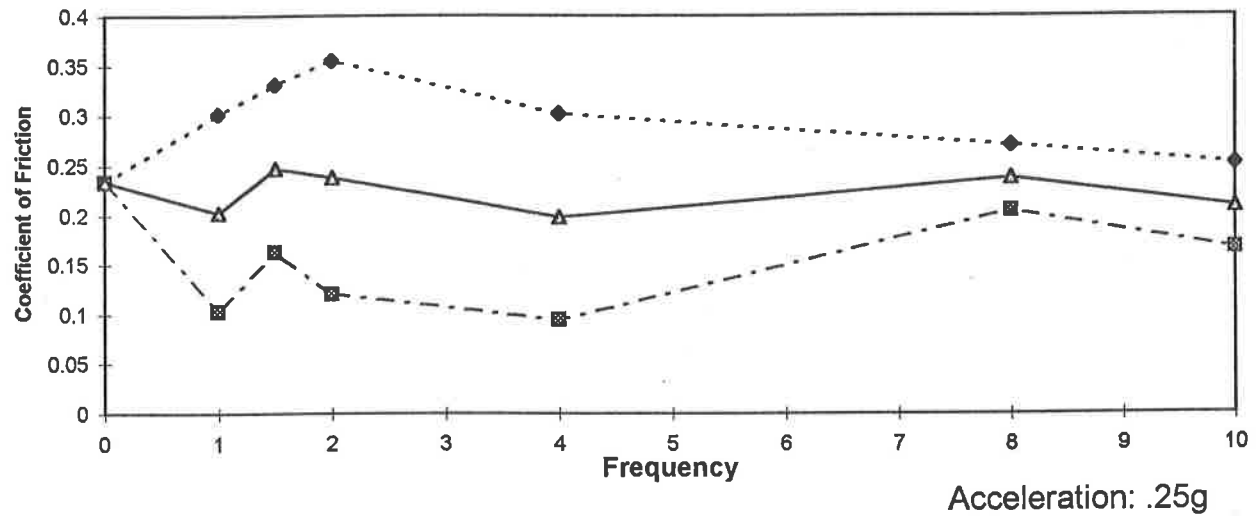
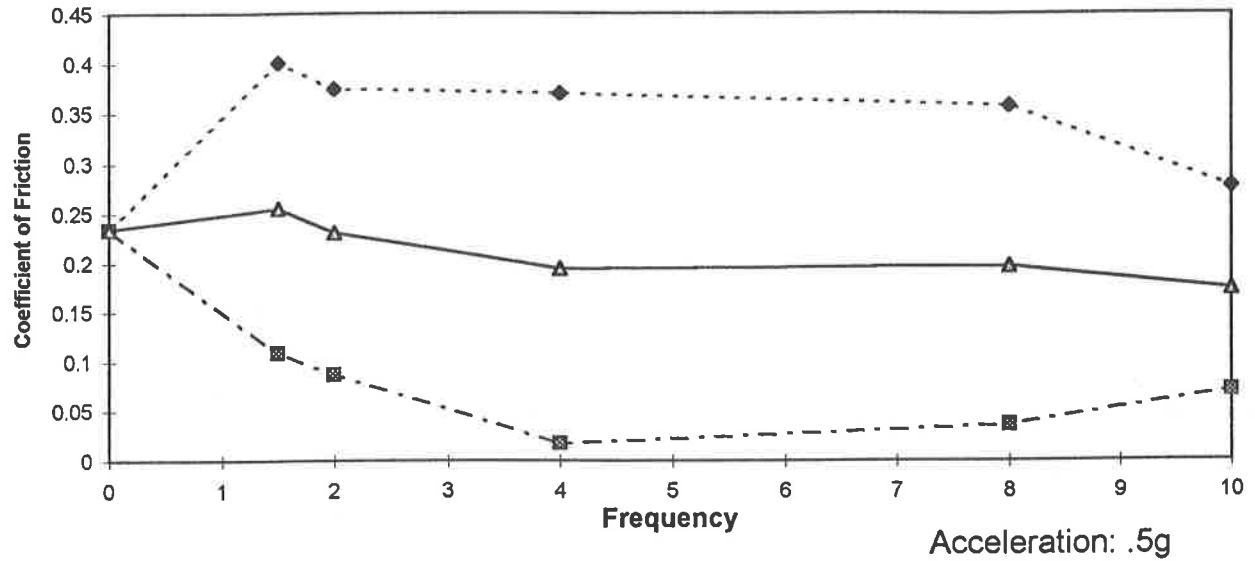


Figure 4.56: Influence of vertical vibration on the coefficient of friction

Deck: X-Groove Aluminum

Load: H

Skid: Plastic Skid

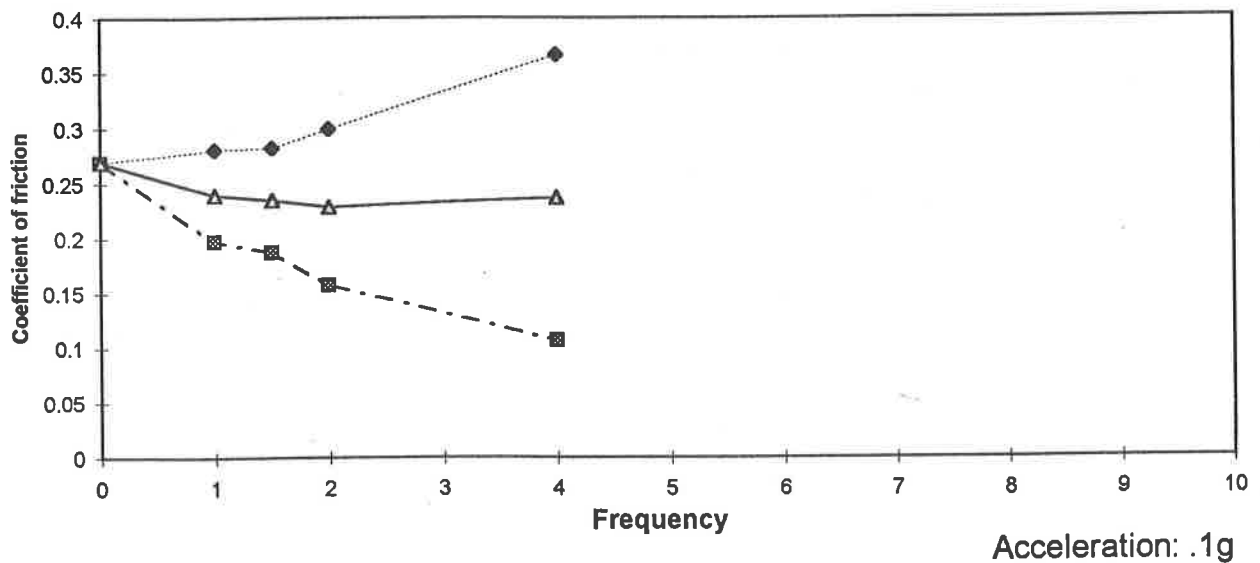
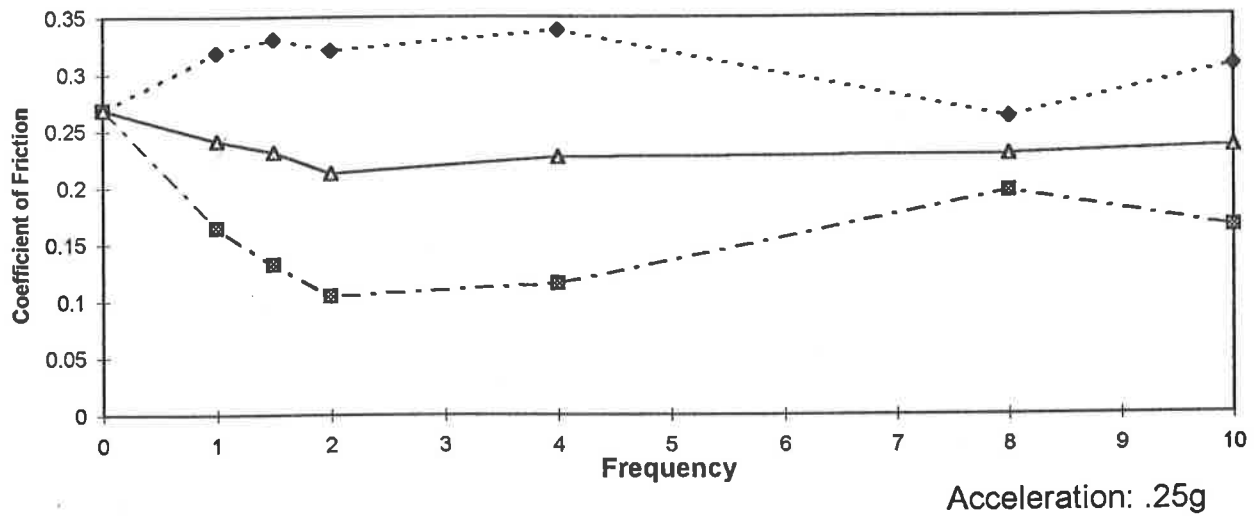
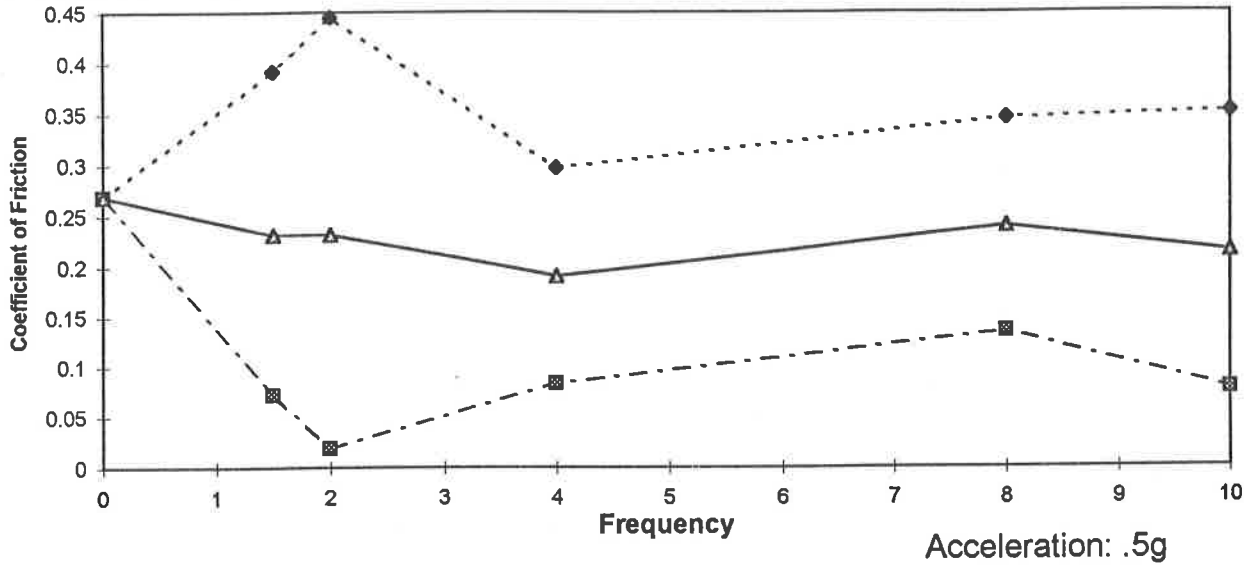


Figure 4.57: Influence of vertical vibration on the coefficient of friction



Deck: X-Groove Aluminum

Skid: Plastic Skid

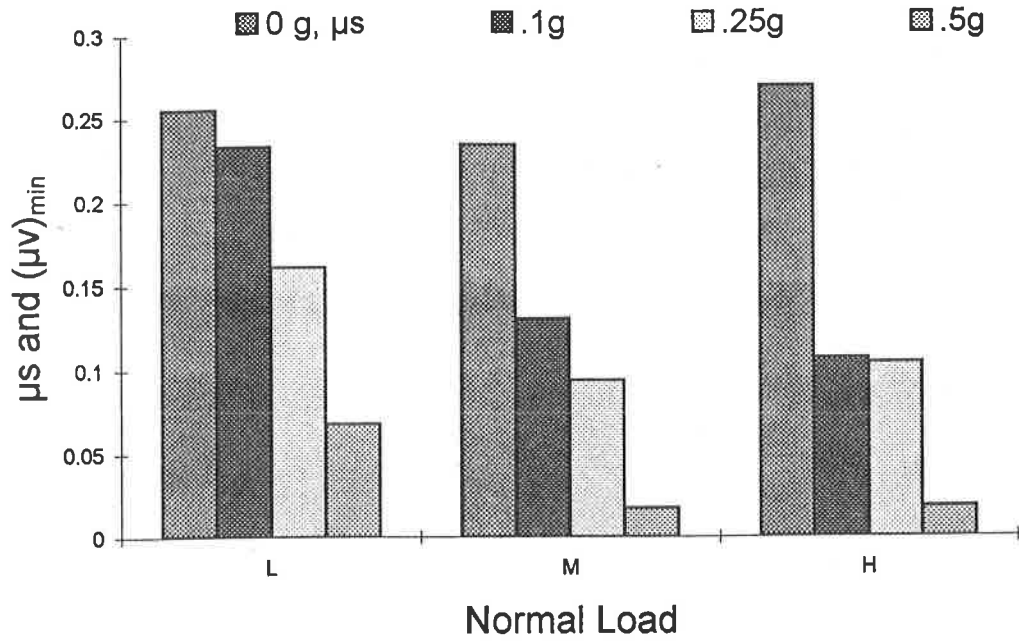


Figure 4.58: Influence of vertical acceleration and normal load on the minimum value of friction coefficient

values of  $\mu_v$  measured between the X-groove aluminum deck and the three skid materials (steel pads, concrete and plastic). Steel pads with light load revealed near loss of contact in the 4-8 Hz frequency range due to poor levelling of the feet, while the plastic skid with medium and high loads resulted in near loss of contact under high level vibration excitations near 4 Hz.

### 4.3 FRICTION COEFFICIENTS UNDER RANDOM VIBRATIONS

The friction forces between the selected deck and skid materials are measured under field measured vertical random vibration synthesized in the laboratory. The measured friction forces are initially analyzed using the *B&K-2035 Signal Analyzer*. The data analysis revealed that the predominant frequency components of the friction force are almost identical to those of the field measured trailer bed vibration. While the frequency spectrum of the friction force does not quantify the magnitude of friction force, the results clearly illustrated the significance of vertical trailer vibration on the friction force between the load and deck surfaces.

The friction forces measured during three trials for each skid and deck material combination are further analyzed to determine the mean, maximum and minimum values of  $\mu_v$ . The measured friction force signals are filtered through a low-pass filter with cut-off frequency of 20 Hz in order to eliminate the peaks, if any, caused by occasional breakaway. The measured friction force is normalized with respect to the normal load (mg) to determine the coefficients of friction,  $\mu_v$ . The measured data were further analyzed to determine the influence of magnitude of acceleration on the friction force, by normalizing the friction force with respect to the effective apparent weight,  $m(g - a)$ . The resulting coefficients of friction were examined to gain insight to the influence of level of vibration on the friction force. The results revealed inconsistent results due to phase difference between the friction force and input acceleration, which is primarily

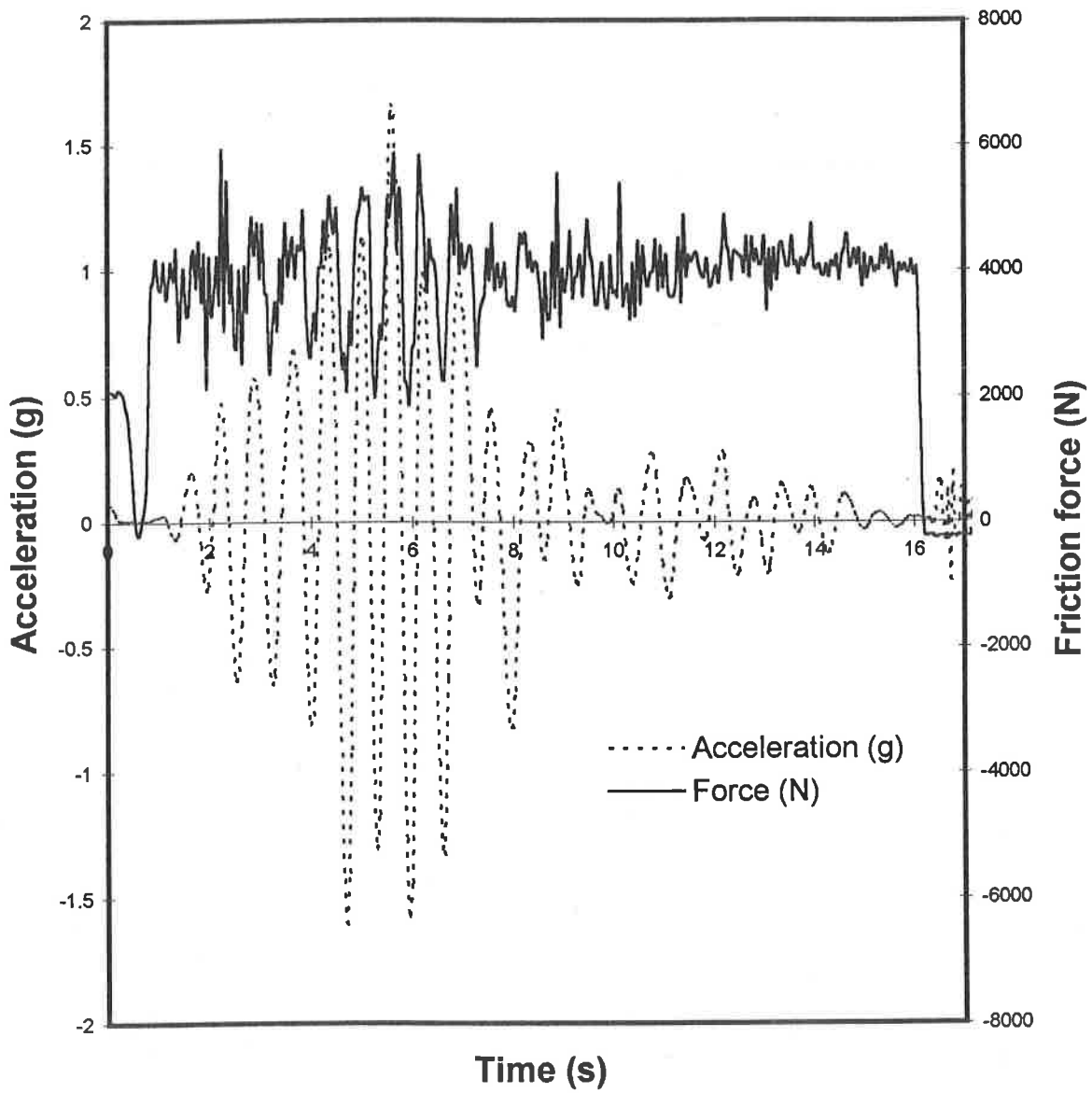


**Figure 4.59: Time history of measured friction force and vertical acceleration (Deck: Aluminum X-Grooved ; Skid: Concrete)**

caused by the flexibility of the skid and deck materials. The analysis of the influence of instantaneous vibration will necessitate the measurement of response acceleration of the skid. The results of the study, derived upon normalizing the friction force with respect to  $mg$ , are therefore discussed in the following section.

#### **4.3.1 Discussion of Results (Random Vibration)**

Figure 4.59 illustrates the time history of friction force and vertical acceleration measured during a test. The results characterize the typical measurements obtained with different skid and deck materials. The breakaway forces are not apparent from the time history of the friction force, and the friction force follows the vertical acceleration history. The measured data is thus analyzed to yield the mean value of friction and the amplitude distribution of the friction coefficient,  $\mu_v$ . The amplitude distribution can be used to derive the more realistic values of  $\mu_v$  and the corresponding percent duration of a specific value of  $\mu_v$  in the typical trailer vibration environment. The results are discussed below for each of the deck material.

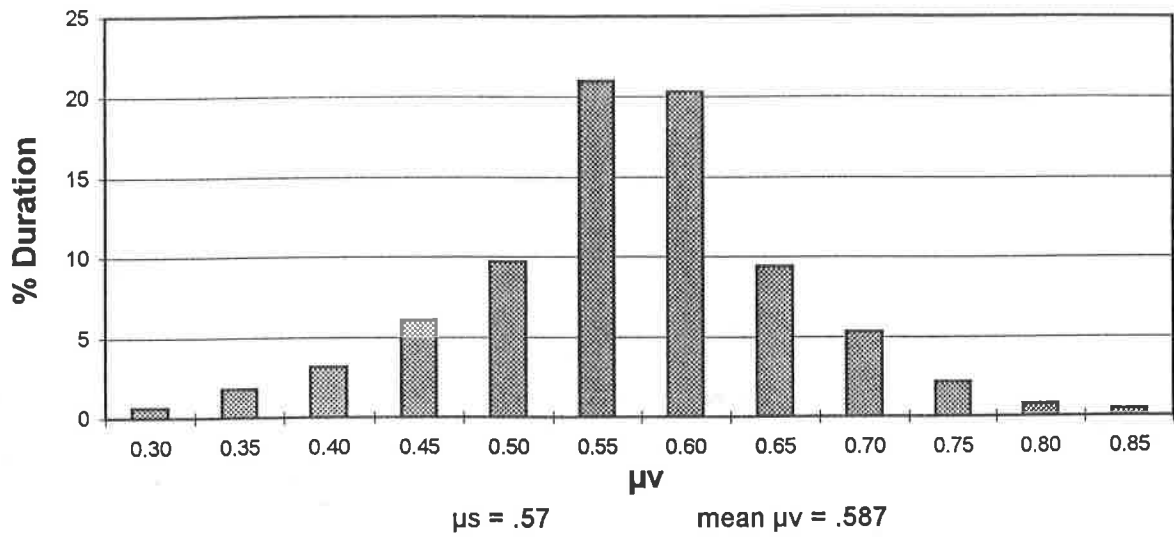
##### **4.3.1.1 COARSE HARDWOOD DECK**

The amplitude distribution of  $\mu_v$  measured between machine feet and coarse hardwood deck subject to trailer vertical vibration due to asphalt and gravel roads are presented in Figures 4.60 and 4.61, respectively. The amplitude distribution is presented to describe the percent duration of existence of a given  $\mu_v$  value over approximately 14s vibration signal. The  $\mu_v$  values, presented on the x-axis, are selected in increments of 0.05, with the exception of plastic skid where the increment is reduced to 0.025. The results show that  $\mu_v$  values in the 0.53 - 0.59 range occur most frequently for the load range considered in this study, for both gravel and asphalt roads. This range of mean  $\mu_v$  values correlates well with the range of  $\mu_s$  values (0.50 - 0.59) measured in a static environment. The measurements performed under excitations

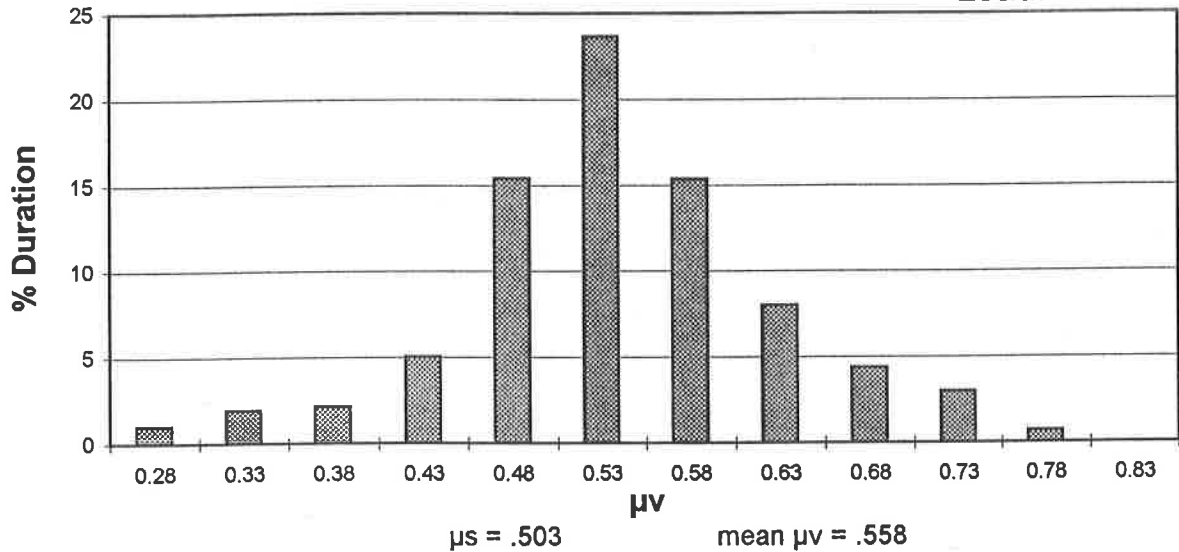
Deck: Coarse Hardwood

Skid: Machine Feet

Load: L



Load: M



Load: H

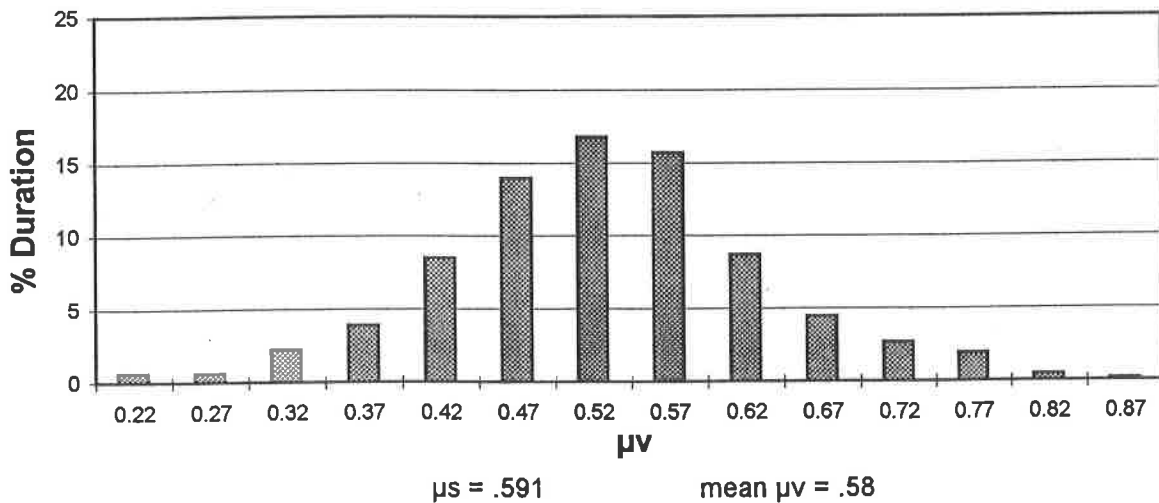
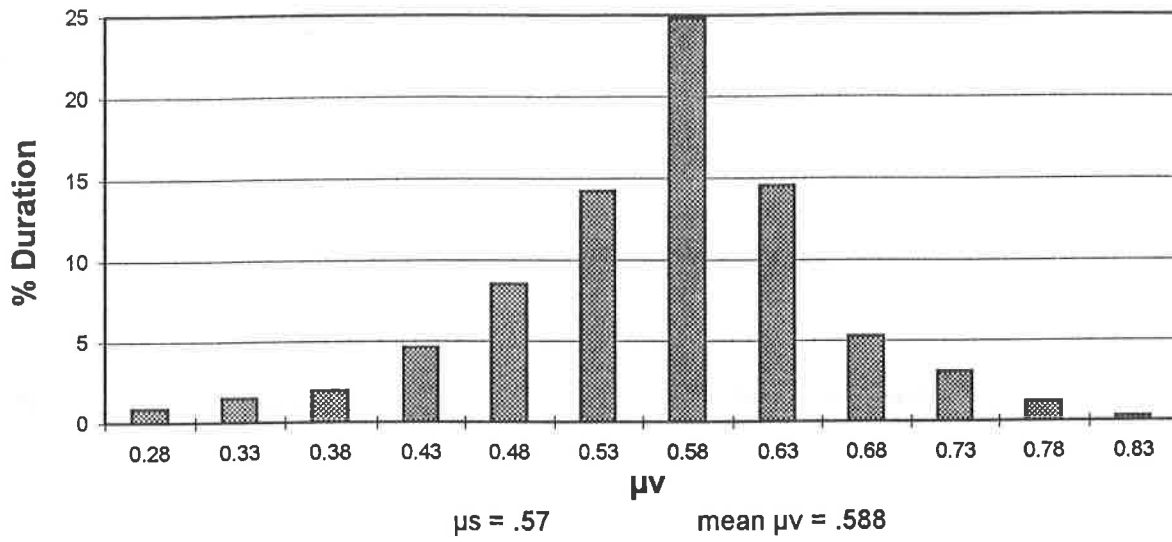


Figure 4-60: Amplitude distribution of coefficient of friction under vertical trailer vibration arising from the asphalt road

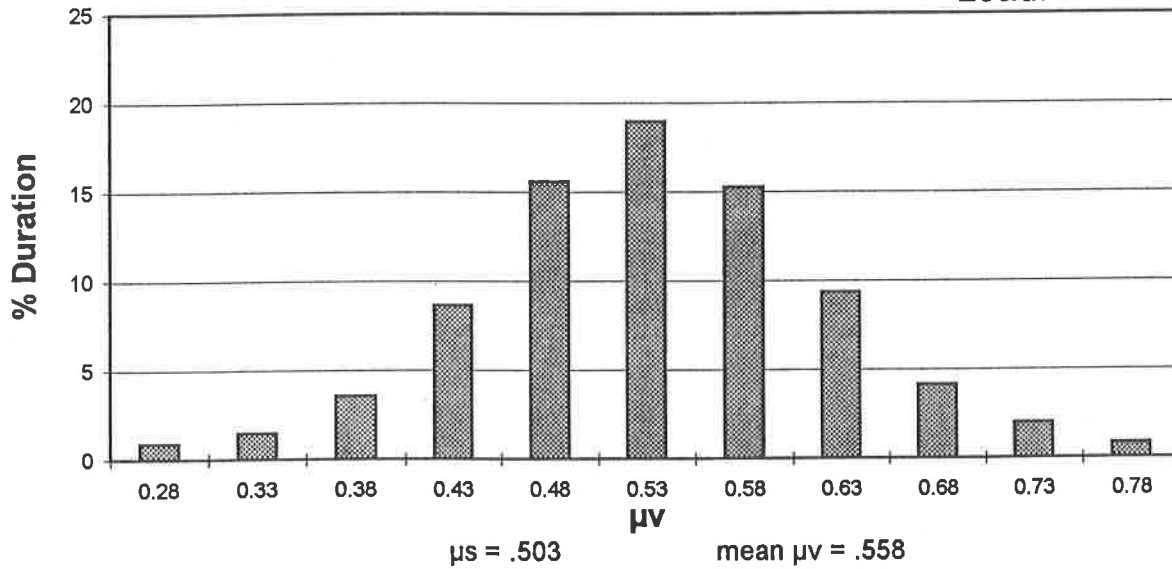
Deck: Coarse Hardwood

Skid: Machine Feet

Load: L



Load: M



Load: H

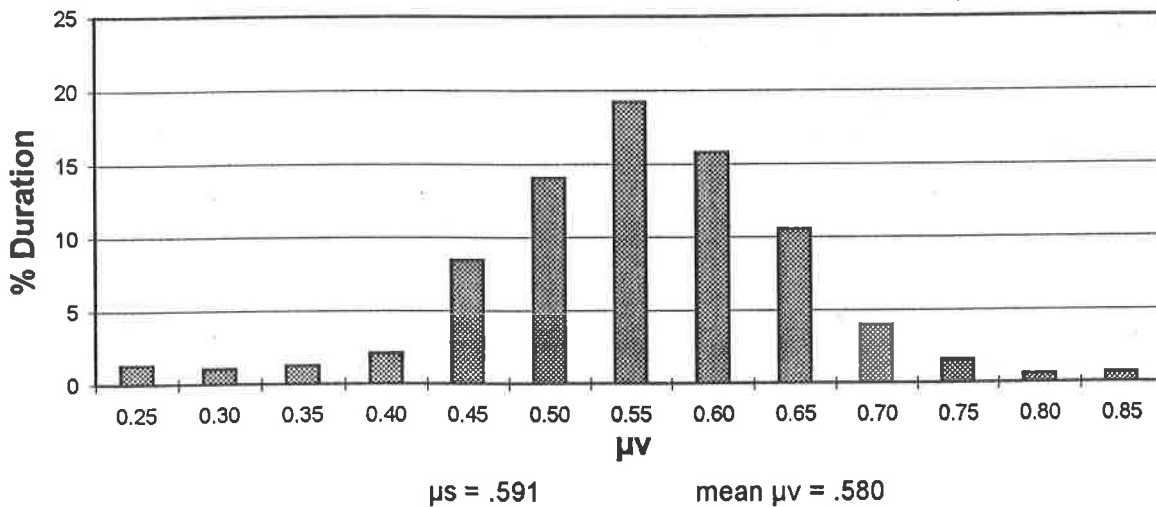


Figure 4-61: Amplitude distribution of coefficient of friction under vertical trailer vibration arising from the gravel road

arising from gravel and asphalt roads are quite similar due to similar vibration spectra obtained for both roads. The results further show relatively insignificant influence of the normal load on the mean values of  $\mu_v$ , which may be attributed to the inertia effects and the frequent stick-slip motion observed during each trial.

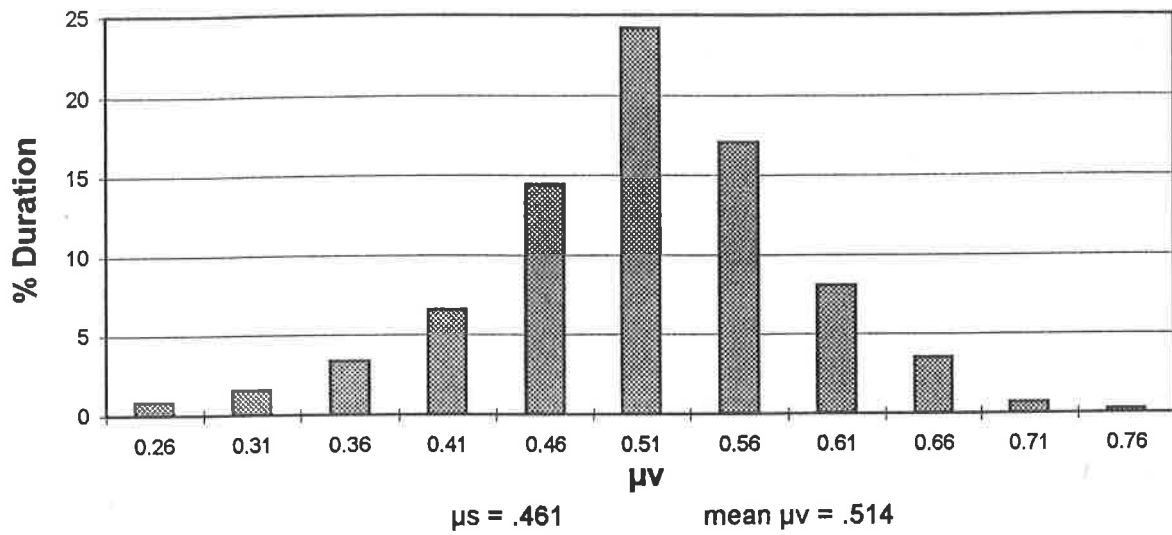
The measurements performed under sinusoidal vibration clearly illustrated the symmetric variations of  $\mu_v$  about the mean value, and extreme maximum and minimum values of friction coefficients. The load security guidelines, however, can not be relied upon either the mean or the extreme minimum values, which occur only for a small segment of the vibration cycle. The amplitude distribution, presented in Figures 4.60 and 4.61, yields the percent of time a low value of  $\mu_v$  may be expected. The high percent duration in conjunction with low value of  $\mu_v$  can lead to movement of the inadequately secured load under braking and directional maneuvers. For development of a load security mechanism, it is thus vital to examine the percent of time corresponding to the existence of a lower value of  $\mu_v$ . The analysis of the amplitude distribution shows that the  $\mu_v$  values remain well below 0.5 for over 25% of the time.

Figures 4.62 and 4.63 illustrate the amplitude distribution of  $\mu_v$  measured between spruce and coarse hardwood deck under excitations arising from asphalt and gravel roads, respectively. The measurements performed under both excitations show almost identical values of  $\mu_v$ . Vertical vibration arising from asphalt road resulted in mean values of 0.514, 0.512 and 0.516, under light, medium and high normal loads, respectively. The corresponding values obtained under gravel road excitations are 0.515, 0.512 and 0.518, respectively. The mean values are observed to be slightly higher than those measured in a static environment (0.461, 0.485, 0.513 under L, M and H loads). The difference, however, is within 10%. The measurements further reveal

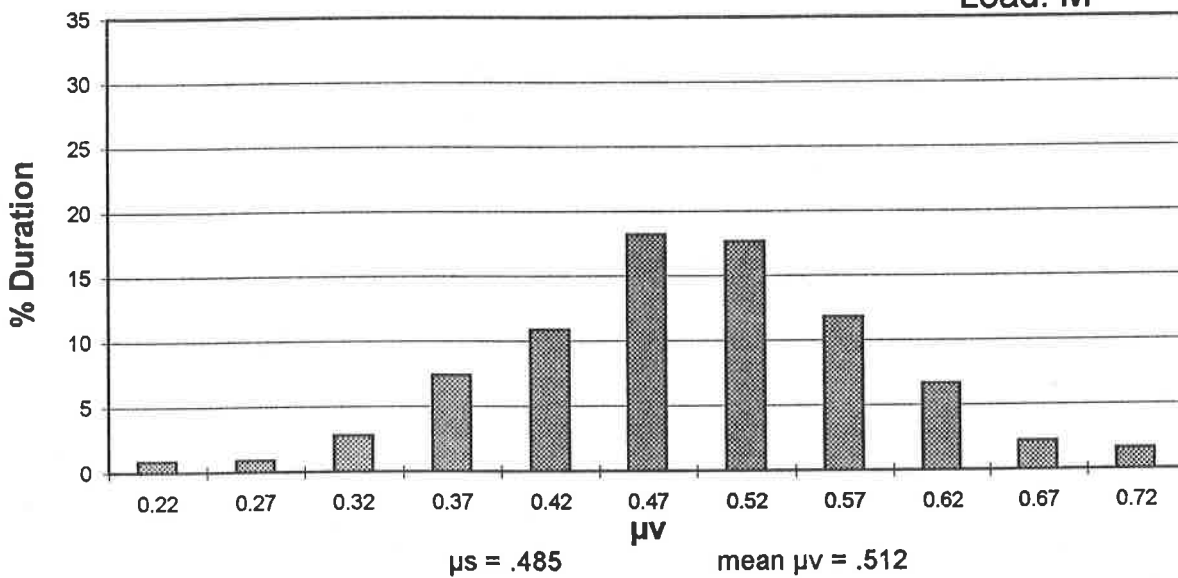
Deck: Coarse Hardwood

Skid: Spruce Board

Load: L



Load: M



Load: H

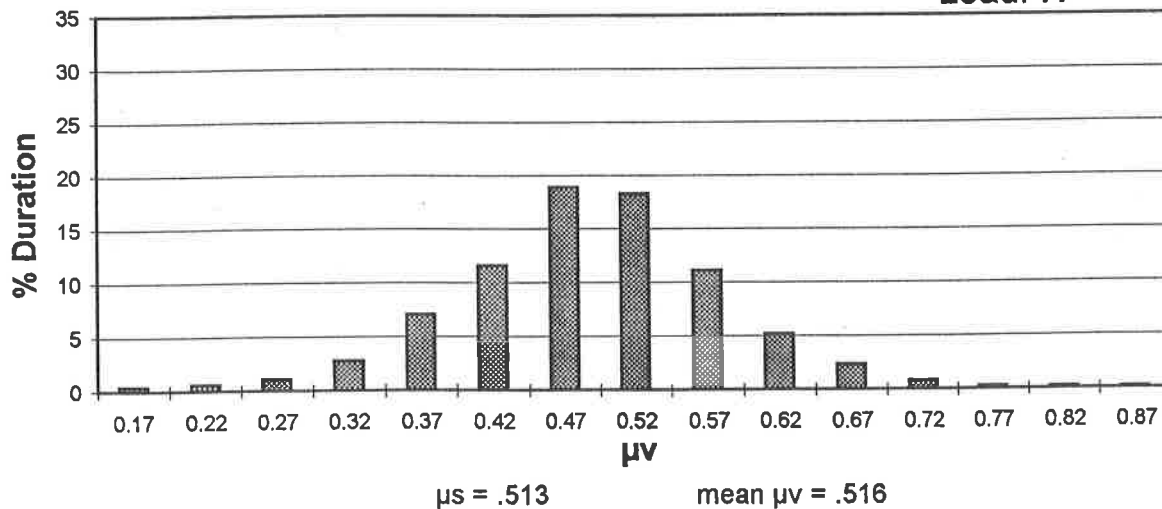


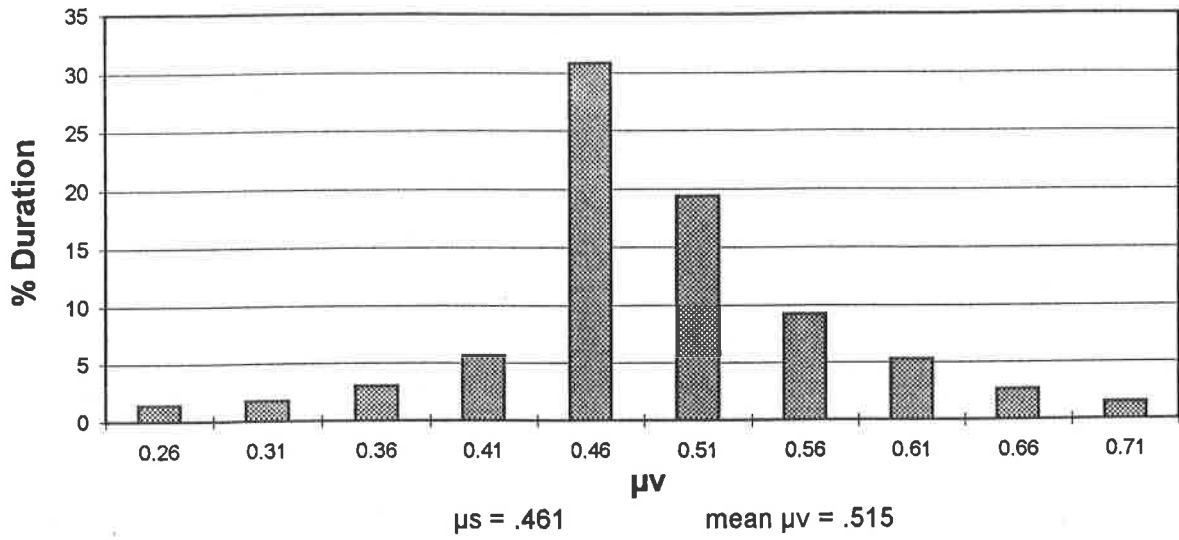
Figure 4-62: Amplitude distribution of coefficient of friction under vertical trailer vibration arising from the asphalt road



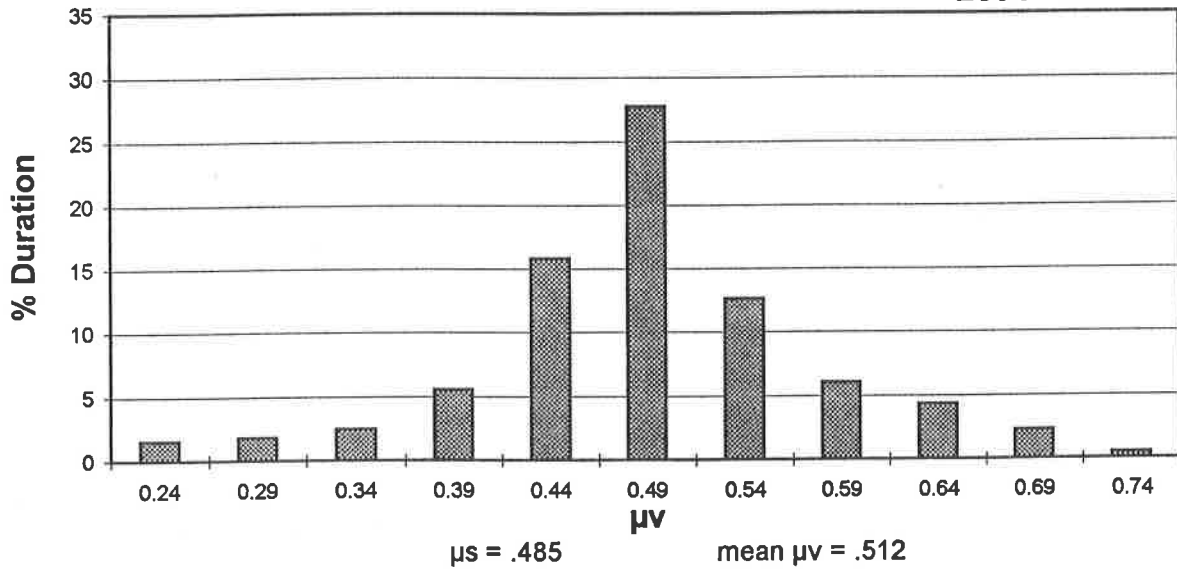
Deck: Coarse Hardwood

Skid: Spruce Board

Load: L



Load: M



Load: H

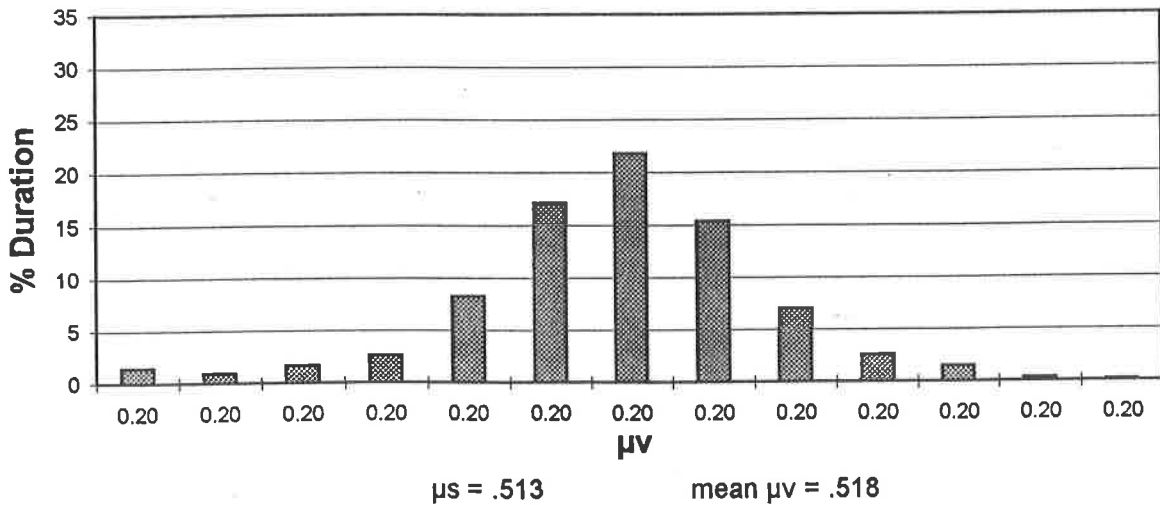


Figure 4-63: Amplitude distribution of coefficient of friction under vertical trailer vibration arising from the gravel road

insignificant dependence on the normal load. While the mean value of  $\mu_v$  is 0.515, the  $\mu_v$  values remain below 0.4 for approximately 12% of the duration.

The amplitude distribution of  $\mu_v$  measured between concrete and coarse hardwood deck subject to asphalt and gravel road vibrations are presented in Figures 4.64 and 4.65, respectively. Both the road excitations yield similar results with mean values of  $\mu_v$  of 0.63 and 0.6, respectively, under medium and high loads. These mean values are approximately 19% and 6% higher than those obtained under static conditions with medium and high normal loads. Although the mean value of  $\mu_v$  under both road excitations is 0.615, in most cases the coefficient of friction remains below 0.5 for nearly 12% of the duration.

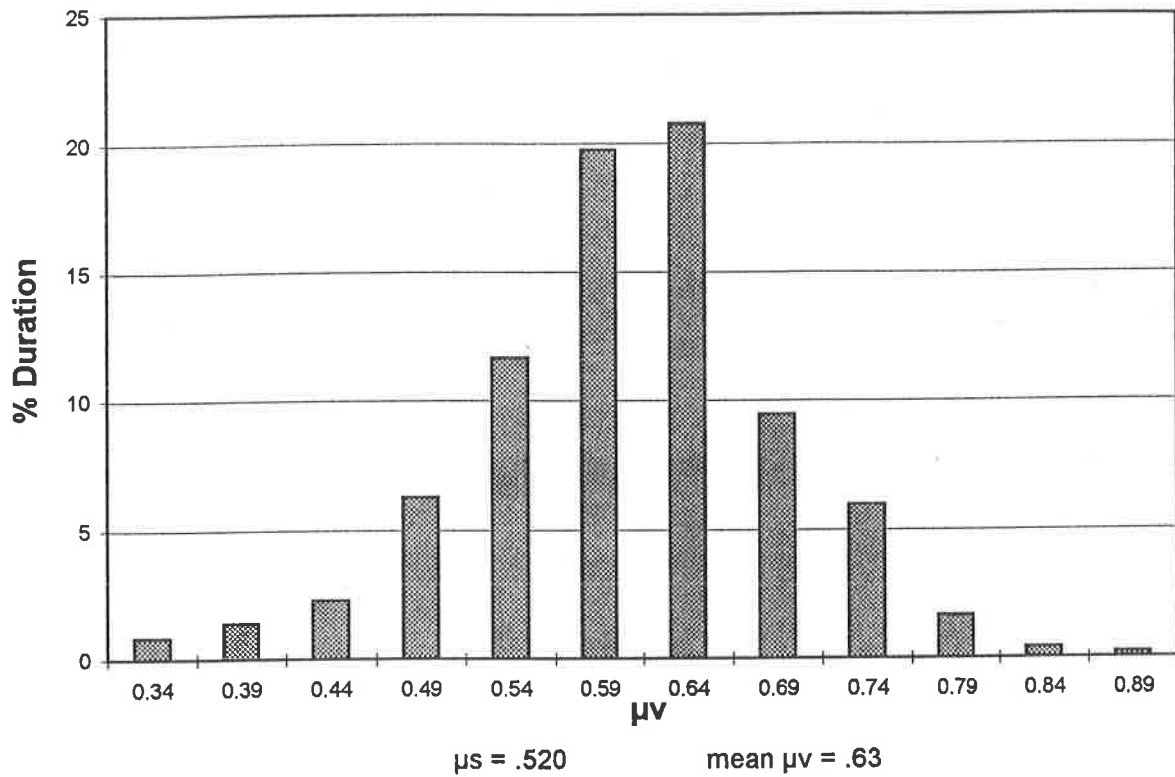
The amplitude distributions of  $\mu_v$  measured between steel pads and coarse hardwood deck under the field measured trailer vibration are illustrated in Figures 4.66 and 4.67. Both the road excitations yield similar results, as observed for other skid materials. The mean values of  $\mu_v$  under light, medium and high loads are obtained as 0.507, 0.513 and 0.512, respectively, for the asphalt road excitation, and 0.496, 0.525, and 0.501 for the gravel road excitations. The corresponding values obtained under static pulls are 0.49, 0.518 and 0.518, respectively. The results show good correlation between the  $\mu_s$  and mean values of  $\mu_v$ . The mean of mean values of  $\mu_v$ , obtained as 0.510 for asphalt road and 0.507 for the gravel road excitation, occur most frequently as shown in the figures. The  $\mu_v$  values below 0.4, however, occur for 10 - 12% of the duration.

The measurements performed under random road measured vibration exhibit the mean values of  $\mu_v$ , which are comparable to those measured under static environment, with the exception of concrete skid material. The concrete skid material resulted in significant increase in the  $\mu_v$  value, specifically, under medium normal load.

Deck: Coarse Hardwood

Skid: Concrete Blocks

Load: M



Load: H

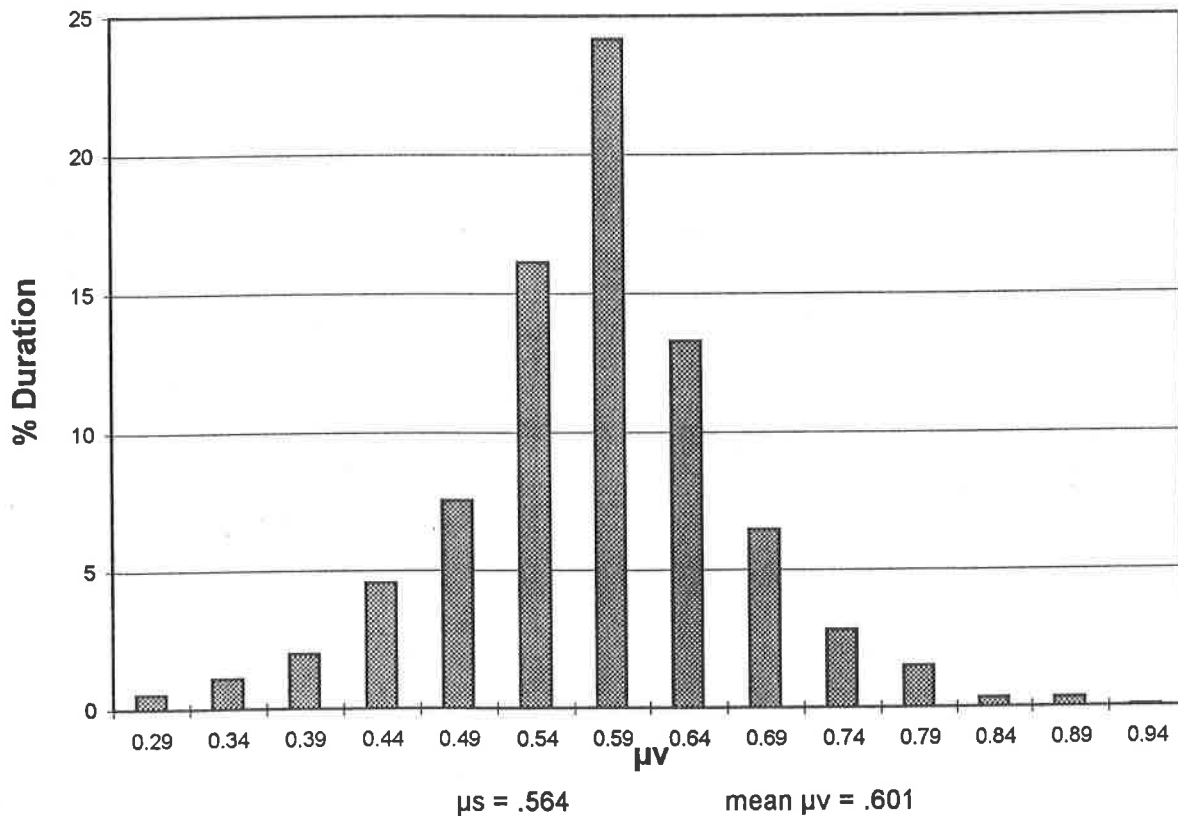
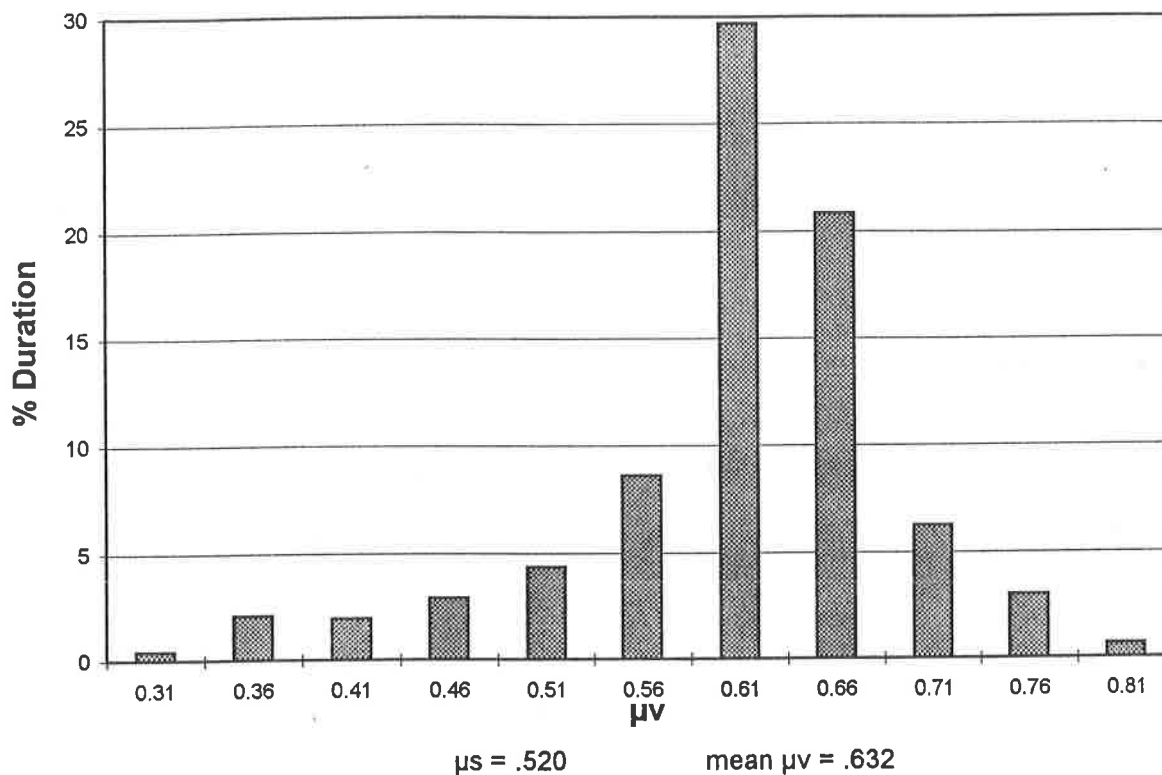


Figure 4-64: Amplitude distribution of coefficient of friction under vertical trailer vibration arising from the asphalt road

Deck: Coarse Hardwood

Skid: Concrete Blocks

Load: M



Load: H

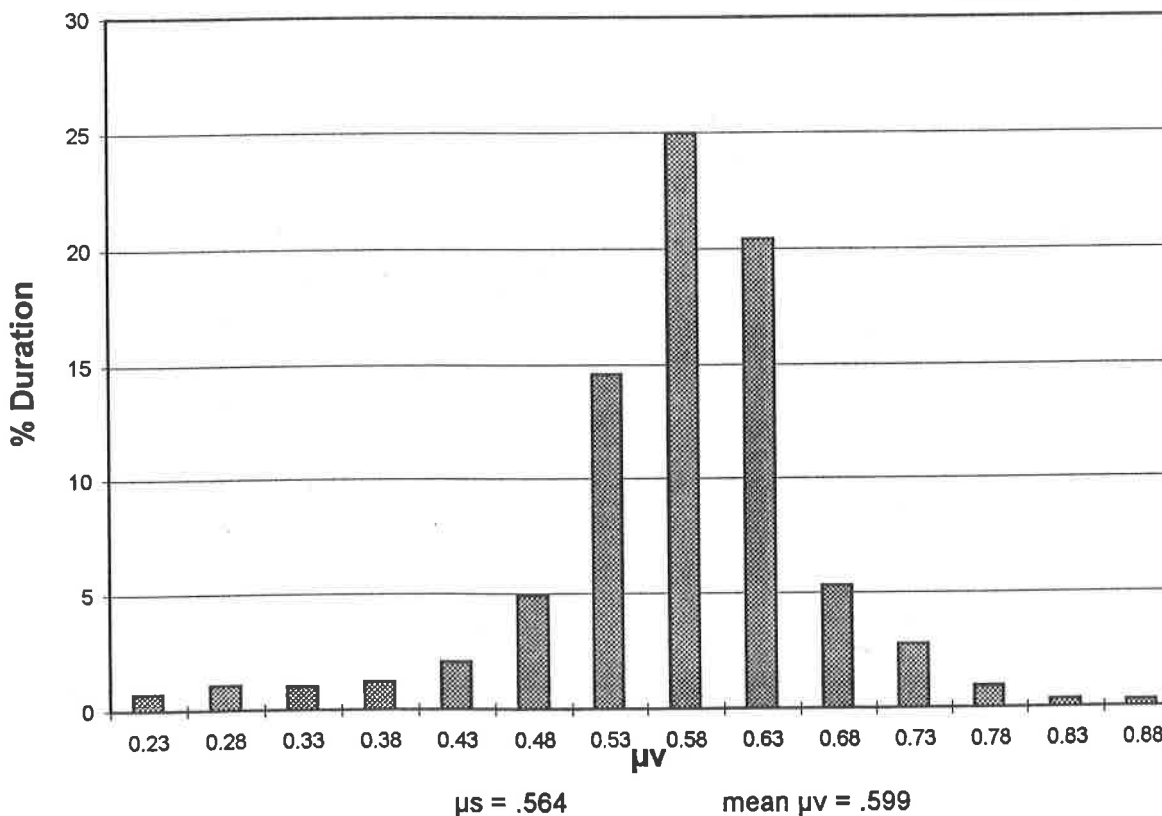
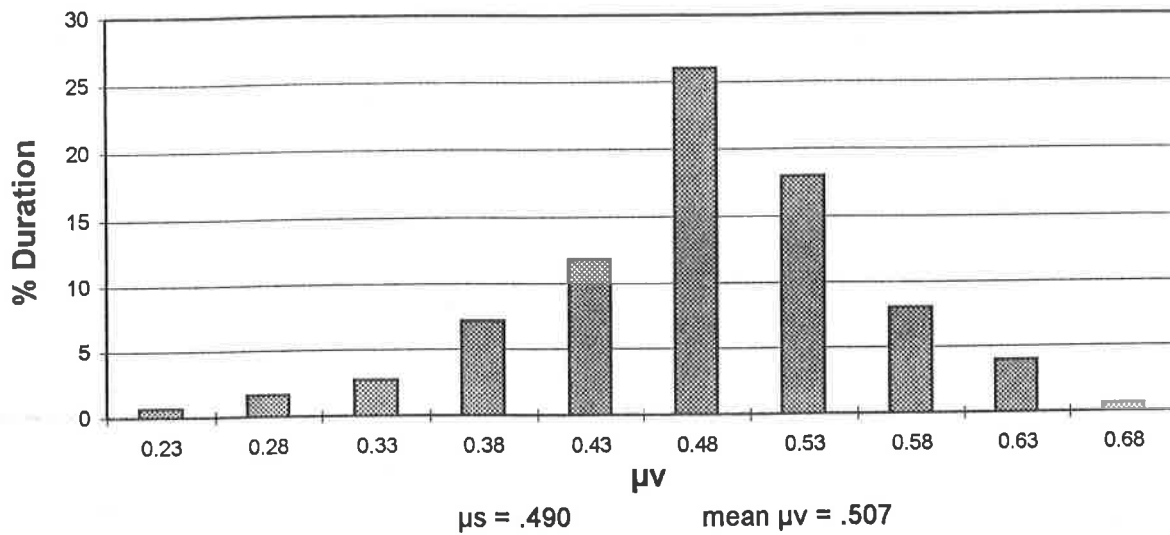


Figure 4-65: Amplitude distribution of coefficient of friction under vertical trailer vibration arising from the gravel road

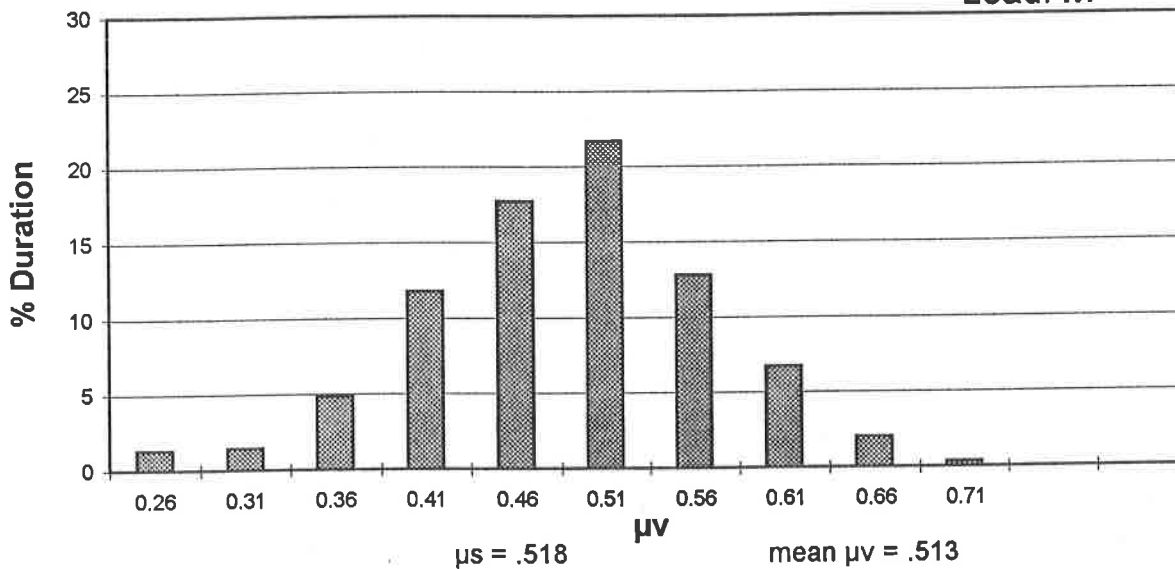
Deck: Coarse Hardwood

Skid: Steel Pads

Load: L



Load: M



Load: H

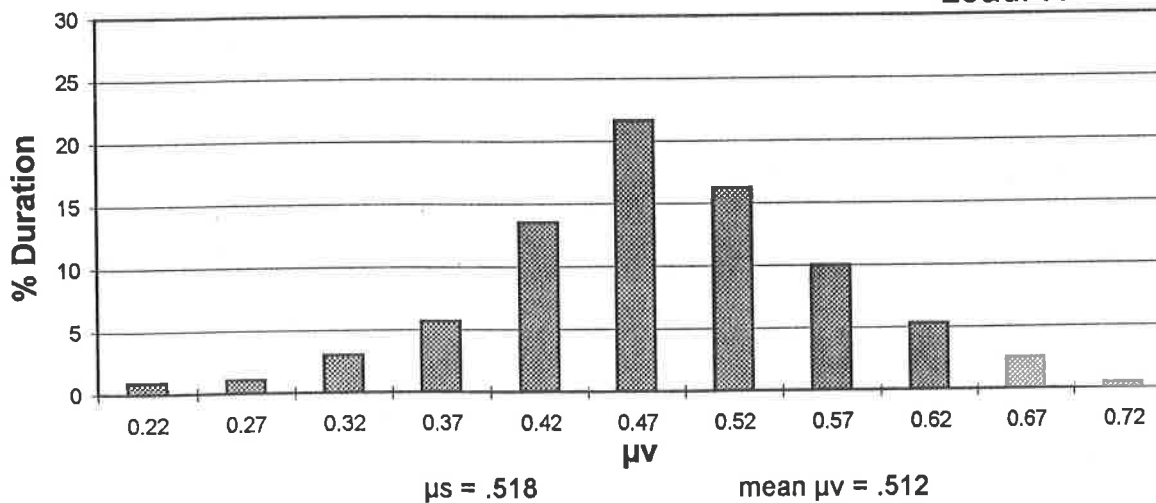
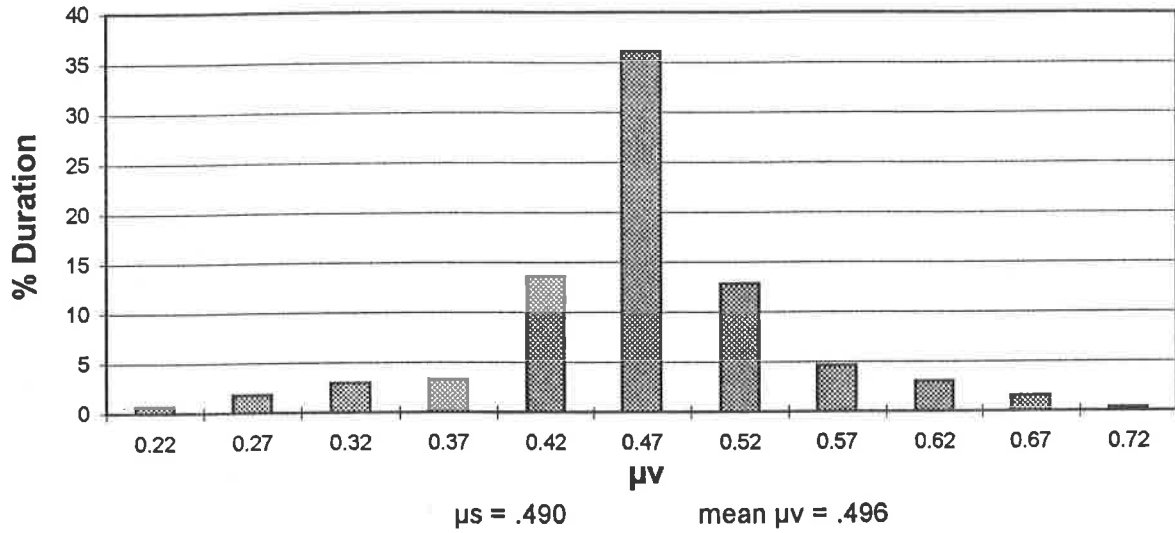


Figure 4-66: Amplitude distribution of coefficient of friction under vertical trailer vibration arising from the asphalt road

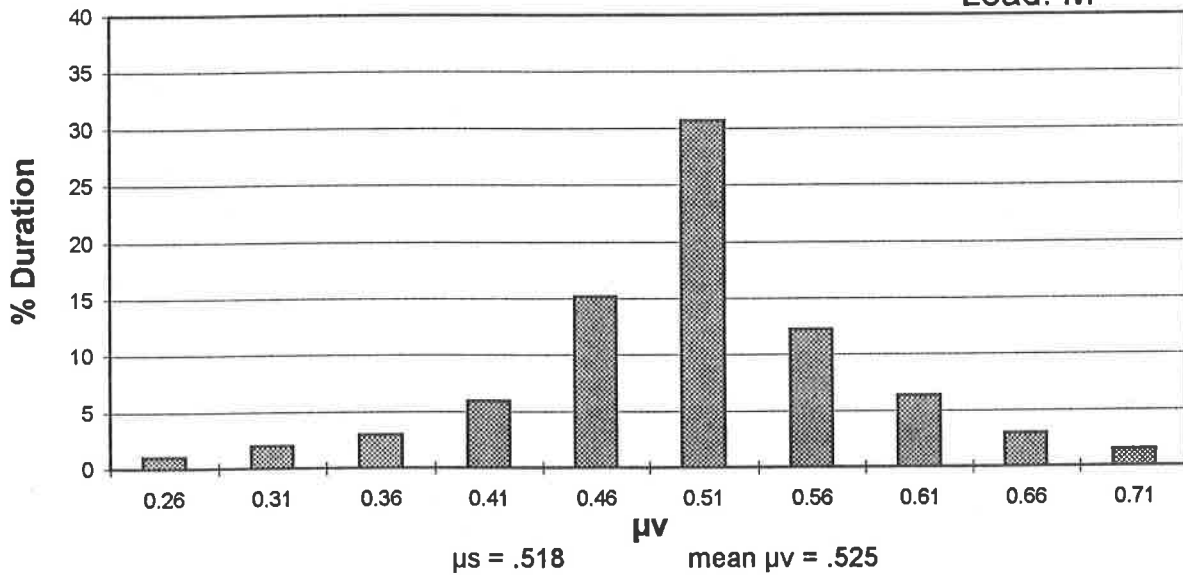
Deck: Coarse Hardwood

Skid: Steel Pads

Load: L



Load: M



Load: H

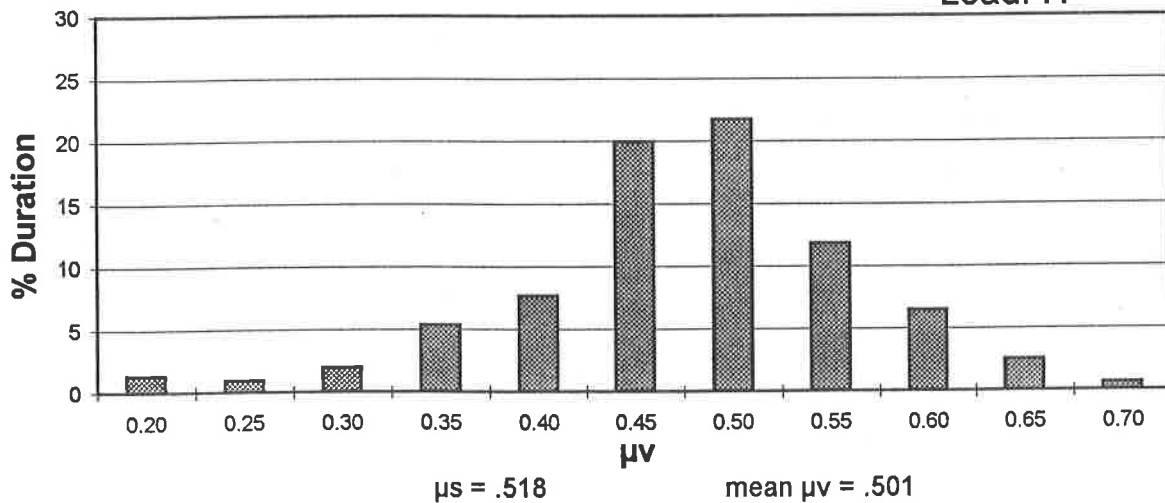


Figure 4-67: Amplitude distribution of coefficient of friction under vertical trailer vibration arising from the gravel road

Furthermore, the measurements performed under trailer vibration arising from asphalt and gravel roads resulted in nearly similar mean values of  $\mu_v$  and amplitude distribution of  $\mu_v$ . In view of this similarity, the results obtained for the smooth hardwood and grooved aluminum decks are presented for gravel road excitations alone.

#### 4.3.1.2 SMOOTH HARDWOOD DECK

Figures 4.68 to 4.71 illustrate the amplitude distribution of  $\mu_v$  measured between the smooth hardwood deck, and paper, rubber, smooth steel and plastic skid materials, respectively. The figures present the distribution of  $\mu_v$  measured under field measured vertical vibration of the trailer operating on a gravel road. The measurements performed with paper skid material resulted in mean values of 0.35 and 0.362 under light and medium loads, respectively, which correlate very well with the respective values obtained under static conditions (0.398 and 0.379). The mean values obtained for rubber mat (0.671 and 0.64 under light and medium normal loads) also correlate very well with the corresponding static values (0.67 and 0.68).

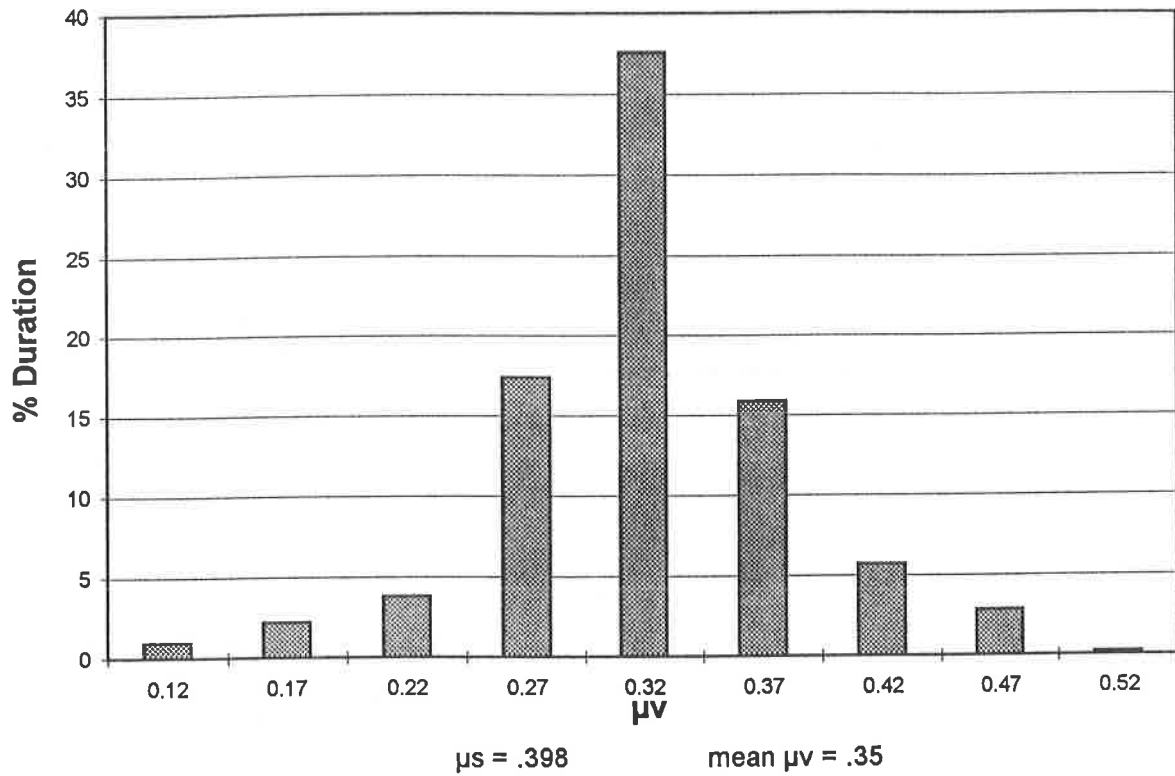
The measurements performed with smooth steel under light load resulted in mean value of 0.462, which is almost identical to the  $\mu_s$  value of 0.463. The corresponding mean values measured under medium and high loads (0.513 and 0.514) are only slightly higher than the respective  $\mu_s$  values (0.479 under medium load and 0.463 under high load). Measurements performed with the plastic skid resulted in mean values of 0.146, 0.147 and 0.143 under light, medium and high loads, respectively, which are quite close to the respective static values of 0.15, 0.135 and 0.142.

The analysis of amplitude distribution data for the paper material reveals that the  $\mu_v$  value below 50% of the mean value (0.18) occurs for 3% of duration only, while  $\mu_v$  below 75% of the mean value (0.27) occurs for 7% of the test duration. Similarly for the

Deck: Smooth Hardwood

Skid: Kraft Paper

Load: L



Load: M

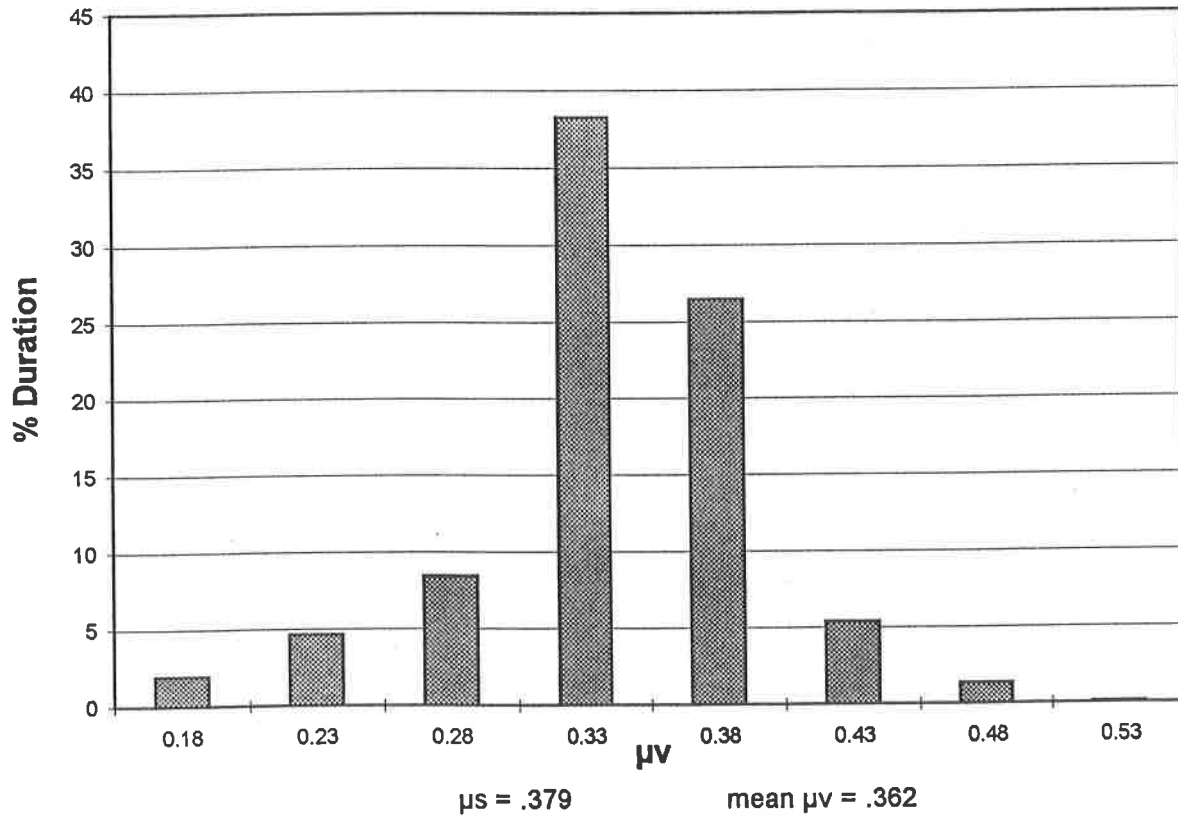


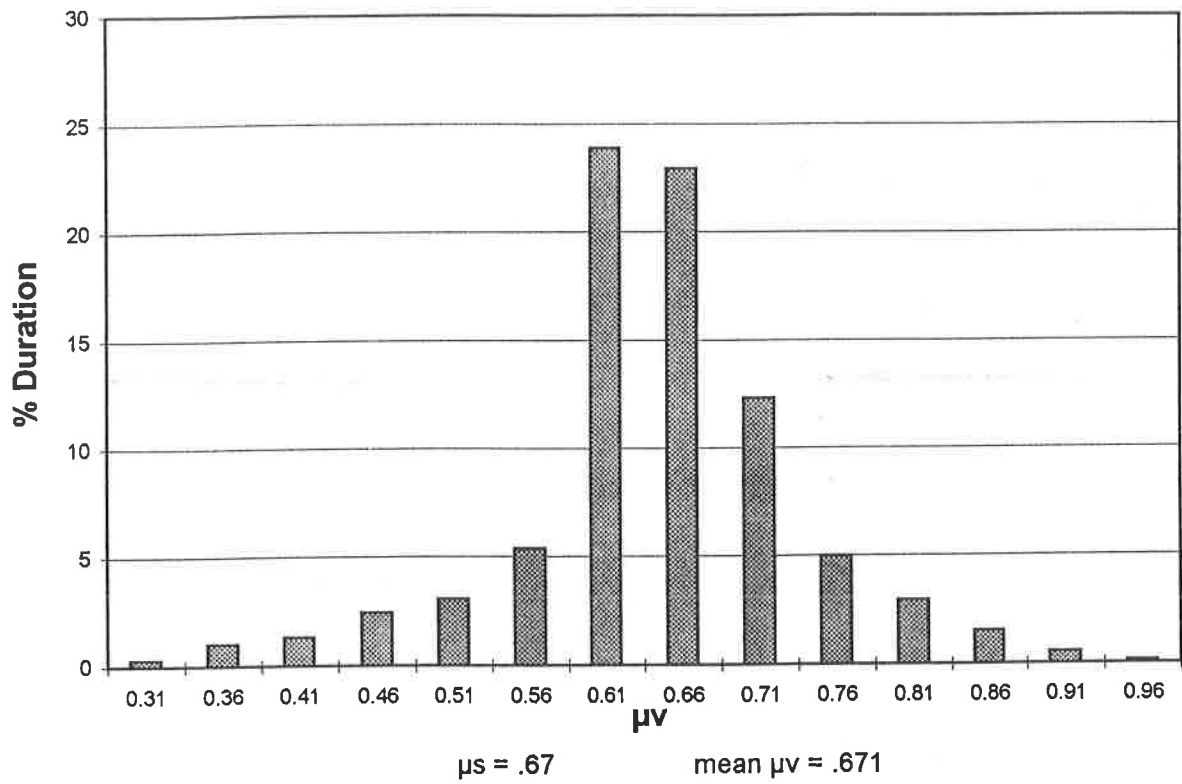
Figure 4-68: Amplitude distribution of coefficient of friction under vertical trailer vibration arising from the gravel road



Deck: Smooth Hardwood

Skid: Rubber Mat

Load: L



Load: M

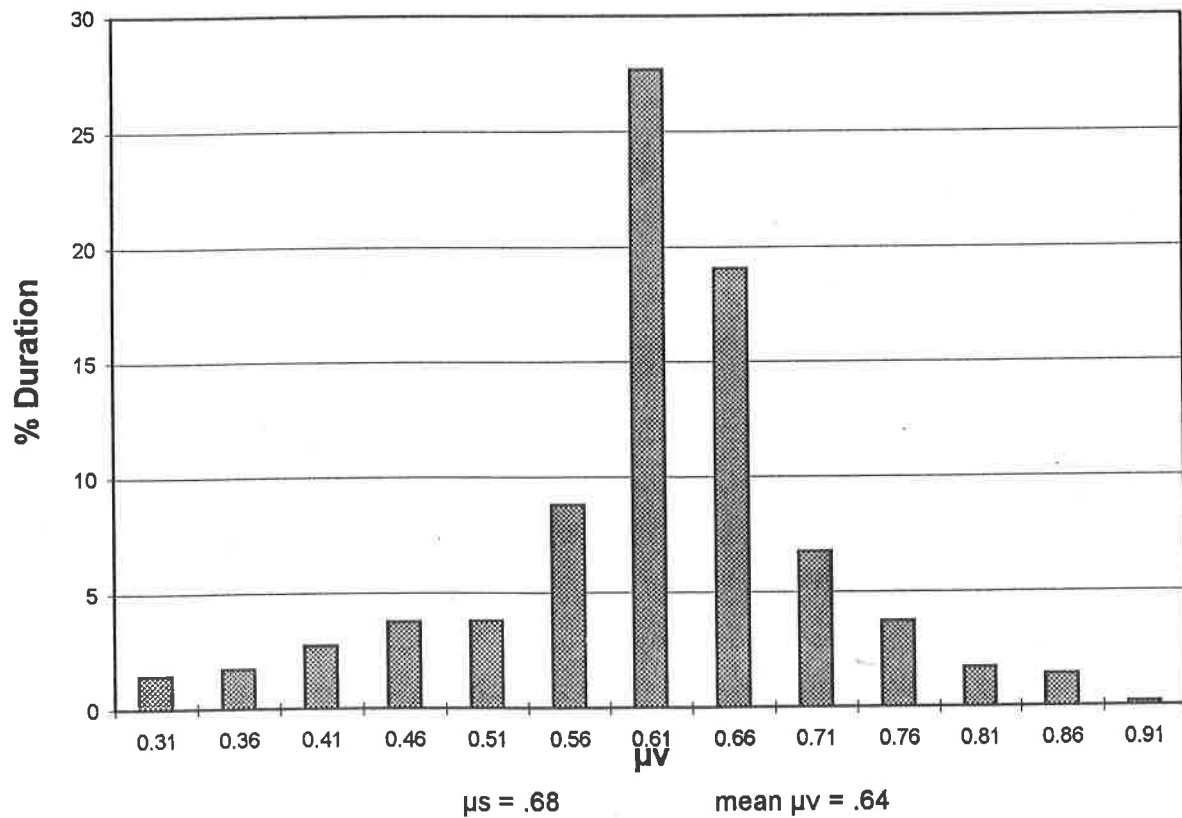
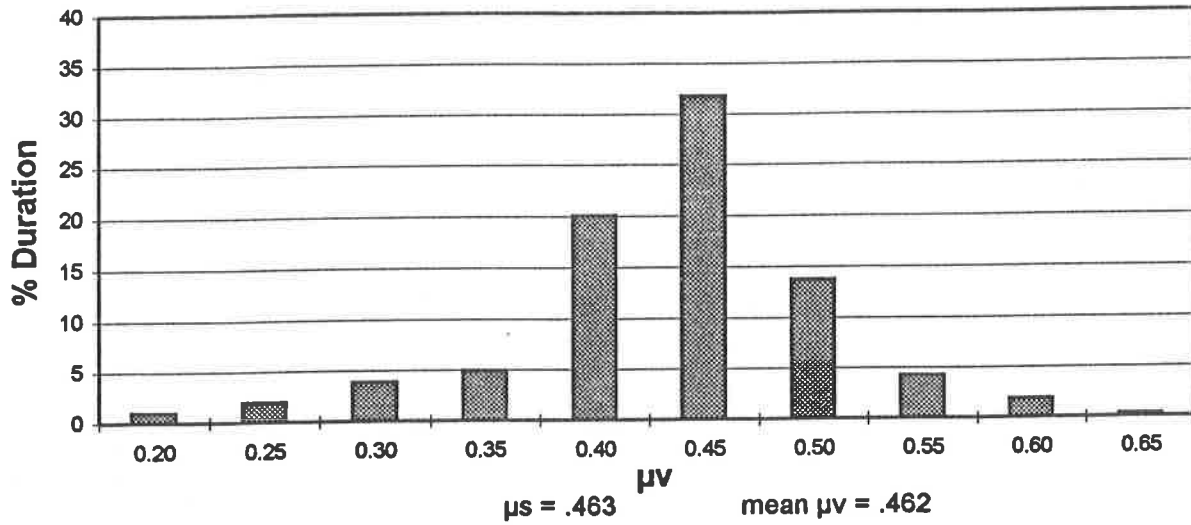


Figure 4-69: Amplitude distribution of coefficient of friction under vertical trailer vibration arising from the gravel road

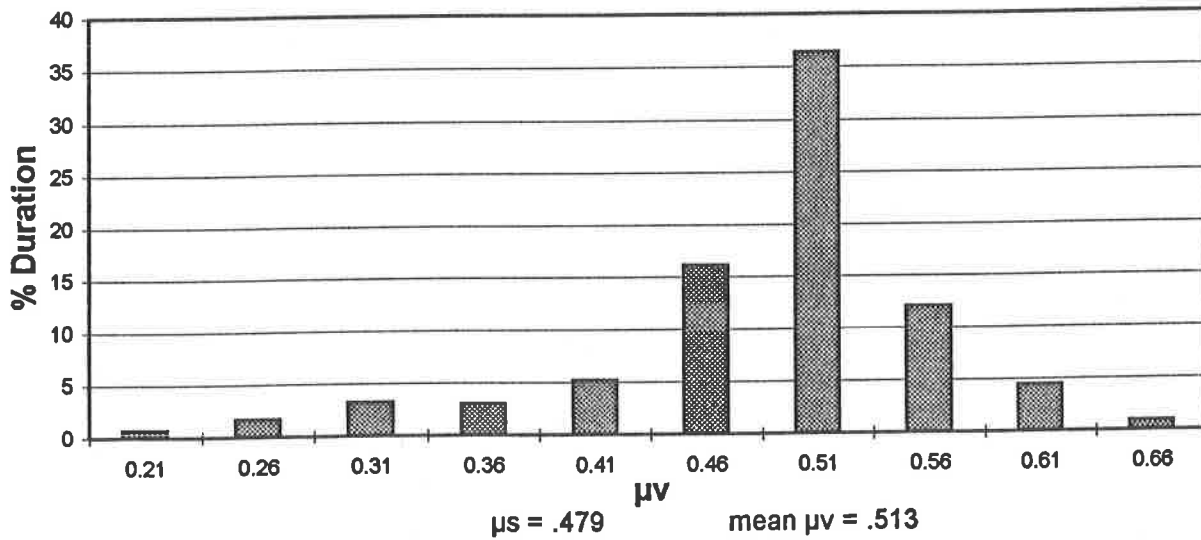
Deck: Smooth Hardwood

Skid: Steel Pads

Load: L



Load: M



Load: H

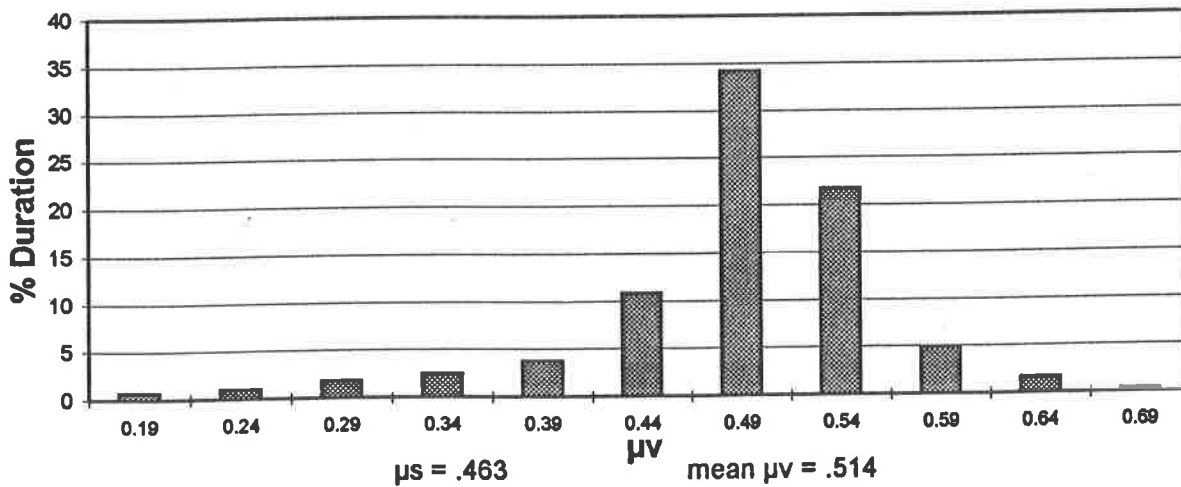
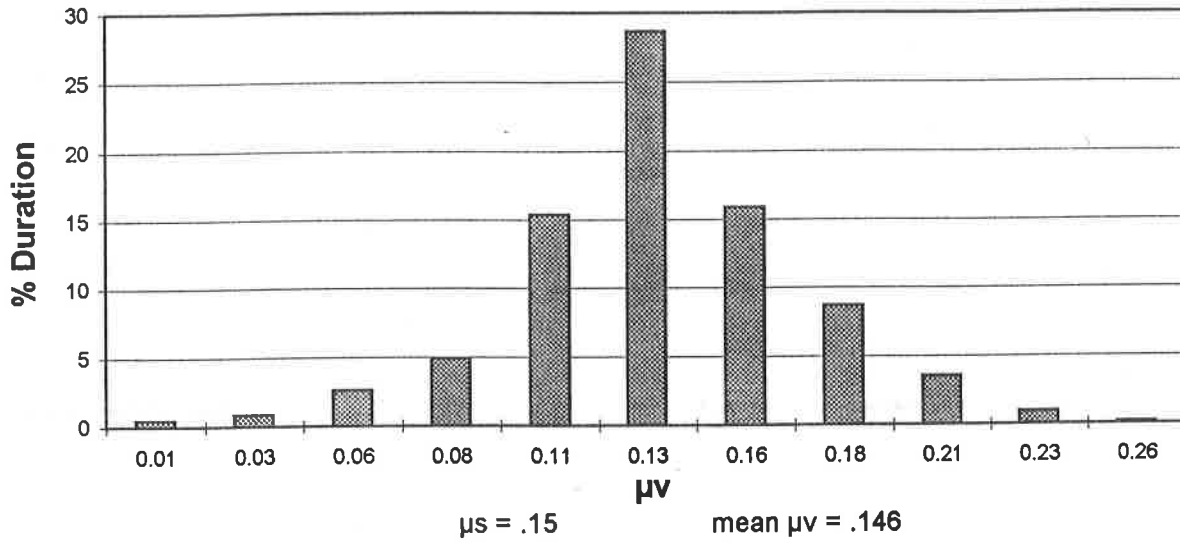


Figure 4-70: Amplitude distribution of coefficient of friction under vertical trailer vibration arising from the gravel road

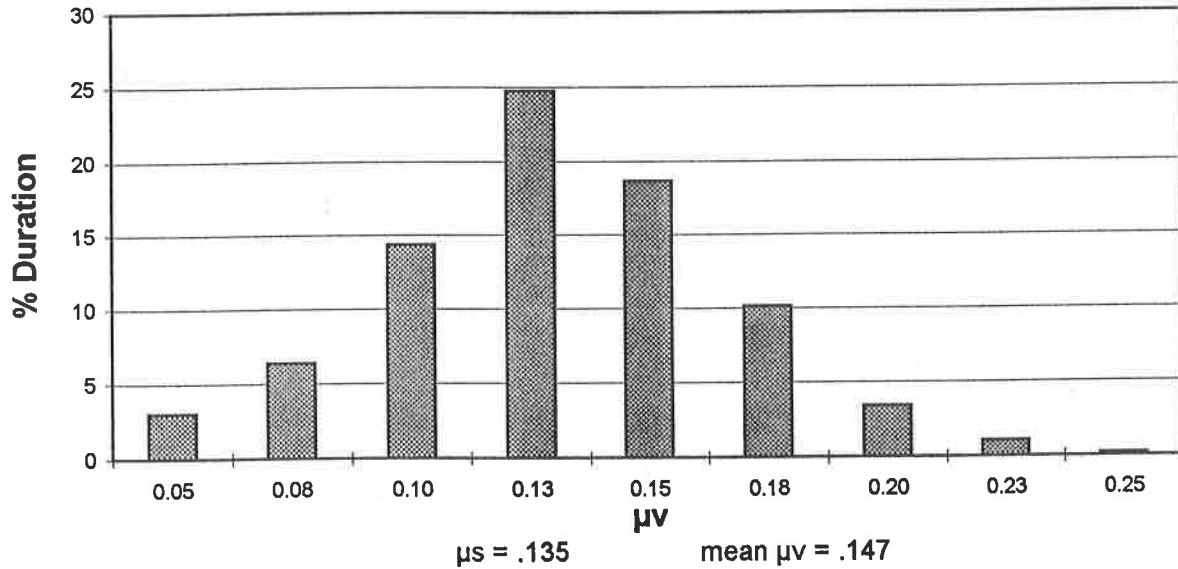
Deck: Smooth Hardwood

Skid: Plastic Skid

Load: L



Load: M



Load: H

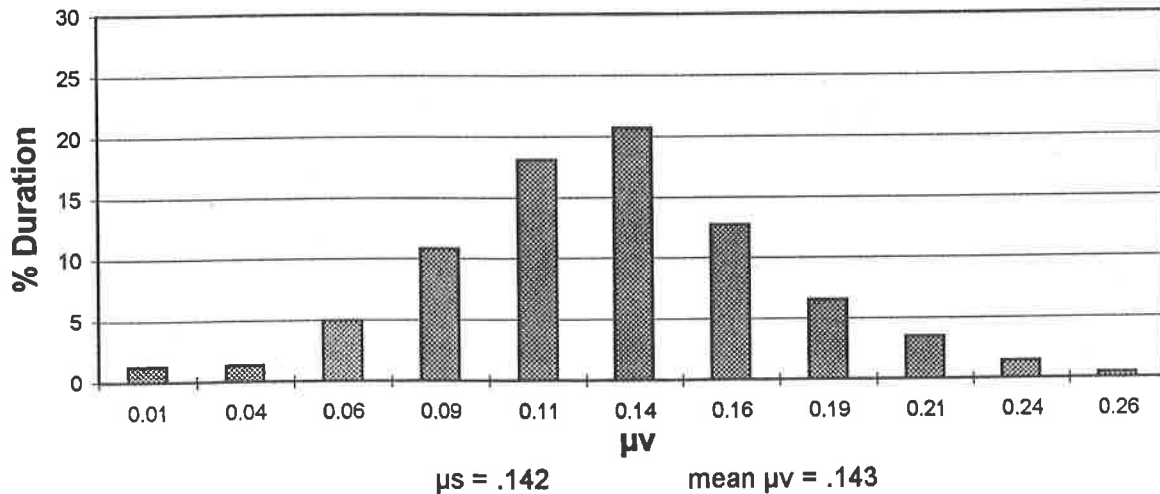


Figure 4-71: Amplitude distribution of coefficient of friction under vertical trailer vibration arising from the gravel road

rubber material a  $\mu_v$  value below 75% of mean value (0.49) occurs over 11% of the duration. While the amplitude distribution data for smooth steel is not analyzed, the analysis of the plastic skid data under high load reveals that the  $\mu_v$  values below 75% of the mean value (0.109) occur over 18% of the test duration.

#### 4.3.1.3 Y-GROOVE ALUMINUM DECK

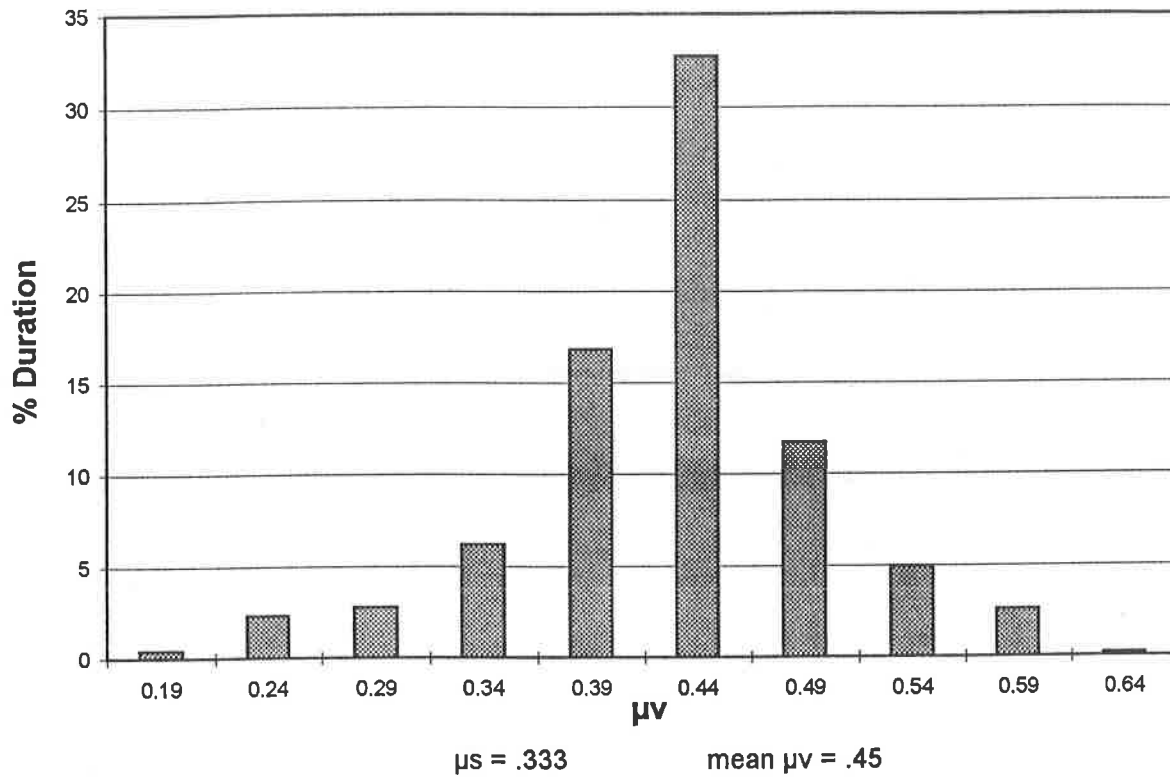
Figures 4.72 to 4.74 illustrate the amplitude distribution of  $\mu_v$  measured between the Y-groove aluminum deck, and concrete, plastic skid and steel pads, respectively. The results are presented for measurements performed under synthesized trailer vibration encountered while operating on a gravel road. The measurements performed with concrete skid under medium load revealed relatively high mean value of  $\mu_v$  (0.45), when compared to the  $\mu_s$  value of 0.333, as observed earlier in the case of coarse hardwood deck. The mean value of  $\mu_v$  obtained under high load (0.42), however, correlates well with the  $\mu_s$  value (0.442). The plastic skid material resulted in mean values of 0.175, 0.178 and 0.172 under light, medium and high loads, respectively, which compare well with respective  $\mu_s$  values (0.210, 0.210 and 0.180). The measurements performed with steel pads under the light, medium and high loads resulted in mean values of 0.439, 0.366 and 0.446, respectively, which are within 10% of  $\mu_s$  values (0.470, 0.400 and 0.452).

The mean of mean values of  $\mu_v$  obtained under three different normal loads are computed for the selected skid materials and the amplitude distribution data is analyzed to determine the percent duration over which  $\mu_v$  values fall below 75% of the mean of mean value. The analysis revealed that  $\mu_v$  drops below 75% of the mean for 11% of the duration for concrete, 12 - 13% for plastic skid under light and medium normal loads, 23% for plastic skid under high normal load, and up to 17% for the steel pads.

Deck: Y-Groove Aluminum

Skid: Concrete Blocks

Load: M



Load: H

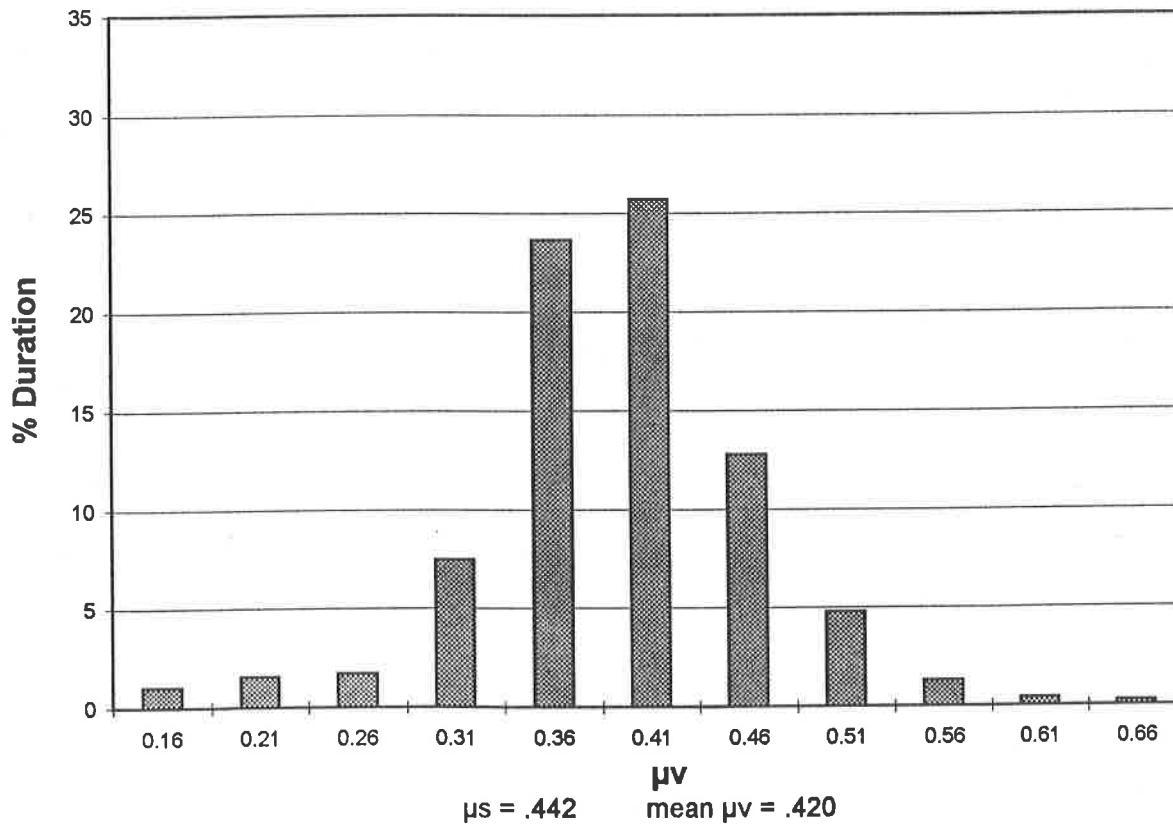
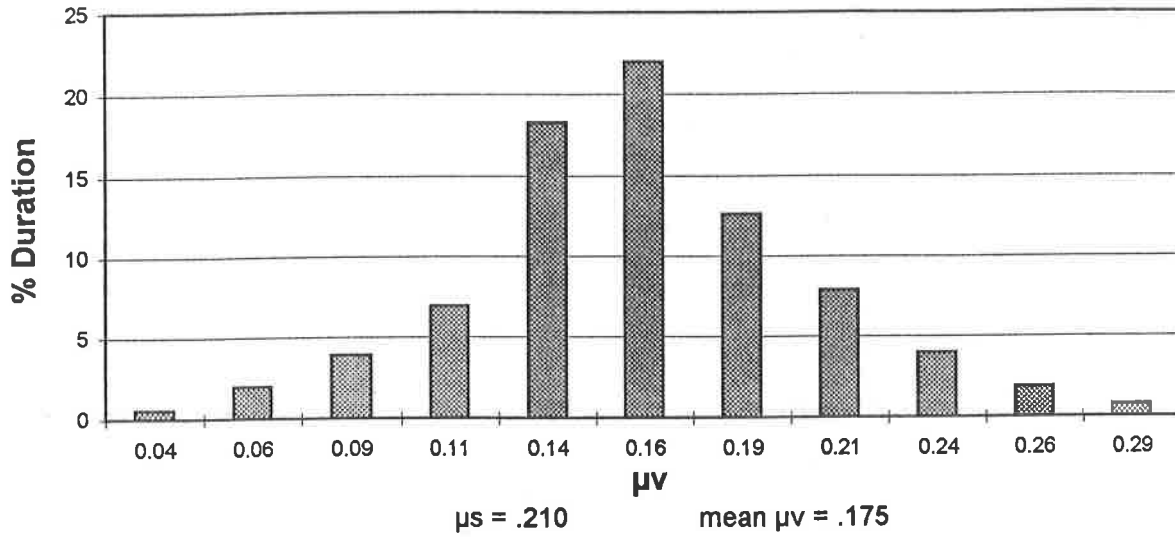


Figure 4-72: Amplitude distribution of coefficient of friction under vertical trailer vibration arising from the gravel road

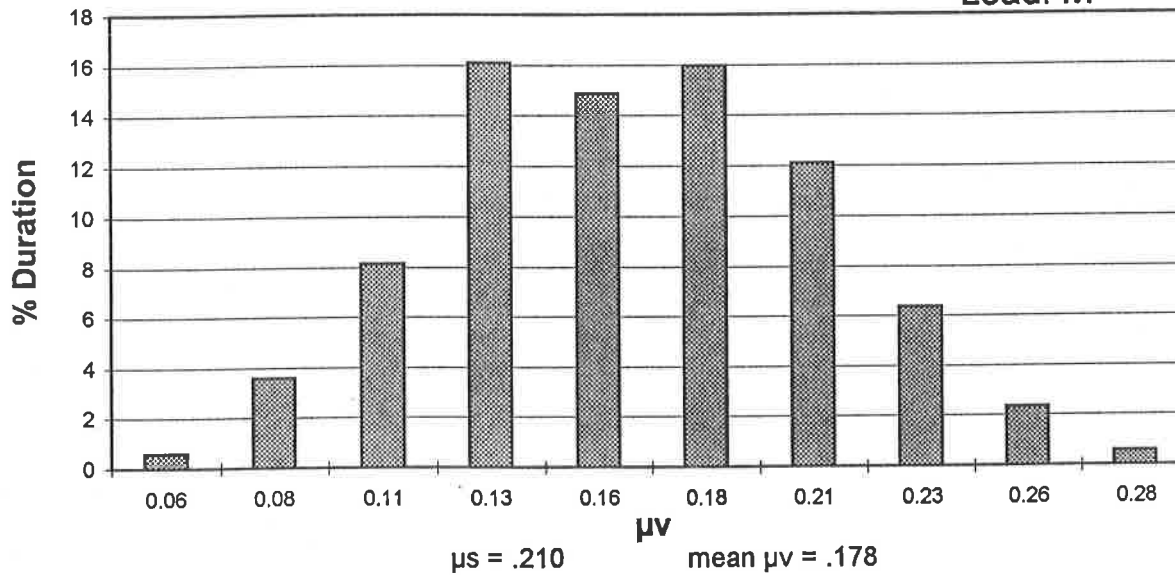
Deck: Y-Groove Aluminum

Skid: Plastic Skid

Load: L



Load: M



Load: H

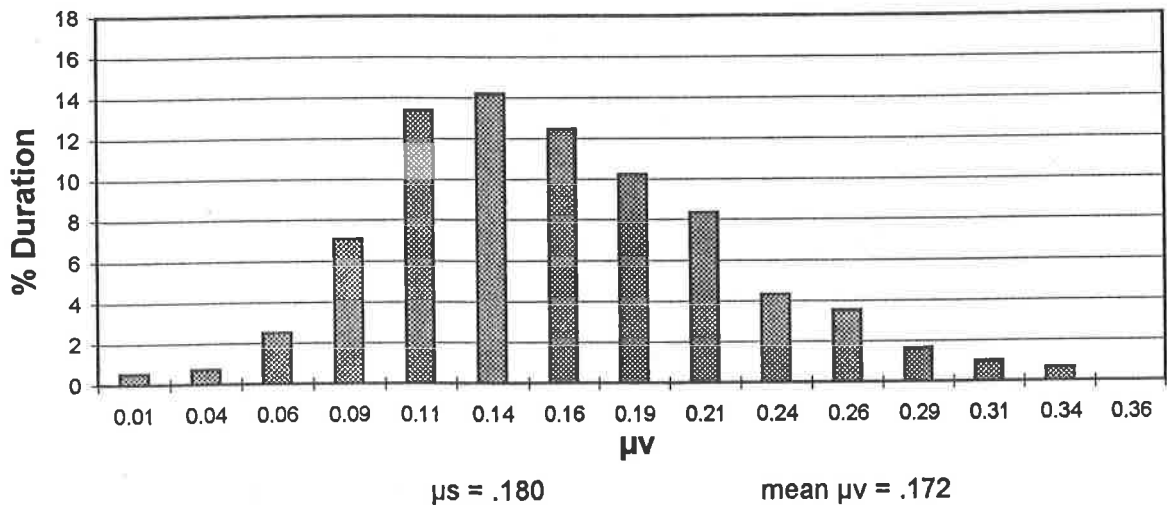
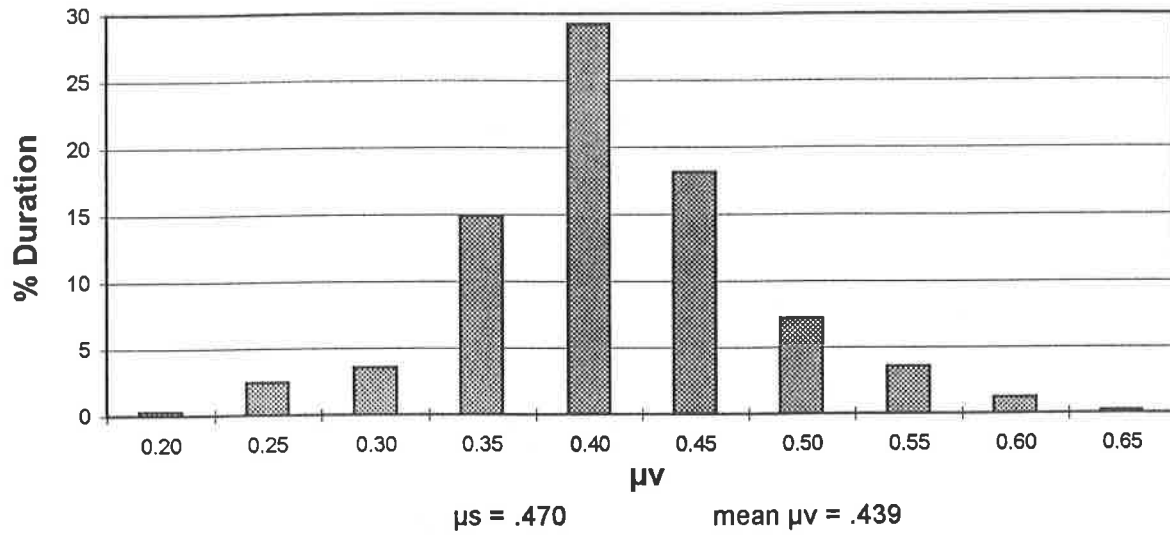


Figure 4-73: Amplitude distribution of coefficient of friction under vertical trailer vibration arising from the gravel road

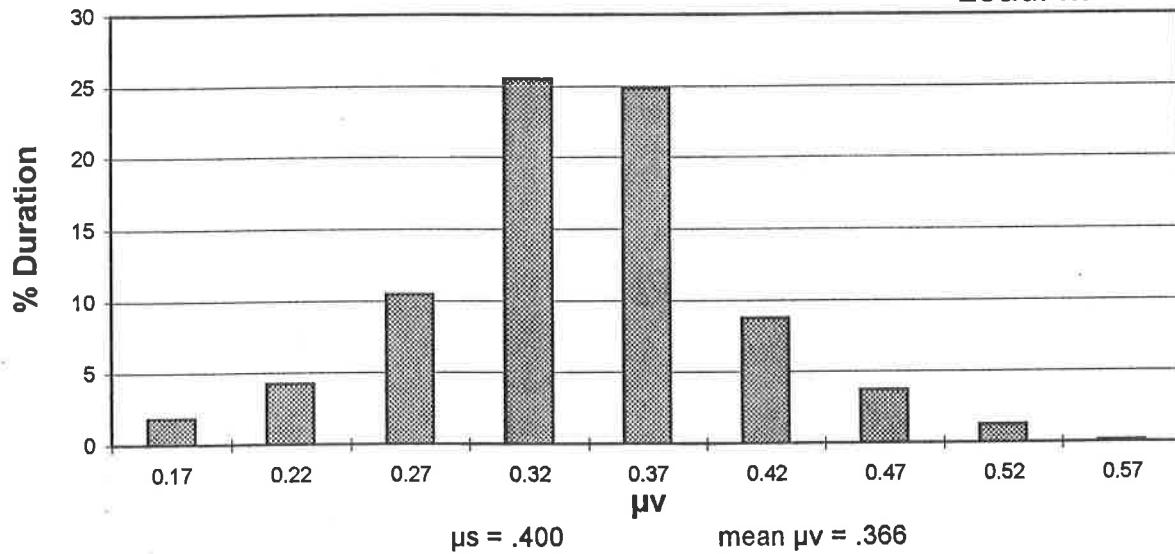
Deck: Y-Groove Aluminm

Skid: Steel Pads

Load: L



Load: M



Load: H

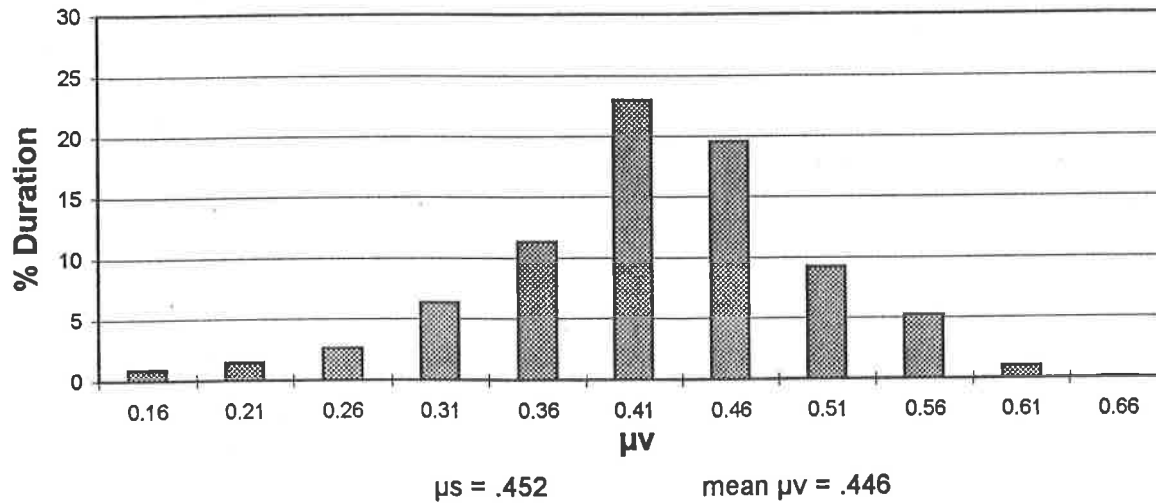


Figure 4-74: Amplitude distribution of coefficient of friction under vertical trailer vibration arising from the gravel road

#### 4.3.1.4 X-GROOVE ALUMINUM DECK

Figures 4.75 of 4.77 illustrate the amplitude distribution of  $\mu_v$  measured between X-groove aluminum deck and concrete, plastic skid and steel pad materials, respectively. The results describe the distribution of  $\mu_v$  values obtained under synthesized trailer vibration encountered while operating on a gravel road. The measurements performed with concrete skid under medium and high loads revealed mean values of 0.378 and 0.413, respectively. A comparison with the corresponding  $\mu_s$  values (0.333 and 0.472) reveal that exposure to random vibration results in higher friction with medium load, as observed earlier with the Y-groove aluminum and coarse hardwood decks. The friction coefficient measured under random vibration and high load, however, is approximately 12.5% lower than the respective  $\mu_s$  value. The measurements performed with plastic skid resulted in mean values of 0.269, 0.231 and 0.247, respectively, under light, medium and high loads. These mean values are observed to be quite close to the respective  $\mu_s$  values of 0.269, 0.231 and 0.247. The measurements performed with steel pads resulted in mean values of  $\mu_v$  (0.310, 0.360 and 0.310), which are within 11.6% of the corresponding  $\mu_s$  values (0.274, 0.327 and 0.362).

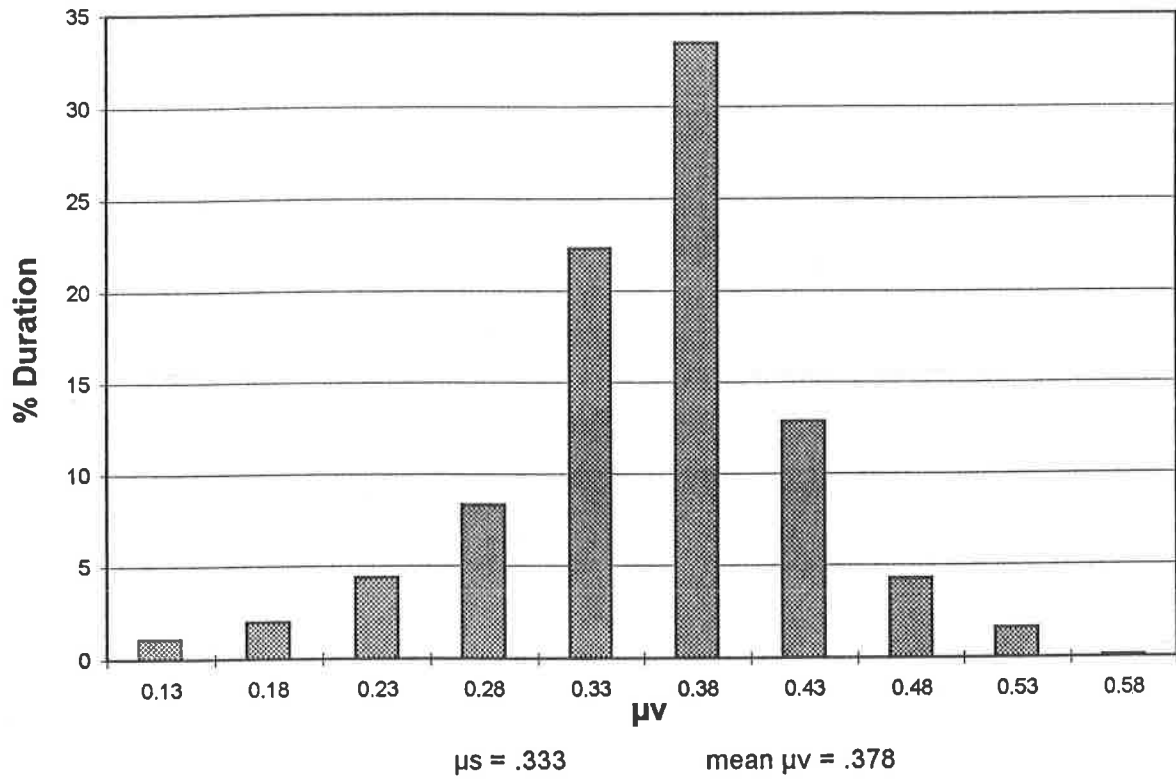
The analysis of the amplitude distribution data revealed that the  $\mu_v$  values fall below 75% of the mean of mean values for up to 15% of the test duration for the concrete and plastic skid materials, nearly 25% for the lightly loaded steel pads, and up to 12% for the steel pads under medium and high loads. Significantly higher occurrence of lower values of  $\mu_v$  for the lightly loaded steel pads is most likely attributed to poor contact (level) between the pads and the deck material.



Deck: X-Groove Aluminum

Skid: Concrete Blocks

Load: M



Load: H

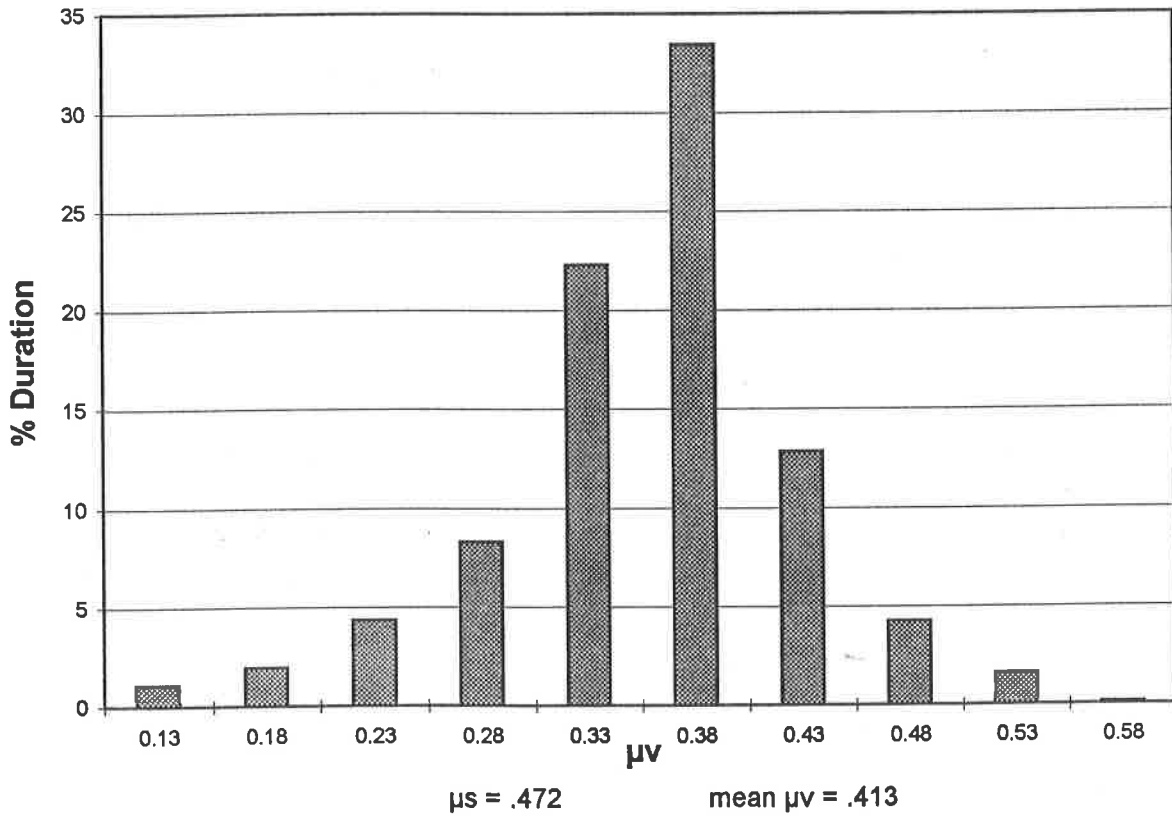
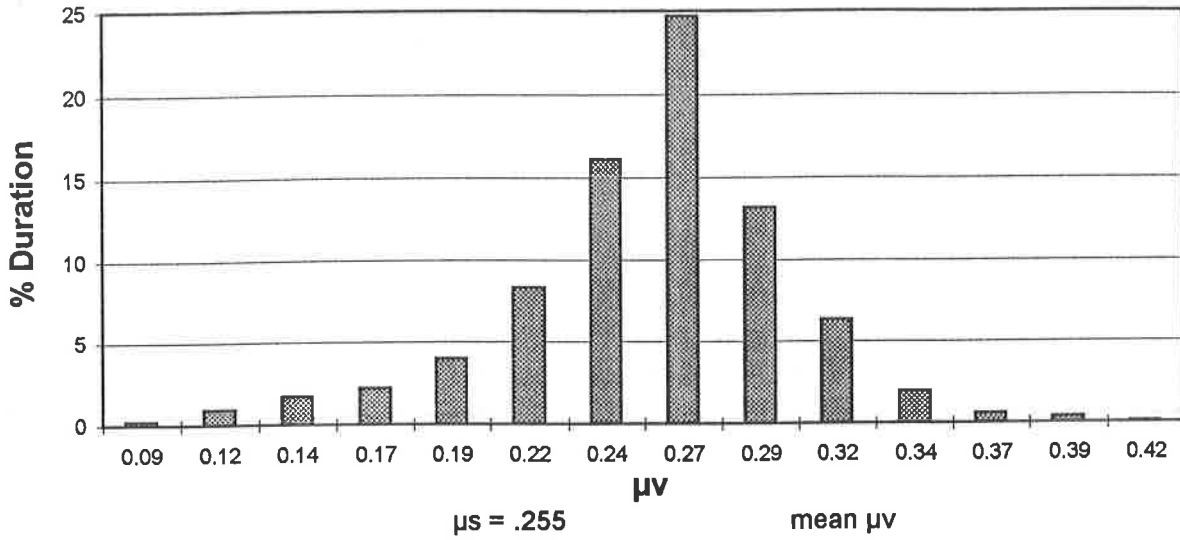


Figure 4-75: Amplitude distribution of coefficient of friction under vertical trailer vibration arising from the gravel road

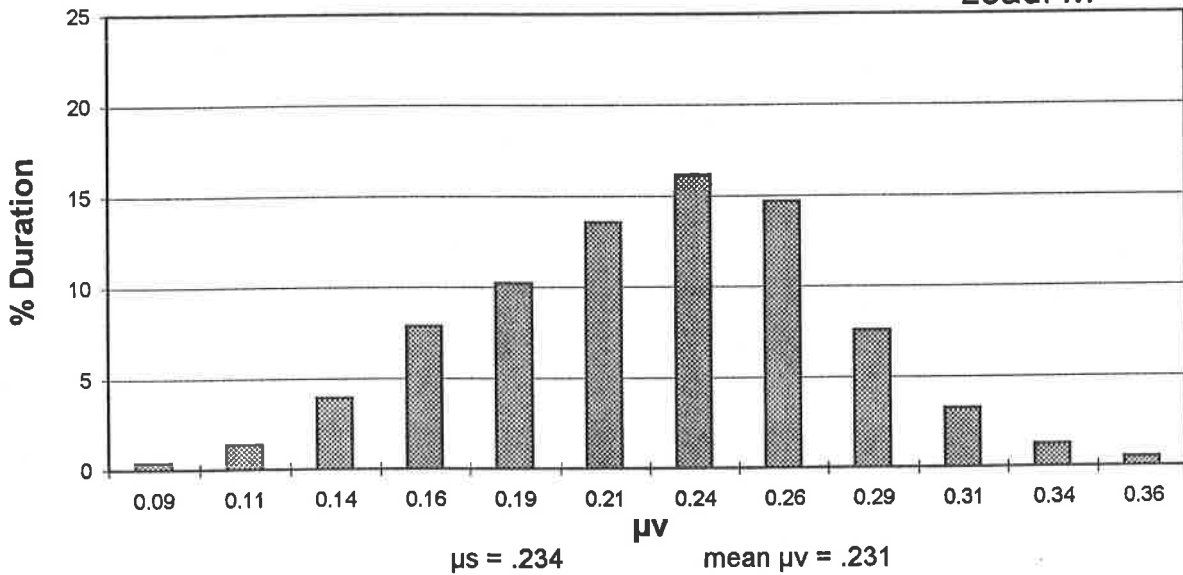
Deck: X-Groove Aluminum

Skid: Plastic Skid

Load: L



Load: M



Load: H

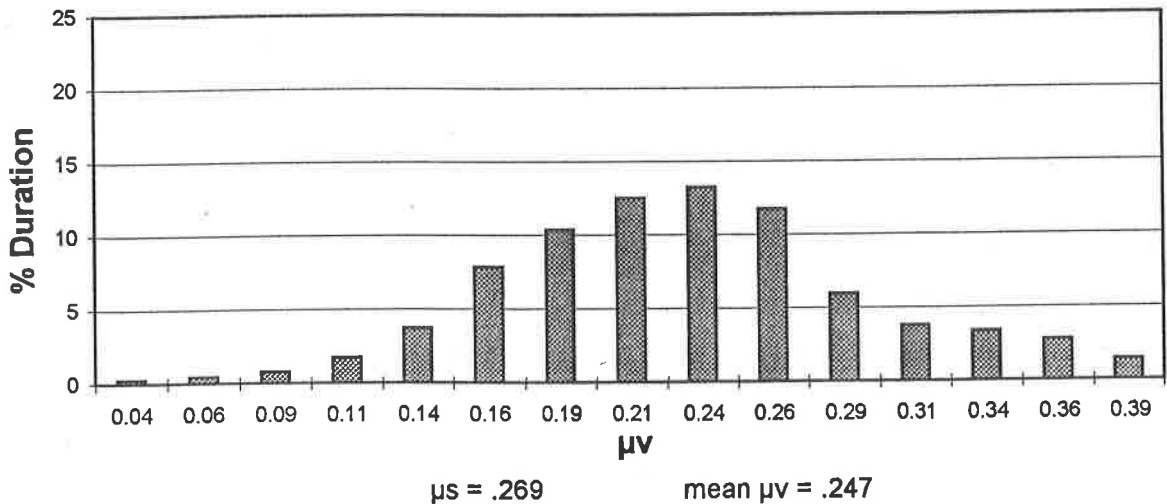
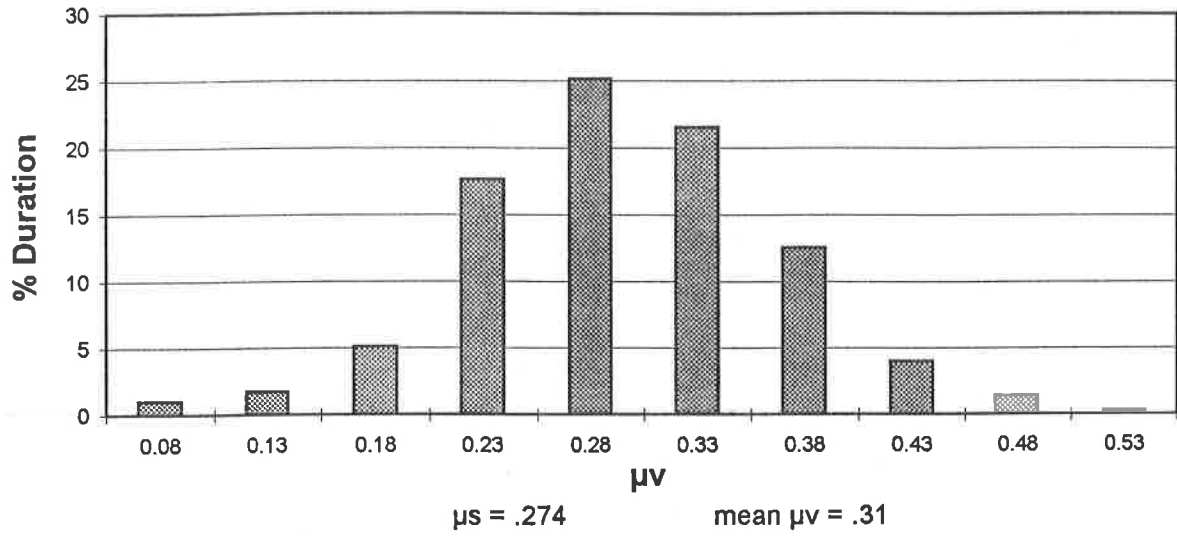


Figure 4-76: Amplitude distribution of coefficient of friction under vertical trailer vibration arising from the gravel road

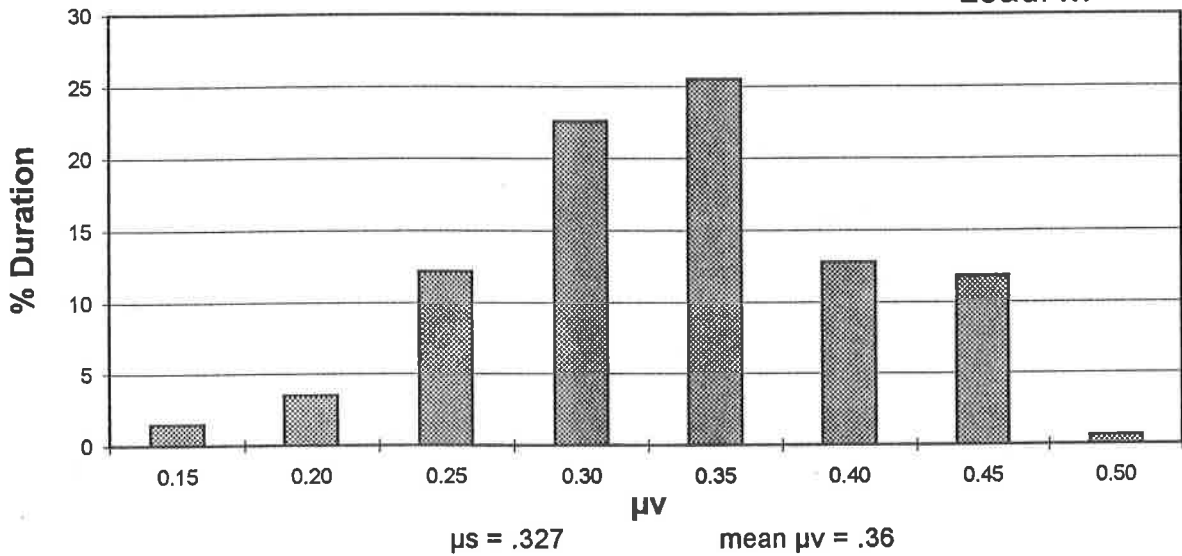
Deck: X-Groove Aluminm

Skid: Steel Pads

Load: L



Load: M



Load: H

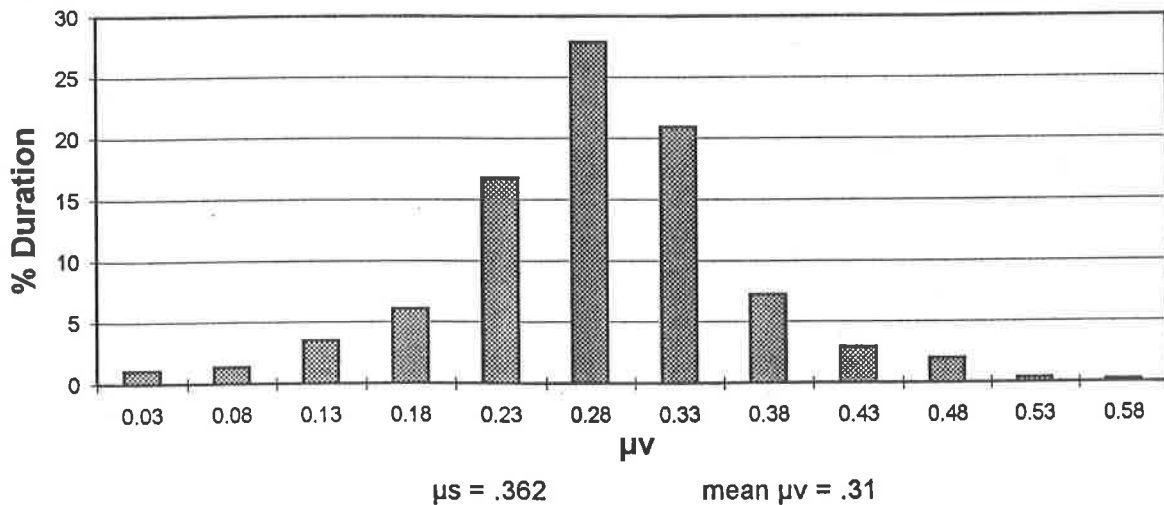
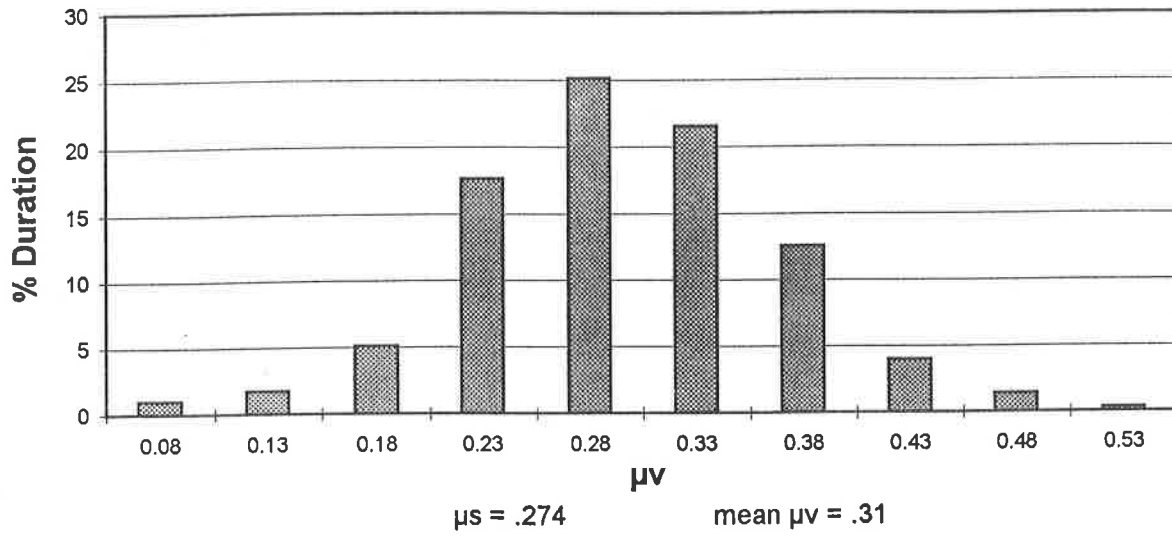


Figure 4-77: Amplitude distribution of coefficient of friction under vertical trailer vibration arising from the gravel road

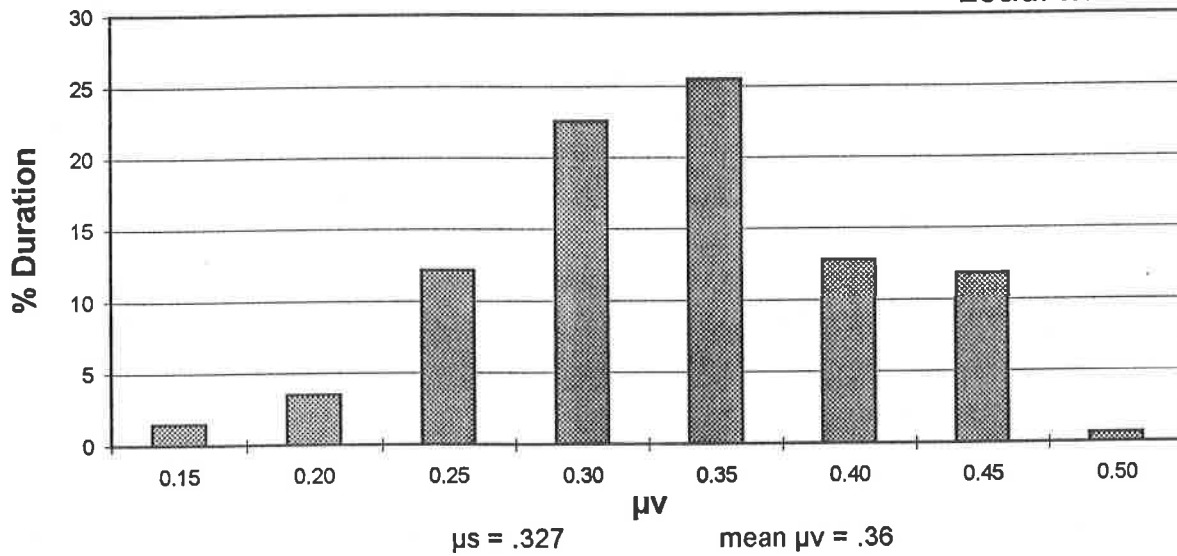
Deck: X-Groove Aluminm

Skid: Steel Pads

Load: L



Load: M



Load: H

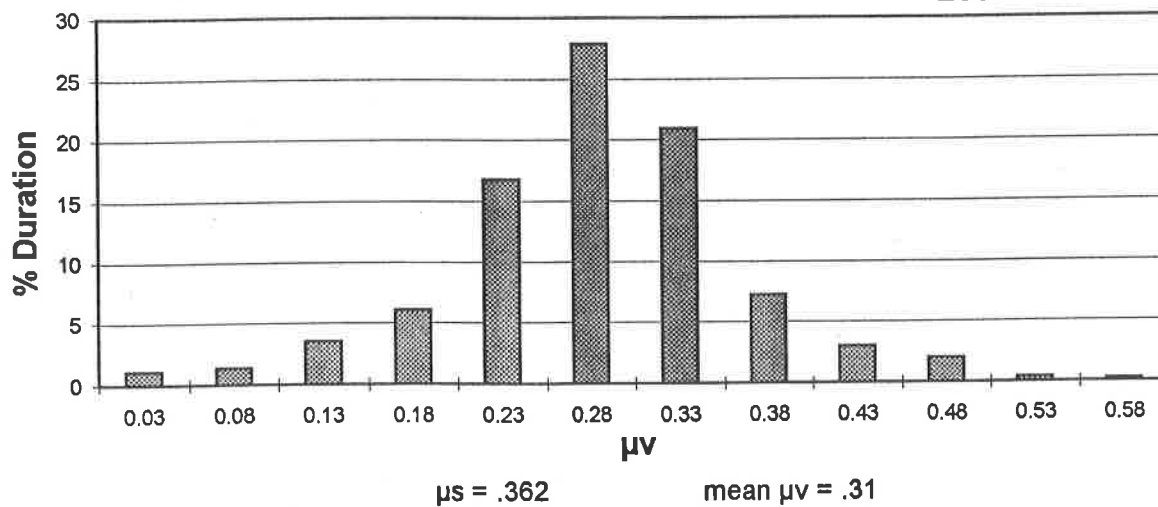


Figure 4-77: Amplitude distribution of coefficient of friction under vertical trailer vibration arising from the gravel road

## 5. CONCLUSIONS

Friction coefficients of selected skid and deck materials were measured under static and vertical vibration environments. The measurements were performed under sinusoidal and field measured random vibration of a three-axle trailer. The measurements performed under static conditions clearly illustrated the influence of normal load on the friction coefficients. The variations in friction coefficients with changes in the normal load were observed to be strongly dependent upon the relative flexibility of the skid and deck materials. Among the different skid materials examined, the plastic skid resulted in lowest values of sliding friction coefficients (0.142 on smooth hardwood and 0.2 on X-groove aluminum), while the rubber mat resulted in the highest values (0.66). The concrete, steel pads and machine feet skid surfaces also revealed relatively high values of friction coefficients, ranging from 0.509 between steel pads and coarse hardwood to 0.556 between machine feet and coarse hardwood.

The measurements performed under vertical sinusoidal vibration of acceleration amplitude ranging from 0.1g to 0.5g in the 1 to 12 Hz frequency range revealed cyclic nature of the friction force, mostly in-phase with the vertical acceleration. The experiments performed under acceleration levels exceeding 0.75g resulted in total loss of contact between the mating surfaces even at low excitation frequencies. The measured data was analyzed to derive the mean, and extreme minimum and maximum values of the friction coefficients, obtained by normalizing the dynamic friction force with respect to the normal load. The conclusions drawn from the results are summarized below:

- The mean values of friction coefficients measured under sinusoidal vibration either remained close to or only slightly higher than those measured under static conditions, irrespective of the magnitude and frequency of excitation. Slightly higher mean values were obtained when frequent stick-slip motion occurred.

- The minimum values of friction coefficients decreased gradually with increase in the excitation frequency up to 2 Hz, and remained nearly constant (in most cases) at higher frequencies.
- The minimum and maximum values of friction coefficients varied considerably with increase in the normal load and magnitude of acceleration. The variations, in the absence of hopping motion, however, were observed to be symmetric about the mean values. The loss of contact between the mating surfaces resulted in asymmetric variations about the mean values.
- The minimum values of friction coefficients were observed to be up to 80% lower than the mean values under high normal loads and high magnitude of vertical vibration.
- The minimum values of friction coefficients were observed to depend upon the flexibility of the deck and skid materials. The flexible plastic skid resulted in lowest values near frequencies of 2 Hz, while the aluminum deck revealed lowest values in the 4 - 8 Hz frequency range.

The measurements performed under field measured trailer vibration, synthesized in the laboratory, revealed mean values comparable to those measured under static conditions. The analysis of the measured data revealed the following:

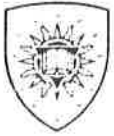
- The measurements performed under excitations arising from gravel and asphalt roads resulted in similar friction forces, due to nearly similar vibration response of the trailer operating on both roads.
- The mean values of friction coefficients were observed to correlate well with those measured under static condition, with the exception of concrete material. The concrete material under medium load revealed relatively high mean values of friction with all the deck surfaces. The mean values measured under high loads, however, were slightly lower.
- An analysis of the amplitude distribution of the measured friction coefficients revealed that the coefficient of friction falls below 75% of the mean value for duration as high as 25% of the total test duration.

## 6. REFERENCES

1. Rakheja, S., Ranganathan, R. and Sankar, S., "Load spill analysis of an articulated vehicle transporting wooded logs", *Proceedings of the Ninth Symposium on Engineering Applications of Mechanics*, London, Ontario, May 1988, pp 380-388.
2. Billing, J.R., Mercer, W.R.J. and Cann, W., "A proposal for research to provide a technical basis for a revised national standard on load security for heavy trucks", *Ontario Ministry of Transportation Report CV-93-02*, November 1993.
3. Billing, J.R., "Need for evaluation of friction between a load and a truck deck subject to vibration", *CCMTA Load Security Project Proposal*, 18 May 1995.
4. Kragelskii, I.V. and Mikhin, N.M., "*Handbook of friction units of machines*", ASME Press, New York, 1988.
5. Shackelford, J. and Alexander, W., "*CRC material science and engineering handbook*", CRC Press, 1992.
6. Baumeister, T. et al., "*Marks engineering handbook for mechanical engineers*".
7. Billing, J.R. and Lam, C.P., "Friction between typical beds and loads, CCMTA Load Security Research Project, Section 10.2", *Ontario Ministry of Transportation Draft Report*, 19 March 1996.
8. Demian, T. and Pascu, Adrian, "*Lagâre si ghidaje pentru aparate*", Editura Academiei Republicii Socialiste România, 1980.
9. Harris, C.M. and Crete, C.E., "*Shock and vibration handbook*", McGraw Hill Book Co., 1976.







September 24, 1996

Mr. Sean McAlister  
Programs Manager  
CCMTA  
2323 St. Laurent Blvd.  
Ottawa, Ontario  
K1G 4K6

Dear Mr. McAlister:

It was indeed a pleasure visiting you and meeting my friends and colleagues. We have finally completed the statistical analysis of the measured data, as we discussed. I am pleased to enclose the self-explanatory results of the probability distribution of the friction coefficients. Apart from the statistical analysis of the friction coefficients, we have also re-examined the time-histories of measured trailer vibration. This primarily evolved from the comments raised by Mr. John Billing on relatively high magnitudes of acceleration considered in the study. Over my many years of association with John involving several discussions on various technical issues, I have learnt to take his comments considerably more seriously. Although this invariability resulted in more work for me, however the end results have consistently been good. Apparently, the present case was not any different.

I am pleased to bring to your attention that both the analyses resulted in very positive findings, more or less good news for the committee (I hope), which are described below.

1. Statistical Analysis of the Friction Coefficients Measured under Trailer Bed Vibration

The friction coefficients ( $\mu_v$ ) measured under synthesized trailer vibration are analyzed to determine the mean, standard deviation, and cumulative probability distribution. The enclosed figures illustrate the above and unsmoothed probability distribution derived from the measured data. Since the histogram presented in our report did not enable us to derive the probabilities more accurately, these results have been derived using the incremental step in  $\mu_v=0.01$ . The results are also summarized in the enclosed table. It should be noted that the mean and standard deviation values listed in the table represent the overall mean values for all three loads (L, M and H). The results show some very interesting trends, which may provide us to arrive at certain values with minimal risk.

.../2

- The dynamic variation in the friction coefficient, defined as the ratio of standard deviation to the mean value, yields very consistent results. This dynamic variation ranges from 12% to 18.7% for most combinations of deck-skidder materials, with the exception of steel pads and plastic skid. The dynamic variation for the steel pads on the Y-groove aluminum and coarse hardwood is also within the above range. It results in relatively high variation (23%) only for the X-groove aluminum deck. This dynamic variation for the plastic skid is obtained as 22% with X-groove aluminum, 28% with Y-groove aluminum and 27% for the smooth-hardwood deck.

I am inclined to speculate that high variation for the steel pad - X-groove aluminum combination is most likely due to inadequate leveling. The plastic skid, however, certainly leads to consistently high dynamic variations.

In view of the relatively small and highly consistent range of dynamic variations or the standard deviation (12% - 18.7%), the effect of vibration may be accounted for by considering the available friction coefficient as:

$$\begin{aligned} \text{Available friction coefficient, } \mu_a &= \mu_v (1 - \text{peak dynamic variation}) \\ \mu_a &= \mu_s (1 - \text{peak dynamic variation}) \end{aligned}$$

Based upon the normal distribution, the above proposed criteria can lead to 16% probability of friction coefficient being below  $\mu_a$ . I, therefore, consider the risk factor associated with this criteria is 16%.

- Alternatively, a risk factor may be defined directly from the static friction coefficients in the following manner:

Risk Factor = Probability that the friction coefficient under vertical vibration falls below  $p\mu_s$ ,

where p is the safety factor that may be established from the range of dynamic variations. In the above analysis, p will assume a value of 0.813 ( $p = 1 - \text{peak dynamic variation, } 0.187$ ). As discussed in our report, the factor  $p=0.75$  may be considered due to uncertainties associated with characteristics of vibration. This factor represents a safety factor of approximately 1.33 above the peak dynamic variation (.187). A value of  $p=0.75$  implies that the risk factor is equal to the probability of dynamic friction coefficient being 25% lower than the corresponding friction coefficient measured under static condition.

Using this criteria and neglecting the data obtained for plastic skid and steel pads - X-groove-aluminum combinations, the risk factor ranges from a low of 4% for concrete to a high of 11.27% for the paper, as summarized in the table. I have also listed the corresponding values for  $p=0.9$  and  $p=0.5$  in the event committee wishes to consider alternate factors.

2. Analysis of the Field Measured Time History of the Trailer Acceleration

An examination of the time-history of the measured trailer vibration over a period of 30 minutes was undertaken. The results discussed below are partly embarrassing for me and certainly very positive for the committee.

- The data revealed only occasional peaks of magnitude nearly 2g, the majority of data was observed to be within  $\pm 0.5g$ .
- The test spectra considered in this study was extracted to represent majority of the events, i.e. within  $\pm 0.5g$ . Now here is the embarrassing part, the results presented in Figure 4.59 of the report somehow omitted the acceleration and presented the displacement only. It was intended to include both displacement and acceleration. I apologize for the error. A revised figure is enclosed.
- The probability density and cumulative distribution of the test acceleration (enclosed) reveals that the peak acceleration is below 0.5g.

I sincerely hope that this analysis will be of some help to the committee. In the event you may require any further assistance, please do not hesitate to contact me. Once again, I thank you for providing the CONCAVE group with an opportunity to participate in the study.

Sincerely yours,



Subhash Rakheja  
Director and Professor

SR/az

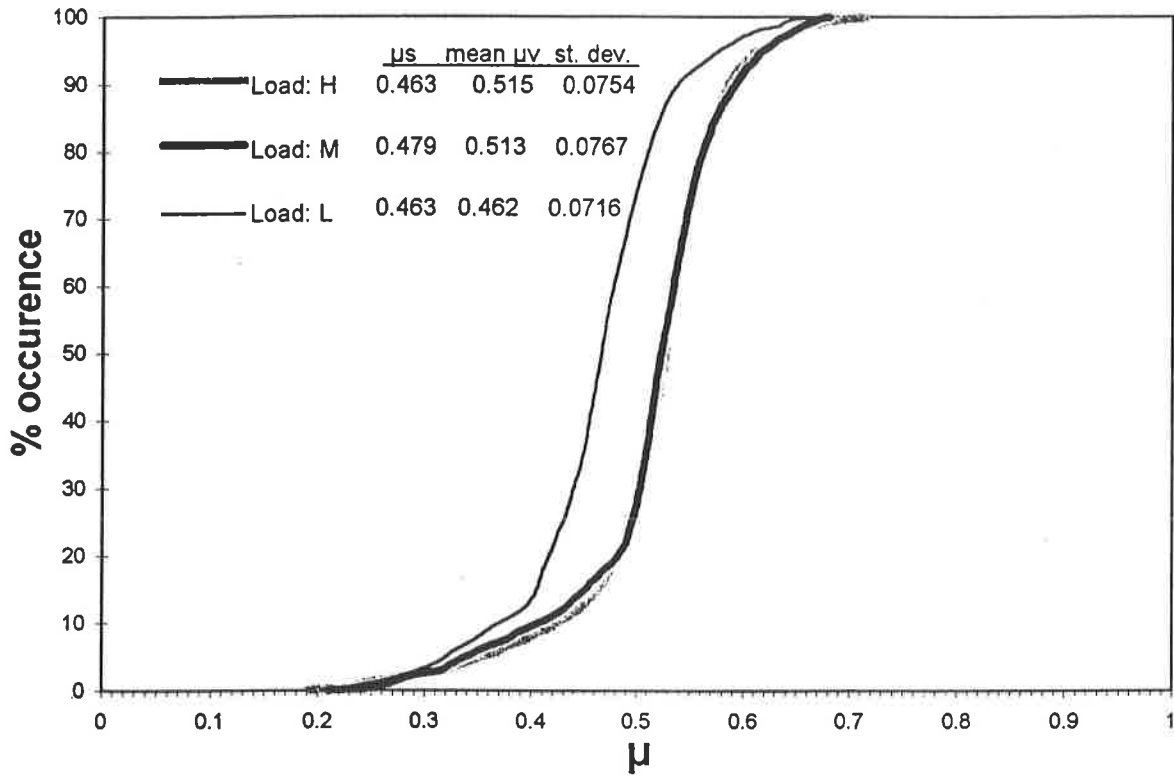
**SUMMARY OF MEAN, STANDARD DEVIATION AND DYNAMIC VARIATIONS IN FRICTION COEFFICIENTS  
MEASURED UNDER SYNTHESIZED TRAILER VERTICAL VIBRATION**

DECK	SKID	FRICTION COEFFICIENTS UNDER VIBRATION			PROBABILITY OF MEAN $\mu$ (%)		
		MEAN	STANDARD DEVIATION	DYNAMIC VARIATION (%)	$\leq 0.5\mu$ ,	$\leq 0.75\mu$ ,	$\leq 0.9\mu$ ,
Aluminum X-Groove	Concrete	0.396	0.074	18.7	0.4	5.3	12.1
	Plastic Skid	0.249	0.0539	21.7	1.9	14.0	32.3
	Steel Pads	0.327	0.0755	23.1	2.2	12.1	29.2
Aluminum Y-Groove	Concrete	0.388	0.0707	18.2	0.3	4.0	8.25
	Plastic Skid	0.175	0.0490	28.0	6.1	32.2	58.4
	Steel Pads	0.417	0.0498	12.0	1.0	12.3	42.2
Coarse Hardwood	Machine Feet	0.575	0.0928	16.0	0.2	5.6	19.0
	Concrete	0.616	0.0871	14.0	0.3	4.0	8.4
	Spruce Board	0.514	0.0865	17.0	0.4	5.6	13.5
	Steel Pads	0.507	0.0811	16.0	0.5	7.2	20.1
Smooth Hardwood	Kraft Paper	0.356	0.0566	15.9	1.4	11.3	44.9
	Rubber Mat	0.656	0.0967	14.8	0.4	8.4	20.7
	Plastic Skid	0.145	0.0393	27.0	5.2	19.6	34.7
	Smooth Steel	0.497	0.0746	15.0	0.4	6.2	13.8

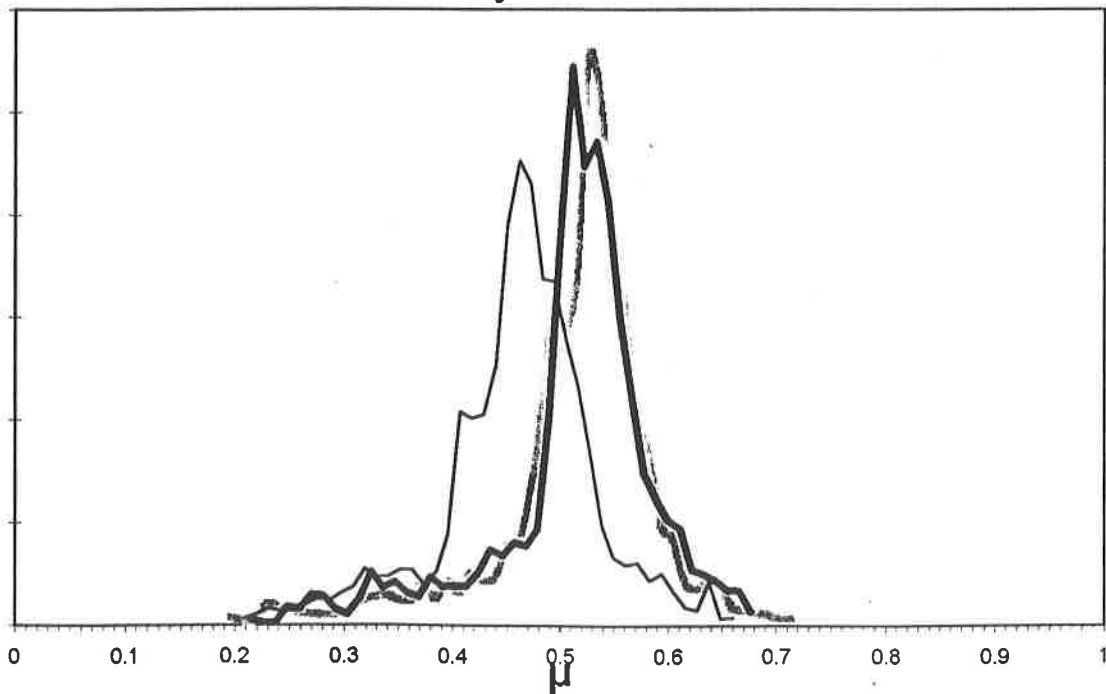
# Cumulative Probability Distribution

Deck: Smooth Hardwood

Skid: Smooth Steel



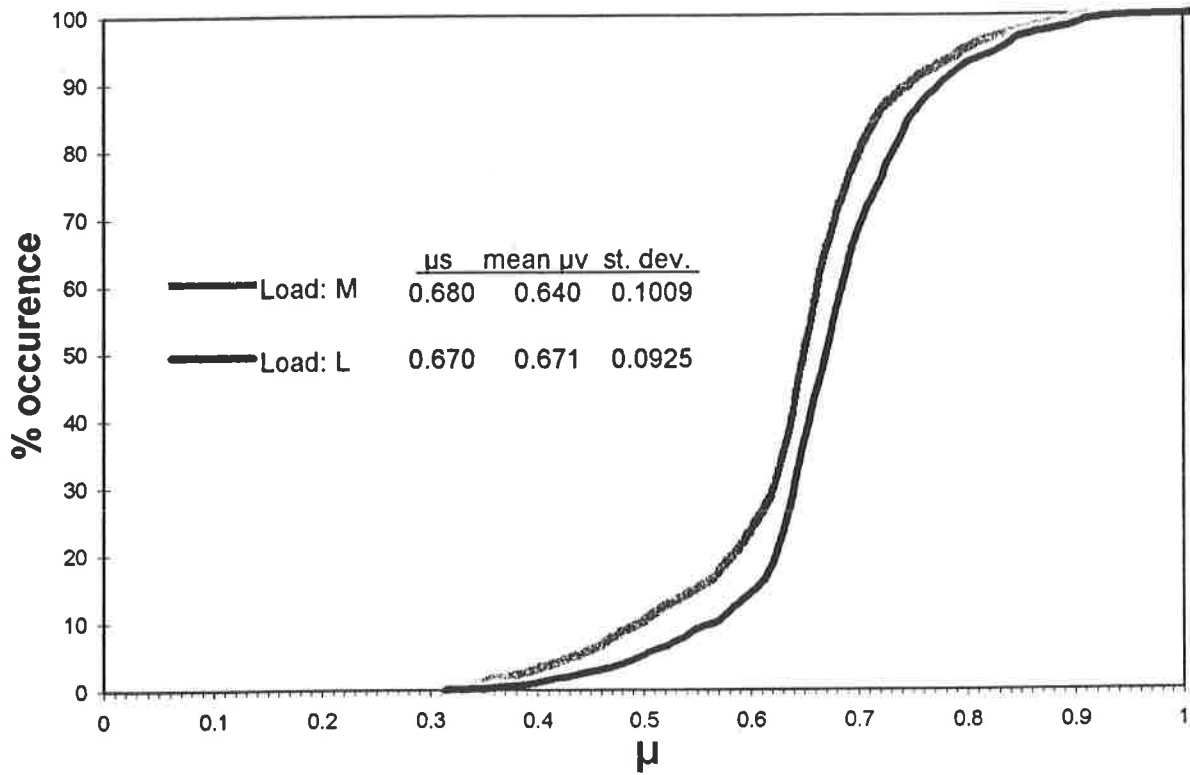
# Probability Distribution



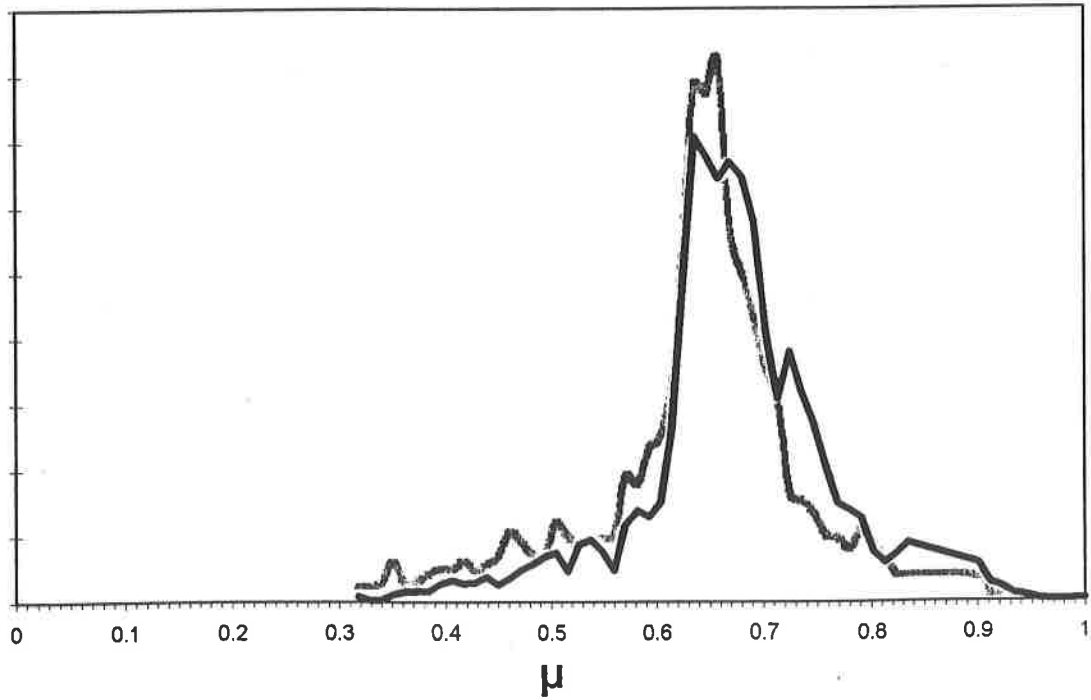
## Cumulative Probability Distributions

Deck: Smooth Hardwood

Skid: Rubber Mat



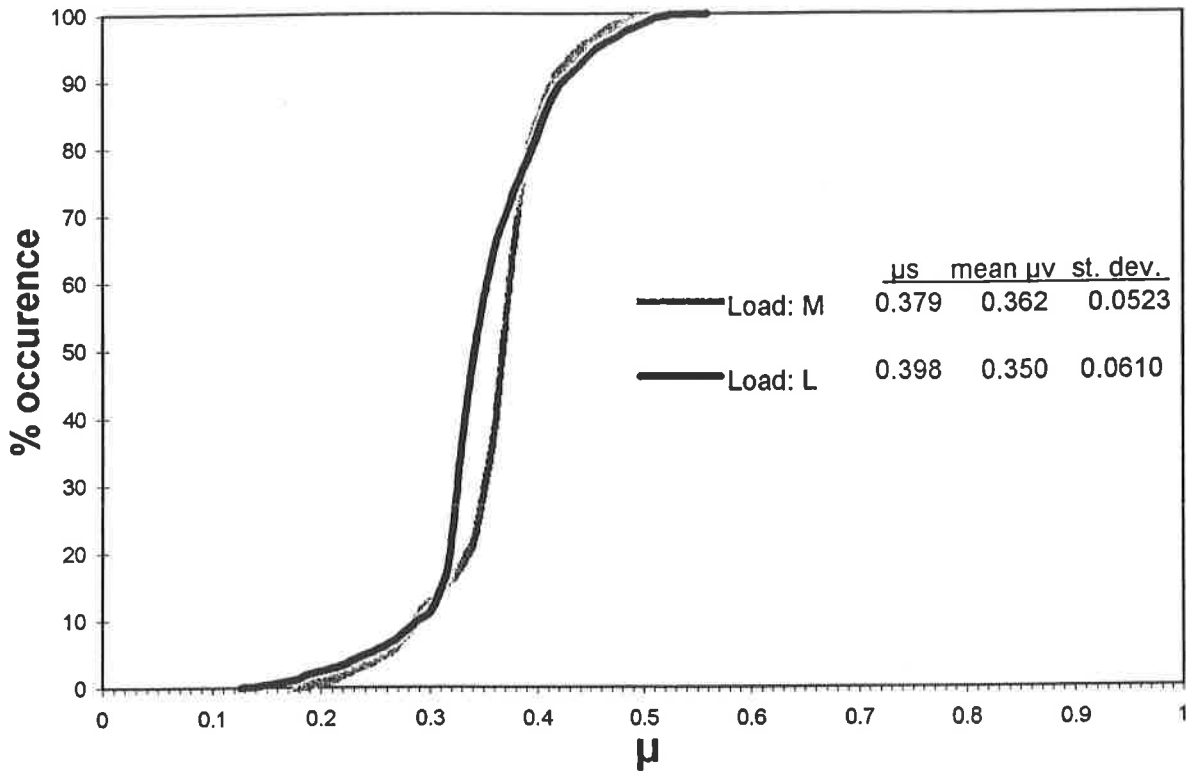
## Probability Distribution



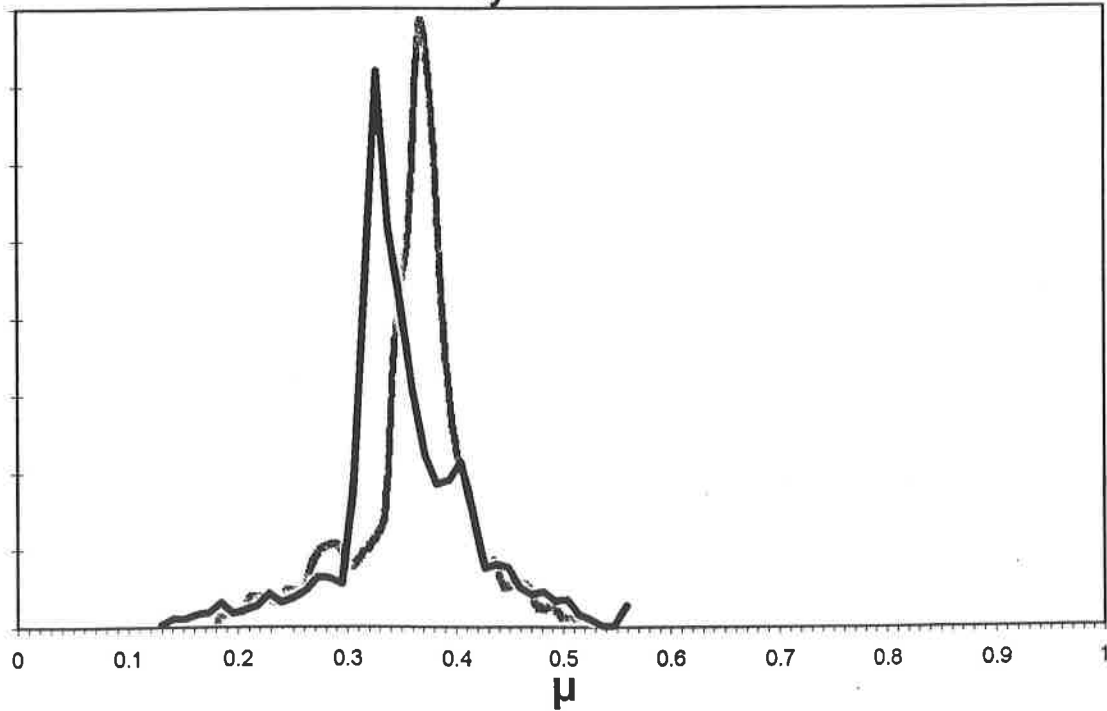
# Cumulative Probability Distribution

Deck: Smooth Hardwood

Skid: Kraft Paper



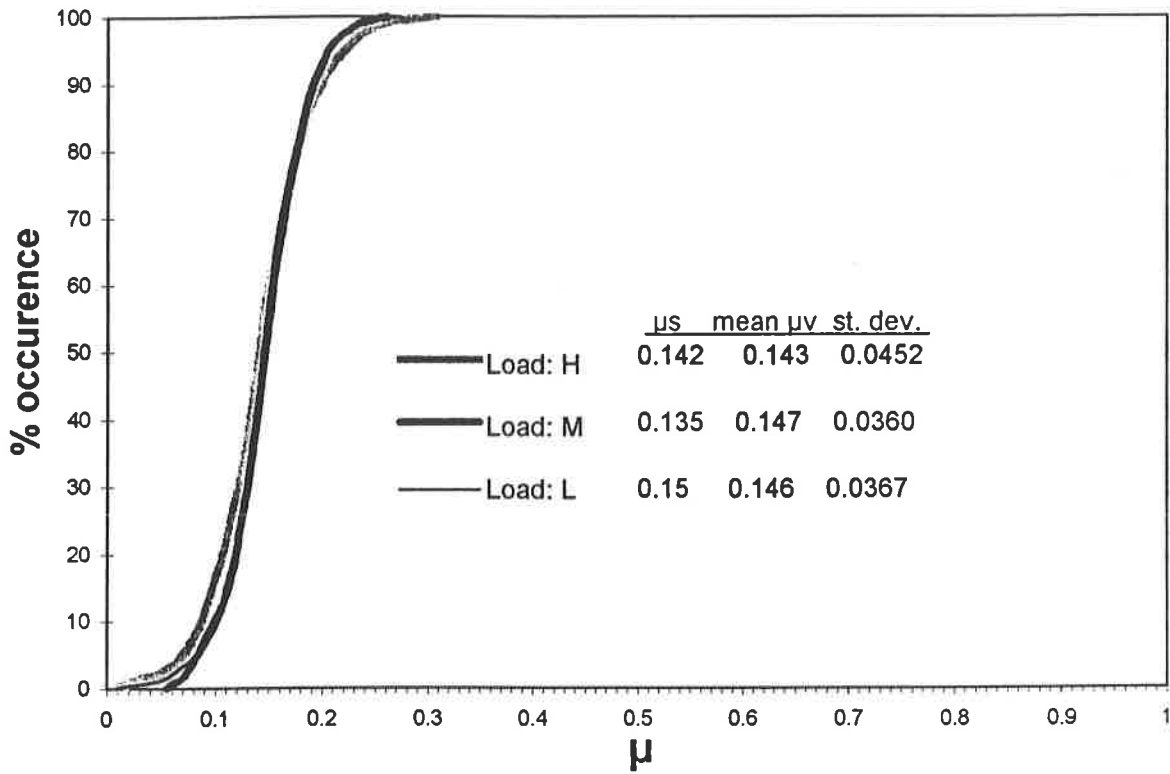
# Probability Distribution



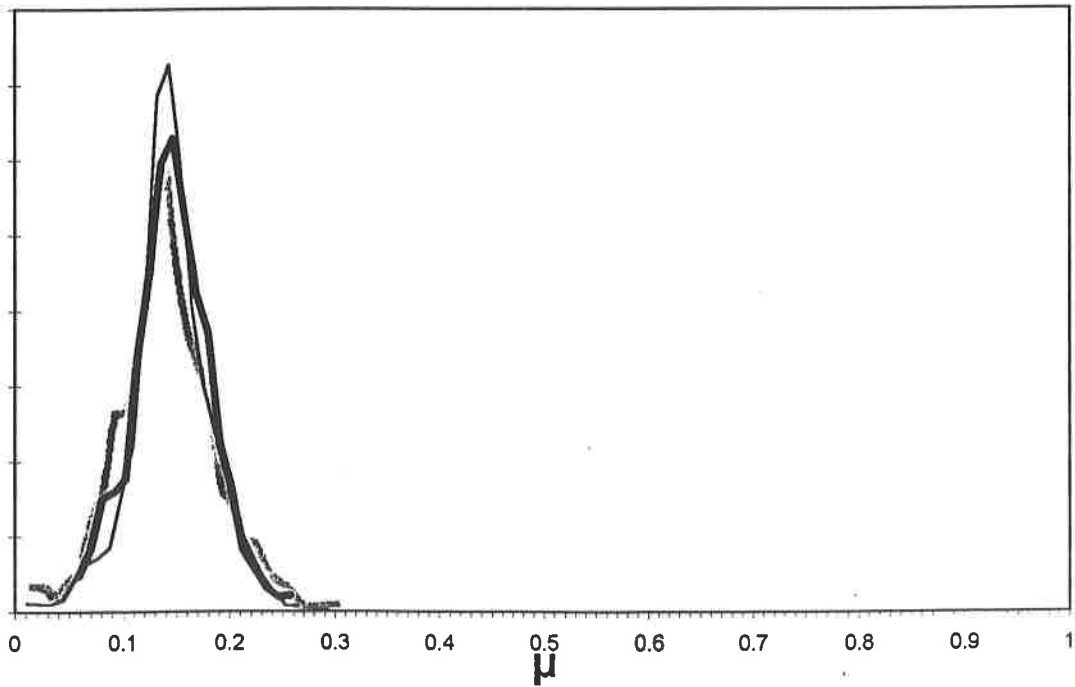
# Probability Distributions

Deck: Smooth Hardwood

Skid: Plastic Skid



# Probability Distribution

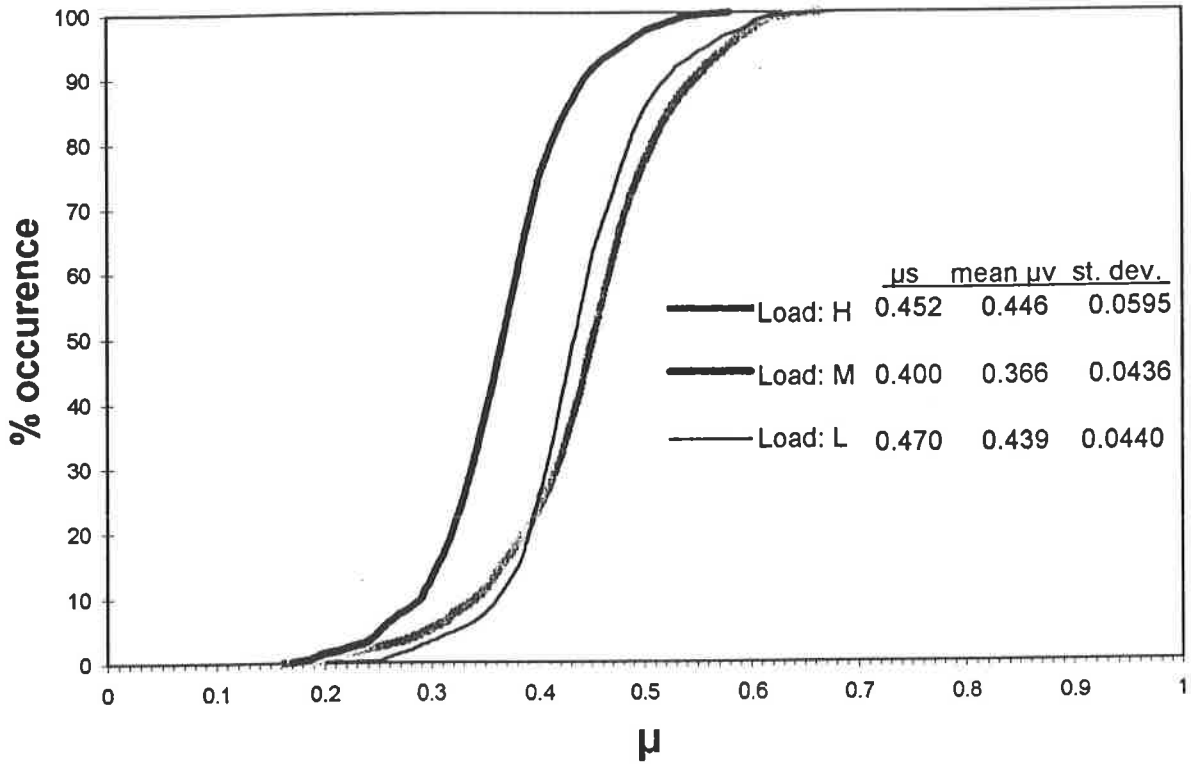




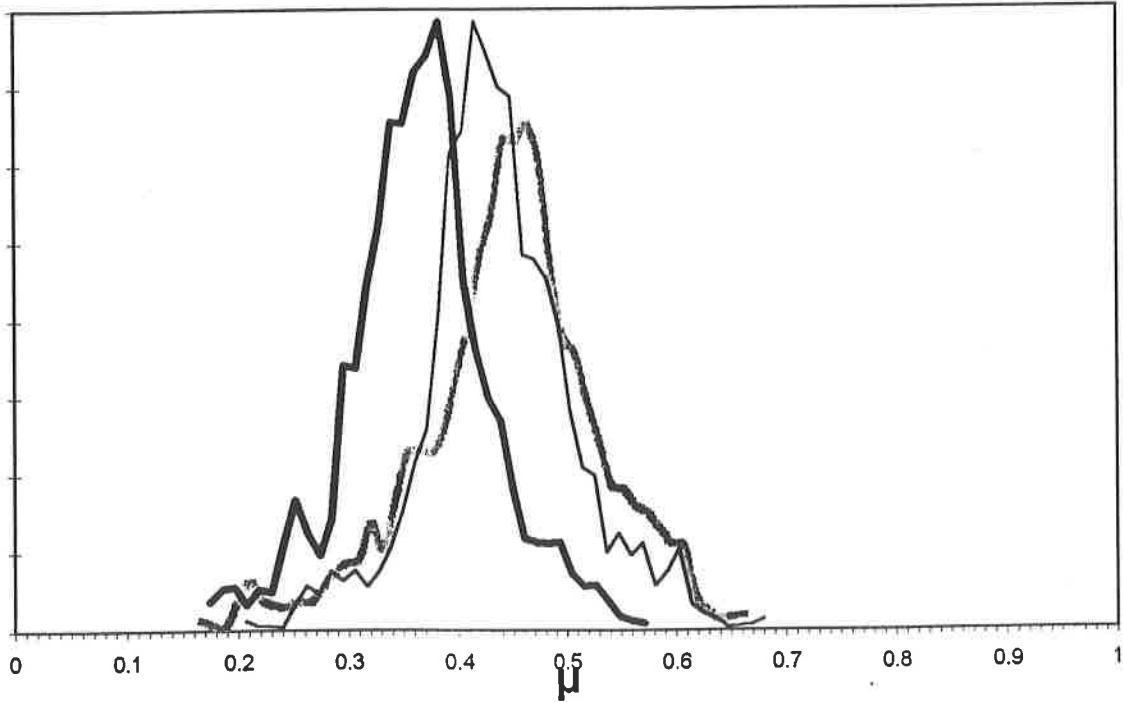
# Cumulative Probability Distribution

Deck: Y-Groove Aluminum

Skid: Steel Pads



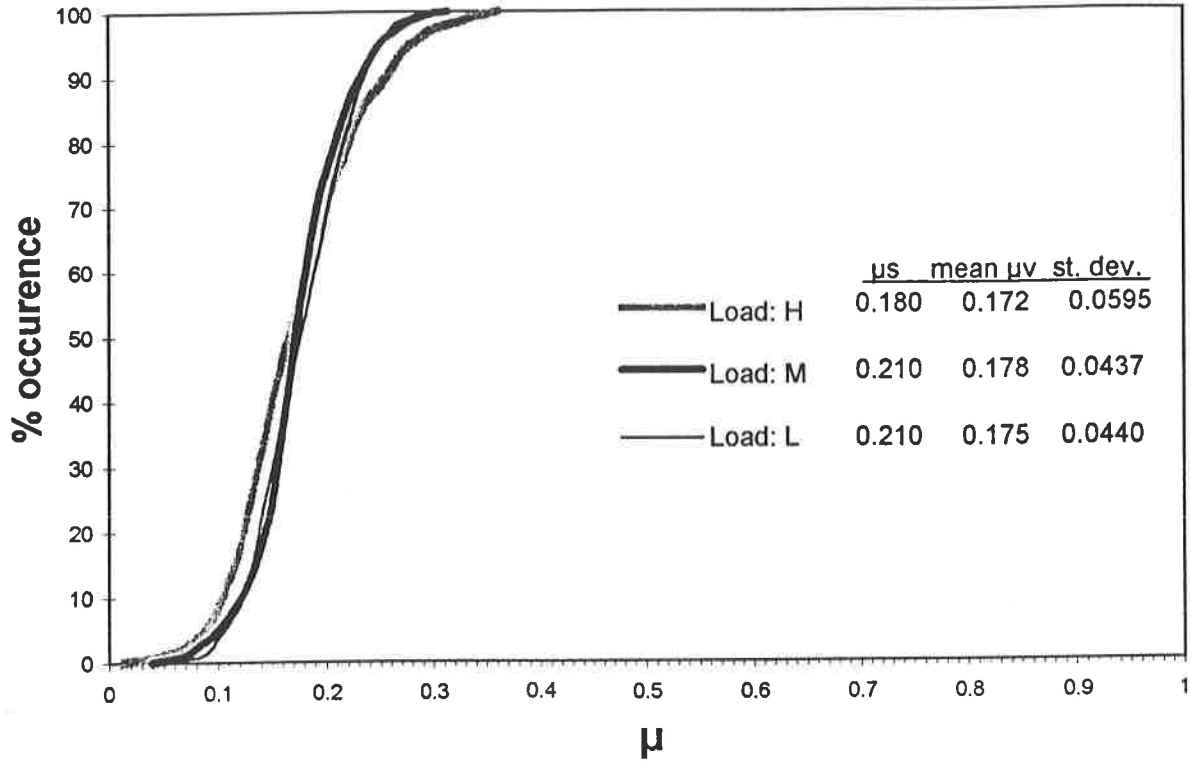
# Probability Distribution



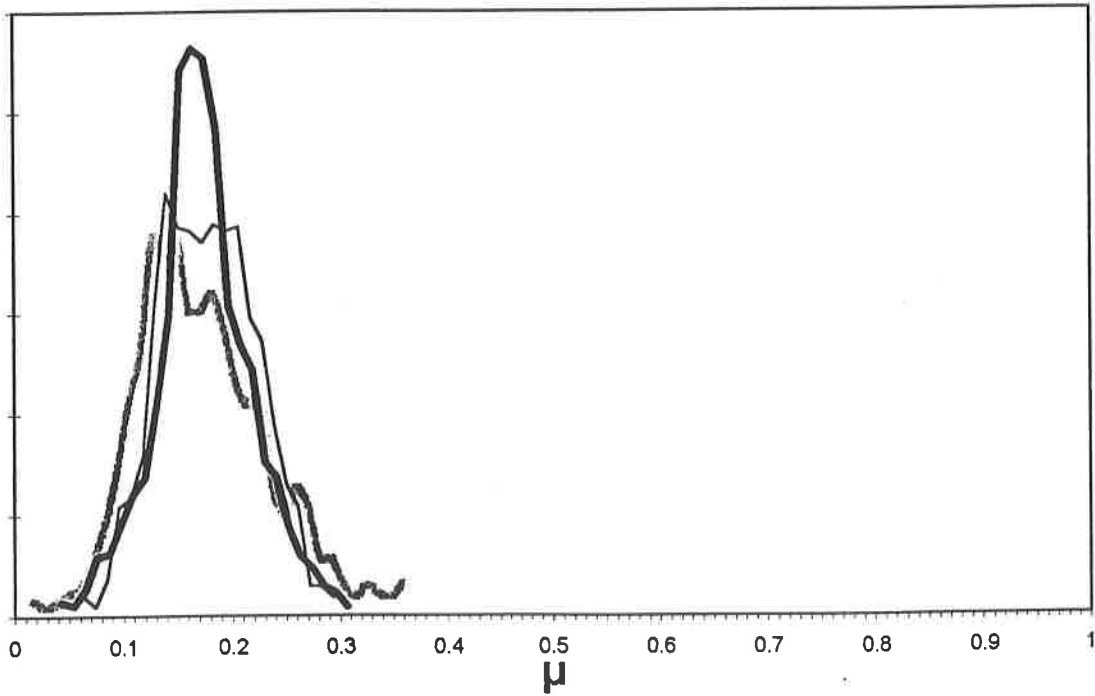
## Cumulative Probability Distribution

Deck: Y-Groove Aluminum

Skid: Plastic Skid



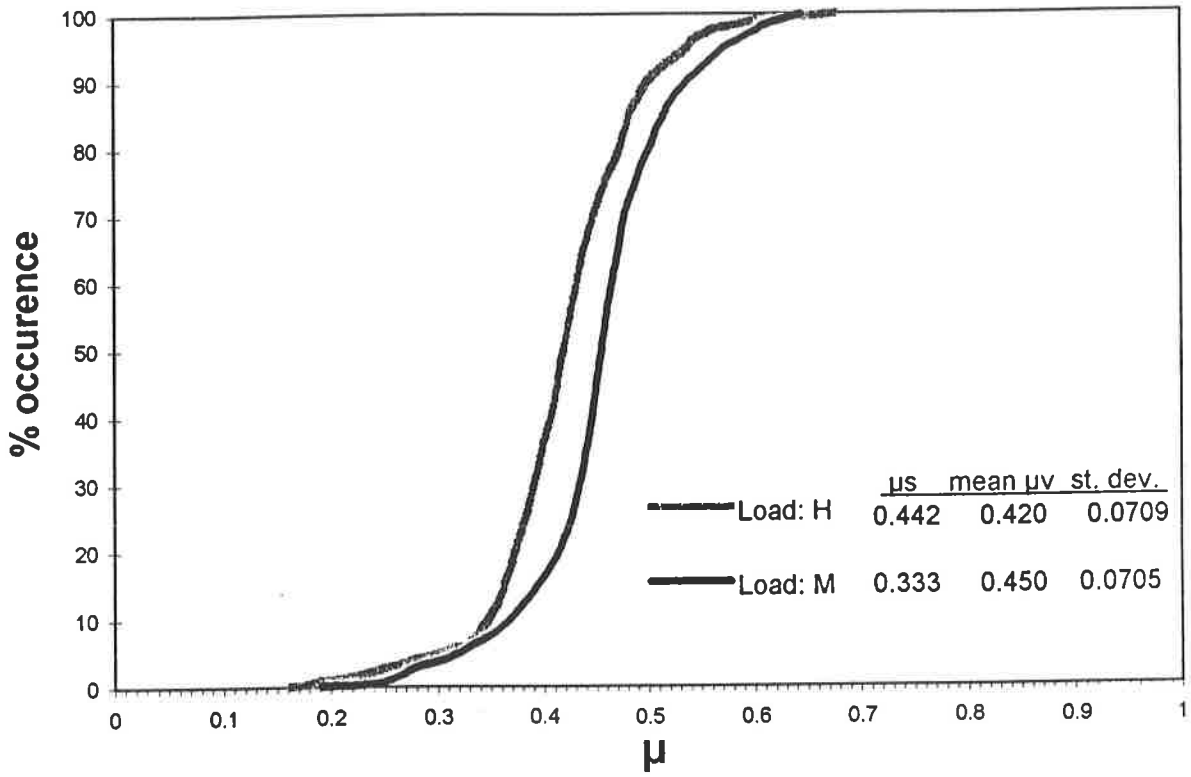
## Probability Distribution



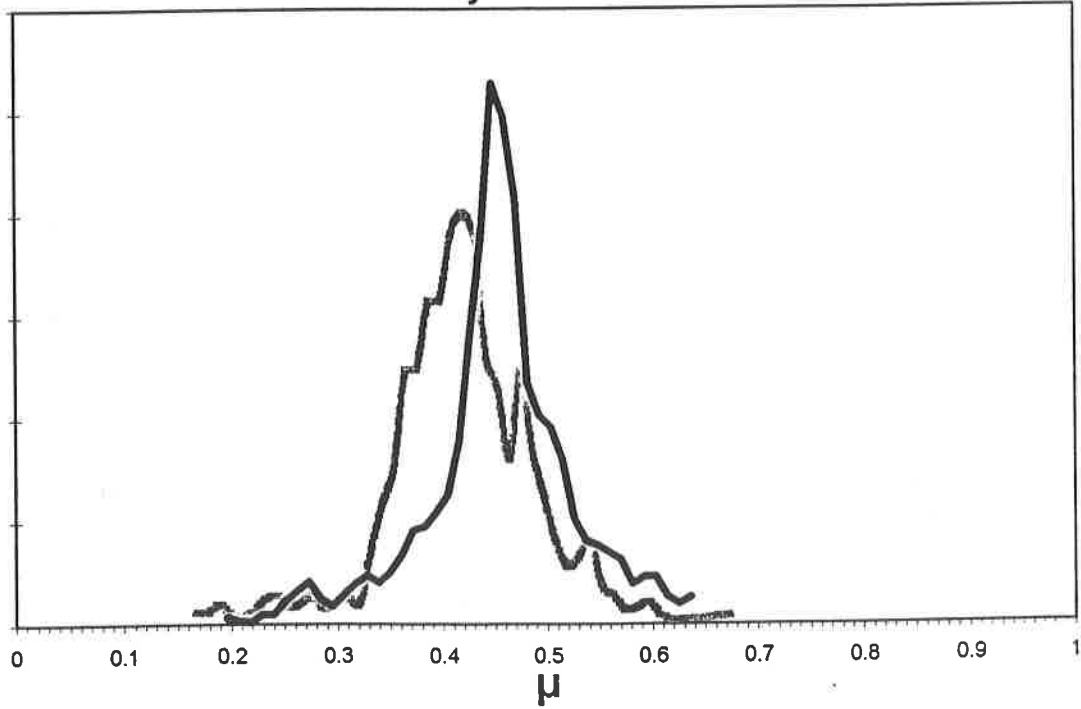
## Cumulative Probability Distribution

Deck: Y-Groove Aluminum

Skid: Concrete Blocks



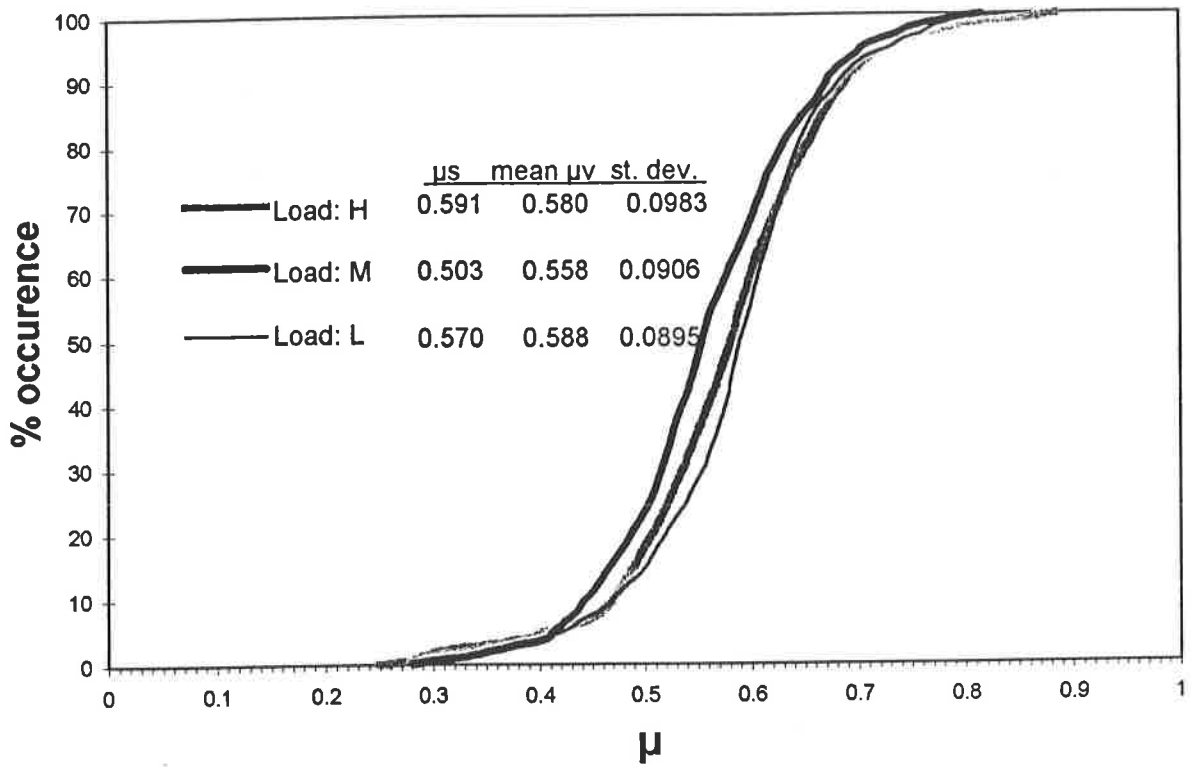
## Probability Distribution



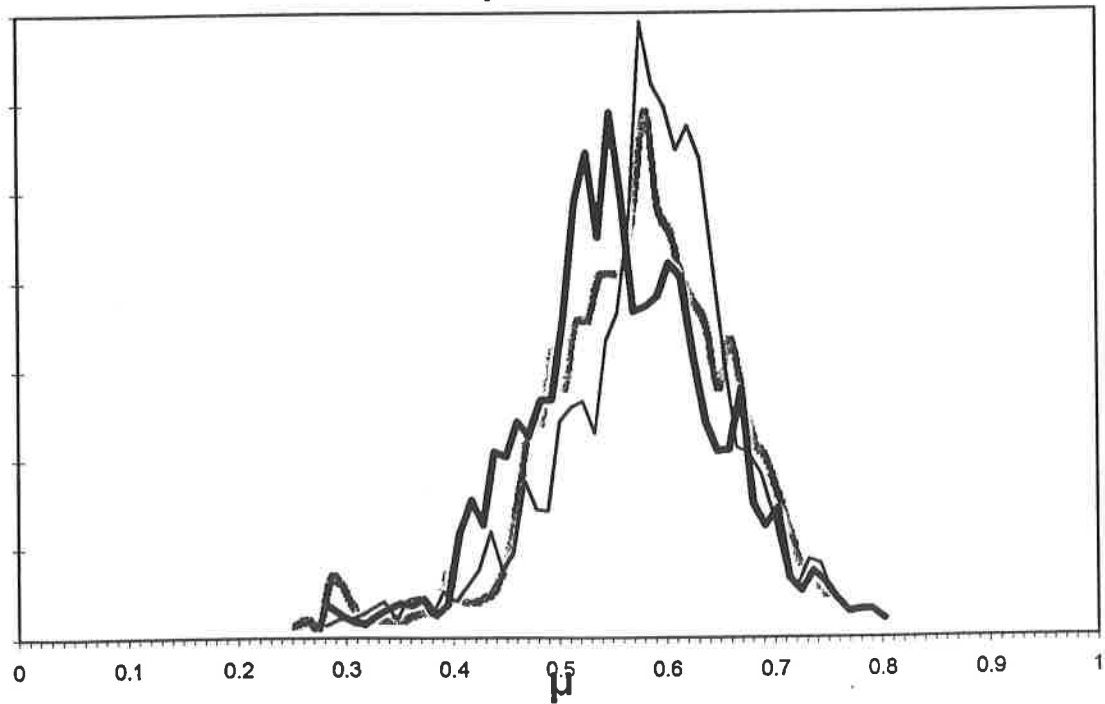
## Cumulative Probability Distribution

Deck: Coarse Hardwood

Skid: Machine feet



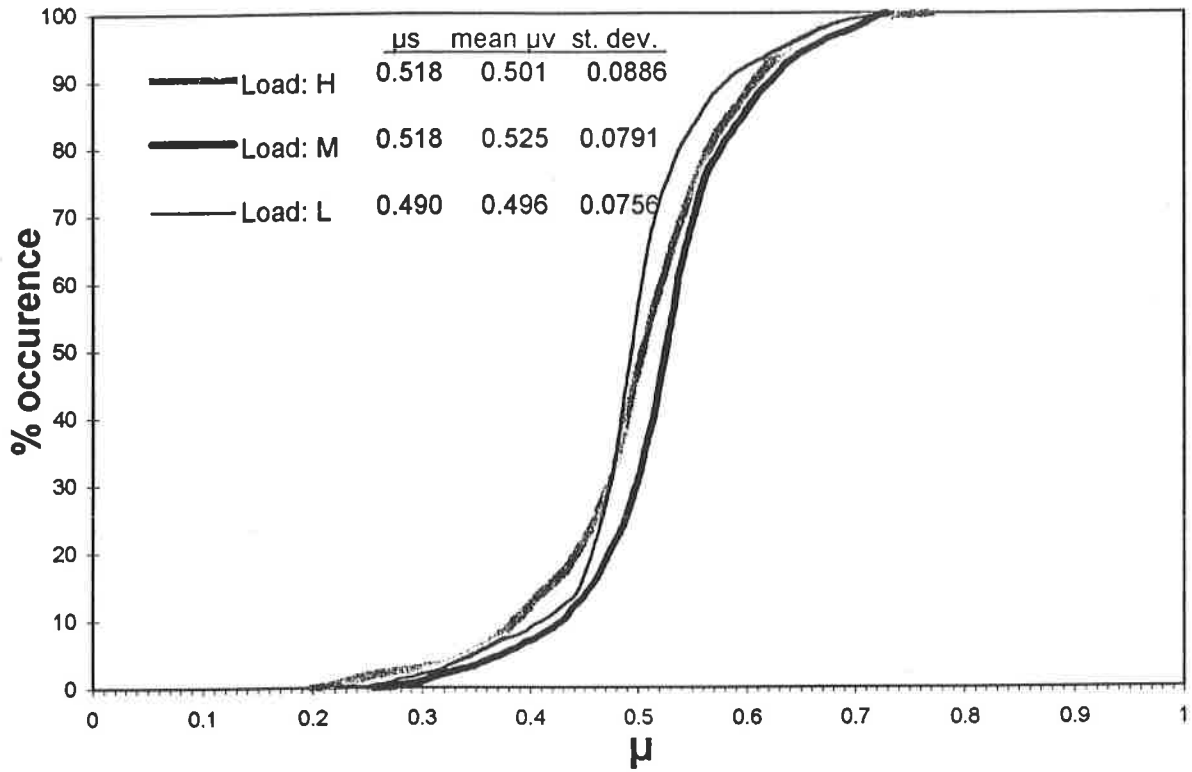
## Probability Distribution



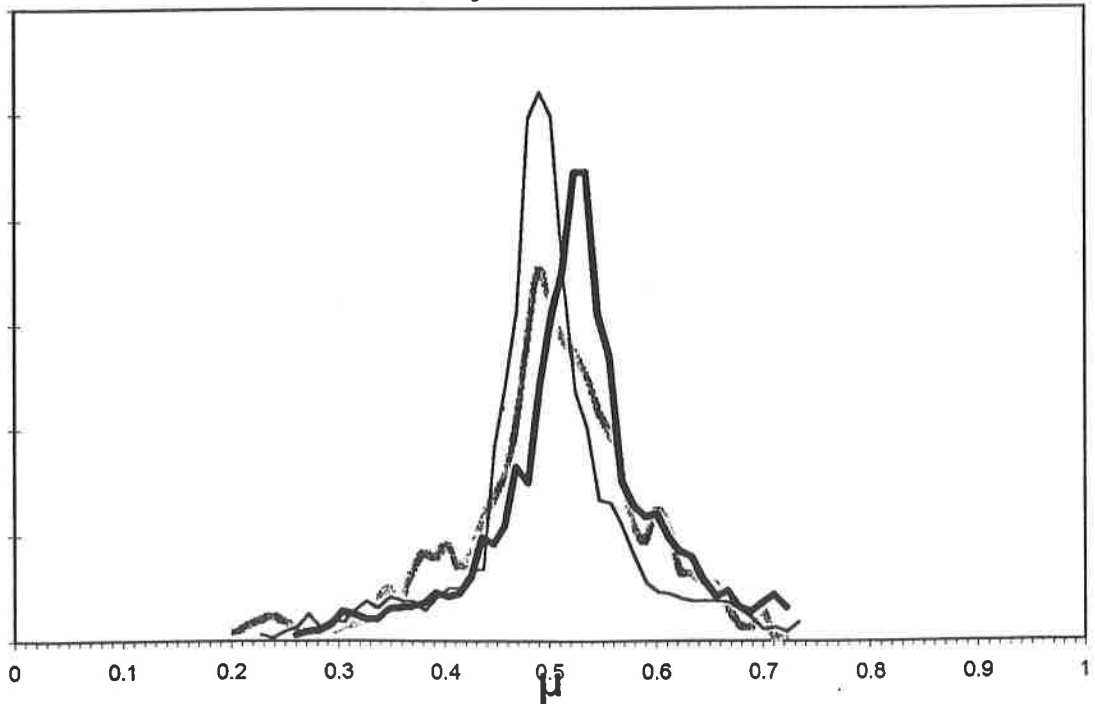
## Cumulative Probability Distribution

Deck: Coarse Hardwood

Skid: Steel Pads



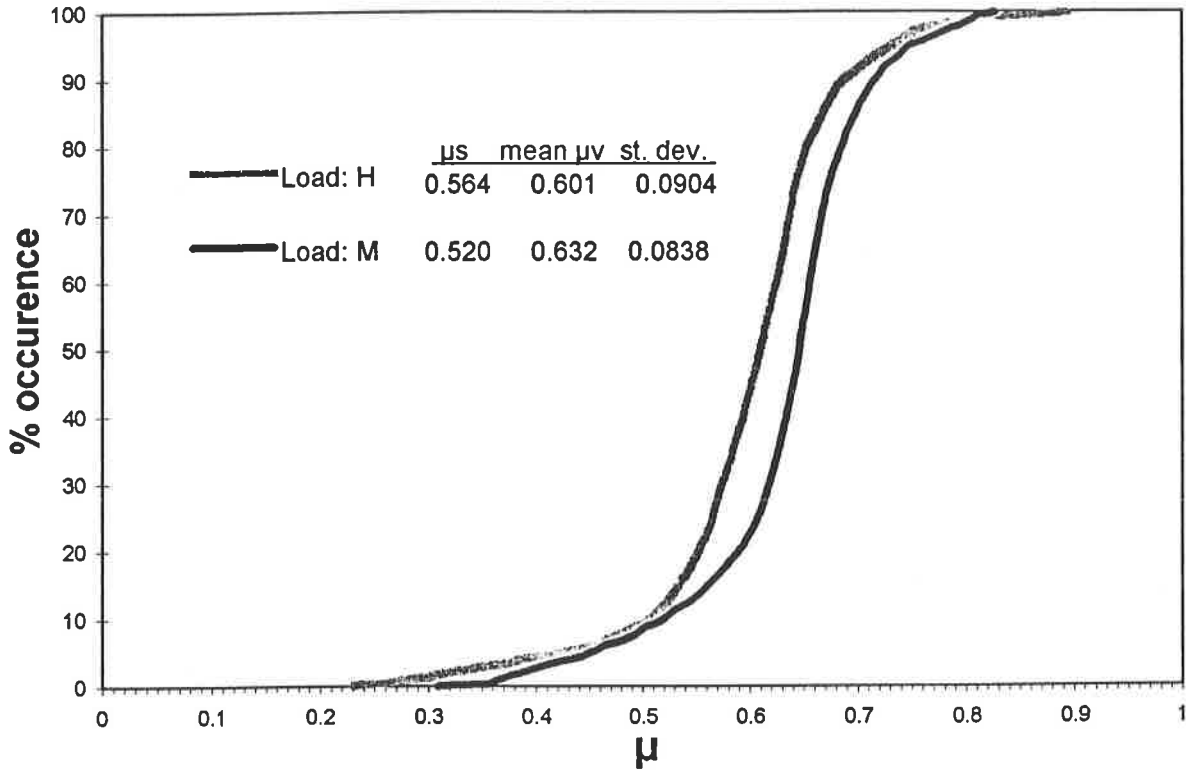
## Probability Distribution



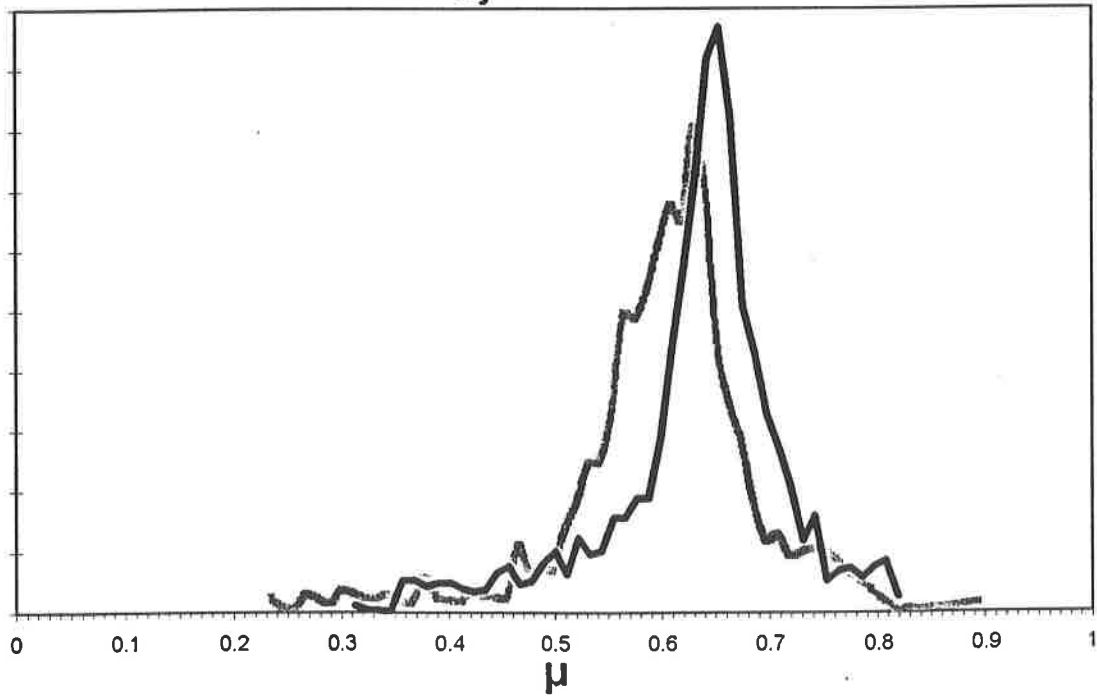
## Cumulative Probability Distribution

Deck: Coarse Hardwood

Skid: Concrete Blocks



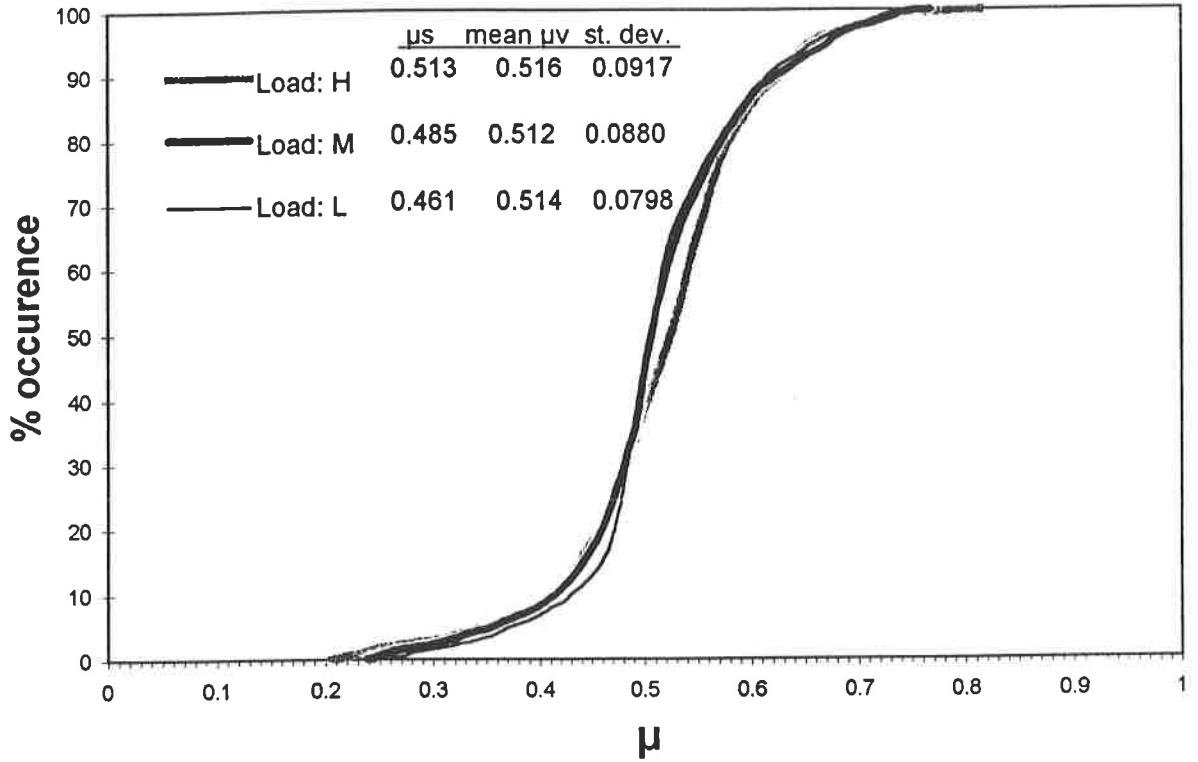
## Probability Distribution



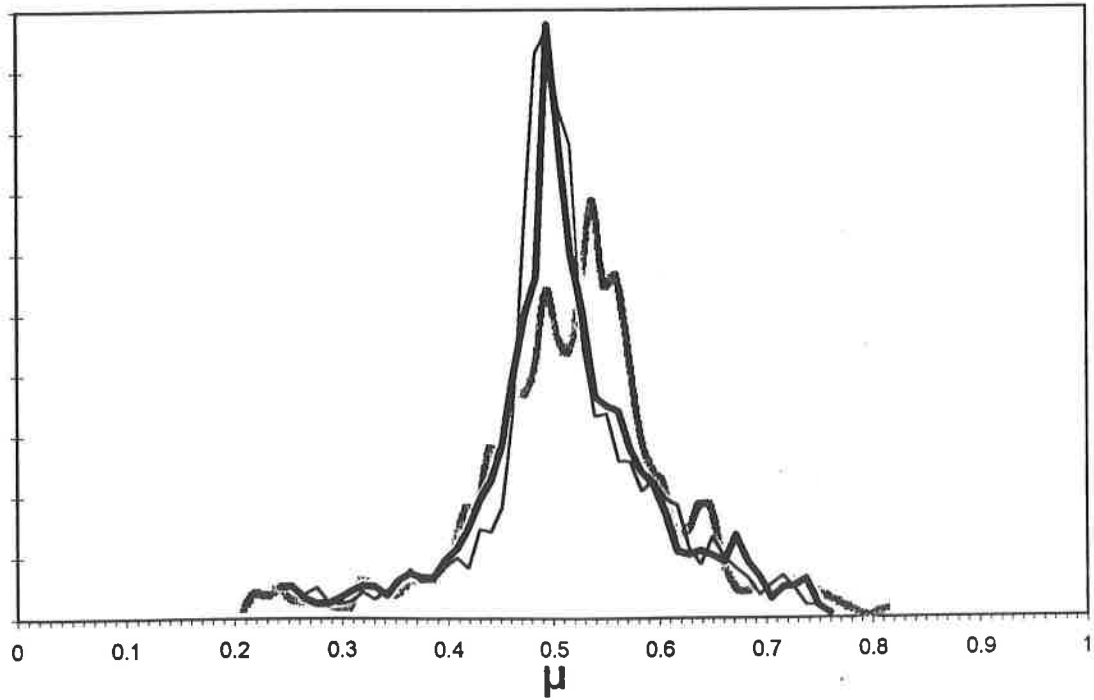
# Cumulative Probability Distribution

Deck: Coarse Hardwood

Skid: Spruce Board



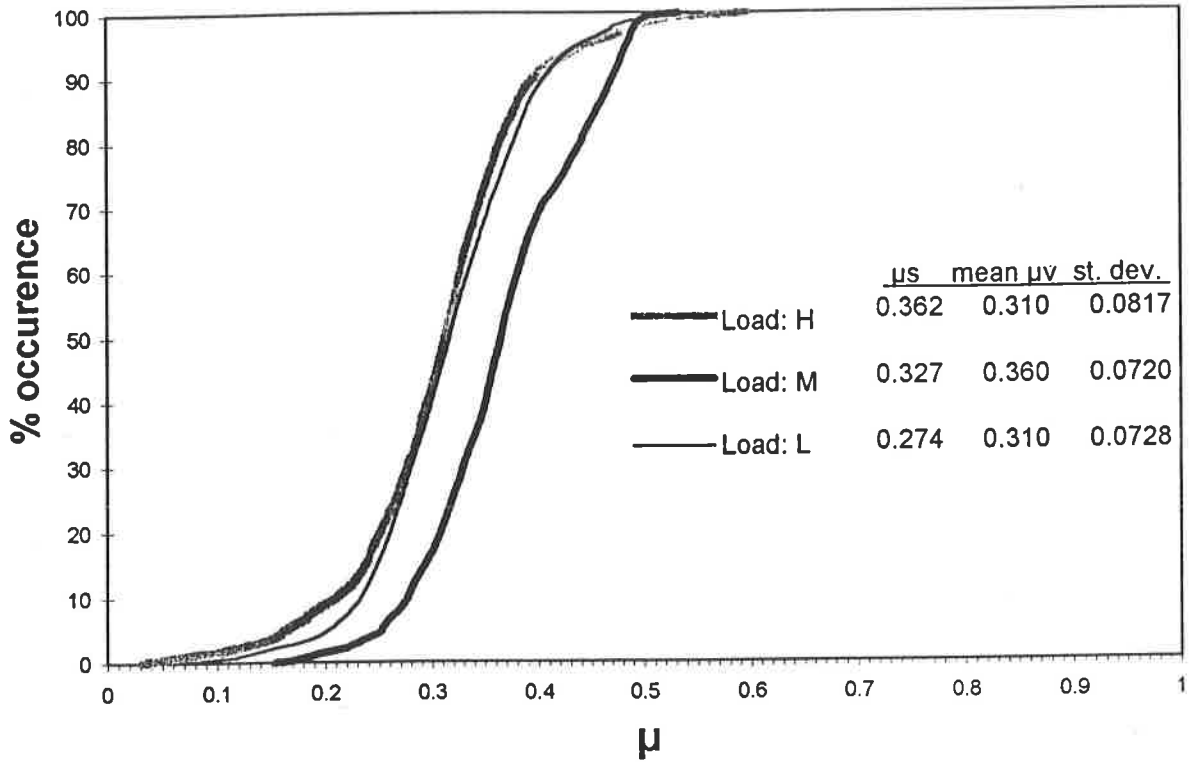
# Probability Distribution



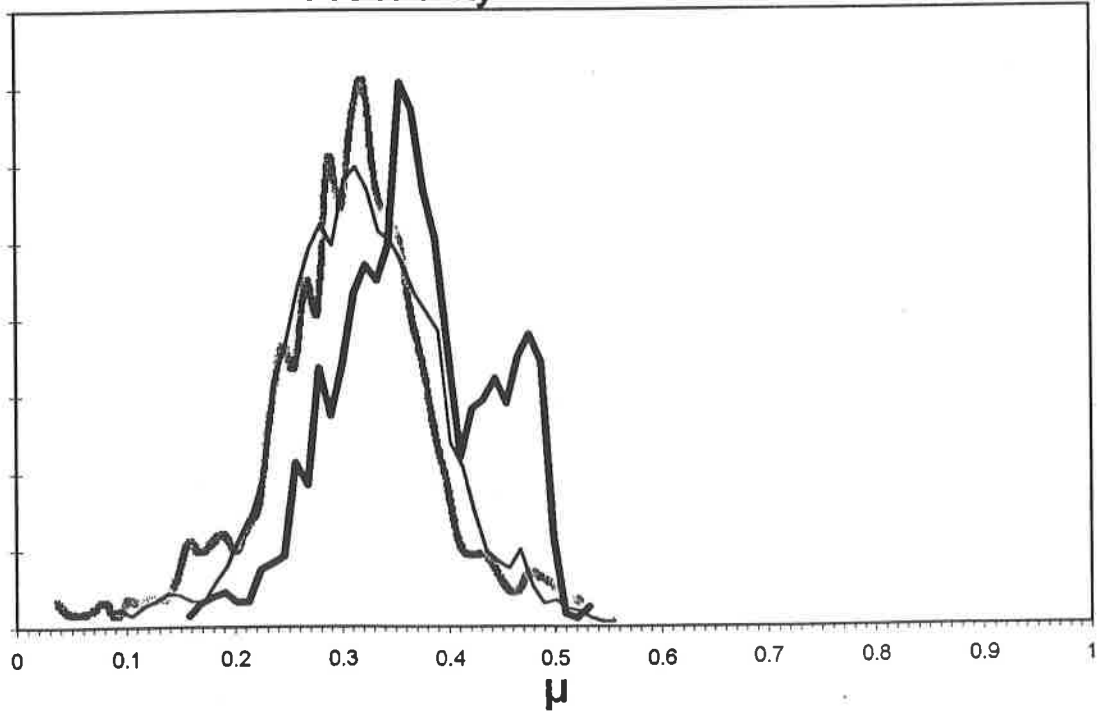
## Cumulative Probability Distribution

Deck: X-Groove Aluminum

Skid: Steel Pads



## Probability Distribution

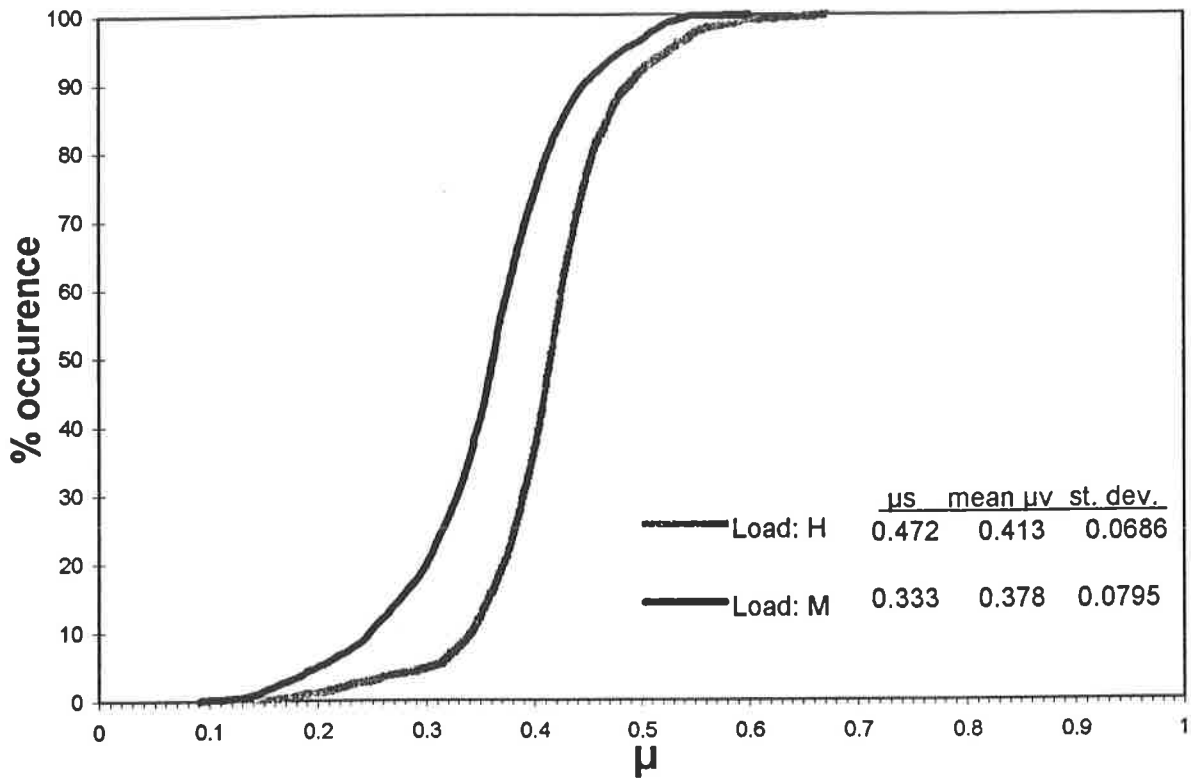




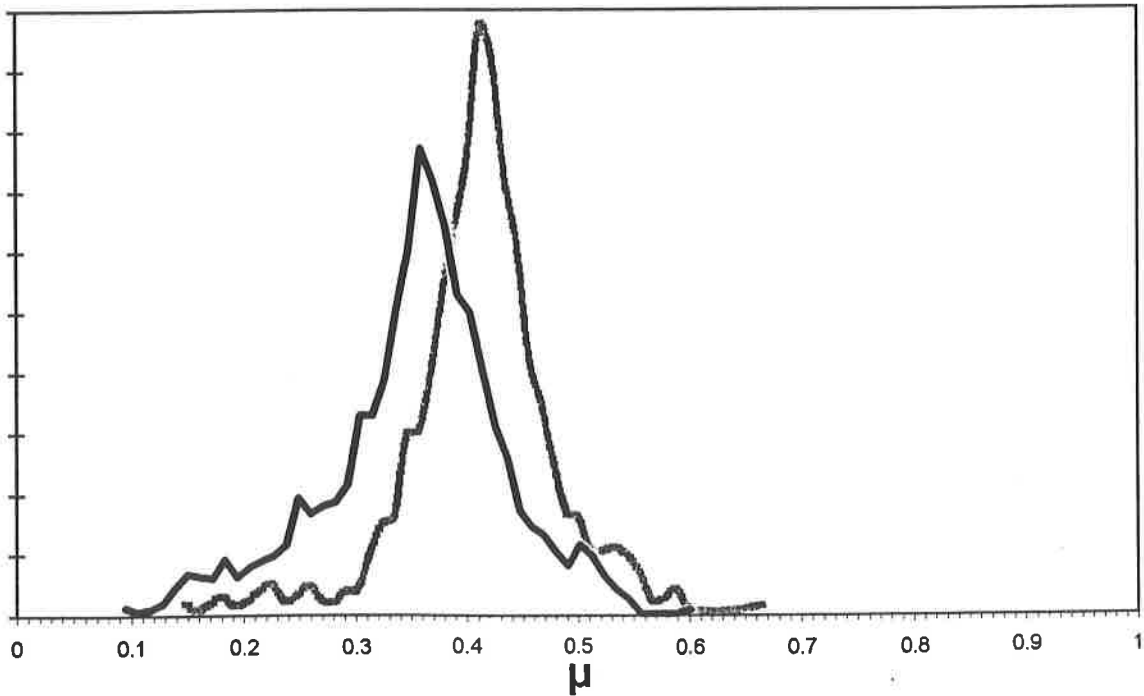
## Cumulative Probability Distribution

Deck: X-Groove Aluminum

Skid: Concrete Blocks



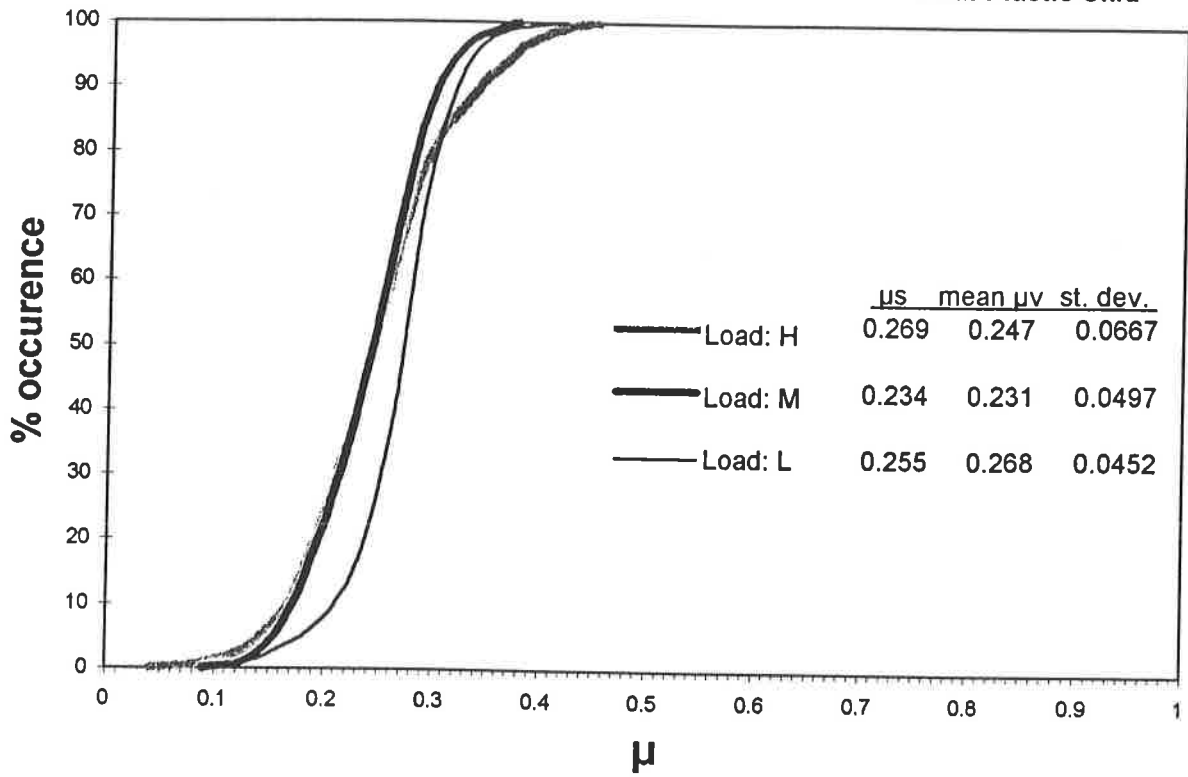
## Probability Distribution



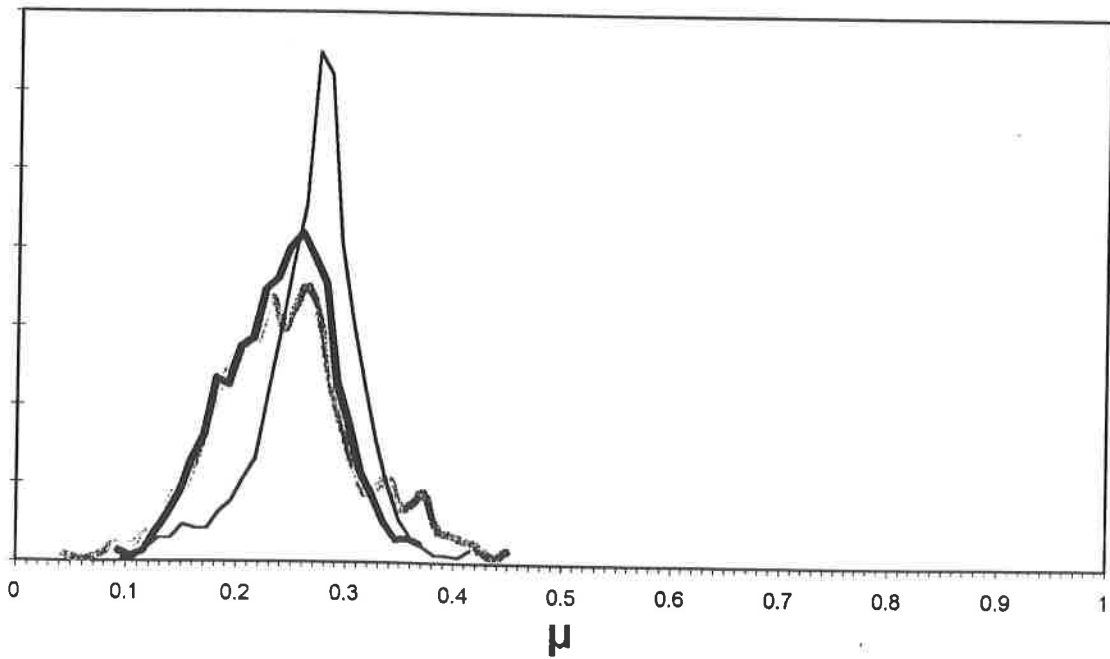
# Cumulative Probability Distribution

Deck: X-Groove Aluminum

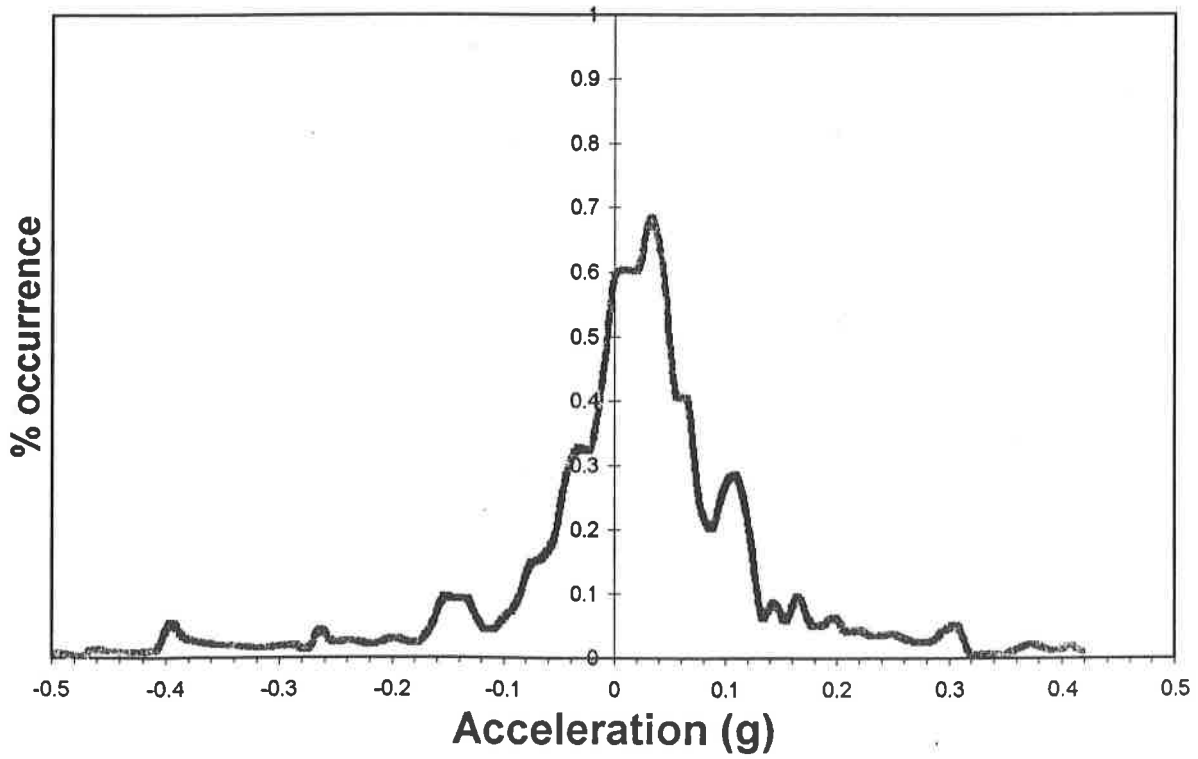
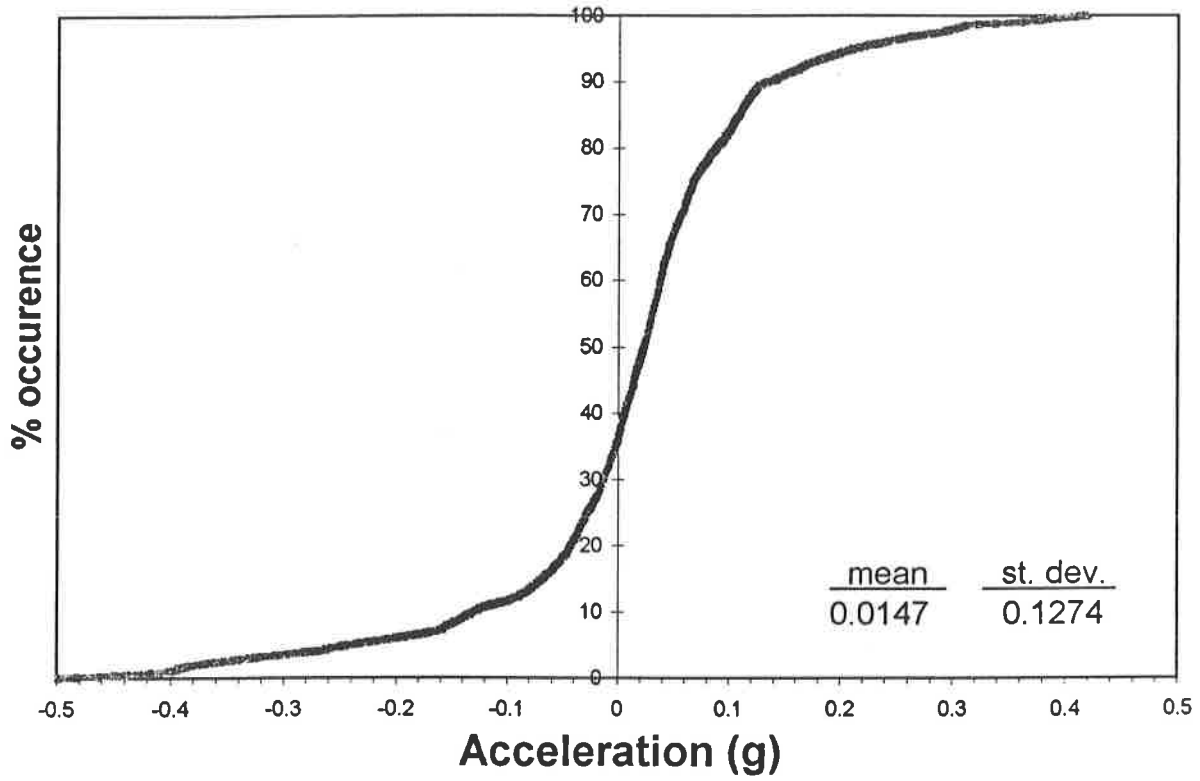
Skid: Plastic Skid



# Probability Distribution



# Probability Distributions



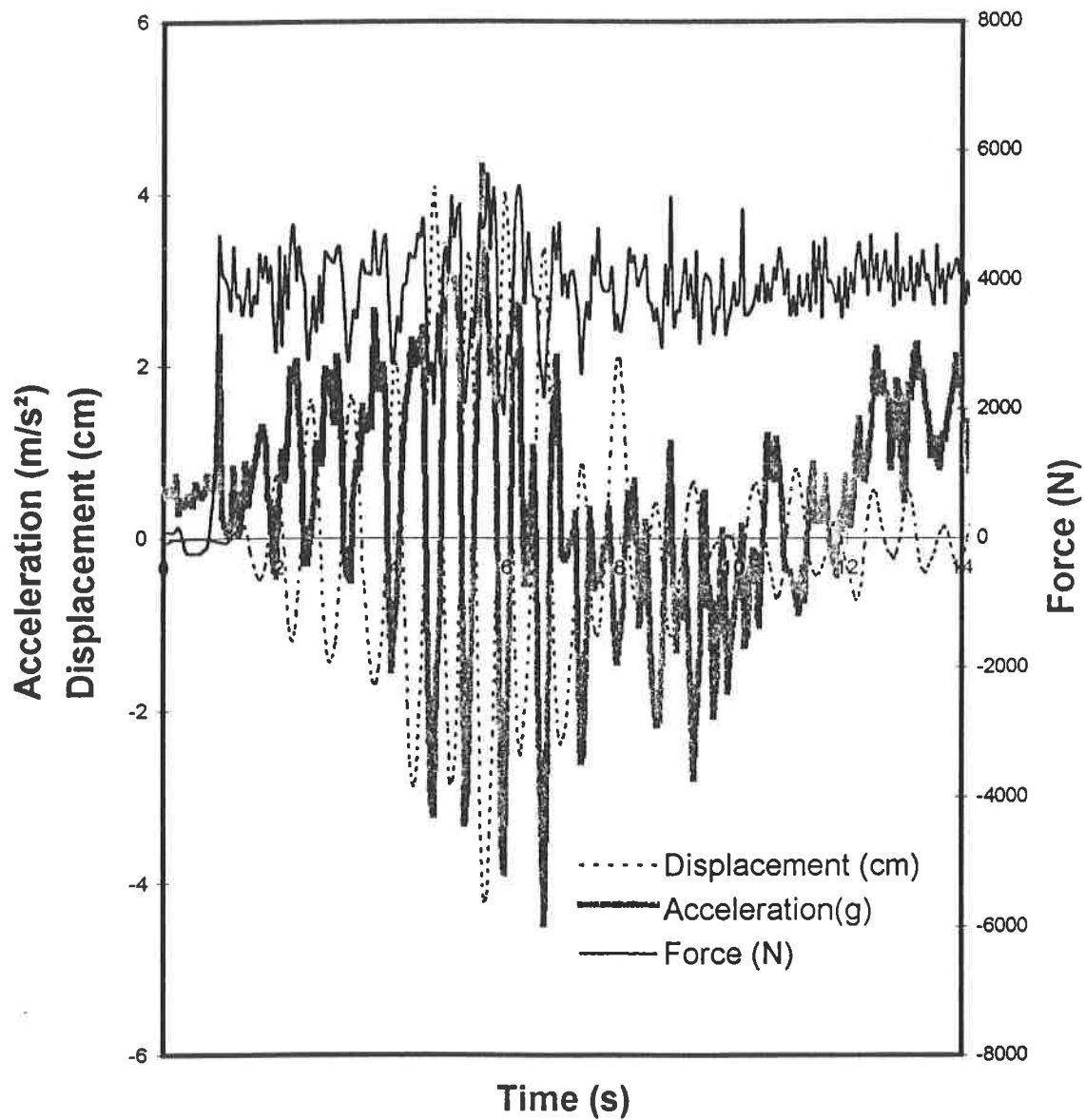


**Figure 4.59: Time history of measured friction force, displacement and vertical acceleration.  
(Deck: Aluminum X-Grooved ; Skid: Concrete)**



## North American Load Security Research Project Reports

- [1] Billing J.R., Mercer W.R.J. and Cann W., "A Proposal for Research to Provide a Technical Basis for a Revised National Standard on Load Security for Heavy Trucks", Transportation Technology and Energy Branch, Ontario Ministry of Transportation, Report CV-93-02, November 1993.

---

- [2] Rakheja S., Sauvé P. and Juras D., "Experimental Evaluation of Friction Coefficients of Typical Loads and Trailer Decks under Vertical Vibration", North American Load Security Research Project, Report 2, Canadian Council of Motor Transport Administrators, Ottawa, Ontario, 1997.
- [3] Heidersdorf E. and Hay E., "Slippage Tests with Anti-skid Mats", North American Load Security Research Project, Report 3, Canadian Council of Motor Transport Administrators, Ottawa, Ontario, 1997.
- [4] Hay E., Williams W. and Heidersdorf E., "Dressed Lumber Tiedown Tests", North American Load Security Research Project, Report 4, Canadian Council of Motor Transport Administrators, Ottawa, Ontario, 1997.

---

- [5] Mercer W.R.J. and Billing J.R., "Effect of Cargo and Tiedown Characteristics on Equalization of Tension in the Spans of Tiedowns", North American Load Security Research Project, Report 5, Canadian Council of Motor Transport Administrators, Ottawa, Ontario, 1997.
- [6] Mercer W.R.J. and Billing J.R., "Effect of Binder Type and Chain Length on Tension in Chain Tiedowns", North American Load Security Research Project, Report 6, Canadian Council of Motor Transport Administrators, Ottawa, Ontario, 1997.
- [7] Billing J.R. and Lam C.P., "Friction Coefficients between Typical Cargo and Truck Decks", North American Load Security Research Project, Report 7, Canadian Council of Motor Transport Administrators, Ottawa, Ontario, 1997.
- [8] Mercer W.R.J. and Billing J.R., "Load Capacity of Nailed Wood Blocking", North American Load Security Research Project, Report 8, Canadian Council of Motor Transport Administrators, Ottawa, Ontario, 1997.
- [9] Billing J.R. and Lam C.P., "Effect of Cargo Movement on Tension in Tiedowns", North American Load Security Research Project, Report 9, Canadian Council of Motor Transport Administrators, Ottawa, Ontario, 1997.
- [10] Billing J.R. and Leung D.K.W., "Evaluation of the Strength and Failure Modes of Heavy Truck Cargo Anchor Points", North American Load Security Research Project, Report 10, Canadian Council of Motor Transport Administrators, Ottawa, Ontario, 1997.

- [11] Mercer W.R.J. and Billing J.R., "Tests on Methods of Securement for Thick Metal Plate", North American Load Security Research Project, Report 11, Canadian Council of Motor Transport Administrators, Ottawa, Ontario, 1997.
- [12] Mercer W.R.J. and Billing J.R., "Tests on Methods of Securement for Large Boulders", North American Load Security Research Project, Report 12, Canadian Council of Motor Transport Administrators, Ottawa, Ontario, 1997.
- [13] Mercer W.R.J. and Billing J.R., "Bending Strength of Trailer Stakes", North American Load Security Research Project, Report 13, Canadian Council of Motor Transport Administrators, Ottawa, Ontario, 1997.
- [14] Mercer W.R.J. and Billing J.R., "Effect of Tiedowns on Wood Blocks Used as Dunnage", North American Load Security Research Project, Report 14, Canadian Council of Motor Transport Administrators, Ottawa, Ontario, 1997.
- [15] Billing J.R. and Lam C.P., "Tests on Methods of Securement for Metal Coils", North American Load Security Research Project, Report 15, Canadian Council of Motor Transport Administrators, Ottawa, Ontario, 1997.
- [16] Mercer W.R.J. and Billing J.R., "Tests on Methods of Securement for ISO Containers", North American Load Security Research Project, Report 16, Canadian Council of Motor Transport Administrators, Ottawa, Ontario, 1997.
- [17] Billing J.R. and Leung D.K.W., "Analysis of Heavy Truck Cargo Anchor Points", North American Load Security Research Project, Report 17, Canadian Council of Motor Transport Administrators, Ottawa, Ontario, 1997.
- [18] Billing J.R. and Couture J., "North American Load Security Research Project Summary Report", North American Load Security Research Project, Report 18, Canadian Council of Motor Transport Administrators, Ottawa, Ontario, 1997.
- 
- [19] Grandbois J., "Assessing a Securement Method for the Transportation of Heavy Machinery Using a Combination of Highway Vehicles", North American Load Security Research Project, Report 19, Canadian Council of Motor Transport Administrators, Ottawa, Ontario, 1997.
-